

Molecular control of ureter development in the mouse

Von der Naturwissenschaftlichen Fakultät
der Gottfried Wilhelm Leibniz Universität Hannover
zur Erlangung des Grades

Doktorin der Naturwissenschaften
(Dr. rer. nat.)

genehmigte Dissertation
von Dipl.-Biol. Anna-Carina Weiss
geboren am 31.08.1983 in Hannover

2015

Referent: Prof. Dr. rer. nat. Andreas Kispert
Erste Korreferentin: PD Dr. med. Sandra Ciesek
Zweite Korreferentin: Prof. Dr. rer. nat. Monika Hassel
Tag der Promotion: 07. Januar 2015

Erklärung zur kumulativen Dissertation von Anna-Carina Weiss (geboren am 31.08.1083 in Hannover)

Diese kumulative Dissertation basiert auf folgenden Artikeln und einem bisher unveröffentlichten Manuskript:

1. Weiss AC, Airik R, Greulich F, Foik AB, Trowe MO, Rudat C, Costantini F, Adams RH and Kispert A. "Nephric duct insertion requires EphA4/EphA7 signaling from the pericloacal mesenchyme". *Development* 2014, September 141(17) 3420-30.
2. Bohnenpoll T and Bettenhausen E, Weiss AC, Foik AB, Trowe MO, Blank P, Airik R and Kispert A. "Tbx18 expression demarcates multipotent precursor populations in the developing urogenital system but is exclusively required within the ureteric mesenchymal lineage to suppress a renal stromal fate". *Developmental Biology* 2013, August 380(1), 25-36.
3. Trowe MO and Airik R, Weiss AC, Farin HF, Foik AB, Bettenhausen E, Schuster-Gossler K, Taketo MM and Kispert A. "Canonical Wnt signaling regulates smooth muscle precursor development in the mouse ureter." *Development* 2012, September 139(17), 3099-108.
4. Weiss AC, Bohnenpoll T, Blank P, Airik, R, Mamo T, Trowe MO and Kispert A. "The zinc finger transcription factor Gata2 promotes differentiation of the ureteric mesenchyme by controlling Hedgehog- and RA-signaling".
Manuscript in preparation.

Alle Abbildungen in **Artikel 1** (außer Abb. S11) sowie das Verfassen des Manuskripts wurden von mir erstellt und durchgeführt. R. Airik hat das Projekt initiiert, F. Greulich, A. Foik und T. Bohnenpoll haben technische Hilfestellung gegeben. C. Rudat hat die Pax2(8.5)-cre Zellschicksalsanalyse durchgeführt (Abb. S11). F. Costantini, RH Adams und M.-O. Trowe haben verschiedene Mausstämme generiert und/oder zur Verfügung gestellt. A. Kispert lieferte das inhaltliche Konzept sowie Anregungen, verfasste und editierte Teile des Manuskripts und finanzierte das Projekt.

In **Artikel 2** habe ich die Abb. 2A, Abb. 5D, Abb. 6B sowie die Abb. S3 J-P experimentell und graphisch angefertigt sowie zum inhaltlichen Konzept des Manuskripts beigetragen. A. Kispert hat das Manuskript geplant, geschrieben sowie das Projekt finanziert.

In **Artikel 3** habe ich die Abb. S7 sowie die Abb. S8 experimentell und graphisch erstellt. M.-O. Trowe und R. Airik haben die Hauptarbeiten für diesen Artikel durchgeführt, AB Foik und E. Bettenhausen gaben technische Hilfestellung. H. Farin, K. Schuster-Gossler und M.M. Taketo generierten oder stellten Mauslinien zur Verfügung. M.-O. Trowe und A. Kispert haben das Manuskript geschrieben und A. Kispert hat das Projekt finanziert.

Der Großteil der Arbeiten in **Artikel 4** sowie das Verfassen des Manuskripts wurden von mir durchgeführt. T. Bohnenpoll hat Abb. 4 erstellt sowie das Sammeln des Gewebes sowie die RNA-Extraktion für die Microarray-Analysen durchgeführt. R. Airik, P. Blank, T. Mamo und M.-O. Trowe haben technische Hilfestellung gegeben. M.-O. Trowe entwickelte das technische Tool zur Analyse der Microarrays. A. Kispert lieferte Anregungen zum inhaltlichen Konzept und finanzierte das Projekt.



Medizinische Hochschule
Hannover



Angefertigt am
Institut für Molekularbiologie
der Medizinischen Hochschule Hannover
unter der Betreuung von
Prof. Dr. rer. nat. Andreas Kispert

Meinem Großvater

“Wunder stehen nicht im Gegensatz zur Natur, nur im Gegensatz zu dem, was wir über die Natur wissen..” (St. Augustin)

1. Summary

The mouse excretory system is a multi-organ entity consisting of the kidneys, the ureters, the urinary bladder and the urethra. Although forming a functional continuum in the adult, the different organs and tissues of this system arise from different epithelial and mesenchymal cells lineages in different germ layers in early embryogenesis. Continuous cross-talk between the different lineages is required to establish both functional tissues in the individual organs as well as proper connectivity between them. Developmental defects within one lineage can cause failure of the entire system as evidenced in the severity of defects observed in congenital anomalies of the kidneys and the urinary tract, that are frequently diagnosed in newborns and may even lead to kidney failure in early childhood.

Development of the excretory system begins at embryonic day (E) 8.5 at the level of the forelimbs with the emergence of an epithelial tube, the nephric duct (ND), within the intermediate mesoderm. The ND migrates in caudal direction and induces the formation of mesonephric tubules in the surrounding mesenchyme. When the ND reaches cloacal level at E9.5, it turns to the midline and fuses with the epithelium of the cloaca, the endothelial primordium of the urinary bladder, establishing the primary connection between the upper and lower urinary tract. How the ND is guided during migration, how the epithelial integrity of the tube is maintained and how both epithelia of the ND and the cloaca interact to finally fuse, have remained poorly understood.

In this dissertation, I demonstrate that Eph/ephrin signalling, a unique signaling module of receptor protein tyrosine kinases (RTKs), plays a crucial role in this process. The Eph receptors *EphA4* and *EphA7* were found to be co-expressed in the pericloacal and ureteric mesenchyme. To address the significance of this expression, embryos deficient for both *EphA4* and *EphA7* (DKO) were generated. DKO embryos exhibited with 50% penetrance distal ureter malformations including ureterocele, blind and ectopically ending ureters with associated hydroureter, megaureter and secondary hydronephrosis shortly before birth. The phenotypic changes were traced to a late or absent fusion of the ND with the cloaca that, in turn, was caused by disintegration of the ND tip. Conditional deletion of *ephrinB2* from the ND largely phenocopied these changes, suggesting that EphA4 and EphA7 from the pericloacal mesenchyme signal via ephrinB2 to mediate ND insertion. This study emphasizes the importance of the precise timing of ND-to-cloacal fusion for the development of a normal urogenital system.

ND insertion into the cloaca is preceded by development of the ureters and the kidneys. At E10.5 at the hindlimb level, the ureteric bud (UB) emerges from the ND and invades an adjacent mesenchymal condensation, the metanephric blastema (MB). The proximal part of the ureter, which lies within the blastema, engages in repetitive rounds of dichotomous branching to generate the collecting duct system of the kidney, while the distal part that remains outside simply elongates to establish the contractile tube that transports the urine from the

kidney to the bladder. The T-box transcription factor *Tbx18* is expressed early in embryonic development in the ureteric mesenchyme (UM), a small stripe of mesenchymal cells that lie between the MB and the ND. Utilizing reporter genes and lineage tracing experiments, we showed that *Tbx18* positive cells contribute to the UM, the kidney stroma, the bladder muscle and the cortex of the adrenal glands. However, *Tbx18* is dispensable for the differentiation of the majority of these organs except the ureter. Upon loss of *Tbx18*, cells of the UM mislocalize to the surface of the kidney and differentiate into fibrocytes, which prenatally results in a severely shortened hydroureter and hydronephrosis. The few remaining *Tbx18*-deficient cells of the UM fail to respond to epithelial signals and differentiate into smooth muscle (SM) cells.

SM differentiation of the UM is a pivotal process for the integrity of the entire excretory system, as failure or delay in differentiation results in a less rigid tube that does not withstand the urinary pressure but dilates together with the renal pelvis (hydroureter and hydronephrosis). Differentiation of the UM depends on signals from the adjacent epithelium, and earlier work characterized the crucial role of Shh from the epithelium and its mesenchymal mediator Bmp4 in this process. As we detected activity of canonical Wnt signaling in the UM, we addressed the functional requirement of this pathway in ureteric SM differentiation by conditionally deleting *Ctnnb1*, the intracellular signal transducer, from the UM. In conditional *Ctnnb1* mutants, the inner mesenchymal domain of the ureter was lost and cells of the outer domain expanded and differentiated into fibrocytes at the expense of SM cells. Moreover, we observed downregulation of *Tbx18* expression at early stages in the mutant UM. Reexpression of *Tbx18* in the *Ctnnb1*-deficient UM, however, did not rescue the hydroureter phenotype discarding an important function for Tbx18 downstream of Wnt signaling in UM differentiation.

In order to allow proper ureteric SM differentiation, transcription factor and signalling activities need to be tightly regulated in space and time. In a fourth project, I showed that the zinc-finger transcription factor gene *Gata2*, the key regulator of hematopoietic system development, is transiently expressed in the undifferentiated UM. Upon conditional deletion of *Gata2* in the UM, SMC differentiation was delayed culminating in severe hydroureter and hydronephrosis at birth. Transcriptional profiling by RNA-microarray analysis allowed deeper insight into the molecular changes in the mutant UM and provided gateways to further molecular and functional analyses.

Taken together, this doctoral thesis provided novel insight into the molecular control of ND migration and insertion by Eph/ephrin signaling, the specification and contribution of progenitor cells to the mature urogenital system, and the molecular control of UM differentiation by the transcription factor *Gata2* and the canonical Wnt signaling pathway. The findings not only decipher regulatory circuits guiding normal ureter development, they also provide new insight into the aetiology of CAKUT in human newborns.

Keywords: Nephric duct, *EphA4*, *EphA7*, *Tbx18*, ureter, smooth muscle differentiation

2. Zusammenfassung

Das Harn- oder Exkretionssystem hat eine essentielle Funktion in der Aufrechterhaltung der Körperhomöostase, in dem es den Ionen- und Wasserhaushalt des Blutes kontrolliert und sowohl überschüssige Ionen als auch Wasser und Stoffwechselendprodukte aus dem Körper eliminiert. Das Exkretionssystem besteht aus einer Filtrationseinheit, den Nieren, und einem anschließenden Harnableitungssystem, das sich aus dem Harnleiter (Ureter), der Blase und der Harnröhre konstituiert. Da sich diese Organe aus verschiedenen embryonalen Vorläufergeweben ableiten, ist die Entwicklung des Gesamtsystems durch komplexe Zell- und Gewebeinteraktionen gekennzeichnet. Bedingt durch die gegenseitige Abhängigkeit kann die gestörte Entwicklung in einem Gewebe oder Organ zum Versagen des gesamten Harnsystems führen. Angeborene Anomalien der Nieren und des Harntrakts („congenital anomalies of the kidneys and urinary tract“, kurz CAKUT) können sogar zu Nierenversagen im Säuglings- oder Kleinkindalter führen, welches eine Nierentransplantation unabdingbar macht.

Die Entwicklung des Harnsystems beginnt in der Maus am Embryonaltag (E) 8,5 mit der Bildung des tubulären nephrischen Ganges. Dieser Gang wird auf der Höhe der Vordergliedmaßenknospen im intermediären Mesoderm angelegt und verlängert sich nach kaudal, bis er auf der Höhe der Hintergliedmaßenanlagen die Kloake, die Vorläuferstruktur der Harnblase, erreicht und mit dieser fusioniert. Dieser Prozess stellt die erste Verbindung zwischen dem oberen und unteren Teil des Harnsystems dar; ist somit Grundlage für die Ausbildung eines kontinuierlichen Harnableitungssystems. Wie der nephrische Gang während seiner Migration geleitet wird, wie seine epitheliale Integrität vermittelt wird und wie die Epithelien der Kloake und des nephrischen Ganges interagieren, um schließlich zu fusionieren, ist nur unzureichend verstanden.

In dieser Dissertation konnte gezeigt werden, dass der Eph/Ephrin Signalweg eine essentielle Rolle in diesem Fusionsprozess spielt. Die Eph Rezeptoren *EphA4* und *EphA7* sind im perikloakalen Mesenchym sowie im Uretermesenchym koexprimiert. Mausembryonen, denen *EphA4* und *EphA7* fehlten (DKO), wiesen in 50% der Fälle pränatale Fehlbildungen des distalen Ureters wie Ureterozöl, Ureterektopie oder blind endende Ureteren, starke Hydro- und Megaureteren auf. Diese phänotypischen Veränderungen konnten auf eine fehlende Fusion des nephrischen Ganges mit dem Kloakenepithel zurückgeführt werden, welche wiederum durch zelluläre Desintegration des distalen nephrischen Ganges bedingt war. Die konditionelle Deletion von *EphrinB2* im nephrischen Gang führte zu ähnlichen Ureteranomalien wie im DKO, was auf eine reverse Signaltransduktion von *EphA4* und *EphA7* im perikloakalen Mesenchym über *EphrinB2* im nephrischen Gang hinweist.

Der Fusion des nephrischen Ganges mit der Kloake schließt sich die Entwicklung des Ureters und der Niere an. Am E10.5 entsteht aus dem nephrischen Gang auf der Höhe der Hintergliedmaßen die epitheliale Ureterknospe, die sich verlängert und in das benachbarte

metanephrische Mesenchyms (MM) eindringt. Während der proximale, im metanephrischen Blastem liegende Anteil der Ureterknospe sich dichotom verzweigt und auswächst, um das Sammelrohrsystem der Niere zu bilden, bleibt der distale Anteil unverzweigt und bildet das Epithel des Ureters. Der T-Box Transkriptionsfaktor *Tbx18* ist im Mesonephros und danach im undifferenzierten Mesenchym des Ureters exprimiert. Zellschicksalsanalysen zeigten, dass Zellen des frühen metanephrischen Felds, die positiv für *Tbx18* waren, zum Stroma der Niere, zum Detrusor der Blase und zur Niebennierenrinde beitragen. *Tbx18* ist jedoch nur für die Differenzierung des Ureters essentiell. Bei einem Verlust von *Tbx18* delokalisieren die Zellen des Uretermesenchyms, lassen sich auf der Nierenoberfläche nieder und differenzieren dort zu Fibrozyten. Dies wiederum führt pränatal zu stark verkürzten Hydroureteren und sekundär assoziierter Hydronephrose.

Die glatte Muskulatur des Ureters differenziert in zeitlich präziser Weise ab E14,5 aus dem Mesenchym des Ureters. Dieser Prozess wird durch Signale aus dem benachbarten Ureterepithel induziert. Frühere Arbeiten beschrieben die wichtige Rolle des Shh Signalwegs und die seines mesenchymalen Zielgens *Bmp4* in diesem Prozess; Arbeiten aus diesem Labor konnten eine wichtige Funktion des Wnt-Signalwegs aufzeigen. Es zeigte sich dabei, dass der kanonische b-Catenin (*Ctnnb1*)-abhängige Wnt-Signalweg für die Aufrechterhaltung der *Tbx18* Expression im Uretermesenchym wichtig ist. Eine Wiederherstellung der *Tbx18* Expression im *Ctnnb1*-defizienten Uretermesenchym konnte den Hydroureter-Phänotyp der *Ctnnb1*-Mutante nicht retten, was eine Funktion von *Tbx18* als Signalvermittler des Wnt-Signalwegs in diesem zellulären Kontext ausschloss.

Damit die Glattmuskeldifferenzierung des Ureters richtig ablaufen kann, muss die Aktivität von Transkriptionsfaktoren und Signalmodulen räumlich und zeitlich kontrolliert werden. In einem vierten Projekt dieser Dissertation konnte gezeigt werden, dass die mRNA des Zinkfinger Transkriptionsfaktorgens *Gata2* transient im undifferenzierten Uretermesenchym exprimiert ist und der konditionelle Verlust von *Gata2* in diesem Gewebe zur Bildung von Hydro- und Megaureteren führt. Molekulare Analysen anhand von RNA *in situ* Hybridisierungen sowie RNA-Mikroarrays haben dazu beigetragen, einen tieferen Einblick in die molekularen Veränderungen im Uretermesenchym der *Gata2*-Mutante zu erlangen.

Diese Dissertation hat zum Verständnis der molekularen Kontrolle der Fusion des nephrischen Ganges mit der Kloake durch den Eph/Ephrin Signalweg beigetragen. Zum anderen hat diese Doktorarbeit den Beitrag und die Spezifizierung der *Tbx18*+ Zellvorläuferpopulation zum adulten Urogenitalsystem geklärt. Schließlich wurden der kanonische Wnt Signalweg und der Zinkfinger-Transkriptionsfaktor *Gata2* als neue regulatorische Faktoren der Glattmuskeldifferenzierung charakterisiert. Diese Ergebnisse leisten nicht nur einen Beitrag für ein tieferes Verständnis der genetischen Kontrolle der Entwicklung des Harnsystems, sie tragen auch zu einem besseren Verständnis pathologischer Prozesse bei, die beim CAKUT-Spektrum von Krankheiten auftreten.

Schlagnworte: Nephrischer Gang, *EphA4*, *EphA7*, *Tbx18*, Ureter, Glattmuskeldifferenzierung

3. Table of content

1. Summary	6
2. Zusammenfassung	8
3. Table of content	10
4. Introduction	11
5. Aim of thesis	20
6. Results	
6.1. Part 1	
“Nephric duct insertion requires EphA4/EphA7 signaling from the pericloacal mesenchyme”	
• Running title: EphA4/EphA7 signaling in ND insertion	21
6.2. Part 2	
“Tbx18 expression demarcates multipotent precursor populations in the developing urogenital system but is exclusively required within the ureteric mesenchymal lineage to suppress a renal stromal fate”	
• Running title: Tbx18 lineage tracing	47
6.3. Part 3	
“Canonical Wnt signaling regulates smooth muscle precursor development in the mouse ureter”	
• Running title: Wnt signalling in SM precursor development	67
6.4. Part 4	
“The zinc finger transcription factor Gata2 promotes differentiation of the ureteric mesenchyme by controlling Hedgehog- and RA-signaling”	
• Running title: Gata2 and SM development	89
7. Concluding remarks	143
8. Acknowledgements	146
9. Curriculum vitae	147
10. List of publications	148
11. Declaration	149
12. Bibliography	150

4. Introduction

The urinary system

The urinary system constitutes a multi-component entity with pivotal roles in the organism that encompass the control of water homeostasis by excretion of excessive water, the electrolyte balance, reabsorption of essential and disposal of toxic substances and the control of blood pressure.

The urinary system can be subdivided into an upper (the kidneys and ureters) and a lower (the bladder and urethra) entity. The kidneys produce the urine by filtration of the blood in their functional units, the nephrons. Each nephron consists of a glomerulus (the capillary network, which is encompassed by the double layered Bowman's capsule), the proximal convoluted tubules, the distal convoluted tubules and the loop-of-Henle [1]. Microfiltration of the blood, that generates the primary urine, is accomplished by endothelial cells, the underlying basal membrane and by the podocytes of the Bowman's capsule. The primary urine is then modified in the proximal and distal tubules as well as in the loop-of-Henle and transported via the renal collecting duct system to the renal pelvis into the proximal ureters. The ureters, the bladder and the urethra constitute a drainage system of the modified urine to the outside. The renal pelvis, the ureters and the urinary bladder are lined with a specialized epithelium, the urothelium, which seals and protects the underlying tissue against the high osmolarity of urine. Adjacent to the urothelium lie the mesenchymal compartment of the ureter that includes the fibrous *lamina propria*, which mediates elasticity of the ureter during contraction. The *lamina propria* is surrounded by a SM layer, which propels the urine towards the urinary bladder by unidirectional peristaltic contractions. The SM layer is covered by the fibrous *tunica adventitia*, which anchors the urinary system in the body cavity.

The distal ureters enter the bladder in an oblique angle in the dorsal bladder neck and are connected to the urothelium of the bladder, where the urine is temporarily stored. Once the renal pelvis is filled with urine, initiation of SM contraction is induced by special pace maker cells in the kidney-pelvis junction [2]. After the urine has entered the urinary bladder, the special anatomy of the bladder muscle around the distal ureters prevents reflux into the distal ureters [3]. Excretion of the urine, however, can only be fulfilled with proper connectivity of the upper and lower units of this organ system in combination with a functional SM coating of both the ureter and bladder [4, 5].

Impairment or blockage of urine drainage can occur in each compartment and at each interface of the urinary system and can have a deleterious outcome.

Malformations of the urinary system portray the most common birth defects affecting 1:500 infants and causing neonatal death in 1:2000 live births [6]. Many newborn patients are diagnosed with so-called congenital anomalies of the kidney and urinary tract (CAKUT), a broad spectrum of malformations, which encompasses hydroureter or megaureter, hydronephrosis, renal duplex systems, horseshoe kidneys, polycystic kidneys (PKD), kidney agenesis or -hypoplasia as well as mega-bladder [7-10].

Abnormalities of the ureter-pelvis intersection lead to a uretero-pelvic junction obstruction (UPJO), a disease entity diagnosed in newborns [11]. UPJO can be acquired by a dysfunctional SM architecture of the very proximal ureter, which prevents the urine to exit the renal pelvis [12, 13]. The accumulated urine and the resulting hydrostatic pressure lead to subsequent destruction of the renal parenchyma. Likewise, a non-functional SM layer of the distal ureter can induce a pathophysiological condition termed hydroureteronephrosis, where primary dilatation of the ureter leads to reflux and succumbs secondary destruction of the kidney [14]. Pivotal to the same extend for the functionality of the urinary system is a proper connectivity of the distal ureter with the bladder. Anatomical blockage of this connection, termed vesico-ureteric junction obstruction (VUJO), results in hydroureter and hydronephrosis [15], respectively.

The aetiology of CAKUT has remained poorly understood. Over the last decades genetically modified mouse models have provided insight into the aetiology of CAKUT but also into the normal development of this organ system by elucidating the underlying molecular pathways and signalling modules, which, upon deletion or ectopic activation in the embryo, cause similar phenotypes as seen in human patients.

Mouse ureter development

Although the ureter is part of the urinary drainage system, its ontogenetic origin clearly differs from that of the bladder and the urethra. The latter organs originate from an endodermal infolding, the urogenital sinus, and its surrounding pericloacal mesenchyme [16], whereas the ureters derive from the intermediate mesoderm (IM) [17]. In the mouse, development of the permanent kidney (the metanephros) starts at embryonic day (E) 8.5 with the emergence of the Wolffian or nephric duct (ND), an epithelial tube that is generated by a process called mesenchymal-to-epithelial-transition (MET) within the IM [18]. The ND extends within the IM in caudal direction while the proximal part induces epithelial tubules in the adjacent mesenchyme, which generates the pronephros. The pronephros constitutes a functional kidney in fish and amphibian larvae, but is without function in amniotes [19]. In mammals the pronephric tubules degenerate and the caudally migrating ND again induces epithelial tubules, which give rise to the mesonephros [20]. In the mouse, the mesonephric tubules vanish in the female, whereas in the male, the ND and anterior mesonephric tubules give rise to the *vas deferens* and the epididymus of the male reproductive system, respectively [18, 21]. At E9.5, the caudal part of the ND reaches the level of the cloaca (the progenitor structure of the urinary bladder), turns to the midline of the embryo and fuses with the cloacal epithelium. This process establishes the pivotal primary connection between the lower (urethra and bladder) and upper (ureters and kidneys) entity of the urinary tract.

Definitive ureter development in the mouse starts at E10.5 at the hindlimb level with the emergence of a small epithelial diverticulum in the caudal ND, the ureteric bud (UB).

The UB invaginates into an adjacent molecularly distinct mesenchymal blastema referred to

as metanephric mesenchyme (MM), a process which is mainly governed by Gdnf/Ret signalling [22]. After entering the MM, the proximal part of the UB acquires a completely different fate than the distal part that remains outside of the MM. The proximal part of the UB engages in several rounds of dichotomous branching to give rise to the collecting duct system of the kidney [17]. The distal part of the UB outside the MM merely elongates and constitutes the ureteric epithelium.

From E10.5 until E13.5, the common nephric duct (CND), the part of the ND that is still connected to the ureter, is eliminated by programmed cell death, which is mainly governed by Ret- and Retinoic acid (RA) signalling as well as by two protein tyrosine phosphatase receptors [23, 24], as I will describe later in more detail. This process is the prerequisite for a proper integration of the distal ureter into the bladder wall in order to establish a functional vesico-ureteric junction (VUJ). At E14.5, the epithelium of the ureteric stalk starts to differentiate into the urothelium. The mature urothelium is a stratified epithelium that is comprised of a basal cell layer (B-cells) expressing the intermediate filament protein keratin 5 (Krt5). Next to the basal cell layer lies the intermediate cell layer (I-cells), which is positive for the transcription factor p63, the hedgehog ligand sonic hedgehog (Shh) and for the asymmetric unit membrane (AUM) proteins uroplakins. The I-cell layer is followed by a superficial layer (S-cells, also termed umbrella cells), which is exposed to the lumen of the ureter and the bladder and expresses several types of uroplakins as well as cytokeratin 20 (Krt20) to seal and protect the urothelium against water and physical stress [25]. Simultaneously, the mesenchyme, which surrounds the ureteric epithelium, starts to express SM marker genes, which indicate terminal differentiation of this tissue compartment. The ambient mesenchymal cells and the mesenchymal cell layer adjacent to the urothelium differentiate into fibrocytes of the inner *lamina propria* and the outer *tunica adventitia*, respectively [26].

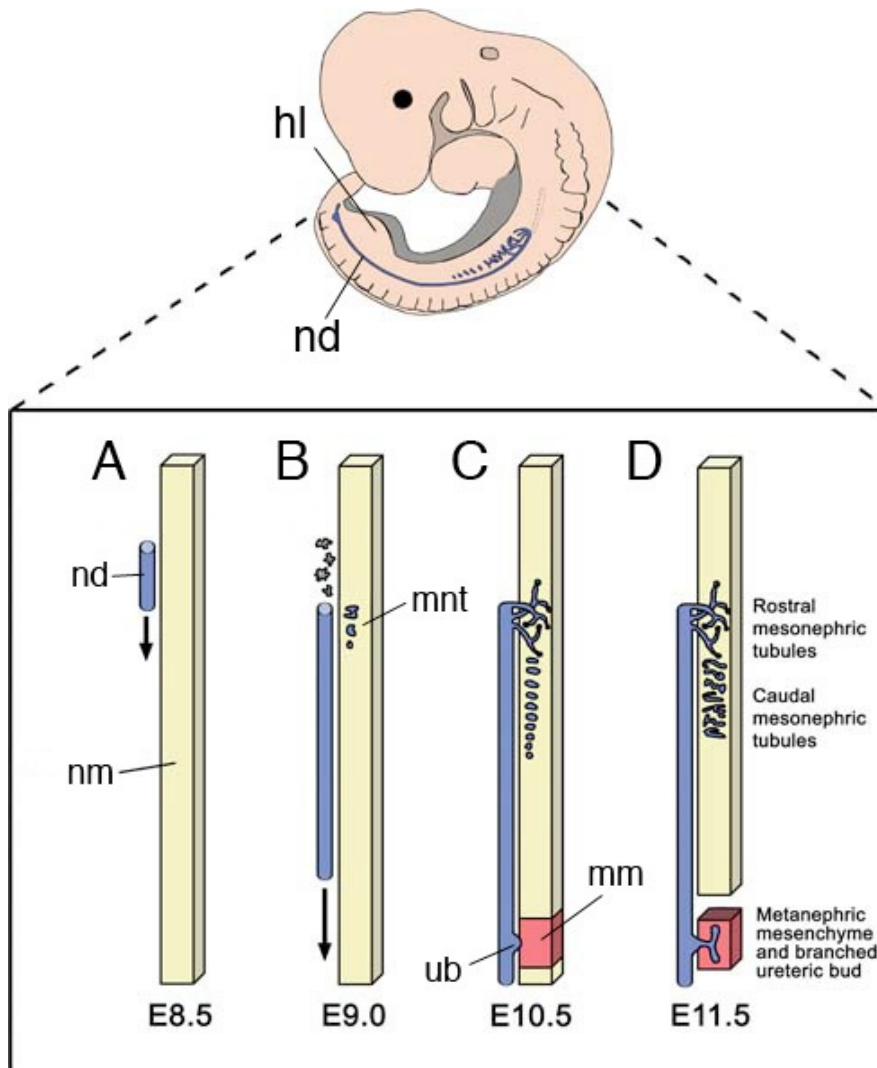


Figure 1. Cartoon of murine nephric lineage induction and ureter development.

(A-D) Schematic illustration of early UGS development. (A) ND emergence from the nephrogenic mesenchyme. (B) Induction of mesonephric tubules. (C) Emergence of the UB from the ND adjacent to the MM. (D) UB invagination into the MM and first branching. Stages are shown. hl, hind limb; nd, nephric duct; nm, nephrogenic mesenchyme; mnt, mesonephric tubules; ub, ureteric bud; mm, metanephric mesenchyme. Modified from Alan J. Davidson published in the Stem Book.

Genetic control of urinary system development

The mouse embryo generates a progressive series of two transient and one permanent kidney during development - the pronephros, the mesonephros and the metanephros. Although development of the metanephros is widely studied, only little is known about the induction of the nephric lineage within the intermediate mesoderm. The ND is induced by signals from the somite and surface ectoderm that instruct cells of the IM to generate the epithelial ND tube by mesenchymal-to-epithelial transition (EMT). Crucial regulators of nephric lineage

induction are two closely related paired box transcription factors, *Pax2* and *Pax8*. Mouse embryos deficient for *Pax2* and *Pax8* fail to develop a ND or any later nephric structures [18]. *Pax2* and *Pax8* are not only essential for nephric lineage induction, but also account for the transcriptional control of *Gata3*, a zinc finger transcription factor, which mediates guidance and morphogenesis of the ND [27]. Furthermore, *Gata3* acts as a downstream factor of *Cttnb1*, the signal transducer of canonical Wnt signalling, to prevent premature differentiation of the ND [28]. Finally, the homeobox transcription factor *Lhx1* (previously referred to as *Lim1*) governs maintenance and extension of the ND toward the cloaca [29].

The ND represents the progenitor structure of the ureter and will differentiate into the sex ducts of the male reproductive system or vanish in the female. To ensure proper urine drainage, the distal ureters need to be separated from the ND and properly inserted into the bladder wall. Prior to this separation, the ND needs to contact and fuse with the cloacal epithelium. While ND morphogenesis and extension are mainly governed by the transcription factors *Lhx1* and *Gata3*, a complex *Aldh1a2-Gata3-Ret* molecular network controls the final insertion process, once the ND has reached the cloacal level [24]. This molecular network controls the expression of specific ND tip cell protrusions which are thought to mediate fusion of both epithelia. However, to date the control of the final fusion process of these two tissue compartments has remained elusive. After ND insertion, separation of the distal ureters from the ND is triggered by stepwise apoptotic removal of the CND. Ductal cell death is initiated by RA signalling emanating from the cloacal epithelium, the two protein tyrosine phosphatase receptors, *Ptprs* and *Ptprf*, and is counteracted by *Ret* (*Ret proto oncogene*) signalling in the ND [15]. In this tissue context, *Ret* signalling acts as survival cues and *Ptprs* and *Ptprf* both act as apoptotic cues. After the CND is completely eliminated at E13.5, the distal ureter lies down on the urogenital sinus, which at this stage massively increases in size and by this moves the distal ureter to its final insertion point in the dorsal bladder neck [23].

Prior to CND elimination, inductive signals from the MM at the hind limb level instruct the ND to swell and give rise to the UB at E10.5, the initial step of metanephros development [22]. The budding process is (mainly) governed by the receptor tyrosine kinase *Ret*, which is expressed in the entire ND epithelium. Secreted *Gdnf* (*Glial derived neurotrophic factor*) signals from the MM are sufficient to induce the outgrowth of the UB at this exact position [22]. Manipulation of this process either mechanically or genetically results in delay or lack of ureteric budding, which in turn leads to kidney hypoplasia or even kidney agenesis. *Gdnf*-deficient embryos die postnatally due to kidney agenesis [30]. The same severe phenotype is observed upon deletion of the *Gdnf* receptor *Ret* and the co-receptor *Gfr α* , which are co-expressed in the ND [22]. *Gdnf* mRNA expression in the MM itself is controlled by the transcription factor group *Six2* [31], *Pax2* and *Eya1* [32]. Ectopic activation of *Gdnf* either by genetic misexpression or by deletion of the bone morphogenetic protein *Bmp4* [33], the cytosolic factor *Sprouty1* or the adhesion molecule *Lcam1* in the MM leads to multiple UBs along

the ND. Super-numerary UBs or budding at a too anterior or too posterior position will generate blind or ectopically ending ureters and VUJO, respectively (Mackie and Stephens, 1975).

The MM is molecularly characterized by the expression of several transcription factors. A first group comprises the paralogous genes *Hoxa11*, *Hoxc11* and *Hoxd11*. Upon deletion of all three genes, differentiation of the MM is arrested and no UB is induced [34]. One further transcription factor is encoded by *Wt1* (*Wilms tumor 1 homolog*). In *Wt1* null embryos, the MM is established but eliminated by apoptosis at E11.5, which succumbs prenatal kidney agenesis [35]. *Wt-1* mRNA expression itself is maintained by *CoupTF-II* [36] and *Fgf2* (*Fibroblast growth factor 2*) signals. In addition, *Fgf2* has been shown to act as an anti-apoptotic factor in the MM and promotes its compactation [37].

While the proximal UB gives rise to the renal collecting duct system, the ureteric epithelium outside the MM reacts to signals from the surrounding mesenchyme that elicit a ureteric fate. One key player in this tissue is the T-box transcription factor *Tbx18*. *Tbx18* is expressed in a stripe of mesenchymal cells between the MM and the ND, the prospective UM. Upon deletion of *Tbx18*, cells of the UM mislocalize to the surface of the kidney as fibrous tissue, which prenatally entails severe shortening of the ureter, absence of SM cells and in hydronephrosis [14]. In the UM, *Tbx18* is coexpressed with the homeobox transcription factor *Six1*. *Six1* interacts genetically and physically with *Tbx18* to govern ureteric SM development [38]. Moreover, *Sox9*, a transcriptional target of *Tbx18*, is expressed early on in the ureteric epithelium and UM. *Sox9* has been shown as an essential regulator of SM development as in *Tbx18^{cre/+};Sox9^{fx/fx}* mutants the SM differentiation program is not induced. Moreover, prenatal *Sox9*-mutants display an altered ECM composition in the UM [39].

Shh (*sonic hedgehog*), a member of the Hedgehog ligand family, is expressed in the ureteric epithelium and regulates proliferation and condensation of UM cells via paracrine signals to its receptor *Ptch1* (*Patched homolog 1*), which is expressed in the adjacent UM. Moreover, *Shh*-signalling is essential for the maintenance of *Bmp4* expression in the UM. *Bmp4* expression is completely lost in *Shh*-mutants, which, in turn, leads to reduction or absence of SM cells in these embryos culminating in hydronephrosis after birth [40].

Bmp4 is a member of the transforming growth factor (Tgf- β) family. Tailbud-derived *Bmp4* is expressed in the pericloacal mesenchyme and in the mesenchyme surrounding the distal ureter, where it directs a ureteric versus metanephric fate of the UM. Moreover, *Bmp4* regulates differentiation of the UM as conditional *Bmp4*-mutants display an disorganized network of only few Acta2-positive cells coating the urothelium [41]. In addition, *Bmp4* has been suggested to inhibit ectopic ureteric budding from the ND and the distal ureteric stalk. Decreasing *Bmp4* levels in the mouse embryo or in organ culture systems leads to ectopic ureter buds along the ND and the distal ureter [33].

The intracellular downstream mediators of *Bmp4*, phosphorylated Smads1/5/8 [42], are abundant in the UM, suggesting that *Bmp4* signalling is transduced by these factors in this

tissue context. The Smad family member 4 (*Smad4*) has been shown to regulate ureteric SM cell differentiation. Conditional *Smad4*-mutants display postnatal UPJO, a less severe phenotype than in *Bmp4*-mutants [43]. A recent study suggested that *Smad4* is crucial for initiation of the SM program in the UM. Conditional deletion of *Smad4* from the UM leads to failure of terminal SM differentiation due to increased apoptosis and decreased proliferation [44].

Moreover, mice deficient for *Id2*, a helix-loop-helix transcription factor and well known transcriptional target of *Bmp4* [45], display postnatal hydronephrosis due to hyperplasia of SM cells at the uretero-pelvic junction [46].

Taken together, various studies in the mouse have shed light on the diverse processes of nephric lineage induction, ND morphogenesis, ureter budding, ureteric SM and metanephric kidney development, which together contribute to the formation of a functional urinary system.

The Eph-Ephrin signalling pathway

The history of the Eph-Ephrin signalling pathway can be traced back to 1987, when a search for new receptor tyrosine kinases involved in cancer pathogenesis and progression, identified a cDNA encoding EphA1, a member of a novel subclass of this protein family, that was named orphan due to the lack of its binding ligand back then [47]. Subsequent work identified a large number of highly related proteins in vertebrates making Eph (erythropoietin-producing hepatocarcinoma cell) receptors the largest sub-family of receptor tyrosine kinases (RTKs). With the help of receptor affinity chromatography, the protein B61 (today referred to as EphrinA1) was subsequently discovered as the first binding partner of an Eph receptor (ECK, today referred to as EphA2). Eph receptors as well as their ligands, the Ephrins are not only conserved in vertebrates, they also appear in invertebrates, such as *Drosophila* and *C. elegans* and surprisingly also in sponges pointing to the evolutionary conserved nature of this pathway [48]. In the mouse, 14 Eph receptors have been characterized and are divided into an A and B subfamily based on sequence and function. The 9 EphA receptors (EphA1-EphA8, EphA10) promiscuously bind to 5 EphrinA ligands, and the 5 EphB receptors (EphB1-4, EphB6) bind to three EphrinB ligands with some exceptions (EphA4 and EphB2 can bind to Ephrins of the other class) [49]. The prototypical Eph receptor consists of an extracellular globular Ephrin binding domain at the N-terminus followed by a cysteine-rich region and two fibronectin III repeats [50]. The Eph receptor is anchored in the cell with a transmembrane domain, which is followed by a short juxtamembrane region, which can be phosphorylated to activate the signalling cascade. Essential for signal transduction is the cytosolic tyrosine kinase domain, which represents the largest domain of the Eph receptor protein. The kinase domain is followed by a sterile alpha motif (SAM) protein-protein interaction domain and a PDZ domain which epitomizes binding sites for effector proteins [51].

EphrinA ligands are tethered to the cell membrane via a GPI- (glycosylphosphatidylinositol) anchor, whereas EphrinB ligands are transmembrane proteins with a small cytoplasmic domain. EphrinA ligands can be released from the cell surface to reach and activate Eph receptors in distance [52]. Eph-Ephrin interaction exclusively occurs upon direct contact of juxtaposed cells. Activation of Eph receptors is mediated by binding of membrane-clustered ligands. The first downstream event after the binding interaction is receptor membrane clustering in dimers or oligomers followed by receptor autophosphorylation. Phosphorylation of conserved tyrosine residues in the juxtamembrane domain removes an inhibitory interaction with the kinase domain to allow efficient kinase activity [53]. The phospho-tyrosine residues of the kinase domain display docking sites for SH2 (Src homology 2) or SH3 (Src homology 3)-containing adaptor proteins including the non-receptor tyrosine kinase families like Src (Src kinase) and Abl (Abelson oncogene). These kinases then activate or inhibit downstream proteins like the small GTPases RhoA, Rac or Cdc42 to alter the actin cytoskeleton ultimately resulting either in a cell rounding or cell spreading response [54]. The Eph-Ephrin signalling pathway constitutes a cellular communication module which harbors the ability to not only transduce signals in the receptor bearing cell as “forward signalling”, but also into the Ephrin ligand expressing cell referred to as “reverse signalling”. Hereby, the cytosolic domain of the Ephrin ligand is phosphorylated and thereby acts like a “mini-receptor” to recruit signalling effector proteins such as GRB4 or STAT3 [55]. As a consequence focal adhesion kinase gets activated, cytoskeletal changes occur and/or transcriptional programs are initiated [56-58] phosphorylation-independent downstream signalling via the PDZ domain is also known [59]. This bidirectional signal transduction is unique and, although assumed for other pathways like e.g. Notch signaling [60], has not been demonstrated for any other signalling pathway to date. Eph-Ephrin interaction cannot only occur in *trans*. It has been shown that receptor-ligand interaction in *cis* can alter or even inhibit signal transduction into the juxtaposed cell [52]. Termination of receptor-ligand adhesive interaction can be achieved by internalization of the receptor-ligand complex [61].

Eph-Ephrin signaling is required in the embryo as well as in the adult to acquire and maintain an organized tissue architecture. Ephs and Ephrins enable cells to communicate contact-dependently to control cell morphology, adhesion, repulsion and migration; emerging evidence suggest a role of this signalling module in mediating survival and apoptosis as well [62]. During embryonic development Eph-Ephrin signalling controls cell sorting, axon guidance, topographical mapping, synaptic plasticity, neural tube differentiation, blood vessel formation as well as epithelial integrity [49, 54]. However, only little is known about this unique signaling module and its function in murine UGS development to date. The first article of this thesis will elucidate the function and significance of this pathway in early development of the urogenital system in the mouse embryo.

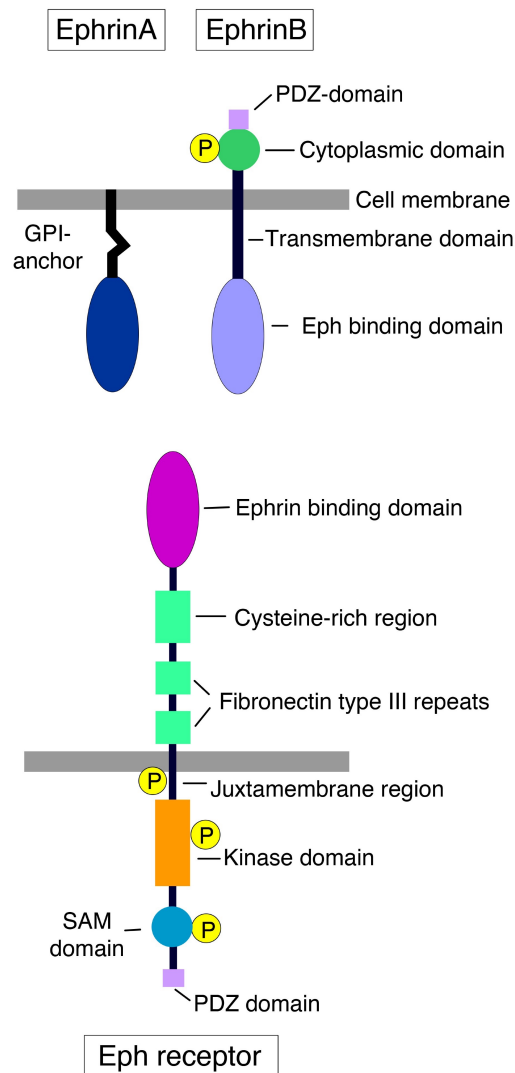


Figure 2: Schematic portrayal of the structural and binding domains of Eph receptors and Ephrins.

EphrinA ligands are tethered to the cell membrane via a glycosylphosphatidylinositol (GPI-) anchor. The globular extracellular part of the EphrinA ligand serves as the Eph receptor binding domain. EphrinB ligands are transmembrane proteins with a small cytoplasmic anchor and a PDZ domain which displays a docking domain for effector proteins. The Eph receptor is comprised of an Ephrin binding domain, a cysteine-rich region and two fibronectin type III repeats and a transmembrane domain. The biggest part of the Eph receptor is represented by the catalytically active kinase domain, which is followed by a sterile alpha motif (SAM) and PDZ-domain.

5. Aim of this thesis

Loss of function studies of the T-box transcription factor *Tbx18* in the mouse have shown its pivotal role in ureter development [14, 63]. In *Tbx18* null embryos (*Tbx18^{GFP/GFP}*) the ureter is severely shortened, dilated and the smooth muscle (SM) differentiation program is not initiated. Moreover, the kidneys of *Tbx18^{GFP/GFP}* embryos display severe hydronephrosis, the gonads remain attached to the kidneys (cryptorchidism) and the ureteric mesenchyme (UM) mislocalizes to the kidney surface to become fibrous tissue, suggesting a function of *Tbx18* in boundary formation, selective adhesion and/or in the regulation of the ureteric SM program. To get a deeper insight into the molecular function of this transcription factor, the transcriptome of E13.5 ureters of *Tbx18^{GFP/+}* and *Tbx18^{GFP/GFP}* embryos was compared utilizing RNA-microarray technology prior to this doctorate. Among the downregulated genes were *EphA4* and *EphA7*, two members of the Eph receptor family. In preliminary experiments, the mRNA expression of both genes in the urinary system of wildtype and *Tbx18^{GFP/GFP}* embryos was analyzed and revealed coexpression of *EphA4* and *EphA7* in the UM as well as a severe downregulation of both genes in the mesenchyme of *Tbx18*-deficient ureters. These findings suggested a potential function of both Eph receptors in establishing a tissue boundary in the UM downstream of *Tbx18*.

This doctoral thesis aimed to unravel the functional relevance of *EphA4* and *EphA7* expression in the development of the mouse ureter. For this purpose *EphA4* and *EphA7* single as well as *EphA4/EphA7* double mutant (DKO) embryos were to be generated and analyzed on morphological, histological and molecular level.

In the initial phase of this doctorate, preliminary experiments in the lab revealed a strong downregulation of *Tbx18* in the UM of conditional *Ctnnb1*-mutants (lacking the intracellular signal transducer of the canonical Wnt pathway), suggesting *Tbx18* as putative target gene of Wnt signalling in this tissue context. With the help of a *Tbx18* misexpression mouse line, it was to be tested whether a genetic reconstitution of *Tbx18* in the *Ctnnb1*-mutant background is able to rescue the hydroureter phenotype of this mouse mutant.

A few signalling pathways and transcription factors have been described to control the development of the UM. How these pathways are transcriptionally integrated, has remained largely unclear. In the search for transcription factors expressed early in the UM, the mRNA of the zinc finger transcription factor *Gata2* was detected in the ureteric epithelium and UM. An initial phenotype analysis of a conditional *Gata2* mutant was performed in the lab and revealed hydroureter and hydronephrosis in prenatal mutant embryos.

In this thesis, a timeline of *Gata2* expression during ureter development was to be depicted using RNA *in situ* hybridization technology. Moreover, the functional significance of *Gata2* expression was to be analysed on morphological, histological and molecular level.

This dissertation aimed to decipher new transcription factors and signalling modules controlling normal ureter development to allow a better understanding of the aetiology of CAKUT, and, moreover, to unravel new upstream and downstream mediators of *Tbx18* in the UM.

Nephric duct insertion requires EphA4/EphA7 signaling from the pericloacal mesenchyme

Anna-Carina Weiss¹, Rannar Airik¹, Tobias Bohnenpoll¹, Franziska Greulich¹, Anna Foik¹, Mark-Oliver Trowe¹, Carsten Rudat, Frank Costantini², Ralf H. Adams³ and Andreas Kispert^{1,§}

¹Institut für Molekularbiologie, Medizinische Hochschule Hannover, 30625 Hannover, Germany

²Department of Genetics and Development, Columbia University Medical Center, New York, New York 10032, USA

³Max-Planck-Institute for Molecular Biomedicine, Department of Tissue Morphogenesis, and University of Münster, Faculty of Medicine, 48149 Münster, Germany

§ Author for correspondence:

Email: kispert.andreas@mh-hannover.de

Tel: +49511 5324017

Fax: +49511532483

Published in Development (Development (2014) 141, 3420-3430)

Reprinted with permission

RESEARCH ARTICLE

Nephric duct insertion requires EphA4/EphA7 signaling from the pericloacal mesenchyme

Anna-Carina Weiss¹, Rannar Airik¹, Tobias Bohnenpoll¹, Franziska Greulich¹, Anna Foik¹, Mark-Oliver Trowe¹, Carsten Rudat¹, Frank Costantini², Ralf H. Adams³ and Andreas Kispert^{1,*}

ABSTRACT

The vesico-ureteric junction (VUJ) forms through a complex developmental program that connects the primordium of the upper urinary tract [the nephric duct (ND)] with that of the lower urinary tract (the cloaca). The signals that orchestrate the various tissue interactions in this program are poorly understood. Here, we show that two members of the EphA subfamily of receptor tyrosine kinases, EphA4 and EphA7, are specifically expressed in the mesenchyme surrounding the caudal ND and the cloaca, and that *Epha4*^{-/-}; *Epha7*^{+/-} and *Epha4*^{-/-}; *Epha7*^{-/-} (DKO) mice display distal ureter malformations including ureterocele, blind and ectopically ending ureters with associated hydroureter, megaureter and hydronephrosis. We trace these defects to a late or absent fusion of the ND with the cloaca. In DKO embryos, the ND extends normally and approaches the cloaca but the tip subsequently loses its integrity. Expression of *Gata3* and *Lhx1* and their downstream target *Ret* is severely reduced in the caudal ND. Conditional deletion of ephrin B2 from the ND largely phenocopies these changes, suggesting that EphA4/EphA7 from the pericloacal mesenchyme signal via ephrin B2 to mediate ND insertion. Disturbed activity of this signaling module may entail defects of the VUJ, which are frequent in the spectrum of congenital anomalies of the kidney and the urinary tract (CAKUT) in human newborns.

KEY WORDS: CAKUT, Eph, Ephrin, Nephric duct, Vesicoureteric junction obstruction, Mouse

INTRODUCTION

Congenital anomalies of the kidney and urinary tract (CAKUT) are amongst the most common human birth defects. They comprise a wide range of structural and functional malformations of the individual components of the urinary system as well as their interfaces. A prominent subclass of CAKUT is characterized by improper ureter-bladder connectivity including distal ureters that end blindly, ectopically or form a ureterocele, which is a fluid-filled sac in or at the bladder. These vesico-ureteric junction (VUJ) anomalies obstruct urinary drainage into the bladder and result in dilation of the ureter (hydro- or megaureter) and renal pelvis (hydronephrosis), a disease entity that may culminate in destruction of the renal parenchyme (Nakai et al., 2003; Kerecuk et al., 2008; NAPRTCS, 2007).

Formation of a patent VUJ is the result of a complex morphogenetic program that connects the primordium of the upper urinary tract [the nephric duct (ND)] with that of the lower urinary tract (the cloaca) during embryonic development. The ND is an epithelial tube that in the mouse forms around embryonic day (E) 8.0 at the level of the forelimb buds and subsequently extends posteriorly within the intermediate mesoderm. At ~E9.75, the ND turns towards the midline and inserts into the cloaca that arises as an endodermal infolding. At E10.5, an epithelial diverticulum called the ureteric bud (UB) evaginates from the ND at the level of the hindlimb buds and invades the surrounding mesenchyme termed the metanephric blastema. The tip of the UB subsequently engages in repetitive rounds of elongation and branching and ultimately generates the collecting duct system of the kidney. The stalk region merely elongates to form the epithelial component of the ureter. From E12.5 onwards, the distal end of the stalk separates from the ND and integrates into the developing bladder wall. This process depends on the apoptotic removal of the common nephric duct (CND), which is the most caudal segment of the ND, and the subsequent growth of the bladder to move the ureter orifice to its final position. The epithelial lining of the collecting duct system, of the ureter and of the bladder subsequently differentiates into the urothelium, and the surrounding mesenchyme of these organs differentiates into layers of smooth muscle (SM) cells. Thus, the functional architecture of the urinary drainage system is established at ~E16.5 (Airik and Kispert, 2007; Uetani and Bouchard, 2009; Woolf and Davies, 2013).

Although the molecular and cellular causes of human VUJ anomalies have remained poorly understood (Weber, 2012), mutational analyses in the mouse have identified a number of crucial factors and steps for the proper integration of the distal ureter into the bladder (Mendelsohn, 2009; Uetani and Bouchard, 2009). Analysis of mice deficient for the transcription factor gene *Gata3*, the retinoic acid (RA) synthesizing gene *Aldh1a2* and the gene encoding the receptor tyrosine kinase *Ret* revealed that a delay or a failure of ND insertion into the cloaca can cause ectopic ureters that join the bladder abnormally or remain fused to the ND. RA signaling and *Gata3* independently regulate *Ret* expression in the ND, which in turn seems to be required for the formation of cellular protrusions that guide the posterior extension of the tube (Chia et al., 2011). *Ret* signaling is also crucial in UB formation and subsequent branching morphogenesis (Costantini and Shakya, 2006). Mispositioning of the UB by altered expression of the *Ret* ligand *Gdnf* or perturbed downstream signaling dramatically affects how the ureter will join the bladder. UBs emerging posterior to the normal sprouting site will insert in the primitive bladder prematurely, which can lead to ectopically positioned distal ureters and, hence, vesico-ureteric reflux. Ureters emerging at an abnormally anterior site remain attached either to the ND, the urethra or to the bladder neck, leading to VUJ obstruction (Mackie and Stephens, 1975; Uetani and Bouchard, 2009). Hydro- or

¹Institut für Molekularbiologie, Medizinische Hochschule Hannover, D-30625 Hannover, Germany. ²Department of Genetics and Development, Columbia University Medical Center, New York, NY 10032, USA. ³Max-Planck-Institute for Molecular Biomedicine, Department of Tissue Morphogenesis, and University of Münster, Faculty of Medicine, D-48149 Münster, Germany.

*Author for correspondence (kispert.andreas@mh-hannover.de)

Received 5 June 2014; Accepted 14 July 2014

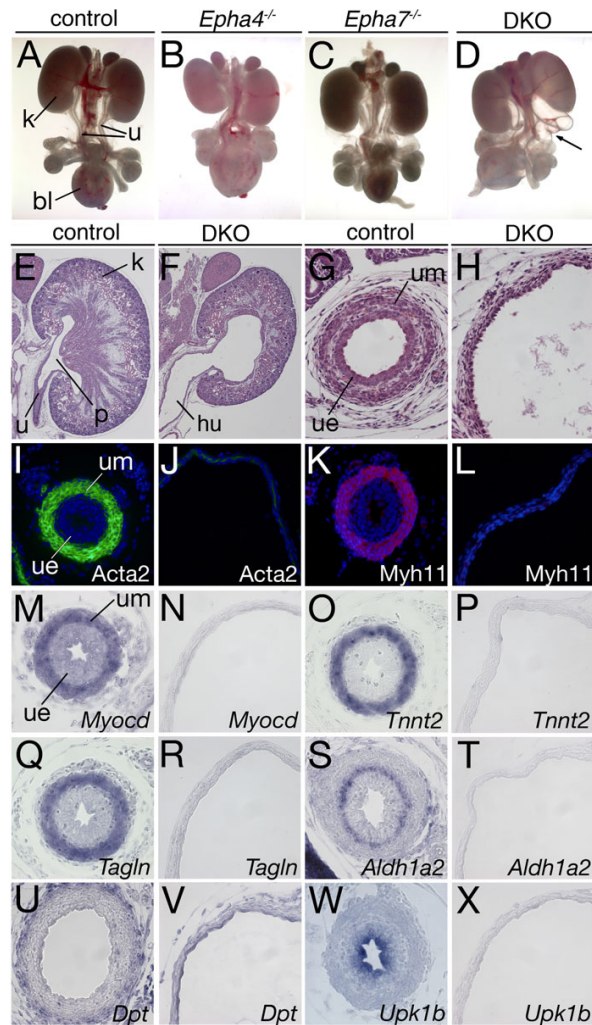


Fig. 2. Kidney and ureter anomalies in *Epha4*^{-/-};*Epha7*^{-/-} (DKO) embryos at E18.5. (A-D) Morphology of whole urogenital systems of male embryos. (E-H) Hematoxylin and Eosin stainings of sagittal sections of kidneys (E,F) and of transverse sections of the proximal ureter (G,H). (I-X) Cytodifferentiation of the ureteric mesenchyme (I-V) and epithelium (W,X) as shown by immunofluorescence (I-L) and *in situ* hybridization analysis (M-X) on transverse sections of the proximal ureter at E18.5. bl, bladder; hu, hydronephrosis; k, kidney; p, pelvis; u, ureter; ue, ureteric epithelium; um, ureteric mesenchyme.

hydronephrosis and/or megaureter with hydronephrosis (Fig. 2D; supplementary material Fig. S2A,B). Quantification of the gross morphological defects of the urogenital system of embryos of both genotypes uncovered sex independence but an incomplete penetrance (47% in DKO and 19% in *Epha4*^{-/-};*Epha7*^{+/-} mice) and variability (unilateral and/or bilateral hydronephrosis and/or megaureter) (supplementary material Table S1).

Histological analyses of DKO and *Epha4*^{-/-};*Epha7*^{+/-} urogenital systems with megaureter revealed dilatation of the entire renal collecting system including the collecting ducts, calyx, pelvis and the absence of the papilla. The ureter was strongly dilated and featured a flat and single-layered urothelium with a thin layer of surrounding mesenchyme (Fig. 2E-H; supplementary material Fig. S2C-H).

To characterize the cellular changes associated with megaureter formation in DKO mice, we analyzed the expression of cell differentiation markers within the epithelial and mesenchymal compartments at the proximal ureter level at E18.5. In the mesenchymal compartment, expression of SM structural proteins (*Acta2* and *Myh11*), of genes encoding SM structural components (*Tagln* and *Tnnt2*), and of the key regulator of SM cell differentiation, *Myocd*, was absent. *Aldh1a2*, a marker for the lamina propria, was not expressed. *Dpt*, a marker for the outer adventitial layer of fibroblasts, was severely reduced (Fig. 2M-V). Epithelial differentiation was also affected in the mutant, as shown by the strong reduction of the urothelial marker *Upk1b* (Fig. 2W,X).

Expression of all of these markers was similarly absent at proximal levels of *Epha4*^{-/-};*Epha7*^{+/-} megaureters (supplementary material Fig. S2I-T), indicating that megaureter formation is associated with a failure of cytodifferentiation along the entire tube in both genotypes. By contrast, the hydronephrosis phenotype in DKO embryos was associated with a slight reduction of SM markers and unchanged expression of *Upk1b* at proximal levels (supplementary material Fig. S3). We conclude that combined loss of *Epha4* and *Epha7* results in severe defects of ureteric cytodifferentiation that correlate with the degree of dilatation.

Onset and progression of ureter defects in DKO embryos

To further explore the relationship between cytodifferentiation defects of DKO ureters and urinary pressure, we analyzed urogenital systems at E14.5, E15.5 and E16.5, i.e. before, at and after the onset of urine production in the kidneys. On the morphological and histological level, the urogenital systems of DKO embryos showed no defects at E14.5 and E15.5, whereas ureter and pelvicalyceal dilatation was detectable at E16.5 (supplementary material Fig. S4A-C). Expression of *Myocd* was initiated at E14.5 and maintained at E15.5 and expression of *Tagln*, *Tnnt2*, *Myocd* and *Upk3b* was observed at E15.5 in DKO ureters, indistinguishable from the control. However, SM and urothelial markers were collectively downregulated in DKO ureters at E16.5 (supplementary material Fig. S4D,E). Furthermore, the expression of genes required in the undifferentiated ureteric mesenchyme to initiate the SM differentiation program was unaffected in DKO ureters at E14.5 (supplementary material Fig. S5). This suggests that *Epha4* and *Epha7* are not required (downstream of *Tbx18*) in the undifferentiated ureteric mesenchyme to initiate the SM differentiation program. Loss of cytodifferentiation in DKO embryos is most likely a consequence and not a cause of increased hydrostatic pressure and might relate to physical obstruction along the ureter.

Aberrant ureter-bladder connectivity in DKO embryos

To test for the continuity of the ureter and the patency of its junctions, we injected ink into the renal pelvis in isolated urogenital systems of E18.5 embryos. In control embryos, the ink passed readily through the ureter and filled the entire bladder (*n*=4; Fig. 3A). In the megaureter situation of DKO embryos, the ink was either retained within the ureter that ended blindly or on the vas deferens (*n*=3; Fig. 3B), or the ink accumulated within a sac in the bladder to be released through the urethra (*n*=2; Fig. 3C). In the DKO situation with hydronephrosis, the ink was retained in the ureter that terminated on the urethra (*n*=1; data not shown). Serial histological sections and 3D reconstructions revealed that in control embryos the distal ureters entered the bladder at an oblique angle at the dorsal bladder neck and the lumen was continuous (*n*=3; Fig. 3D,G). In DKO embryos with megaureter, the distal ureters ended as an intravesical (*n*=3) or an extravascular (*n*=2) pouch-like

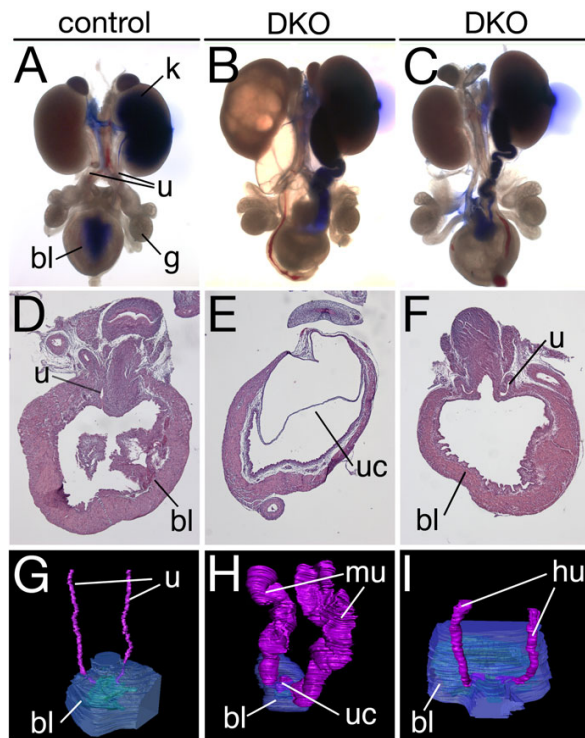


Fig. 3. Vesico-ureteric junction (VUJ) anomalies in DKO embryos at E18.5. (A–C) Distribution of ink injected in the pelvic region of whole urogenital systems. (D–F) Hematoxylin and Eosin stainings of frontal sections of the bladder. (G–I) Three-dimensional reconstructions of serial histological sections of the ureter (pink), the bladder muscle (blue) and the bladder lumen (green). bl, bladder; hu, hydroureter; k, kidney; mu, megaureter; g, gonad (testis); u, ureter; uc, ureterocele.

structure, termed the ureterocele (Fig. 3E,H; data not shown). In the case of hydroureter, the distal ureter terminated ectopically in the urethra ($n=2$; Fig. 3F,I). We conclude that anatomical obstruction caused by aberrant connectivity of the bladder and the distal ureter underlies hydro/megaureter in DKO embryos.

Defects in fusion of the ND with the cloaca

In order to elucidate the morphogenetic origin of this aberrant ureter-bladder connectivity, we analyzed urogenital systems by 3D reconstruction of serial histological sections at earlier embryonic stages (Fig. 4). At E10.5 in the wild type, the UB had emerged from the ND and the CND was fused with the cloaca. In DKO embryos, the position of the UB was unaffected; the CND approached the cloaca in the midline but contact and fusion of the two epithelia either occurred ectopically in a more anterior position ($n=3$) or was not detected at all ($n=2$) (Fig. 4A,B). In E12.5 wild-type embryos, the CND was still present and fused with the urogenital sinus but the lumen was not yet continuous. In all DKO embryos analyzed the CND was present but appeared longer than in controls (supplementary material Fig. S6). In three of five, cases the CND was fused with the primitive bladder, whereas a gap between the CND and the urogenital sinus was observed in two specimens (Fig. 4C,D). In E13.5 and E14.5 wild-type embryos, the CND was eliminated and the distal ureter and the ND were well separated; they were inserted into the bladder but the lumen was not yet continuous. In the DKO situation, the CND persisted and gained an ampulla-like

swelling within the bladder wall at these stages (Fig. 4E–I), as confirmed by GFP epifluorescence using the *Hoxb7-GFP* reporter line, which marks the ND and all of its descendants (Fig. 4J) (Srinivas et al., 1999). In four of five cases the CND was fused with the urogenital sinus, whereas in one specimen a gap between the two epithelia was still detectable. We suggest that ureterocele and megaureter in DKO embryos is caused by the persistence of the CND, which in turn results from a failure or delayed fusion of the ND with the cloaca.

Cellular changes in the distal ND of DKO embryos

To analyze the cellular changes in the mutant ND in more detail, we performed live cell imaging of explants of E9.5 trunks of embryos carrying the *Hoxb7-GFP* transgene. At E9.5, the tip of the ND was characterized by the presence of cellular protrusions both in wild-type and in DKO embryos, as previously reported (Chia et al., 2011). During the 18 h culture period these protrusions were highly dynamic, switching between extension and retraction cycles, but remained associated with a compact tip that moved progressively forward in the wild type. By contrast, in DKO embryos, individual cells dramatically stretched during the formation of these protrusions and started to lose contact with the tip of the ND after 5 h of culture to finally scale off [$n=3$; Fig. 5A–D; supplementary material Movies 1A,B (control) and 2A,B (DKO)].

Confocal immunofluorescence analysis on sections of E10.5 embryos confirmed these observations. In wild-type embryos, GFP expression from the *Hoxb7-GFP* transgene was confined to cells of the distal ND, whereas in DKO embryos GFP-positive cell material was additionally found in the periphery of the distal ND (Fig. 5E,F). Furthermore, collagen type IV (ColIV) staining revealed an uninterrupted basal lamina underlying the ND in the wild type, whereas several gaps were detected in DKO embryos (Fig. 5G,H). Finally, *Cdh1*, a marker for basolateral membranes of epithelial cells, was severely downregulated in DKO embryos (Fig. 5I,J), supporting the notion that tissue integrity is perturbed in the distal ND of DKO embryos.

Analysis of the expression of endothelial [*eng* (Eng), vimentin (*Vim*), endomucin (Emcn)] and neuronal [*Hand2*, neuropilin 1 (*Nrp1*), neurofilament light chain (*Nefl*)] markers (supplementary material Fig. S7) did not detect differences in the mesenchymal tissue surrounding the E10.5 ND between wild-type and DKO embryos, arguing against the possibility that changes in endothelial and neuronal networks have misguided the ND in DKO embryos.

Previous studies have shown that distal ureter maturation requires the apoptotic removal of the CND (Batourina et al., 2002, 2005; Uetani et al., 2009). Analysis of programmed cell death by the TUNEL assay revealed that in wild-type embryos apoptosis was initiated at E10.5 and maintained at E12.5 in the CND. Apoptosis was similarly observed in the CND of DKO embryos, in which the CND was fused with the cloaca/bladder epithelium. By contrast, apoptosis was absent in specimens in which the CND was separated from the cloaca (supplementary material Fig. S8). Together, these findings suggest that EphA4/EphA7 signaling is required to maintain adhesion between ND tip cells to allow fusion with the cloaca, which in turn is prerequisite for the stepwise apoptotic removal of the CND until E13.5.

Perturbation of the *Ret/Gata3* molecular network in the caudal ND in DKO embryos

To determine molecular changes that are associated with the fusion defect of the caudal ND in DKO embryos, we analyzed

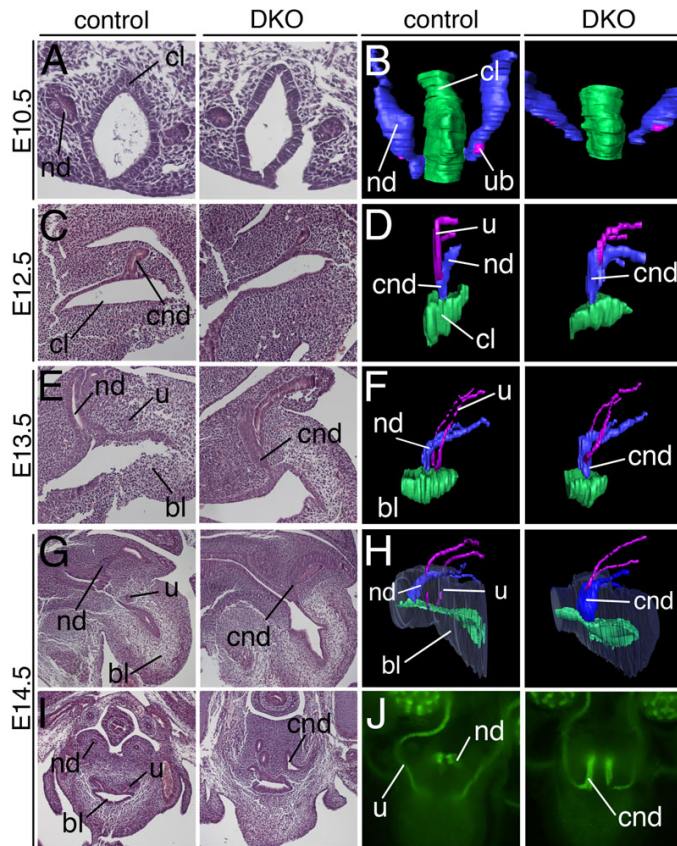


Fig. 4. Onset of VUJ anomalies in DKO embryos. (A,C,E,G,I) Histological analysis by Hematoxylin and Eosin staining of transverse (A,I) and sagittal (C,E,G) sections at the junction between the developing bladder and the distal ND and ureter. (B,D,F,H) Three-dimensional reconstructions of serial histological sections of the distal ND (blue), ureter (pink) and bladder region (bladder lumen in green, bladder wall in transparent gray). (J) GFP epifluorescence of ND derivatives marked by the *Hoxb7-GFP* reporter. (A,B) Dorsal is up; (C-H) anterior is to the left, dorsal is up. bl, bladder; cl, cloaca; cnd, common nephric duct; nd, nephric duct; u, ureter; ub, ureteric bud.

the expression of a panel of genes previously implicated in ND extension and fusion in E9.5 whole embryos and on sections through the posterior trunk of E10.5 embryos. At E9.5 (when the ND has reached the cloacal level) expression of *Pax2*, *Gata3* (not shown), *Lhx1* and *Ret* was found along the entire ND of DKO embryos, indistinguishable from controls (Fig. 6A–D). At E10.5 the expression of *Emx2* was unaffected, whereas *Pax2* was slightly diminished, and *Lhx1*, *Gata3* and *Ret* were severely reduced in the caudal ND of DKO embryos (Fig. 6E–P). Expression of *Gdnf*, which encodes the ligand of the Ret receptor (Treanor et al., 1996), was restricted to the metanephric blastema both in wild-type and DKO embryos (Fig. 6K,L). As expression of *Ret* also depends on RA signaling (Chia et al., 2011), we analyzed expression of the genes encoding the biosynthetic enzyme *Aldh1a2* and the receptor and target of RA signaling *Rarb* (Matt et al., 2003). Expression of *Aldh1a2* in the pericloacal mesenchyme of DKO embryos was unaltered, whereas expression of *Rarb*, which in control embryos is restricted to the fusion site in the cloacal epithelium, appeared scattered and reduced (Fig. 6Q–T). Expression of *Ptch1*, which is a target of Hedgehog signaling (Ingham and McMahon, 2001), in the pericloacal mesenchyme, and of *Shh* in the cloacal epithelium was observed in both wild-type and DKO embryos (Fig. 6U–X). Expression of ND marker genes was not affected on more anterior metanephric and mesonephric levels in DKO embryos (supplementary material Fig. S9), indicating that pericloacal EphA4/EphA7 signaling affects the *Lhx1/Gata3/Ret* network specifically in the adjacent caudalmost aspect of the ND.

The caudal ND is the target of pericloacal mesenchymal EphA4/EphA7 signaling

Failure of ND insertion might indicate a non-cell-autonomous requirement of pericloacal mesenchymal EphA4/EphA7 signaling in the epithelium of the cloaca and/or the caudal ND to regulate adhesion and/or fusion within and between the two compartments. In order to determine the target tissue of EphA4/EphA7 signaling in the lower urinary tract, we incubated E9.5 wild-type embryos with fusion proteins of the soluble part of EphA4 or EphA7 with the constant domain of antibodies and subsequently recorded the distribution of the bound ligand by anti-IgG-AP fusion protein-mediated enzymatic detection (Gale et al., 1996). EphA4 and EphA7 binding patterns were virtually identical and comprised the branchial arches, the ventral forebrain, the forelimb bud and – most relevant to this project – the caudal ND and the cloaca (Fig. 7A,B). To identify ligand(s) of EphA4 and/or EphA7, we screened for expression of all known ephrin A and ephrin B genes by section RNA *in situ* hybridization analysis at E10.5 (supplementary material Fig. S10). Expression of ephrin B2 (*Efnb2*), which encodes a known ligand of EphA4 signaling (Watanabe et al., 2009), was found in the caudal ND and the cloaca as well as in the pericloacal mesenchyme from E10.5 until E14.5 (Fig. 7C–F). Immunofluorescence analysis confirmed these expression domains and identified membranous localization of ephrin B2 protein in the epithelia of the ND and the cloaca and in endothelial cells (Fig. 7G).

In order to determine whether the signal that results from binding of EphA4/EphA7 to ephrin B2 was transduced into the ligand-bearing cell, we performed anti-phospho-ephrin B (Y316) antibody

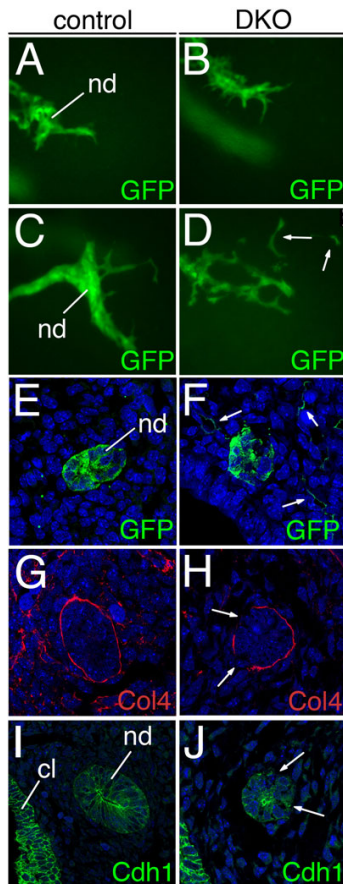


Fig. 5. Cellular changes in the caudal ND of DKO embryos at E9.5 and E10.5. (A-D) GFP epifluorescence of the caudal ND visualized by the *Hoxb7-GFP* reporter in explants of E9.5 trunk at the onset of the culture (A,B) and after 18 h (C,D). (E-J) Confocal analysis on transverse sections through the distal ND region by immunofluorescence for GFP (E,F), the basal lamina marker *Col4a4* (G,H), and the epithelial marker *Cdh1* (I,J). Arrows point to scaled off ND cells (D,F), to disruption of the basal lamina (H), and to disrupted epithelial integrity (J). nd, nephric duct; cl, cloaca.

staining. This specific tyrosine phosphorylation site has been described to activate downstream Src family or associated kinases as a result of active ephrin B reverse signaling (Palmer et al., 2002; Wu et al., 2011; Georgakopoulos et al., 2011). In the wild type, we found phospho-specific staining in membranes of epithelial cells of the ND, the cloaca and endothelial cells at E10.5, whereas strongly reduced phospho-specific staining was detectable in the ND and the cloaca in the DKO situation (Fig. 7H,I). Taken together, these findings argue for active EphA4/EphA7-ephrin B2 reverse signaling in the ND and cloacal epithelium.

Loss of *Efnb2* in the ND leads to urinary tract anomalies

To determine whether ephrin B2 is functionally involved in ND development, we used a conditional gene targeting approach with a floxed allele of *Efnb2* (*Efnb2^{fl}*) and a *Pax2(8.5)-cre* driver line that mediates specific recombination in the ND and its derivatives (supplementary material Fig. S11) (Kuschert et al., 2001; Trowe et al., 2011). At E18.5, *Pax2(8.5)-cre;Efnb2^{fl/fl}* embryos ($n=17$) displayed urinary anomalies in 60% of specimens analyzed. These

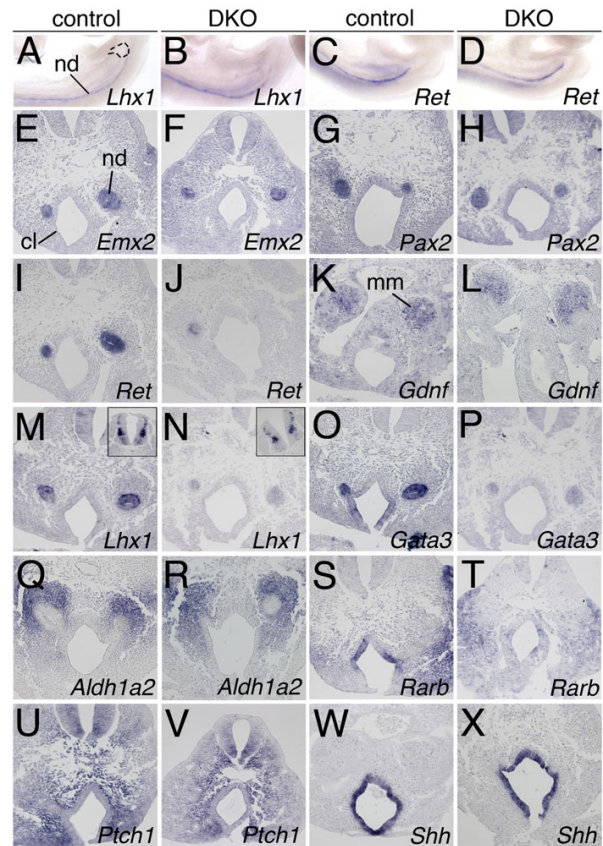


Fig. 6. Molecular changes in the ND of DKO embryos at E9.5 and E10.5. RNA *in situ* hybridization analysis on whole E9.5 embryos (A-D) and on transverse sections of the posterior trunk of E10.5 embryos (E-X). Dashed line in A outlines the cloaca. Insets (M,N) show the neural tube. nd, nephric duct; cl, cloaca; mm, metanephric mesenchyme.

anomalies were sex independent and included bilateral hydronephrosis ($n=7$) and unilateral megaureter ($n=3$) (Fig. 8A-D; supplementary material Table S2). Histological analysis of mutant urogenital systems revealed a strong dilatation of the ureter and renal pelvis with occasional absence of the renal papilla (Fig. 8E,F). In order to unravel a potential physical obstruction in *Efnb2*-deficient embryos, we performed histological analysis of sagittal bladder sections at E18.5 to visualize the VUJ. In mutant specimens with CAKUT-like phenotypes ($n=7$), we found distal ureters that were embedded in the bladder muscle but were without connection to the bladder lumen ($n=3$) or distal ureters that terminated in the urethra ($n=1$) (Fig. 8G,H; data not shown). This suggests physical obstruction as the cause of hydronephrosis.

To determine the status of CND removal, we investigated sagittal sections of the E14.5 urogenital sinus. In wild-type embryos ($n=4$) the CND was eliminated and ND and ureter were separated. In mutant embryos ($n=4$), the CND was either still present and fused with the urogenital sinus ($n=1$) or the CND was eliminated but the ND and ureter were not well separated ($n=1$) (Fig. 8I,J; data not shown). Moreover, we found ND fusion defects (mainly unilaterally) at E10.5 in three out of five *Pax2(8.5)-cre;Efnb2^{fl/fl}* mutants analyzed, similar to DKO embryos (Fig. 8K,L). Molecular markers associated with ureter SM development were unchanged in

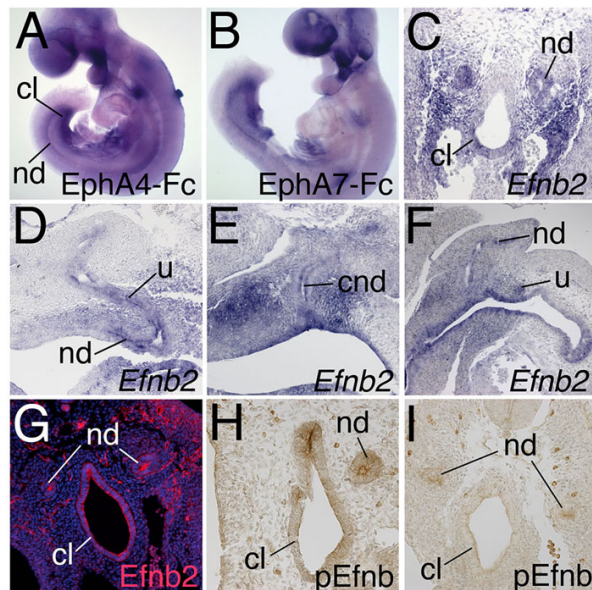


Fig. 7. The ND is a target of pericloacal EphA4/EphA7 reverse signaling. (A,B) Whole-mount EphA4/EphA7-Fc staining of E9.5 wild-type embryos. (C-F) *Efnb2* expression analysis by RNA *in situ* hybridization on a transverse section of a E10.5 posterior trunk (C), and on sagittal sections through the posterior trunk region at E11.5 (D), E12.5 (E) and E14.5 (F). (G) *Efnb2* immunofluorescence on sections of wild-type embryos at E10.5. (H,I) Immunohistochemistry of phosphorylated ephrin B (pEfnb) on transverse sections of wild-type (H) and DKO (I) embryos at E10.5. nd, nephric duct; cl, cloaca; u, ureter.

Pax2(8.5)-cre;Efnb2^{fl/fl} embryos at E14.5 (supplementary material Fig. S12). We conclude that *Efnb2*, similar to EphA4/EphA7, is required to establish proper ureter-bladder connectivity by promoting ND insertion into the cloaca.

Loss of *Lhx1* and downregulation of *Gata3* expression in the distal ND of *Pax2(8.5)-cre;Efnb2^{fl/fl}* embryos

We next sought to elucidate whether the loss of *Efnb2* in the ND results in similar molecular changes as observed in DKO embryos. We performed RNA *in situ* hybridizations on sections of E10.5 posterior trunks with the previously employed panel of genes associated with ND extension or fusion. Marker expression was unchanged at the mesonephros level (supplementary material Fig. S13). At the cloacal level, *Emx2*, *Pax2* and *Axin2* expression was unaltered, but expression of *Gata3* and *Lhx1* was strongly diminished and that of *Ret* was slightly reduced in the caudal ND of *Pax2(8.5)-cre;Efnb2^{fl/fl}* embryos (Fig. 9K,L). Expression of *Aldh1a2* and *Ptch1* in the pericloacal mesenchyme and of *Rarb* and *Shh* in the cloacal epithelium was unaffected at this stage in the mutant. Taken together, these findings confirm *Lhx1*, *Gata3* and *Ret* as molecular targets of ephrin B2 signaling in the caudal ND.

DISCUSSION

Pericloacal Eph signaling maintains caudal ND integrity via the *Lhx1/Gata3/Ret* network

ND elongation and fusion are poorly defined processes that depend on permissive and instructive cues from surrounding tissues (Drawbridge et al., 2000; Morris et al., 2003; Obara-Ishihara

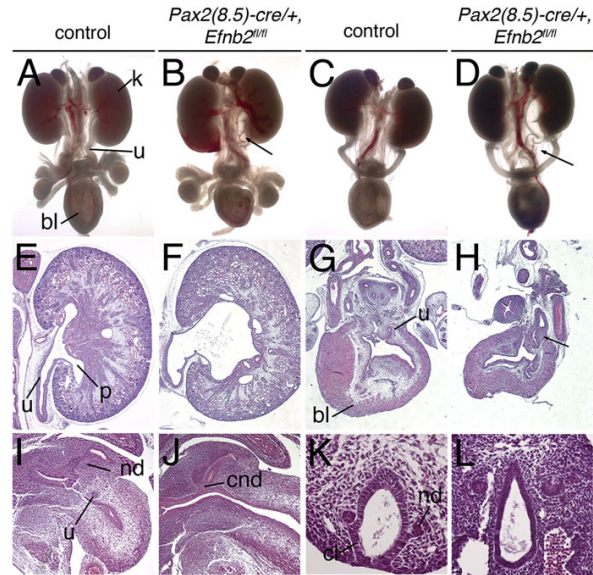


Fig. 8. Loss of *Efnb2* in the ND leads to CAKUT-like phenotypic changes. (A-D) Morphology of urogenital systems of male (A,B) and female (C,D) E18.5 embryos. (E-L) Hematoxylin and Eosin stainings of sagittal sections of E18.5 kidney (E,F) and bladder (G,H), of the E14.5 urogenital sinus (I,J), and of transverse sections of E10.5 trunk (K,L). Arrows (B,D,H) indicate hydronephrosis in the mutant. k, kidney; u, ureter; bl, bladder; p, pelvis; cl, cloaca; nd, nephric duct; cnd, common nephric duct.

et al., 1999). These cues are likely to be sensed by a specialized tip that translates them into directional growth towards and integration into the cloaca. Recent live cell imaging revealed the presence of protrusions at ND tip cells, similar to growth cones of nerve cells (Chia et al., 2011). Our videomicroscopy confirmed these tip cell protrusions and revealed that they switch dynamically between extension and retraction during ND migration. In DKO embryos, the ND tip was similarly dynamic in the formation of cellular protrusions during most of the posterior extension, but cells detached from the tip cell community in the last phase of migration once they had turned towards the cloaca in the midline of the embryo. Unfortunately, we were not able to simultaneously visualize the cloacal epithelium in our explant system in order to relate the cellular changes of the ND tip with the presence of the cloaca. Therefore, we cannot exclude the possibility that the disintegration of the ND tip is the consequence rather than the cause of failed interaction with the cloaca. However, we consider it more likely that ND tip disintegration precedes contact with the cloaca, as our molecular analysis showed that factors known to be required for caudal ND extension are collectively downregulated and that the cloacal epithelium seems largely unaffected.

Our molecular analysis identified *Ret*, *Gata3* and *Lhx1* as targets of EphA4/EphA7 signaling in the ND tip. Loss of *Gata3*, *Ret* and *Aldh1a2* has recently been associated with the absence of cellular protrusions of ND tip cells and a failure of ND integration. It was suggested that *Gata3* in the ND and RA signaling from the pericloacal mesenchyme act in parallel to maintain *Ret* expression in the caudal ND (Chia et al., 2011). *Lhx1* has also been shown to be required for the caudal portion of the ND to reach the urogenital sinus. It appears to act upstream of *Ret* but independently of *Gata3* (Pedersen et al., 2005), arguing

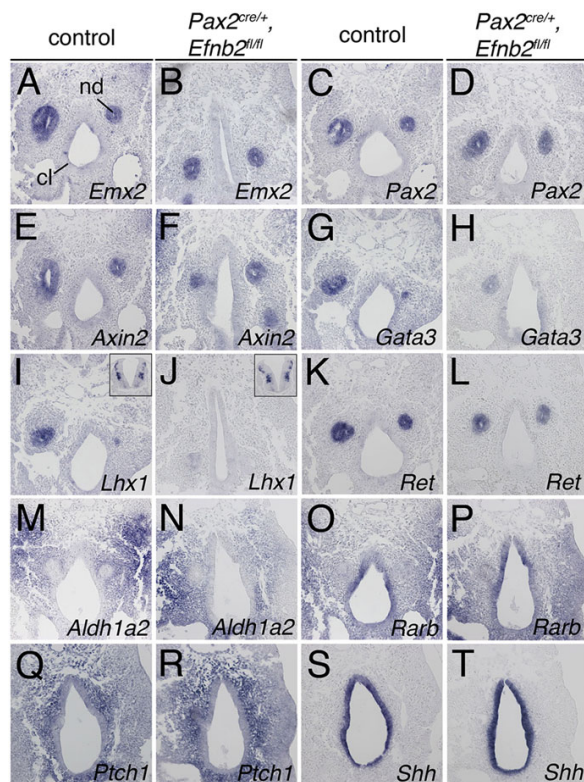


Fig. 9. Molecular changes in the caudal ND of *Pax2(8.5)-cre/+;Efnb2^{fl/fl}* embryos at E10.5. RNA *in situ* hybridization analysis of genes associated with ND extension or fusion on transverse sections of posterior trunks of E10.5 embryos. Insets (I, J) show spinal cord expression as an internal control. nd, nephric duct; cl, cloaca.

together that *Gata3* and *Lhx1* represent the primary targets of Eph/ephrin activity in the ND.

EphA4/EphA7 act in *trans* via ephrin B2-mediated reverse signaling

Eph/ephrin signaling represents an unusual intercellular communication module in the sense that the signals can elicit molecular changes both in the receptor-bearing as well as the ligand-bearing cell. As our study suggests that the caudal ND is the crucial target of EphA4/EphA7 activity in the pericloacal mesenchyme, it is possible that EphA4/EphA7 control the expression of a diffusible ligand in the pericloacal mesenchyme by forward signaling. Alternatively, EphA4/EphA7 might use the reverse signaling mode to directly activate transcriptional and/or cytoskeletal changes in the caudal ND. For a number of reasons, we deem the second possibility more likely. First, we found binding of EphA4/EphA7 to cells in the ND and the cloaca but not in the pericloacal mesenchyme. Second, specific expression of the ephrin B2 ligand was found in these two tissue compartments. Third, ephrin B2 signaling was greatly reduced in these compartments in mice with combined loss of *Epha4* and *Epha7*. Fourth, the observed loss of cell adhesion between ND tip cells is more compatible with the known role of reverse signaling in mediating adhesive cell interactions than with cell repulsion, which has been recognized as a consequence of Eph forward signaling (Kao et al., 2012).

Intriguingly, reverse ephrin B2 signaling has been implicated in the control of epithelial cell adhesion in urorectal maturation by promoting tubularization of the urethra and septation of the urinary and the anorectal system (Dravis et al., 2004). Fifth, although EphA receptors preferentially bind to ephrin A ligands, ephrin B2 has been described as a ligand for EphA4 in some contexts (Watanabe et al., 2009); ephrin B2 binding to EphA7 still needs to be validated on the biochemical level. Last, and most importantly, conditional deletion of *Efnb2* in the ND phenocopied the urinary tract defects of DKO embryos to a substantial extent, including blind or ectopically ending ureters, delayed CND removal, lack or delayed ND insertion and downregulation of *Gata3/Lhx1/Ret* in the caudal ND.

It remains to be seen how ephrin B2 signaling maintains the expression of *Gata3* and *Lhx1* and adhesion between cells in the ND tip. MAPKs, such as Erk1/2 (Mapk3/1), act downstream of ephrin B2-activated Src kinases but are also the main downstream signaling pathway activated by receptor tyrosine kinases including Ret (Hoshi et al., 2012; Sebolt-Leopold and Herrera, 2004). Independent of the precise epistatic relationship or of direct phosphorylation by Src kinases or by Ret, MAPK signaling might control the cytoskeletal changes that confer adhesive properties between ND tip cells.

EphA4/EphA7 signaling is also transduced into the cloacal epithelium, suggesting that ephrin B2 mediates some kind of heterotypic adhesion between the ND and the cloaca. Thus far, we have not found direct evidence for this hypothesis, as expression of cell adhesion molecules in the two compartments was unaffected and the integrity of the cloacal epithelium was preserved in DKO embryos.

We also observed reduced *Rarb* expression, a target gene of RA signaling in the cloacal epithelium (Tsou et al., 1994). RA is produced in the pericloacal mesenchyme by Aldh1a2. We did not find a change in the expression of *Aldh1a2* in the pericloacal mesenchyme of DKO embryos, but this might be due to the insensitivity of the *in situ* hybridization technique to detect small expression changes. Hence, it is conceivable that RA is reduced as a consequence of disturbed EphA4/EphA7 forward signaling in the pericloacal mesenchyme, resulting in reduced activation of RA target genes such as *Rarb* and also *Ret* in the caudal ND and cloaca.

A previous study revealed that, during the establishment of limb innervation by motor neurons, Ret and EphA signaling do not act in series but in parallel (Kramer et al., 2006). Gdnf from the dorsal limb bud mesenchyme acts as an attractive cue for motor neurons via binding to the Ret receptor. Ret additionally seems to act as a co-receptor for attractive reverse ephrin A signaling, thus integrating two attractive cues for pathfinding (Bonanomi et al., 2012). A similar interaction might hypothetically guide the ND to its target tissue. However, we did not detect *Gdnf* expression in the cloaca or pericloacal mesenchyme but in the metanephric blastema. In summary, we suggest that reverse ephrin B2-mediated EphA4/EphA7 signaling from the pericloacal mesenchyme maintains via the *Lhx1/Gata3/Ret* network the epithelial integrity of the ND tip, which is required for proper fusion with the cloaca.

ND defects underlie aberrant VUJ and ureter dilatation

DKO and *Pax2(8.5)-cre/+;Efnb2^{fl/fl}* embryos exhibited with ~50% penetrance a continuum of upper urinary tract defects ranging from weak unilateral hydroureter to strong bilateral megaureter. Our molecular analysis excluded a functional obstruction as the causative agent. However, we detected a range of VUJ malformations that corresponded in severity to the dilative uropathies: megaureters were associated with ureterocele and blind-ending ureters, and hydroureters

with ureters ending ectopically (e.g. in the urethra). Such a range of structural malformation and penetrance seems unusual for a monogenetic disease and might indicate genetic interaction with as yet unknown factors, or might stem from the mosaic composition of the genetic background that we obtained by continuous outcrossing from an initially C57BL/6 background. However, as we obtained the same range of structural malformation after each outcrossing, we consider it more likely that it simply relates to slight variations in the extension of the ND resulting in the absent, delayed or ectopic fusion with the cloaca that occurred in 100% of DKO embryos analyzed at E10.5. Lack of ND integration impaired CND removal by apoptosis and ureters remained attached to the NDs. Following massive growth of the bladder, the CND became incorporated into the bladder resulting in intravesical ureterocele, or remained outside ending blindly, resulting in hydronephrotic/megaureter and associated hydronephrosis upon onset of urine production in the kidney. By contrast, delayed or ectopic fusion of the ND with the cloaca may result in ureters ending ectopically with much less severe phenotypic manifestations at E18.5, or might be partially or completely resolved during further morphogenetic steps. These findings strongly support the conclusions of a recent study of mice mutant for *Ret*, *Gata3* or *Aldh1a2*, which reported that a defect in ND integration is a novel cause of CAKUT (Chia et al., 2011).

It was recently reported that mice deficient for a mutant allele of *Epha4* exhibit spontaneous hydronephrotic lesions in adulthood. The low rate (17%) and late onset (3–10 months) of the defects strongly support our findings that *Epha4* and *Epha7* act redundantly to establish a proper VUJ (Sallstrom et al., 2013).

MATERIALS AND METHODS

Microarray analysis

Preliminary microarray analysis used for the identification of candidate genes was performed by the core facility Transcriptomics of Medizinische Hochschule Hannover using Agilent mouse whole-genome arrays with RNA isolated from E13.5 wild-type and *Tbx18*-deficient ureters.

Mice

Mice carrying null alleles for *Tbx18* (*Tbx18^{tm2Aki}*; synonym *Tbx18^{GFP}*) (Christoffels et al., 2006), *Epha4* (*Epha4^{tm1Pvan}*; synonym *Epha4⁻*) (Kullander et al., 2001) and *Epha7* (*Epha7^{tm1Ud}*; synonym *Epha7⁻*) (Dufour et al., 2003), mice with a floxed allele of *Efnb2* (*Efnb2^{tm4Kln}*; synonym *Efnb2^f*) (Grunwald et al., 2004), transgenic mouse lines *Hoxb7-GFP* [*Tg(Hoxb7-EGFP)33Cos*] (Srinivas et al., 1999) and *Pax2(8.5)-cre* (Trowe et al., 2011), and the double fluorescent Cre reporter line *Gt(ROSA)26Sor^{tm4(ACTB-tdTomato,-EGFP)Luo}* (synonym *R26^{mTmG}*) (Muzumdar et al., 2007) were maintained on an NMRI outbred background. *Epha4/Epha7* compound mutant mice were obtained from matings of *Epha7^{-/-};Epha4^{+/-}* males and *Epha4^{+/-};Epha7^{+/-}* or *Epha7^{-/-};Epha4^{+/-}* females. *Epha7^{+/-};Epha4^{+/-}* and *Epha7^{+/-};Epha4^{+/-}* littermates were interchangeably used as controls. *Pax2(8.5)-cre/+;Efnb2^{f/f}* embryos were obtained from matings of *Pax2(8.5)-cre/+;Efnb2^{f/f}* males with *Efnb2^{f/f}* females. Embryos for Eph/ephrin gene expression analysis were derived from matings of NMRI wild-type and *Tbx18^{GFP/+}* mice. For timed pregnancies, vaginal plugs were checked in the morning after mating; noon was taken as E0.5. Pregnant females were sacrificed by cervical dislocation; embryos were harvested in phosphate-buffered saline (PBS), decapitated, fixed in 4% paraformaldehyde/PBS overnight, and stored in 100% methanol at -20°C before further use. Genomic DNA prepared from tails or embryonic tissues was used for genotyping by PCR.

Morphological, histological and immunohistochemical analyses

Ink injection experiments were performed as previously described (Airik et al., 2010). For histological stainings, organ rudiments or posterior trunks of embryos were paraffin embedded and sectioned at 5 µm. Sections

were stained with Hematoxylin and Eosin. Three-dimensional (3D) reconstruction of stained serial sections was performed according to published protocols (Soufan et al., 2003).

For Eph receptor-Fc stainings, we modified a previously published protocol (Gale et al., 1996). E9.5 embryos were incubated with recombinant mouse EphA4-Fc or recombinant mouse EphA7-Fc chimeric proteins (#641-A4-200 and #608-A7-200, R&D Systems). For detection of Eph-Fc binding, embryos were incubated with anti-human IgG (H&L) AP conjugate (#S3821, Promega; 1:1500). Embryos were stained with either NBT/BCIP or INT/BCIP (#11681451001 or #11681460001, Roche Diagnostics) in the dark. To permeabilize the tissue, we used Tween 20 in the wash buffer.

For the detection of antigens on 5 µm paraffin sections, the following primary antibodies and dilutions were used: anti-Myh11 (kindly provided by R. Adelstein, NIH, Bethesda, MD, USA; 1:400), mouse anti-Acta2 (#F3777 and C6198, Sigma; 1:200), rabbit anti-Cdh1 (kindly provided by R. Kemler, MPI for Immunobiology and Epigenetics, Freiburg, Germany; 1:200), rabbit anti-ephrin B2 (#sc-15397, Santa Cruz; 1:200), rabbit anti-phospho-ephrin B (Y316) (#PPS047, R&D Systems; 1:50), rat monoclonal anti-endomucin (kindly provided by D. Vestweber, MPI for Molecular Biomedicine, Münster, Germany; 1:10), mouse monoclonal anti-neurofilament (DSHB; 1:200), rat anti-neuropilin 1 (MAB5661, R&D Systems; 1:100), rabbit polyclonal anti-collagen type 4 (#AB756P, Millipore; 1:200) and rabbit polyclonal anti-GFP (#sc-8334, Santa Cruz; 1:200). Fluorophore-coupled secondary antibodies were purchased from Dianova (goat anti-rabbit, #111-065-003) and Life Technologies (goat anti-rabbit and goat anti-rat, #A-11008 and #A-21434) and used at 1:200 or 1:250 dilution. Non-fluorescent staining was performed using kits from Vector Laboratories [Mouse-on-Mouse peroxidase kit, Vectastain ABC peroxidase kit (rabbit IgG), DAB substrate kit].

Explant cultures

For live cell imaging of GFP-labeled NDs, posterior trunks of E9.5 embryos were isolated and cultured with their flanks down on Transwell filters at 37°C in an atmosphere of 5% CO₂ for 18 h as previously described (Airik et al., 2010). GFP epifluorescence of NDs was documented hourly for the entire culture period.

Cellular assays

Apoptotic cells on 5 µm sections were detected by TUNEL assay, modifying genomic DNA via terminal deoxynucleotidyl transferase using the ApopTag Plus Fluorescein In Situ Apoptosis Detection Kit (Chemicon). All sections were counterstained with DAPI to visualize the nuclei.

In situ hybridization analysis

Whole-mount *in situ* hybridization was performed following a standard procedure with digoxigenin-labeled antisense riboprobes (Wilkinson and Nieto, 1993). Stained specimens were transferred to 80% glycerol prior to documentation. RNA *in situ* hybridization on 10 µm paraffin sections was essentially as previously described (Moorman et al., 2001). For each marker at least four independent specimens were analyzed.

Image analysis

Whole-mount specimens were photographed on a Leica M420 microscope with a Fujix HC-300Z digital camera, and sections on a Leica DM5000B with a Leica DFC300FX digital camera. GFP epifluorescence in living tissues was documented with a Leica DMI 6000 microscope, and the images and movies were processed with Leica Application Suite Advanced Fluorescence software (version 2.3.0). Confocal images were taken on a Leica Inverted-2 with TCS SP2 scan head. Images for figures were processed in Adobe Photoshop CS3.

Acknowledgements

We thank Rolf Kemler, Dietmar Vestweber and Robert Adelstein for antibodies; Pierre Vanderhaeghen, Rüdiger Klein and Rolf Zeller for providing mice; and Eva Bettenhausen for technical help.

Competing interests

The authors declare no competing financial interests.

Author contributions

A.-C.W., R.A. and A.K. initiated the project; A.-C.W., R.A., T.B., F.G., A.F., M.-O.T., C.R. and A.K. designed and performed the experiments; F.C. and R.H.A. provided mice; A.-C.W., M.-O.T., F.C., R.H.A. and A.K. wrote and/or edited the paper.

Funding

This work was supported by a grant from the German Research Council [DFG KI728/7-1] to A.K.

Supplementary material

Supplementary material available online at <http://dev.biologists.org/lookup/suppl/doi:10.1242/dev.113928/-/DC1>

References

- Airik, R. and Kispert, A. (2007). Down the tube of obstructive nephropathies: the importance of tissue interactions during ureter development. *Kidney Int.* **72**, 1459-1467.
- Airik, R., Bussen, M., Singh, M. K., Petry, M. and Kispert, A. (2006). Tbx18 regulates the development of the ureteral mesenchyme. *J. Clin. Invest.* **116**, 663-674.
- Airik, R., Trowe, M.-O., Foik, A., Farin, H. F., Petry, M., Schuster-Gossler, K., Schweizer, M., Scherer, G., Kist, R. and Kispert, A. (2010). Hydrourteronephrosis due to loss of Sox9-regulated smooth muscle cell differentiation of the ureteric mesenchyme. *Hum. Mol. Genet.* **19**, 4918-4929.
- Batourina, E., Choi, C., Paragas, N., Bello, N., Hensle, T., Costantini, F. D., Schuchardt, A., Bacallao, R. L. and Mendelsohn, C. L. (2002). Distal ureter morphogenesis depends on epithelial cell remodeling mediated by vitamin A and Ret. *Nat. Genet.* **32**, 109-115.
- Batourina, E., Tsai, S., Lambert, S., Sprengle, P., Viana, R., Dutta, S., Hensle, T., Wang, F., Niederreither, K., McMahon, A. P. et al. (2005). Apoptosis induced by vitamin A signaling is crucial for connecting the ureters to the bladder. *Nat. Genet.* **37**, 1082-1089.
- Bohnenpoll, T., Bettenhausen, E., Weiss, A.-C., Foik, A. B., Trowe, M.-O., Blank, P., Airik, R. and Kispert, A. (2013). Tbx18 expression demarcates multipotent precursor populations in the developing urogenital system but is exclusively required within the ureteric mesenchymal lineage to suppress a renal stromal fate. *Dev. Biol.* **380**, 25-36.
- Bonomi, D., Chivatakarn, O., Bai, G., Abdesslem, H., Lettieri, K., Marquardt, T., Pierchala, B. A. and Pfaff, S. L. (2012). Ret is a multifunctional coreceptor that integrates diffusible- and contact-axon guidance signals. *Cell* **148**, 568-582.
- Chia, I., Grote, D., Marcotte, M., Batourina, E., Mendelsohn, C. and Bouchard, M. (2011). Nephric duct insertion is a crucial step in urinary tract maturation that is regulated by a Gata3-Raldh2-Ret molecular network in mice. *Development* **138**, 2089-2097.
- Christoffels, V. M., Mommersteeg, M. T., Trowe, M.-O., Prall, O. W. J., de Gier-de Vries, C., Soufan, A. T., Bussen, M., Schuster-Gossler, K., Harvey, R. P., Moorman, A. F. M. et al. (2006). Formation of the venous pole of the heart from an Nkx2-5-negative precursor population requires Tbx18. *Circ. Res.* **98**, 1555-1563.
- Costantini, F. and Shakya, R. (2006). GDNF/Ret signaling and the development of the kidney. *Bioessays* **28**, 117-127.
- Dravis, C., Yokoyama, N., Chumley, M. J., Cowan, C. A., Silvany, R. E., Shay, J., Baker, L. A. and Henkemeyer, M. (2004). Bidirectional signaling mediated by ephrin-B2 and EphB2 controls ureteral development. *Dev. Biol.* **271**, 272-290.
- Drawbridge, J., Meighan, C. M. and Mitchell, E. A. (2000). GDNF and GFRalpha-1 are components of the axolotl pronephric duct guidance system. *Dev. Biol.* **228**, 116-124.
- Dufour, A., Seibt, J., Passante, L., Depaepae, V., Ciossek, T., Frisén, J., Kullander, K., Flanagan, J. G., Polleux, F. and Vanderhaeghen, P. (2003). Area specificity and topography of thalamocortical projections are controlled by ephrin/Eph genes. *Neuron* **39**, 453-465.
- Gale, N. W., Holland, S. J., Valenzuela, D. M., Flenniken, A., Pan, L., Ryan, T. E., Henkemeyer, M., Strebhardt, K., Hirai, H., Wilkinson, D. G. et al. (1996). Eph receptors and ligands comprise two major specificity subclasses and are reciprocally compartmentalized during embryogenesis. *Neuron* **17**, 9-19.
- Georgakopoulos, A., Xu, J., Xu, C., Mauger, G., Barthel, G. and Robakis, N. K. (2011). Presenilin1/gamma-secretase promotes the EphB2-induced phosphorylation of ephrinB2 by regulating phosphoprotein associated with glycosphingolipid-enriched microdomains/Csk binding protein. *FASEB J.* **25**, 3594-3604.
- Grunwald, I. C., Korte, M., Adelman, G., Plueck, A., Kullander, K., Adams, R. H., Frotscher, M., Bonhoeffer, T. and Klein, R. (2004). Hippocampal plasticity requires postsynaptic ephrinBs. *Nat. Neurosci.* **7**, 33-40.
- Hoshi, M., Batourina, E., Mendelsohn, C. and Jain, S. (2012). Novel mechanisms of early upper and lower urinary tract patterning regulated by RetY1015 docking tyrosine in mice. *Development* **139**, 2405-2415.
- Ingham, P. W. and McMahon, A. P. (2001). Hedgehog signaling in animal development: paradigms and principles. *Genes Dev.* **15**, 3059-3087.
- Kao, T.-J., Law, C. and Kania, A. (2012). Eph and ephrin signaling: lessons learned from spinal motor neurons. *Semin. Cell Dev. Biol.* **23**, 83-91.
- Kerecuk, L., Schreuder, M. F. and Woolf, A. S. (2008). Renal tract malformations: perspectives for nephrologists. *Nat. Clin. Pract. Nephrol.* **4**, 312-325.
- Klein, R. (2012). Eph/ephrin signaling during development. *Development* **139**, 4105-4109.
- Kramer, E. R., Knott, L., Su, F., Dessaud, E., Krull, C. E., Helmbacher, F. and Klein, R. (2006). Cooperation between GDNF/Ret and ephrinA/EphA4 signals for motor-axon pathway selection in the limb. *Neuron* **50**, 35-47.
- Kullander, K. and Klein, R. (2002). Mechanisms and functions of Eph and ephrin signalling. *Nat. Rev. Mol. Cell Biol.* **3**, 475-486.
- Kullander, K., Mather, N. K., Diella, F., Dottori, M., Boyd, A. W. and Klein, R. (2001). Kinase-dependent and kinase-independent functions of EphA4 receptors in major axon tract formation in vivo. *Neuron* **29**, 73-84.
- Kuschert, S., Rowitch, D. H., Haenig, B., McMahon, A. P. and Kispert, A. (2001). Characterization of Pax-2 regulatory sequences that direct transgene expression in the Wolffian duct and its derivatives. *Dev. Biol.* **229**, 128-140.
- Mackie, G. G. and Stephens, F. D. (1975). Duplex kidneys: a correlation of renal dysplasia with position of the ureteral orifice. *J. Urol.* **114**, 274-280.
- Matt, N., Ghyselinck, N. B., Wendling, O., Chambon, P. and Mark, M. (2003). Retinoic acid-induced developmental defects are mediated by RARbeta/RXR heterodimers in the pharyngeal endoderm. *Development* **130**, 2083-2093.
- Mendelsohn, C. (2009). Using mouse models to understand normal and abnormal urogenital tract development. *Organogenesis* **5**, 32-40.
- Moorman, A. F. M., Houweling, A. C., de Boer, P. A. J. and Christoffels, V. M. (2001). Sensitive nonradioactive detection of mRNA in tissue sections: novel application of the whole-mount in situ hybridization protocol. *J. Histochem. Cytochem.* **49**, 1-8.
- Morris, A. R., Drawbridge, J. and Steinberg, M. S. (2003). Axolotl pronephric duct migration requires an epidermally derived, laminin 1-containing extracellular matrix and the integrin receptor alpha6beta1. *Development* **130**, 5601-5608.
- Muzumdar, M. D., Tasic, B., Miyamichi, K., Li, L. and Luo, L. (2007). A global double-fluorescent Cre reporter mouse. *Genesis* **45**, 593-605.
- Nakai, H., Asanuma, H., Shishido, S., Kitahara, S. and Yasuda, K. (2003). Changing concepts in urological management of the congenital anomalies of kidney and urinary tract, CAKUT. *Pediatr. Int.* **45**, 634-641.
- NAPRTCS (2007). *North American Pediatric Renal Trials and Collaborative Studies*. <http://www.emmes.com/study/ped/annlrept/annlrept2007.pdf>.
- Obara-Ishihara, T., Kuhlman, J., Niswander, L. and Herzlinger, D. (1999). The surface ectoderm is essential for nephric duct formation in intermediate mesoderm. *Development* **126**, 1103-1108.
- Ogawa, K., Wada, H., Okada, N., Harada, I., Nakajima, T., Pasquale, E. B. and Tsuyama, S. (2006). EphB2 and ephrin-B1 expressed in the adult kidney regulate the cytoarchitecture of medullary tubule cells through Rho family GTPases. *J. Cell Sci.* **119**, 559-570.
- Palmer, A., Zimmer, M., Erdmann, K. S., Eulenburg, V., Porthin, A., Heumann, R., Deutsch, U. and Klein, R. (2002). EphrinB phosphorylation and reverse signaling: regulation by Src kinases and PTP-BL phosphatase. *Mol. Cell* **9**, 725-737.
- Pedersen, A., Skjong, C. and Shawlot, W. (2005). Lim1 is required for nephric duct extension and ureteric bud morphogenesis. *Dev. Biol.* **288**, 571-581.
- Pitulescu, M. E. and Adams, R. H. (2010). Eph/ephrin molecules—a hub for signaling and endocytosis. *Genes Dev.* **24**, 2480-2492.
- Sallstrom, J., Peuckert, C., Gao, X., Larsson, E., Nilsson, A., Jensen, B. L., Onozato, M. L., Persson, A. E. G., Kullander, K. and Carlstrom, M. (2013). Impaired EphA4 signaling leads to congenital hydronephrosis, renal injury and hypertension. *Am. J. Physiol. Renal Physiol.* **305**, F71-F79.
- Sebolt-Leopold, J. S. and Herrera, R. (2004). Targeting the mitogen-activated protein kinase cascade to treat cancer. *Nat. Rev. Cancer* **4**, 937-947.
- Soufan, A. T., Ruijter, J. M., van den Hoff, M. J., de Boer, P. A., Hagoort, J. and Moorman, A. F. (2003). Three-dimensional reconstruction of gene expression patterns during cardiac development. *Physiol. Genomics* **13**, 187-195.
- Srinivas, S., Goldberg, M. R., Watanabe, T., D'Agati, V., Al-Awqati, Q. and Costantini, F. (1999). Expression of green fluorescent protein in the ureteric bud of transgenic mice: a new tool for the analysis of ureteric bud morphogenesis. *Dev. Genet.* **24**, 241-251.
- Treanor, J. J. S., Goodman, L., de Sauvage, F., Stone, D. M., Poulsen, K. T., Beck, C. D., Gray, C., Armanini, M. P., Pollock, R. A., Hefti, F. et al. (1996). Characterization of a multicomponent receptor for GDNF. *Nature* **382**, 80-83.
- Trowe, M.-O., Maier, H., Petry, M., Schweizer, M., Schuster-Gossler, K. and Kispert, A. (2011). Impaired stria vascularis integrity upon loss of E-cadherin in basal cells. *Dev. Biol.* **359**, 95-107.
- Tsou, H. C., Si, S. P., Lee, X., González-Serva, A. and Peacocke, M. (1994). A beta 2RARE-LacZ transgene identifies retinoic acid-mediated transcriptional activation in distinct cutaneous sites. *Exp. Cell Res.* **214**, 27-34.
- Uetani, N. and Bouchard, M. (2009). Plumbing in the embryo: developmental defects of the urinary tracts. *Clin. Genet.* **75**, 307-317.

- Uetani, N., Bertozzi, K., Chagnon, M. J., Hendriks, W., Tremblay, M. L. and Bouchard, M.** (2009). Maturation of ureter-bladder connection in mice is controlled by LAR family receptor protein tyrosine phosphatases. *J. Clin. Invest.* **119**, 924-935.
- Watanabe, T., Sato, Y., Saito, D., Tadokoro, R. and Takahashi, Y.** (2009). EphrinB2 coordinates the formation of a morphological boundary and cell epithelialization during somite segmentation. *Proc. Natl. Acad. Sci. USA* **106**, 7467-7472.
- Weber, S.** (2012). Novel genetic aspects of congenital anomalies of kidney and urinary tract. *Curr. Opin. Pediatr.* **24**, 212-218.
- Wilkinson, D. G. and Nieto, M. A.** (1993). Detection of messenger RNA by in situ hybridization to tissue sections and whole mounts. *Methods Enzymol.* **225**, 361-373.
- Woolf, A. S. and Davies, J. A.** (2013). Cell biology of ureter development. *J. Am. Soc. Nephrol.* **24**, 19-25.
- Wu, H.-C., Chang, C.-H., Peng, H.-Y., Chen, G.-D., Lai, C.-Y., Hsieh, M.-C. and Lin, T.-B.** (2011). EphrinB2 induces pelvic-urethra reflex potentiation via Src kinase-dependent tyrosine phosphorylation of NR2B. *Am. J. Physiol. Renal Physiol.* **300**, F403-F411.

SUPPLEMENTARY FIGURES

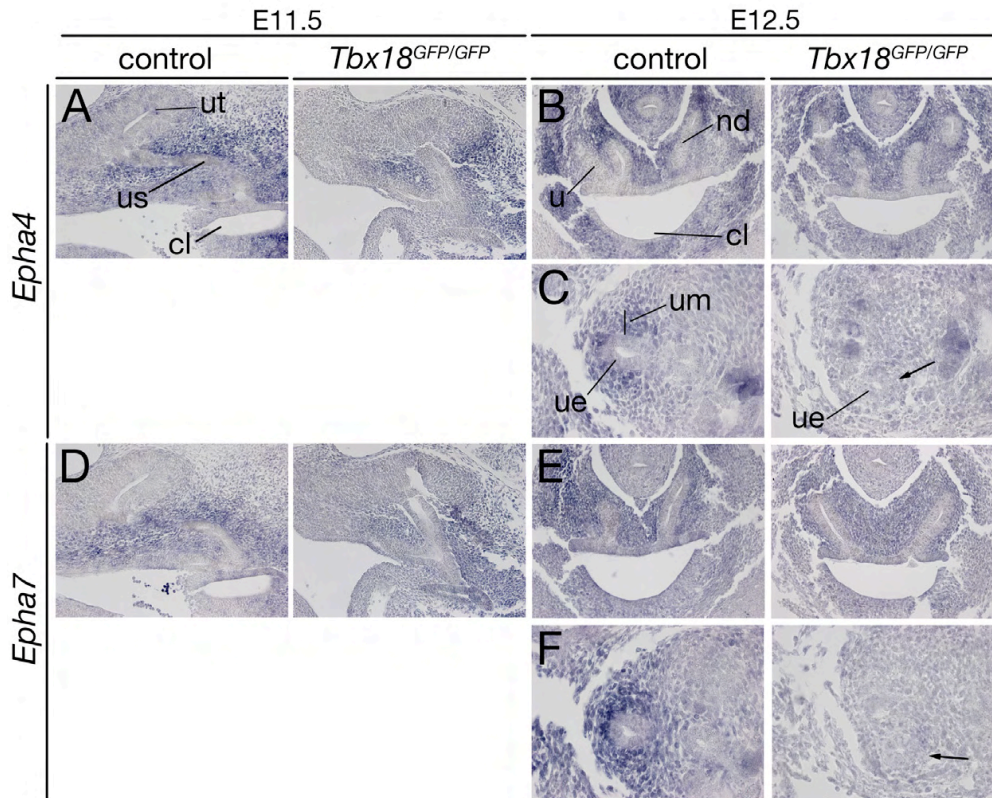


Fig. S1. Expression of *Epha4* and *Epha7* in the ureteric mesenchyme depends on *Tbx18*. (A-F) RNA *in situ* hybridization analysis on sagittal (A,D) and transverse (B,C,E,F) sections through the posterior trunk region at the level of the cloaca (A,B,D,E) and of the proximal ureter (C,F) for expression of *Epha4* and *Epha7* in wildtype and *Tbx18*-deficient (*Tbx18*^{GFP/GFP}) embryos at E11.5 and E12.5. Stages and probes are as indicated. Expression of *Epha4* and *Epha7* is not changed in the pericloacal mesenchyme but is lost in the ureteric mesenchyme at E12.5 in *Tbx18*-deficient embryos (arrows in C and F). cl, cloaca; nd, nephric duct; u, ureter; ue, ureteric epithelium; um, ureteric mesenchyme; us, ureteric stalk; ut, ureteric tip.

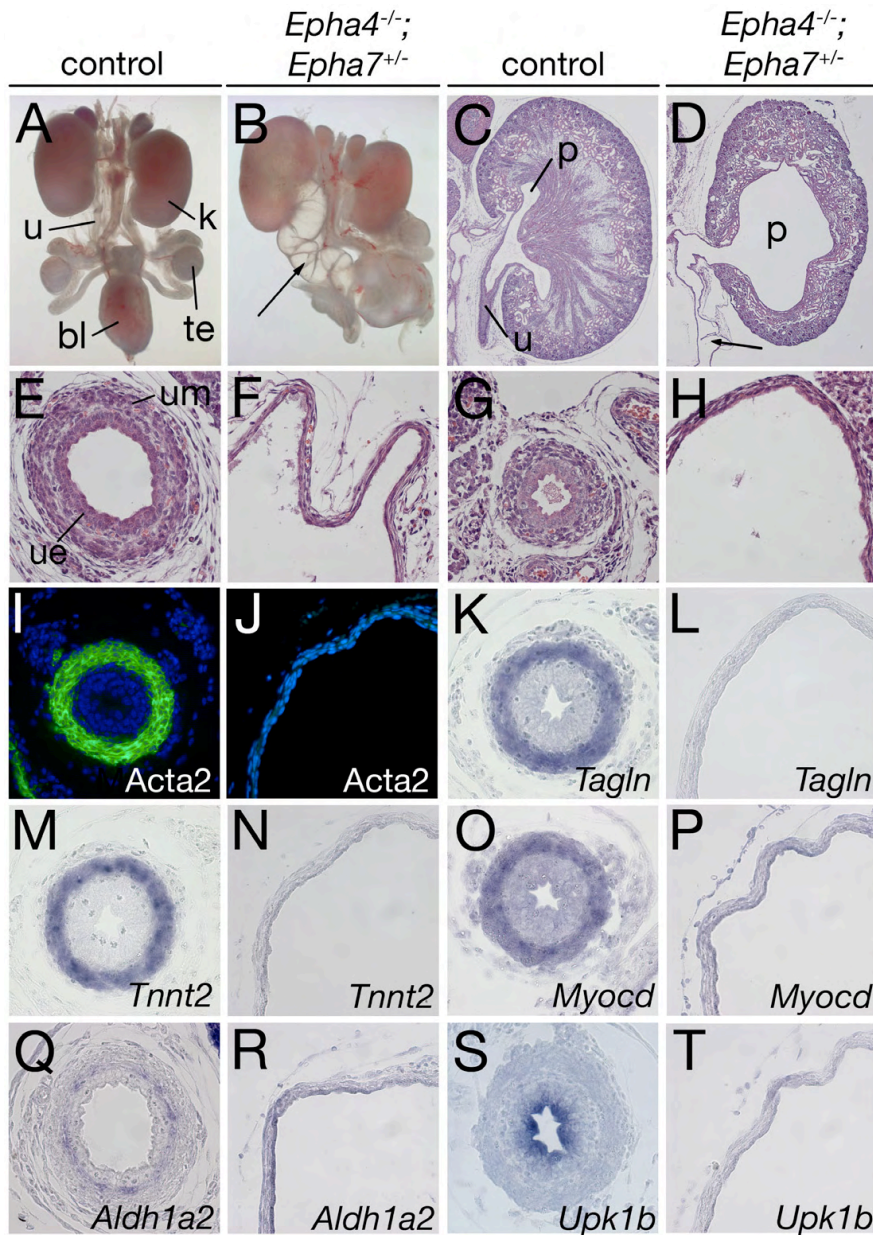


Fig. S2. Megaureter and hydronephrosis in *Epha4*^{-/-};*Epha7*^{+/-} embryos at E18.5. (A,B) Morphology of whole urogenital systems of male embryos. (C-H) Hematoxylin and Eosin stainings (HE) of sagittal sections of kidneys (C,D) and of transverse sections of the proximal ureter (E,F) and the distal ureter (G,H). (I-T) Cytodifferentiation of the ureteric mesenchyme (I-R) and epithelium (S,T) as shown by immunofluorescence (I,J) and *in situ* hybridization analysis (K-T) on transverse sections of the proximal ureter at E18.5. Mutants exhibit a megaureter (arrows in B and D) with a complete lack of cytodifferentiation. Genotypes, probes and antibodies are as indicated. bl, bladder; k, kidney; p, pelvis; pa, papilla; t, testis; u, ureter; ue, ureteric epithelium; um, ureteric mesenchyme.

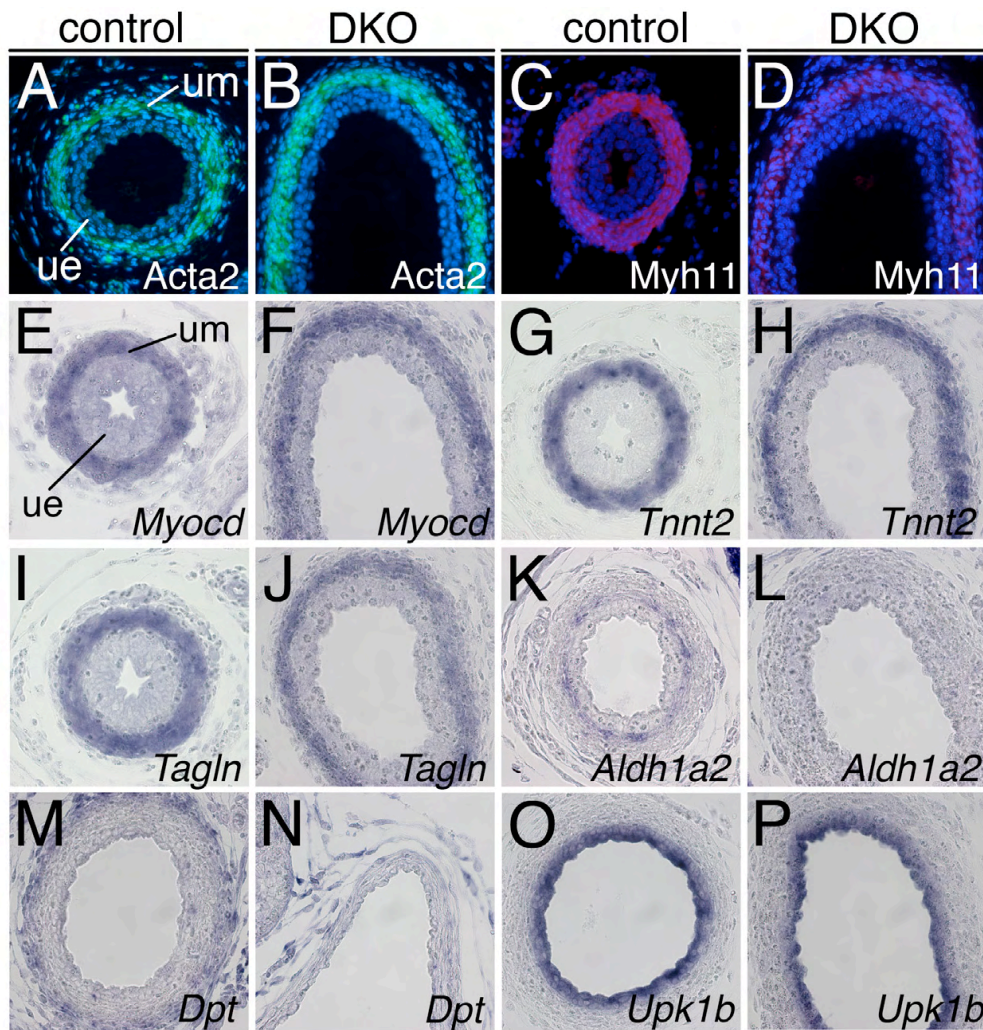


Fig. S3. Cytodifferentiation is only partly affected in the proximal hydroureter in *Epha4*^{-/-};*Epha7*^{-/-} (DKO) embryos. Immunofluorescence (A-D) and RNA *in situ* hybridization analysis (E-P) on transverse sections of the proximal ureter at E18.5 for differentiation of the smooth muscle layer (A-J), the lamina propria (K,L), the tunica adventitia (M,N) and the urothelium (O,P). Mutants exhibit a hydroureter with a partial reduction of cytodifferentiation. Genotypes, probes and antibodies are as indicated. ue, ureteric epithelium; um, ureteric mesenchyme.

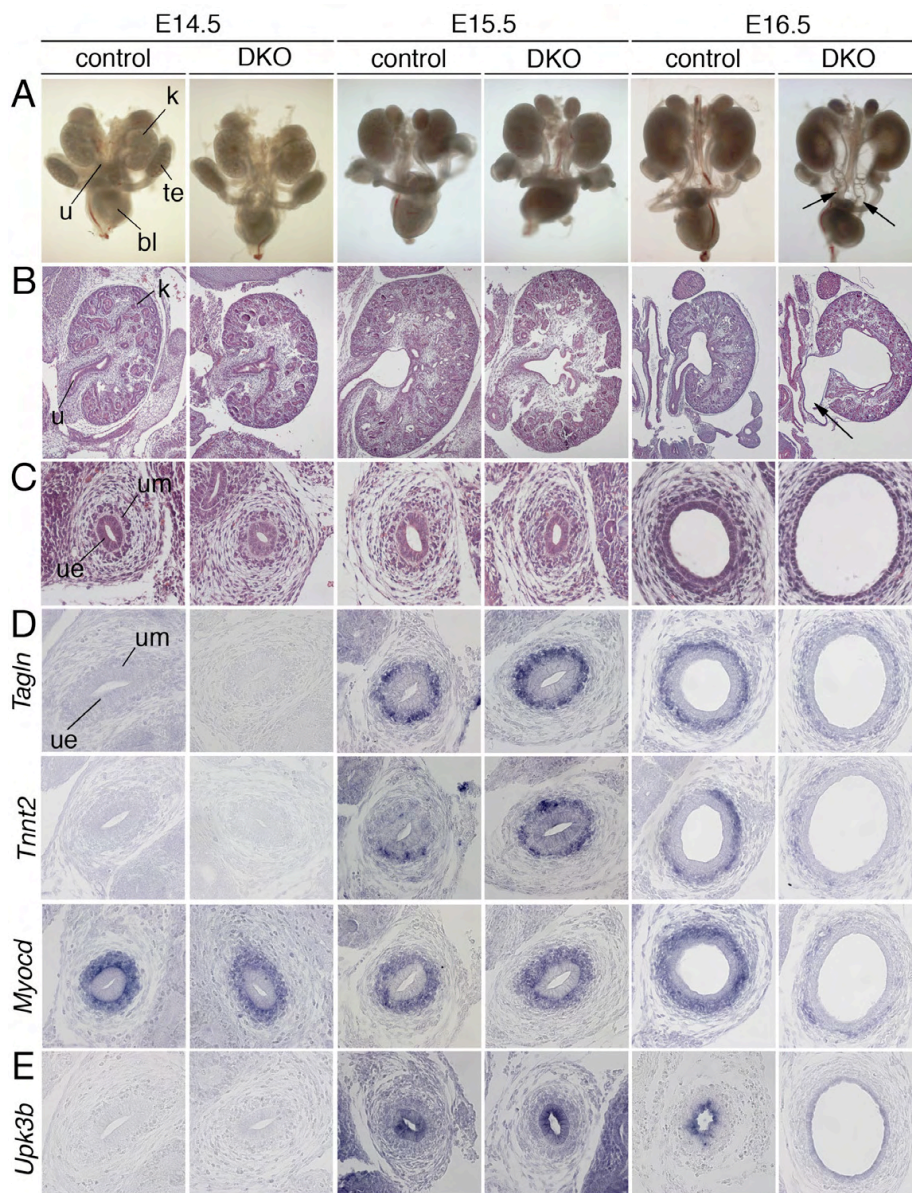


Fig S4. Onset of kidney and ureter anomalies in *Epha4*^{-/-};*Epha7*^{-/-} (DKO) embryos. (A) Morphology of whole urogenital systems. (B,C) Hematoxylin and Eosin stainings of sagittal sections of the kidney (B) and of transverse sections of the proximal ureter (C). (D,E) Cytodifferentiation of the ureteric mesenchyme into smooth muscle cells (D) and of the ureteric epithelium into the urothelium (E) as shown by RNA *in situ* hybridization analysis of marker genes on transverse sections of the proximal ureter. Arrows (in A and B) point to megaureter formation in *DKO* embryos. SM differentiation is initiated in *DKO* embryos at E14.5 and E15.5 indicating that hydroureter results from physical and not functional ureter obstruction. Stages, genotypes and probes are as indicated. bl, bladder; k, kidney; t, testis; u, ureter; ue, ureteric epithelium; um, ureteric mesenchyme.

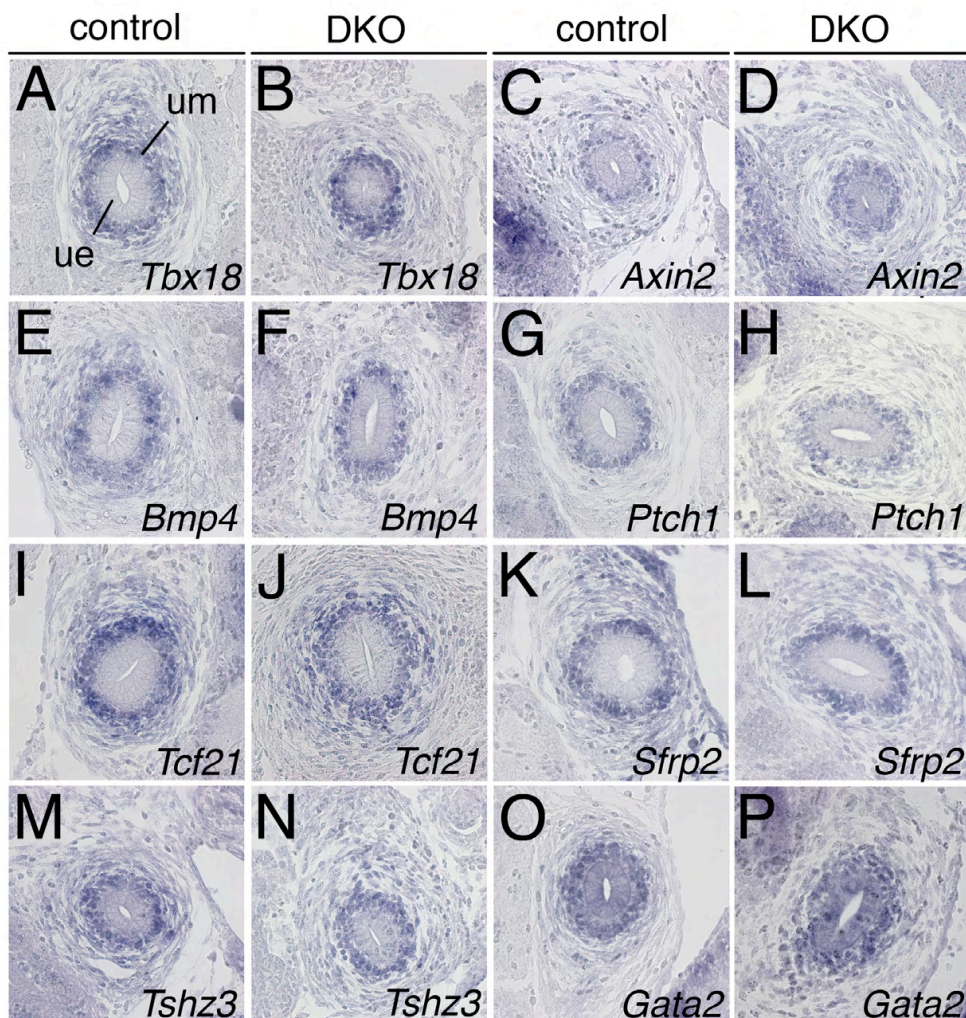


Fig. S5. The ureteric mesenchyme is unchanged in *EphA4*^{-/-};*Epha7*^{-/-} (DKO) embryos at E14.5. RNA *in situ* hybridization analysis on transverse sections of the proximal ureter at E14.5 for expression of markers of prospective smooth muscle cells. All markers are unchanged in DKO ureters at this stage. Genotypes and probes are as indicated. ue, ureteric epithelium; um, ureteric mesenchyme.

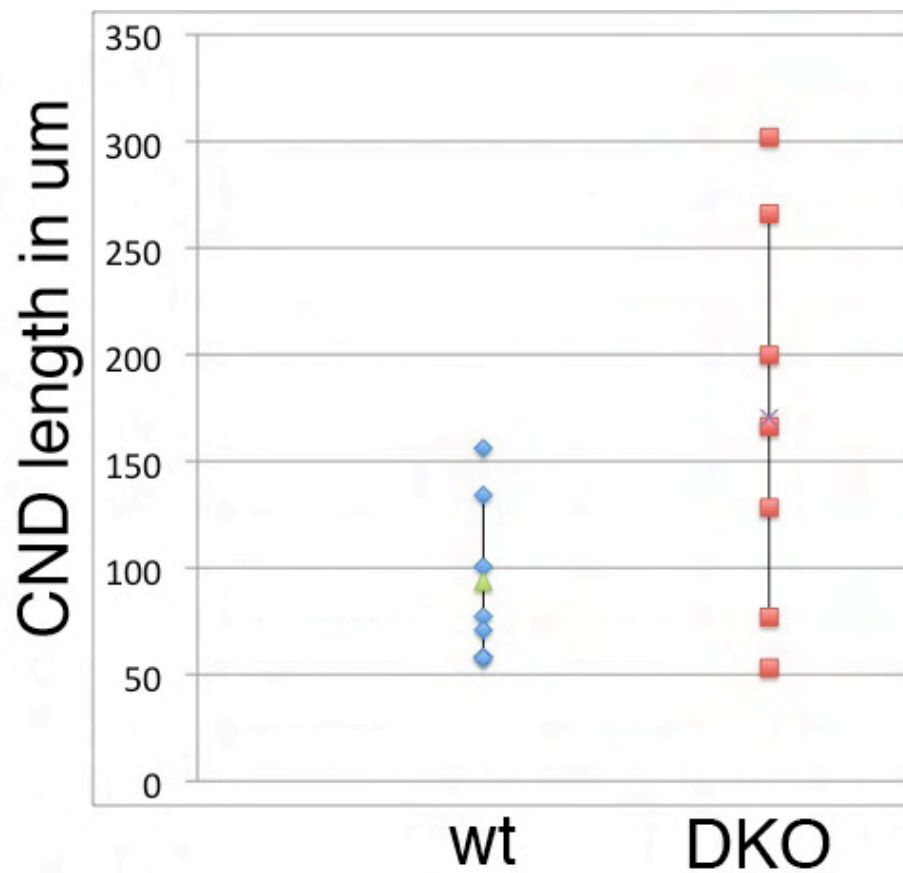


Fig. S6. Variation of CND length of wildtype and *Epha4*^{-/-};*Epha7*^{-/-} (DKO) embryos at E12.5. This scatter plot displays the unilateral CND length (in μm) of wildtype (blue) and DKO (red) embryos at E12.5 ($n=7$). Green triangle in wildtype (93 μm) and black cross in DKO (170 μm) shows the arithmetic mean. Black vertical bars represents the standard deviation in both genotypes (in wildtype 38.55, in DKO 92.74). CND length was measured on sagittal sections of embryos using ImageJ software.

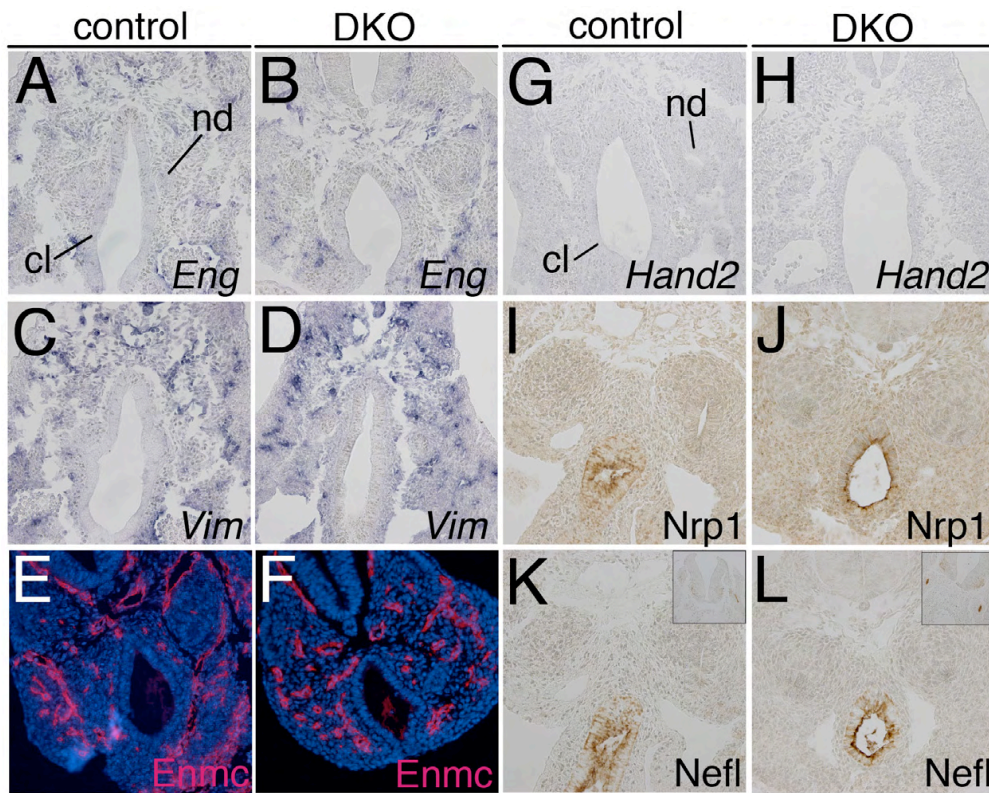


Fig. S7. Endothelial and neuronal cell distribution is unchanged in the pericloacal mesenchyme of DKO embryos at E10.5. (A-D, G,H) RNA *in situ* hybridization analysis on sections through the posterior trunk for expression of the endothelial marker genes endoglin (Eng) and vimentin (Vim) and the neuronal marker *Hand2*. Absence of *Hand2* shows that neural crest cells have not yet invaded this region of the posterior trunk at this stage. (E,F) Immunofluorescence analysis on sections through the posterior trunk for expression of the endothelial marker endomucin (Emcn). (I-L) IHC analysis on sections through the posterior trunk for expression of the neuronal markers neuropilin-1 (Nrp1) and neurofilament light chain (Nefl). Control regions of Nefl staining in upper right boxes (K,L). Note that these two proteins are found in the cloacal epithelium but not in the adjacent mesenchyme. nd, nephric duct, cl, cloaca.

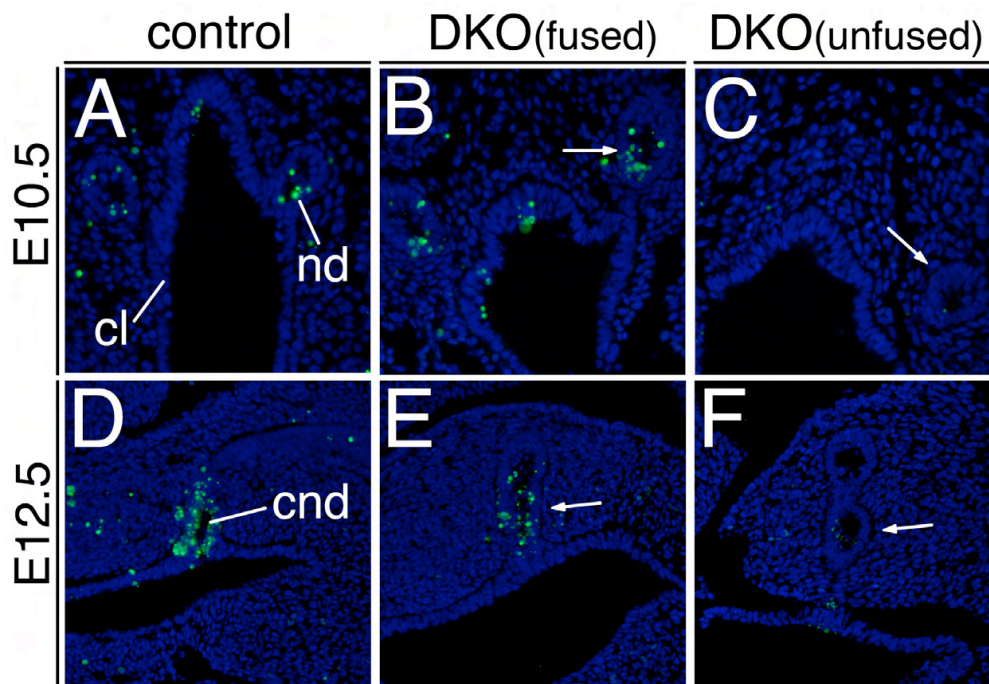


Fig. S8. Defective apoptotic CND removal in DKO embryos. Analysis of programmed cell death by the TUNEL assay of E10.5 transverse (A-C) and E12.5 (D-F) sagittal sections of the urogenital sinus. Apoptosis is absent and CND removal fails in DKO embryos with an unfused ND. Apoptotic bodies in green, nuclei in blue (DAPI). Stages and genotypes as indicated. Arrows point to ND or CND. nd, nephric duct; cl, cloaca; cnd, common nephric duct.

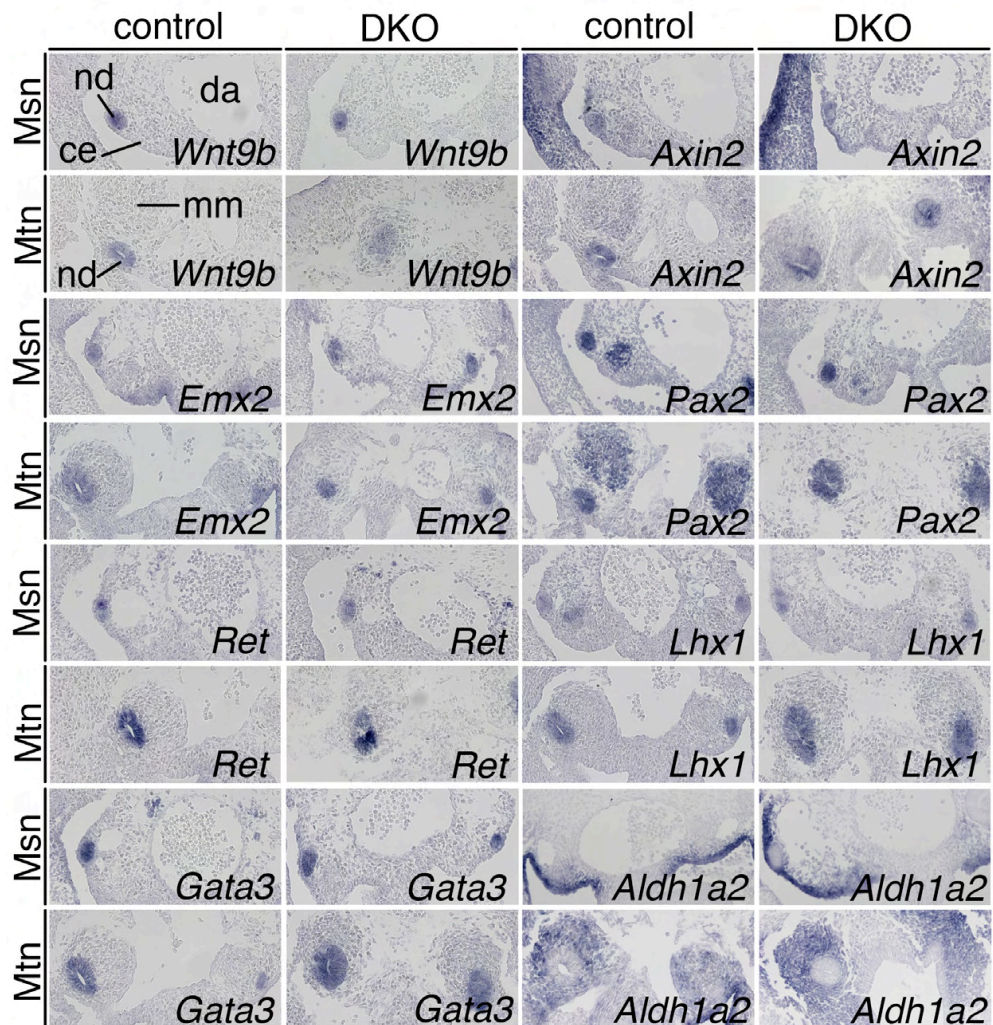


Fig. S9. Expression of ND markers is unchanged on the level of the meso- and metanephros in DKO embryos at E10.5. RNA *in situ* hybridization analysis of transverse sections of the anterior and posterior trunk of E10.5 embryos. Probes and genotypes as indicated. Msn, mesonephros; Mtn, metanephros; ce, coelomic epithelium; da, dorsal aorta; nd, nephric duct; mm, metanephric mesenchyme.

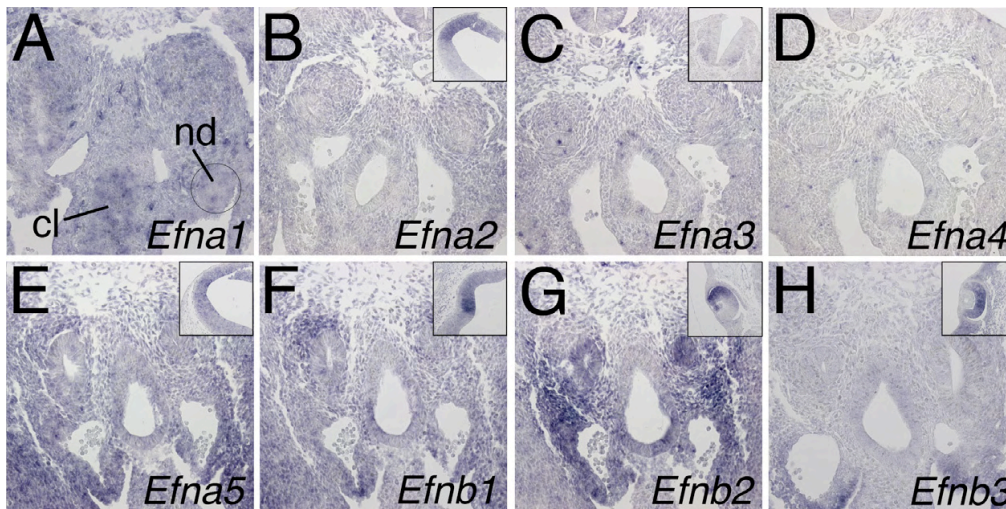


Fig. S10. Ephrin ligand expression in the pericloacal region of wildtype embryos at E10.5. RNA *in situ* hybridization analysis of (A-E) ephrin A (*Efna1-5*) and (F-H) ephrin B (*Efnb1-3*) ligand genes on transverse sections of E10.5 posterior trunks. Control regions eg. brain (B,E,F), neural tube (C) and eye (G,H) are shown in upper right boxes. nd, nephric duct; cl, cloaca.

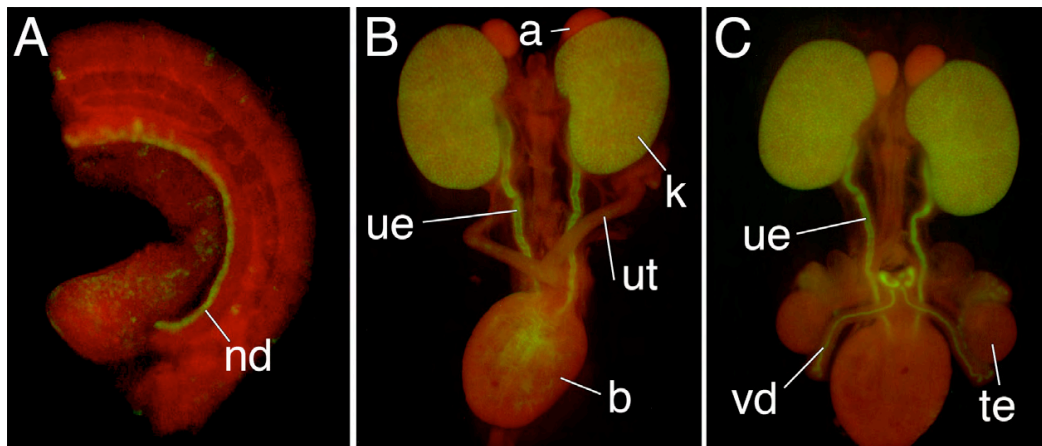


Fig. S11. *Pax2(8.5)-cre* mediates recombination of a reporter allele in the epithelium of nephric duct and its derivatives. (A-C) Analysis of GFP expression by epifluorescence in a whole posterior trunk half of an E10.5 embryo (A) and in E18.5 urogenital systems of male and female *Pax2-cre/+;R26^{mTmG/+}* embryos (B,C). Recombined GFP-positive cells are shown in green, non-recombined RFP-positive cells in red. All epithelial cells of the nephric duct, ureter and collecting duct system are positive for the lineage marker GFP at these stages. a, adrenal; b, bladder; k, kidney; nd, nephric duct; te, testis; ue, ureteric epithelium; ut, uterus; vd, vas deferens.

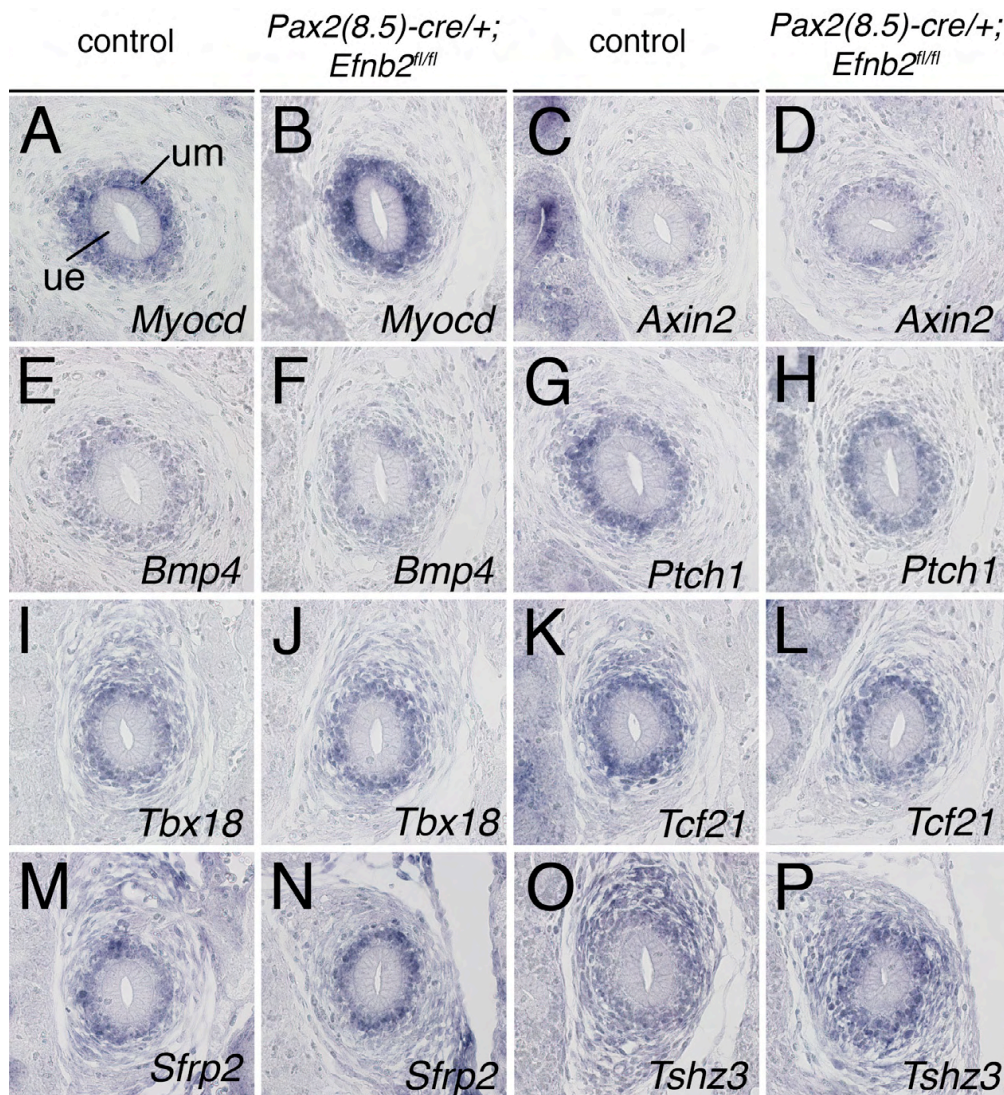


Fig. S12. Markers of the undifferentiated ureteric mesenchyme are unchanged in *Pax2(8.5)-cre/+;Efnb2^{fl/fl}* embryos at E14.5. RNA *in situ* hybridization analysis of transverse sections of the proximal ureter in *Pax2(8.5)-cre/+;Efnb2^{fl/fl}* embryos at E14.5. Probes as indicated. ue, ureteric epithelium; um, ureteric mesenchyme.

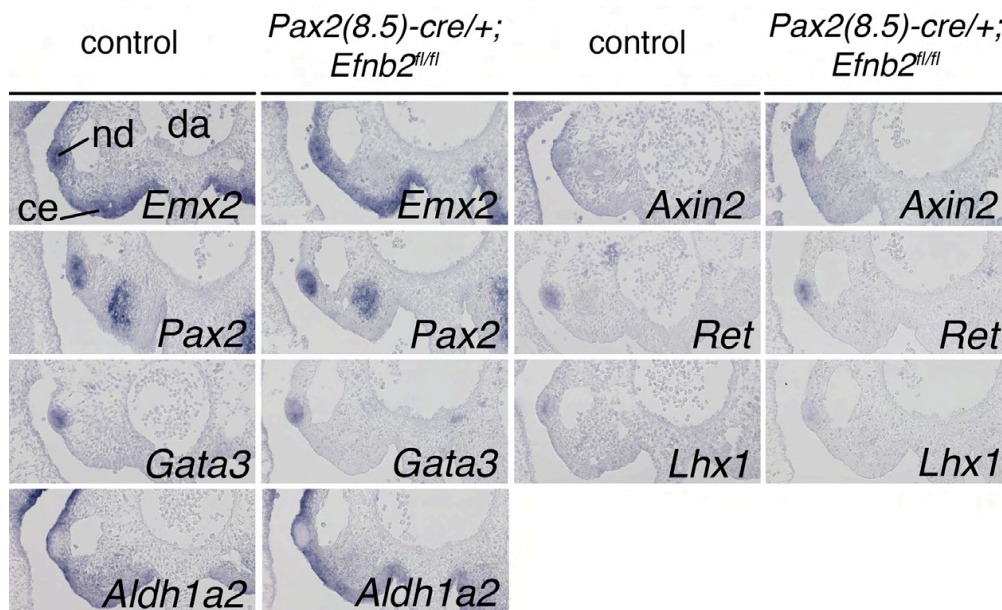


Fig. S13. Expression of ND markers is unchanged on the mesonephros level in *Pax2(8.5)-cre/+;Efnb2^{fl/fl}* embryos. RNA *in situ* hybridization analysis on transverse sections of the anterior trunk of E10.5 embryos. Probes as indicated. da, dorsal aorta; ue, ureteric epithelium; um, ureteric mesenchyme.

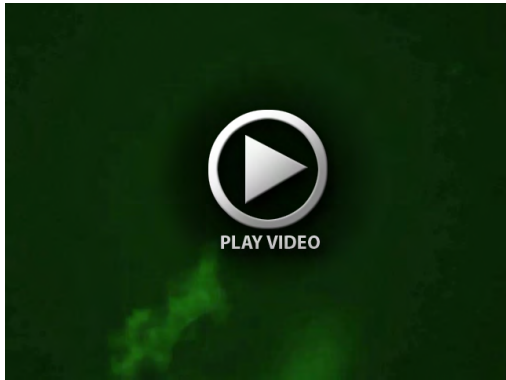
SUPPLEMENTARY TABLES

Genotype		Ratio		Urinary tract malformations				
EphA4	EphA7	predicted	observed	Hydroureter		Megaureter		Hydro/Megaureter
				unilateral	bilateral	unilateral	bilateral	
+/+	+/+	6.25%	0.5%	0% (0/2)	0% (0/2)	0% (0/2)	0% (0/2)	0% (0/2)
+/+	+/-	12.5%	7.3%	0% (0/30)	0% (0/30)	0% (0/30)	0% (0/30)	0% (0/30)
+/+	-/-	6.25%	8.1%	0% (0/33)	0% (0/33)	0% (0/33)	0% (0/33)	0% (0/33)
+/-	+/+	12.5%	2.9%	0% (0/12)	0% (0/12)	0% (0/12)	0% (0/12)	0% (0/12)
+/-	+/-	25%	26.0%	0% (0/108)	0% (0/108)	0% (0/108)	0% (0/108)	0% (0/108)
+/-	-/-	6.25%	28.5%	0% (0/116)	0% (0/116)	0% (0/116)	0% (0/116)	0% (0/116)
-/-	+/+	6.25%	1.9%	0% (0/8)	0% (0/8)	0% (0/8)	0% (0/8)	0% (0/8)
-/-	+/-	12.5%	15.2%	4.8% (3/62)	3.2% (2/62)	9.7% (6/62)	1.6% (1/62)	0 (0/62)
-/-	-/-	6.25%	8.9%	5.6% (2/36)	16.7% (6/36)	13.9% (5/36)	2.8% (1/36)	8.3% (3/36)

Table S1. Frequency of malformations in an *Epha4/Epha7* allelic series at E18.5. Shown are the predicted and observed ratios as well as the percentage and absolute numbers (n=407) of urinary tract malformations of all *Epha4/Epha7* allelic combinations.

Genotype	Predicted ratio	Observed ratio	Urinary tract malformations			Embryos=100	Mutants=17
			Hydroureter unilateral	Hydroureter bilateral	Megaureter unilateral		
							Epididymal cysts
<i>Pax2(8.5)-cre/+; Efnb2^{fl/fl}</i>	12.5 (12.5%)	17 (17%)	2 (12%)	5 (30%)	2 (12%)	1 (6%)	3 (16%)

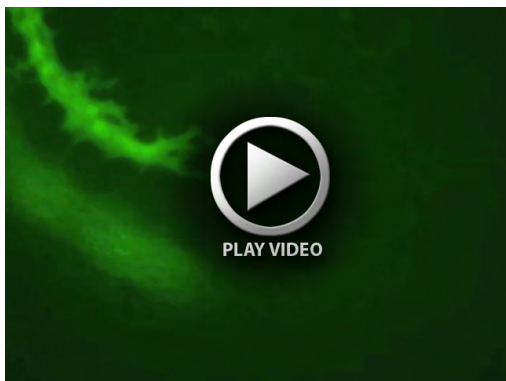
Table S2. Frequency of malformations in *Pax2(8.5)cre/+;Efnb2^{fl/fl}* embryos at E18.5. Shown are the predicted and observed ratios as well as the percentage and absolute numbers (n_{mutants}=17) of urinary tract malformations.



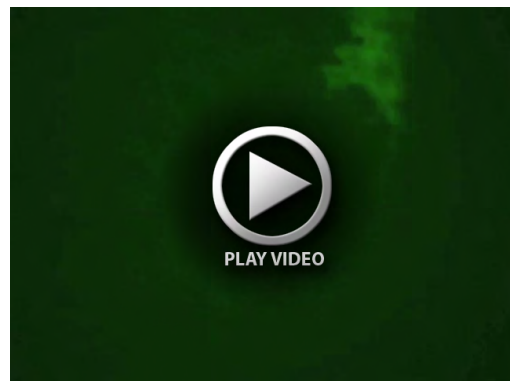
Movie 1A.



Movie 1B.



Movie 2A.



Movie 2B.

Tbx18 expression demarcates multipotent precursor populations in the developing urogenital system but is exclusively required within the ureteric mesenchymal lineage to suppress a renal stromal fate

**Tobias Bohnenpoll^{1,*}, Eva Bettenhausen^{1,*}, Anna-Carina Weiss¹,
Anna B. Foik¹, Mark-Oliver Trowe¹ and Patrick Blank¹, Rannar Airik¹
and Andreas Kispert^{1,§}**

¹Institut für Molekularbiologie, Medizinische Hochschule Hannover, 30625 Hannover, Germany

§Author for correspondence:

Email: kispert.andreas@mh-hannover.de

Tel: +49511 5324017

Fax: +49511532483

* Equal contribution

Published in Developmental Biology (Developmental Biology 380 (2013) 25-36)

Reprinted with permission



Contents lists available at SciVerse ScienceDirect

Developmental Biology

journal homepage: www.elsevier.com/locate/developmentalbiology

Tbx18 expression demarcates multipotent precursor populations in the developing urogenital system but is exclusively required within the ureteric mesenchymal lineage to suppress a renal stromal fate

Tobias Bohnenpoll¹, Eva Bettenhausen¹, Anna-Carina Weiss, Anna B. Foik, Mark-Oliver Trowe, Patrick Blank, Rannar Airik, Andreas Kispert*

Institut für Molekularbiologie, OE5250, Medizinische Hochschule Hannover, Carl-Neuberg-Str. 1, D-30625 Hannover, Germany

ARTICLE INFO

Article history:

Received 11 October 2012

Received in revised form

30 April 2013

Accepted 30 April 2013

Available online 15 May 2013

Keywords:

Tbx18

Cre

Lineage tracing

Ureter

Urogenital system

ABSTRACT

The mammalian urogenital system derives from multipotent progenitor cells of different germinal tissues. The contribution of individual sub-populations to specific components of the mature system, and the spatiotemporal restriction of the respective lineages have remained poorly characterized. Here, we use comparative expression analysis to delineate sub-regions within the developing urogenital system that express the T-box transcription factor gene *Tbx18*. We show that *Tbx18* is transiently expressed in the epithelial lining and the subjacent mesenchyme of the urogenital ridge. At the onset of metanephric development *Tbx18* expression occurs in a band of mesenchyme in between the metanephros and the Wolffian duct but is subsequently restricted to the mesenchyme surrounding the distal ureter stalk. Genetic lineage tracing reveals that former *Tbx18*⁺ cells of the urogenital ridge and the metanephric field contribute substantially to the adrenal glands and gonads, to the kidney stroma, the ureteric and the bladder mesenchyme. Loss of *Tbx18* does not affect differentiation of the adrenal gland, the gonad, the bladder and the kidney. However, ureter differentiation is severely disturbed as the mesenchymal lineage adopts a stromal rather than a ureteric smooth muscle fate. Dil labeling and tissue recombination experiments show that the restriction of *Tbx18* expression to the prospective ureteric mesenchyme does not reflect an active condensation process but is due to a specific loss of *Tbx18* expression in the mesenchyme out of range of signals from the ureteric epithelium. These cells either contribute to the renal stroma or undergo apoptosis aiding in severing the ureter from its surrounding tissues. We show that *Tbx18*-deficient cells do not respond to epithelial signals suggesting that *Tbx18* is required to prepattern the ureteric mesenchyme. Our study provides new insights into the molecular diversity of urogenital progenitor cells and helps to understand the specification of the ureteric mesenchymal sub-lineage.

© 2013 Elsevier Inc. All rights reserved.

Introduction

The urinary system is a multi-component entity consisting of the kidneys, the ureters, the bladder and the urethra that together control the water and ionic balance of the blood by excretion of excess water, solutes and waste products. The urinary system is structurally and functionally tightly associated with the adrenal glands, as well as with the genital system that consists of sexually dimorphic gonads, sex ducts and external genitalia.

A number of studies have begun to identify the progenitor populations, their interaction and the temporal specification of

sublineages for the different components of the urogenital system in the mouse. While the lower parts of the urogenital system including the bladder epithelium, the urethra, and the lower aspect of the vagina derive from an infolding of the endoderm, the cloaca, and its surrounding mesenchyme, most other components are thought to be derivatives of the intermediate mesoderm (Mugford et al., 2008; Wang et al., 2011). Expression of the transcriptional regulator gene *Osr1* is activated broadly within the intermediate mesoderm starting from embryonic day (E) 7.5, and is required for the development of adrenals, gonads, kidneys and sex ducts suggesting that *Osr1* marks the progenitors for all of these components at this stage (James et al., 2006; Wang et al., 2005). Within the urogenital ridge of E9.5-E10.5 embryos, the first sublineages emerge. *Osr1* expression becomes gradually excluded from the (coelomic) epithelium that lines the urogenital ridge and from the epithelial Wolffian duct to be restricted to the

* Corresponding author. Fax: +49 511 5324283.

E-mail address: kispert.andreas@mh-hannover.de (A. Kispert).¹ Equal contribution.

mesenchymal compartment of the intermediate mesoderm, and later at around E10.5, to the most posterior aspect from which all cell types of the metanephros will arise (Mugford et al., 2008). The Wolffian duct epithelium that expresses the transcription factor genes *Lhx1*, *Pax2* and *Gata3* (Grote et al., 2006; Pedersen et al., 2005) contributes exclusively to the vas deferens in the male, the epithelium of the ureter and the collecting duct system of the kidney (Saxen, 1987), whereas the epithelial lining of the ridge harbors a common pool of precursor cells for the gonads and the adrenal glands (Hatano et al., 1996). This adrenogonadal primordium that is marked by expression of the orphan nuclear receptor gene *Sf1* divides between E10–E11 into distinct progenitor populations for the adrenals and gonads (Ikeda et al., 1994; Keegan and Hammer, 2002; Luo et al., 1994). The *Sf1*⁺ cells eventually differentiate into the cortical cells of the adrenal gland, Sertoli and Leydig cells of the testis, and granulosa and theca cells of the ovary (Bingham et al., 2006). At E10.5, signals from the mesenchymal condensation at the posterior end of the intermediate mesoderm, the metanephric blastema, induce the formation of an epithelial diverticulum from the Wolffian duct, the ureteric bud. During further development the ureteric bud invades the metanephric blastema and initiates a program of branching morphogenesis to generate the collecting duct system of the mature kidney. The distal part merely elongates and differentiates into a highly specialized type of epithelium, the urothelium. With each branching event a portion of the metanephric mesenchyme adjacent to the branch tip, is induced by tip signals to condense and undergo a mesenchymal–epithelial transition and form a renal vesicle from which the nephron will mature (for a recent review see (Little and McMahon, 2012)). This cap or metanephrogenic mesenchyme is a self-renewing population of nephron progenitors that expresses the transcription factor genes *Six2* and *Uncx* (Boyle et al., 2008; Karner et al., 2011; Kobayashi et al., 2008; Neidhardt et al., 1997; Self et al., 2006). Nephron progenitors are surrounded by *Foxd1*⁺ mesenchymal cells that will give rise to the stromal cells of the renal capsule, cortex and medulla as well as to mesangial and vascular smooth muscle cells (Hatini et al., 1996; Humphreys et al., 2010; Levinson et al., 2005). Separation of the *Six2*⁺ nephron lineage from the *Foxd1*⁺ stromal lineage within the *Osr1*⁺ precursor pool is thought to occur between E10.5 and E11.5 (Mugford et al., 2008). Finally, *Flk1*⁺ cells within the metanephric mesenchyme may contribute to the renal vasculature system (Gao et al., 2005). While the developmental origin of most of the cell types of the mature kidney has been characterized to an appreciable level, much less is known about the specification of the mesenchymal progenitor pool of the smooth muscle and fibroblast coatings of the ureter and the bladder, and the temporal separation of this lineage from the *Six2*⁺ and *Foxd1*⁺ progenitors of the metanephros. Notably, it has been suggested that stromal cells of the kidney and the ureteric mesenchyme do not actually arise from the intermediate mesoderm but originate in the paraxial and/or tail-bud mesoderm (Brenner-Anantharam et al., 2007; Guillaume et al., 2009).

We have previously shown that the T-box transcription factor gene *Tbx18* marks the undifferentiated ureteric mesenchyme from E12.5 to E14.5. At E11.5, *Tbx18* is expressed in a narrow band of cells between the mesenchyme surrounding the Wolffian duct and the metanephros (Airik et al., 2006). Prior to metanephric development expression of *Tbx18* was also noted in the mesonephros (Kraus et al., 2001). In *Tbx18*^{-/-} mice, descendants of former *Tbx18*-positive cells (short: *Tbx18*⁺ descendants) do not differentiate into smooth muscle cells of the ureter but dislocalize to the kidney and differentiate into fibroblast-like cells. As a consequence, the renal pelvis becomes dramatically enlarged at the expense of the ureter, and hydronephrosis develops at birth (Airik et al., 2006). This suggested that the ureteric mesenchymal lineage is separated

early from other mesenchymal lineages of the renal system, and that separation is disturbed in *Tbx18*-deficient mice. Fate mapping efforts based on a cre knock-in in the *Tbx18* locus harbored on a BAC identified smooth muscle cells of the ureter and the bladder as derivatives of former *Tbx18*⁺ progenitor cells (Wang et al., 2009). However, it remained unclear whether the genomic region covered by the BAC contained all *Tbx18* control elements for specific urogenital expression. Further, we neither know when the ureteric lineage is specified nor do we know the mechanisms by which the ureteric mesenchyme becomes localized around the ureteric epithelium.

Here, we characterize the expression of *Tbx18* in the developing urogenital system. We describe the cell lineages to which *Tbx18*⁺ descendants contribute in the mature urogenital system, and analyze their *Tbx18*-dependency. We investigate the mechanisms that restrict *Tbx18* expression to the ureteric mesenchyme, and provide evidence for the role that *Tbx18* plays within this tissue.

Materials and methods

Mice

R26^{mTmG} (*Gt(ROSA)26Sor^{tm4}(ACTB-tdTomato-EGFP)Luo*) reporter mice (Muzumdar et al., 2007), *Tbx18^{lacZ}* (*Tbx18^{tm3Akis}*), *Tbx18^{GFP}* (*Tbx18^{tm2Akis}*) and *Tbx18^{cre}* (*Tbx18^{tm4}(cre)Akis*) knock-in alleles (Bussem et al., 2004; Christoffels et al., 2006; Trowe et al., 2010) were all maintained on an NMRI outbred background. Embryos for gene expression analysis were derived from matings of NMRI wildtype mice. *Tbx18^{cre/+};R26^{mTmG/+}* mice were obtained from matings of *Tbx18^{cre/+}* males and *R26^{mTmG/mTmG}* females. *Tbx18^{cre/lacZ};R26^{mTmG/+}* mice were obtained from matings of *Tbx18^{cre/+};R26^{mTmG/mTmG}* males and *Tbx18^{lacZ/+}* females. *Tbx18^{GFP/+}* embryos were obtained from matings of *Tbx18^{GFP/+}* males with NMRI females. For timed pregnancies, vaginal plugs were checked in the morning after mating, noon was taken as embryonic day (E) 0.5. Embryos, whole urogenital systems and kidneys were dissected in PBS. For *in situ* hybridization and immunofluorescence analyses specimens were fixed in 4% paraformaldehyde (PFA) in PBS and stored in methanol at -20 °C. Genomic DNA prepared from yolk sacs or tail biopsies was used for genotyping by PCR.

Organ cultures

Explant cultures of embryonic kidneys or urogenital systems were performed as previously described (Airik et al., 2010). The culture medium was replaced every 24 h.

For labeling experiments with the fluorescent carbocyanine dye Dil, a tungsten wire was dipped into the Dil tissue labeling paste (Invitrogen) and excessive material was removed with a tissue towel. The tungsten wire was then clamped into a micromanipulator. Labeling of mesenchymal subpopulations within the metanephric field of E11.5 *Tbx18^{GFP/+}* kidney rudiments was performed under visual control. Kidney explants were documented before and after treatment and the perpendicular distance of labeled cells from the ureteric epithelium was measured using ImageJ software (Schneider et al., 2012). After two days of culture the distribution of Dil labeled cells was assessed and plotted against the distance.

For the detection of apoptotic tissue in the metanephric field E11.5 kidney rudiments (*Tbx18^{GFP/+}*) were explanted and cultured for 24 h. The medium was subsequently replaced with 1 ml of 2.5 μM LysoTracker red DND-99 (L-7528, Invitrogen) in PBS and the explant cultures were incubated for 30 min at 37 °C. Cultures were then rinsed in PBS and documented.

For tissue recombination experiments, E11.5 acceptor kidney rudiments (*Tbx18^{GFP/+}*) were explanted. E12.5 ureters (*Tbx18^{cre/+}*;

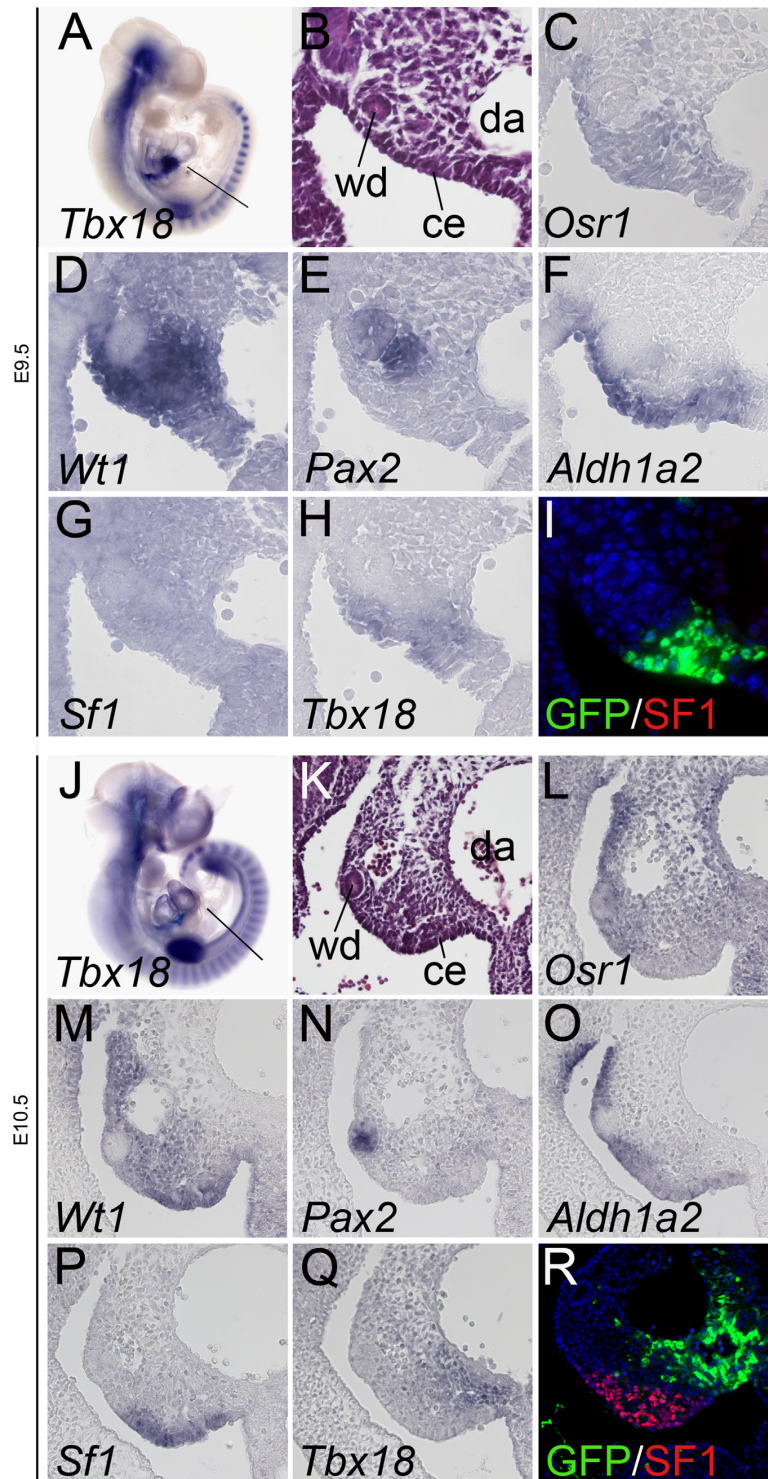


Fig. 1. *Tbx18* expression during early urogenital development: (A,J) *In situ* hybridization analysis of whole wildtype embryos for *Tbx18*: (B,D). Histological staining (HE) of transverse sections through the posterior trunk region on the planes indicated in (A,J) to describe anatomical landmarks. (C–H,L–Q) *In situ* hybridization analysis on adjacent sections to compare expression of *Tbx18* and markers of the intermediate mesoderm. (I,R) Co-immunofluorescence analysis for SF1 and GFP on adjacent sections of *Tbx18*^{GFP/+} embryos. Probes and stages are as indicated. ce: coelomic epithelium; da: dorsal aorta; wd: Wolffian duct.

R26^{mTmG/+} were subsequently prepared and the ureteric epithelium was mechanically separated from the mesenchyme using forceps. The uncoated ureteric epithelium was transplanted into the *Tbx18*⁺ domain of the acceptor tissue distant to the endogenous ureteric epithelium. The recombined tissues were cultured for 3 days with daily documentation.

For bead implantation experiments, E11.5 acceptor kidney rudiments (*Tbx18^{GFP/+}*) were explanted. AffiGel Blue beads (153-7302, Bio-Rad) were rinsed in PBS and incubated with 50 µg/ml rmWNT9B (3669-WN, R&D Systems), 1.6 µg/ml rmSHH (PMC8034, Invitrogen), both or 1 mg/ml BSA for 4 hours at 4 °C. Beads were implanted into the GFP⁺ domain of the acceptor kidneys. Cultures were maintained for 2 days and GFP expression was documented daily.

Histological and histochemical analyses

Fixed embryos were dehydrated, paraffin embedded, and sectioned to 5 µm. For histological analyses sections were stained with haematoxylin and eosin. For the detection of antigens on these sections, the following primary antibodies and dilutions

were used: mouse anti-UPK1B (WH0007348M2-100UG, Sigma, 1:200), mouse anti-ACTA2 (F3777 and C6198, Sigma, 1:200), rabbit anti-CDH1 (kindly provided by R. Kemler, MPI for Immunobiology and Epigenetics, Freiburg, Germany, 1:200), rabbit anti-SF1 (TransGenic Inc., preparation of antibodies by Dr. Ken-Ichirou Morohashi, 1:200), rabbit anti-DDX4 (ab13840, Abcam, 1:50), rabbit anti-FOXD1 (kindly provided by A.P. McMahon, Harvard University, MA, USA, 1:2000), rabbit anti-SIX2 (kindly provided by A.P. McMahon, Harvard University, MA, USA, 1:1000), anti-SOX9 (AB5535, Millipore Chemicon, 1:200), rat anti-EMCN (kindly provided by D. Vestweber, MPI for Molecular Medicine, Münster, Germany, 1:10), mouse anti-GFP (11 814 460 001, Roche, 1:200), rabbit anti-GFP (sc-8334, Santa Cruz, 1:200). Fluorescent staining was performed using Alexa 488/555-conjugated secondary antibodies (A11034; A11008; 711-487-003; A21202; A21422; A21428, Invitrogen/Dianova; 1:500) or biotin-conjugated secondary antibodies (Dianova; 1:500) and the TSA Tetramethylrhodamine Amplification Kit (Perkin-Elmer).

Labeling with primary antibodies was performed at 4 °C overnight after antigen retrieval (Antigen Unmasking Solution, Vector Laboratories; 15 min, 100 °C), blocking of endogenous peroxidases with 3% H₂O₂/PBS for 10 min (required for TSA) and incubation in

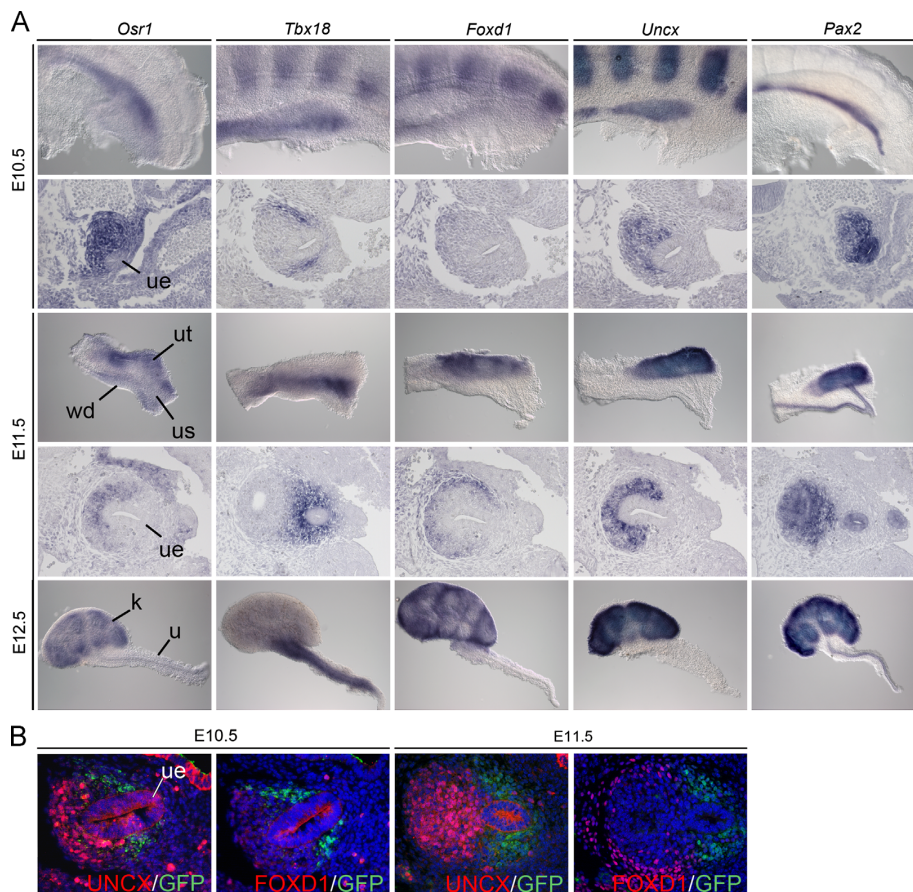


Fig. 2. *Tbx18* expression during early metanephric and ureter development. (A) *In situ* hybridization analysis of whole posterior trunk halves at E10.5 (first row), of transverse sections through the metanephric anlagen of the posterior trunk region at E10.5 (posterior is to the right, ventral to the bottom, second row), of whole E11.5 kidneys (third row), of transverse sections through the E11.5 metanephric kidney (fourth row) and of E12.5 kidneys with ureters (fifth row) to compare expression of *Tbx18* with an early pan-metanephric marker (*Osr1*), and with markers of the nephron lineage (*Uncx*, *Pax2*), of the collecting duct and ureter epithelium (*Pax2*) and of the stromal lineage (*Foxd1*) in wildtype embryos, and (B) Co-immunofluorescence analysis on sections through the metanephros at E10.5 and E11.5 with antibodies against GFP (visualizing TBX18 expression), FOXD1 and UNCX in *Tbx18^{GFP/+}* embryos. k: kidney; u: ureter; ue: ureteric epithelium; us: ureter stalk; wd: Wolffian duct.

blocking solutions provided with the kits. For monoclonal mouse antibodies an additional IgG blocking step was performed using the Mouse-on-Mouse Kit (Vector Laboratories). Sections were mounted with Mowiol (Roth) or IS mounting medium (Dianova).

Paraffin sections used for TUNEL assay were deparaffinized, rehydrated and then treated according to the protocol provided with the Apop Tag Fluorescence Apoptosis detection kit (S7111, Millipore).

In situ hybridization analysis

Whole-mount *in situ* hybridization was performed following a standard procedure with digoxigenin-labeled antisense riboprobes (Wilkinson and Nieto, 1993). Stained specimens were transferred in 80% glycerol prior to documentation. *In situ* hybridization on 10 μ m paraffin sections was done essentially as described (Moorman et al., 2001). For each marker at least three independent specimens were analyzed.

Image analysis

Whole-mount specimens were photographed on Leica M420 with Fujix digital camera HC-300Z, sections on Leica DM5000 B with Leica digital camera DFC300 FX. All images were processed in Adobe Photoshop CS4.

Results

Tbx18 is expressed in a subregion of the urogenital ridge

Earlier work showed expression of *Tbx18* in the urogenital ridge but failed to delineate the precise subdomain (Kraus et al., 2001). We therefore performed comparative *in situ* hybridization analysis of expression of *Tbx18* and of markers of (subregions of) the urogenital ridge on transverse sections of E9.5 and E10.5 wildtype embryos (Fig. 1). At E9.5, the entire urogenital ridge was marked by expression of *Osr1* and *Wt1*; the Wolffian duct by expression of *Pax2*, the adjacent tubule-forming mesonephric mesenchyme by *Pax2*, and the epithelial (coelomic) lining of the ridge by *Aldh1a2*. *Sf1* was not expressed at this stage. *Tbx18* expression was never detected in the epithelial Wolffian duct and the *Pax2*⁺ mesonephric mesenchyme but was present in the more medially located mesenchyme close to the dorsal aorta, and overlapping with *Aldh1a2* expression in the coelomic epithelium (Fig. 1C H). At E10.5, the coelomic epithelium of the urogenital ridge was positive for *Sf1* and *Aldh1a2*, and the Wolffian duct for *Pax2* expression. *Osr1* was confined to the mesenchymal compartment of the intermediate mesoderm. *Tbx18* was found in a subregion of the *Osr1*⁺ mesenchyme in the medial aspect close to the hinge between the urogenital ridge and the dorsal mesenterium, complementary to *Wt1* that was expressed in the epithelium and the lateral mesenchyme. Expression of *Tbx18* was no longer detected

in the epithelial lining of the ridge that was positive for *Sf1* at this stage (Fig. 1K Q). Co-immunofluorescence analysis for GFP and SF1 (in *Tbx18*^{GFP/+} embryos) confirmed the expression domain of *Tbx18*

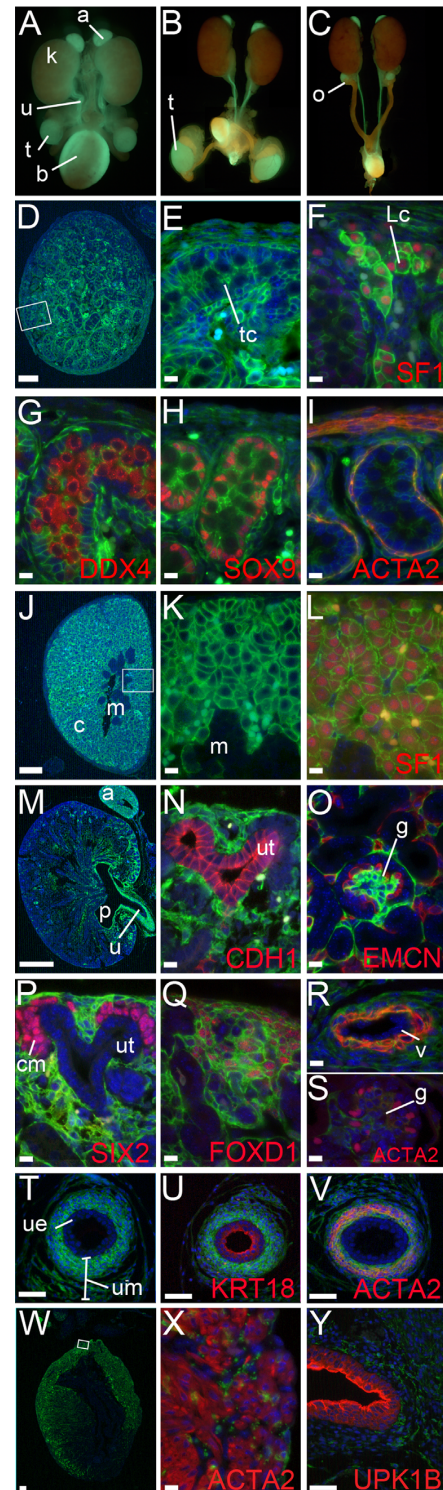


Fig. 3. Lineage analysis of *Tbx18*⁺ descendants in the urogenital system. (A–C) GFP/RFP epifluorescence analysis of urogenital systems from *Tbx18*^{cre/+};*R26*^{mTmG/+} embryos at E18.5 (A) and at 3-weeks of age (B, C) of both male (A, B) and female sex (C). GFP (green) marks *Tbx18*⁺ cells and their descendants, RFP (red) marks all other cells in the urogenital system. (D–Y) Immunofluorescence analysis of expression of the lineage marker GFP on sections of E18.5 testis (D–I), adrenal gland (J–L), kidney (M–S), ureter (T–V) and bladder (W–Y). Boxed areas are magnified for co-expression analysis of GFP and cell type markers as indicated. Scale bars represent 100 μ m (D, J), 500 μ m (M, W), 50 μ m (T–V, Y), 10 μ m (E–I, K, L, N–S, X). a: adrenal gland; b: bladder; c: cortex; cm: cap mesenchyme; g: glomerulus; k: kidney; Lc: Leydig cell; m: medulla; p: pelvis; t: testis; tc: testis cord; u: ureter; ue: ureteric epithelium; um: ureteric mesenchyme; ut: ureter tip; v: vessel. (For interpretation of the references to color in this figure legend, the reader is referred to the web version of this article.)

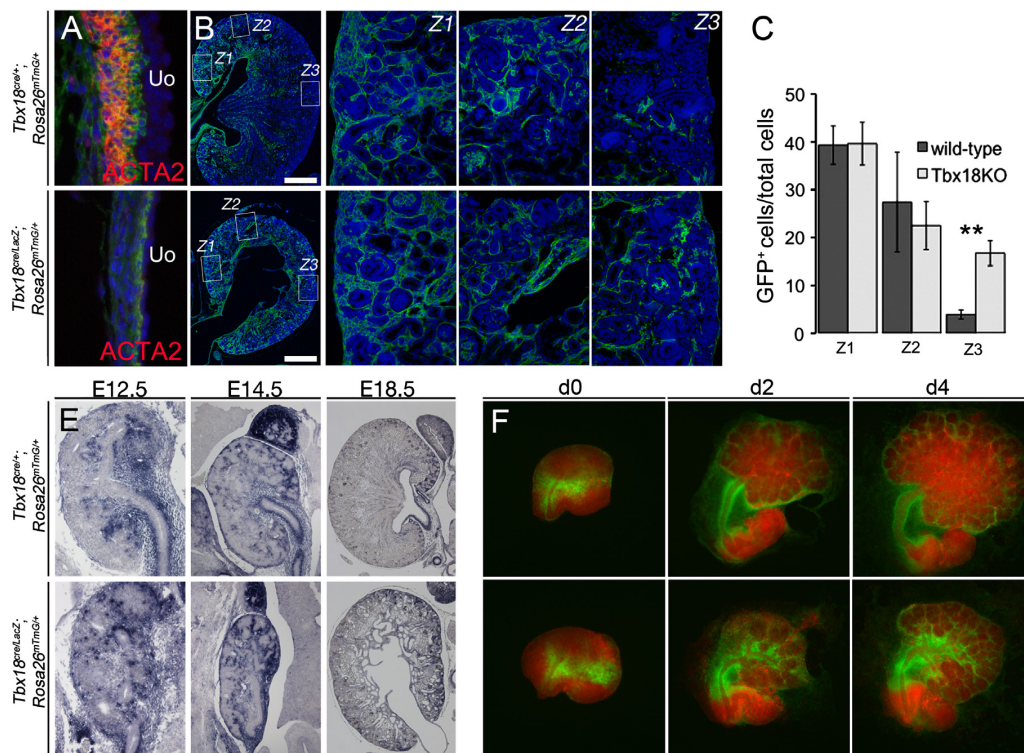


Fig. 4. Lineage analysis of *Tbx18*⁺ descendants in the metanephric/ureteric development. (A) Co-immunofluorescence analysis of expression of the lineage marker GFP and the marker of smooth muscle cells, ACTA2 on sagittal sections of the ureter at E18.5. (B) Co-immunofluorescence analysis of expression of the lineage marker GFP on sagittal sections of the kidney at E18.5. Z1–3 relate to three regions used to determine the contribution of GFP⁺ cells. (C) Quantification of the contribution of GFP⁺ cells to stromal cells in the three regions of the kidney. Z1: control: 39+/-4, mutant: 40+/-4, $p=0.935$; Z2: control: 27+/-10, mutant: 23+/-5, $p=0.504$; Z3: control: 4+/-1, mutant: 17+/-3, $p=0.001$. (D) *In situ* hybridization analysis of GFP expression in *Tbx18*^{cre/+}; *R26*^{mTmG/+} kidneys at different developmental stages as indicated. (E) GFP/RFP epifluorescence analysis of metanephric explants from E11.5 *Tbx18*^{cre/+}; *R26*^{mTmG/+} embryos at 0, 2 and 4 days of culture. GFP (green) marks *Tbx18*⁺ cells and their descendants, RFP (red) marks all other cells in the explants. a: adrenal; k: kidney; u: ureter; ut: ureter tip. (For interpretation of the references to color in this figure legend, the reader is referred to the web version of this article.)

at both stages and the exclusion from SF1⁺ cells (Fig. 11.R). Hence, *Tbx18* is expressed transiently in the coelomic epithelium and in a mesenchymal subdomain of the urogenital ridge.

Tbx18 is expressed in a mesenchymal subregion of the metanephric field before it is restricted to the ureteric mesenchyme

Our previous work showed that during metanephric development *Tbx18* is expressed in a narrow band of mesenchymal cells abutting the mesenchyme of the Wolffian duct and the metanephric kidney at E11.5 before expression becomes confined to the mesenchyme surrounding the ureter from E12.5 onwards (Airik et al., 2006). To determine the onset of *Tbx18* expression in the mesenchymal cells of the metanephric anlage (the metanephric field) and define the relationship to the precursor populations of known metanephric cell lineages, we performed *in situ* hybridization analysis of whole kidney rudiments as well as of adjacent sections through the posterior trunk at E10.5 and E11.5. At each stage, we compared expression of *Tbx18* to that of *Foxd1*, a marker for the stromal lineage of the metanephros (Hatini et al., 1996), to that of *Uncx*, a marker for the cap mesenchyme (Karner et al., 2011), to *Pax2* which marks the cap mesenchyme as well as the Wolffian duct and its epithelial outgrowths (Dressler et al., 1990), and to *Osr1* (Mugford et al., 2008; So and Danielian, 1999).

At E10.5, *Osr1* expression encompassed the mutually exclusive domains of *Tbx18* and *Uncx/Pax2*. Expression of *Foxd1* was scarcely detectable at this stage. At E11.5, *Foxd1* expression surrounded in a

circle-like fashion the cap mesenchyme that was positive for *Osr1*, *Uncx* and *Pax2*. *Tbx18* expression surrounded the ureter stalk in an exclusive fashion. At E12.5, *Tbx18* was restricted to the mesenchyme surrounding the distal ureter whereas expression of *Foxd1* and *Uncx/Pax2/Osr1* was restricted to the stromal and the cap mesenchyme of the kidney, respectively (Fig. 2A). Immunofluorescence analysis of GFP (visualizing TBX18) and FOXD1/UNCX expression on transverse sections of E10.5 and E11.5 *Tbx18*^{GFP/+} embryos confirmed that TBX18 protein was not co-expressed with either of these markers (Fig. 2B). These data show that *Tbx18* expression defines a molecularly distinct sub-population of mesenchymal cells in the early metanephric field.

Tbx18⁺ cells of the urogenital ridge and the early metanephric field contribute to multiple components of the mature urogenital system

To determine the contribution of *Tbx18*⁺ cells in the urogenital ridge and the early metanephric field to the components of the mature urogenital system, we irreversibly labeled the descendants of these populations using a *cre/loxP*-based genetic approach with a *Tbx18*^{cre}-line generated in our laboratory and the sensitive *Rosa26*^{mTmG} reporter (Muzumdar et al., 2007; Trowe et al., 2010). In the *Rosa26*^{mTmG} reporter line cells that have undergone recombination express membrane-bound GFP while non-recombined cells express membrane-bound RFP.

In E18.5 and 3-week old whole urogenital systems, GFP epifluorescence was found in the gonads, the kidneys, the ureters,

the bladder and additionally in the adrenals that are associated with the urogenital system (Fig. 3A–C). To characterize the contribution of *Tbx18*⁺ descendants to the differentiated cell types in these organs, we performed co-immunofluorescence analysis with antibodies directed against GFP and cell-type specific markers on sections of E18.5 *Tbx18*^{cre/+};*Rosa26*^{mTmG/+} embryos. In the testis, GFP expression was found in the tunica albuginea, interstitium and testis cords in a dorsal to ventral gradient (Fig. 3D). Coexpression analysis with cell-type specific markers showed that *Tbx18*⁺ descendants contributed to Leydig cells in the interstitium (SF1) (Luo et al., 1994), to most but not all Sertoli cells (SOX9) (Morais da Silva et al., 1996), to smooth muscle cells of the tunica albuginea (ACTA2) but not to germ cells (DDX4) (Fujiwara et al., 1994) (Fig. 3E–I). In adrenals, GFP⁺ cells were restricted to the SF1⁺ steroidogenic cells of the cortex (Luo et al., 1994) (Fig. 3J–L). Compatible with the notion that *Tbx18*⁺ descendants contribute to steroidogenic cells of the gonad and the adrenal gland, we observed coexpression of the lineage marker GFP with SF1, a marker for the adrenogonadal precursor pool (Bingham et al.,

2006), in the coelomic lining of E10.5 *Tbx18*^{cre/+};*Rosa26*^{mTmG/+} embryos (Supplementary Fig. S1).

In E18.5 kidneys, the distribution of GFP expression appeared graded being more prominent at the medial (where *Tbx18*⁺ cells originally resided) than at the lateral side of the organ (Fig. 3M). In the medial region of the kidney, GFP expression was excluded from cells expressing the epithelial marker CDH1 (Vestweber et al., 1985), the endothelial marker EMCN (Morgan et al., 1999), and the cap mesenchyme marker SIX2 (Karner et al., 2011; Self et al., 2006) indicating that *Tbx18*⁺ descendants do not contribute to the collecting duct system, the endothelial network of the kidney, or the nephron lineage, respectively (Fig. 3N–P). Coexpression in the cortical stroma with FOXD1 and with the smooth muscle marker ACTA2 in arteries and in glomeruli argue that a substantial fraction of interstitial cells, vascular smooth muscle and mesangial cells in the medial kidney region derive from *Tbx18*⁺ progenitors (Fig. 3Q–S). In the ureter, all cells of the mesenchymal coating (fibroblasts of the lamina propria, smooth muscle cells and adventitial fibroblasts) expressed GFP confirming earlier results

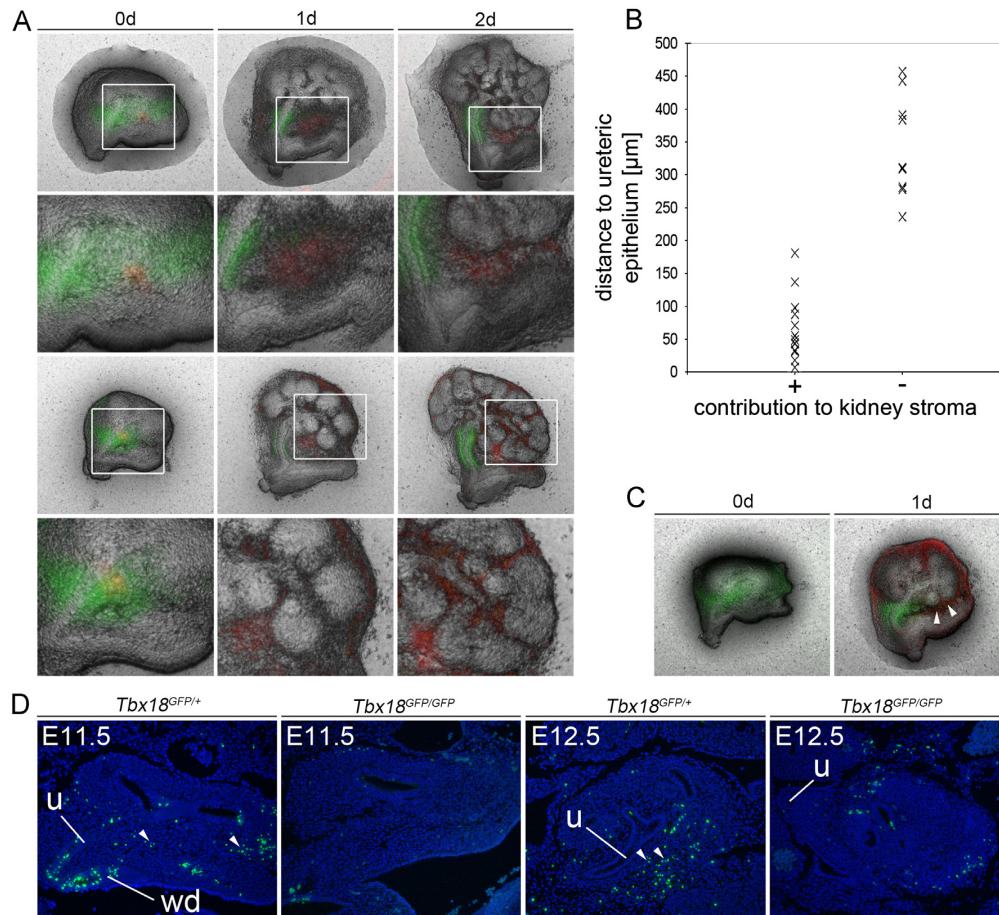


Fig. 5. Lineage analysis and apoptosis of *Tbx18*⁺ mesenchymal cells in early kidney rudiments. (A) Combined brightfield and epifluorescence analysis of metanephric explants from E11.5 *Tbx18*^{GFP/+} embryos at 0, 1 and 2 days of culture. GFP (green) marks the *Tbx18* expression domain, the red fluorescence indicates Dil-injected cell clusters. Shown are two representative examples of Dil-injected cells ending up in the renal stroma (upper row), and of cells localizing to the space between kidneys and the Wolffian duct (lower row). Boxed regions are shown in higher magnifications below. (B) Quantitative evaluation of localization of Dil-injected cells in dependence from the distance from the ureteric epithelium at E11.5. (C) Analysis of cell death by lysotracker staining in explants of E11.5 kidney rudiments from *Tbx18*^{GFP/+} embryos cultured for 0 and 1 day. Arrows point to cell death in the lateral ureteric mesenchyme. (D) Analysis of cell death by the TUNEL assay in E11.5 and E12.5 kidneys rudiments from *Tbx18*^{GFP/+} and *Tbx18*^{GFP/GFP} embryos. Arrows point to cell death in the lateral ureteric mesenchyme. u, ureter; Wd, Wolffian duct. (For interpretation of the references to color in this figure legend, the reader is referred to the web version of this article.)

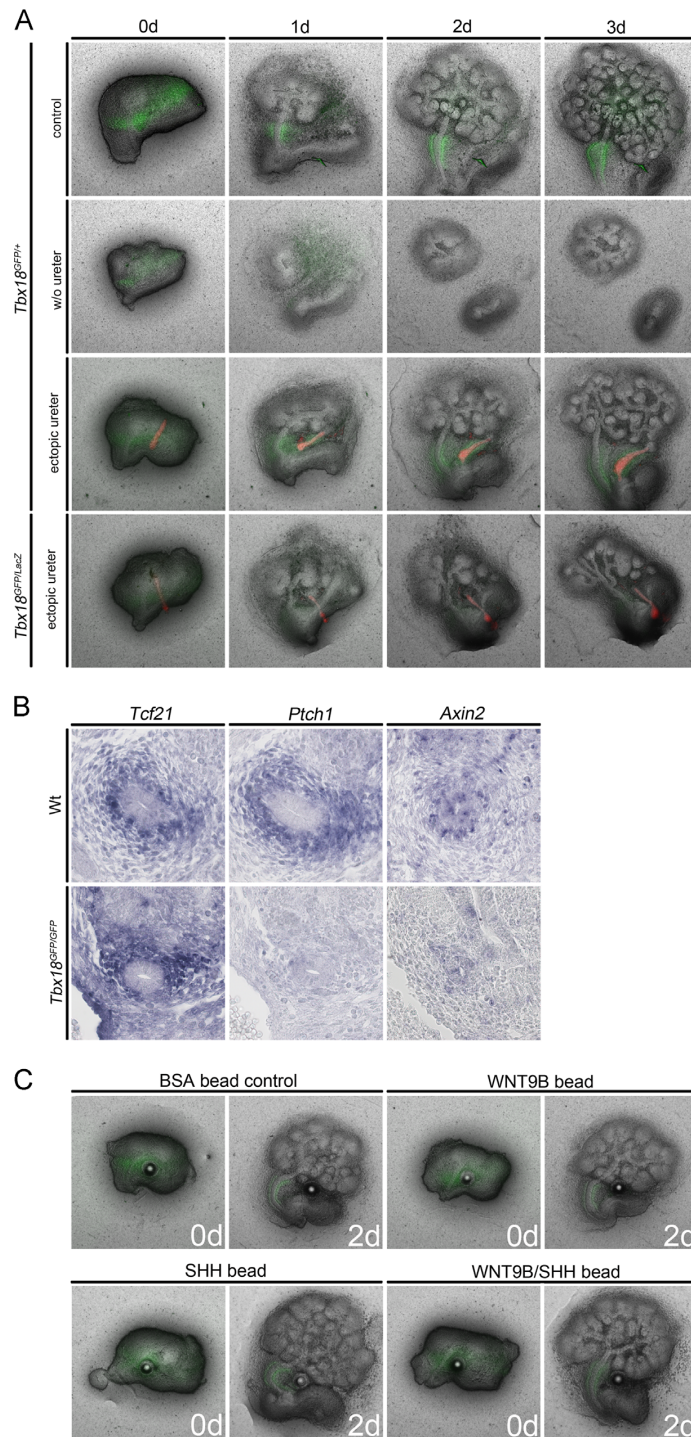


Fig. 6. Regulation of *Tbx18* expression and ureteric fates by signals from the ureteric epithelium. (A) Combined brightfield and GFP/RFP epifluorescence analysis of E11.5 metanephric explants from E11.5 *Tbx18*^{GFP/+} embryos at 0, 1, 2 and 3 days of culture; GFP (green) marks *Tbx18*⁺ cells in unmanipulated cultures (control), in cultures from which the ureter was removed (w/o ureter); after transplantation of an RFP⁺ (red) *R26*^{mTmG/+} ureter stripped of mesenchymal cells into the distal domain of *Tbx18*⁺ cells (ectopic ureter) in *Tbx18*^{GFP/+} and *Tbx18*^{GFP/Δex2} rudiments. (B) *In situ* hybridization analysis of transverse ureter sections of E12.5 control (wt) and *Tbx18*^{GFP/GFP} embryos of expression of *Tcf21*, of the target of SHH-signaling, *Ptch1*, and of the target of canonical WNT-signaling, *Axin2*. (C) GFP epifluorescence analysis of explants from E11.5 *Tbx18*^{GFP/+} embryos cultured for 0 and 2 days in the presence of BSA-, WNT9B-, SHH- or WNT9B/SHH-soaked beads. (For interpretation of the references to color in this figure legend, the reader is referred to the web version of this article.)

of our group that the ureteric mesenchyme completely derives from *Tbx18*⁺ mesenchymal cells (Fig. 3T–V) (Trowe et al., 2012). In the bladder, GFP expression was graded from dorsal to ventral within the smooth muscle cell layer but was absent from the urothelium (Fig. 3W–Y).

We conclude, that *Tbx18*⁺ cells in the developing urogenital system are multipotent and contribute to all mesenchymal cell types in the ureter but also to a large degree to the stromal, mesangial and smooth muscle cells of the medial region of the kidney, to the bladder mesenchyme, to the cortical steroidogenic cells of the adrenal gland and to somatic cells of the gonads.

Tbx18 is required for ureteric differentiation of mesenchymal cells

Our previous analysis has shown that *Tbx18* is required for differentiation of the ureteric mesenchyme into smooth muscle cells but has not addressed a critical involvement of the gene in the development of the other organs of the urogenital system, to which *Tbx18*⁺ descendants largely contribute. We, therefore, analyzed *Tbx18*-deficient embryos (*Tbx18*^{cre/lacZ}; *R26*^{mTmG/+}) at E18.5, i.e. shortly before these mice die due to skeletal defects, for histological and molecular changes in the development of these organs. Analysis of the adrenal gland by histological staining, co-immunofluorescence of the lineage marker GFP and the marker of steroidogenic cells SF1, and quantification of GFP⁺ cells in the cortex did not detect any difference in the distribution and differentiation of *Tbx18*⁺ descendants in wildtype and *Tbx18*-deficient adrenals at this stage. Expression of *Akr1c18* and *Cyp11b1*, markers of the inner cortical layer (Lalli, 2010), and of *Wnt-4*, a marker of the outer cortical layer (Heikkilä et al., 2002), was unaffected in the mutant showing that zonation into medulla and inner and outer cortex occurred normally (Supplementary Fig. S2). Histological staining and co-expression analysis with subsequent quantification of the previously used differentiation markers SOX9 (Sertoli cells), DDX4 (germ cells), and SF1 (Leydig cells) did not detect any difference between wildtype and *Tbx18*-deficient testes at this stage either (Supplementary Fig. S3). Differentiation of mesenchymal and epithelial lineages was also unaffected in the bladder and the kidney in the absence of *Tbx18* (Supplementary Figs. S4,S5).

However, in the kidney, the contribution of GFP⁺ cells to both the medullary and cortical stroma on the lateral side was enhanced, whereas the few GFP⁺ cells of the ureter failed to differentiate into smooth muscle cells (Fig. 4A–C). *In situ* hybridization of the lineage marker *Gfp* on sections of kidneys of earlier stages revealed that *Tbx18*⁺ descendants dislocalized laterally onto the kidney as early as E12.5 (Fig. 4D). To further visualize the altered contribution to stromal cells in *Tbx18*-deficient kidneys, we explanted E11.5 metanephric rudiments and followed the GFP epifluorescence in culture (Fig. 4E). In the control (*Tbx18*^{cre/+}; *R26*^{mTmG/+}) GFP⁺ cells localized to the ureteric mesenchyme and the stromal cells of the kidney particularly those of the medial cortex. In *Tbx18*-deficient embryos (*Tbx18*^{cre/lacZ}; *R26*^{mTmG/+}), GFP expression was reduced around the short ureter but strongly enhanced in the medullary stroma around the distorted pelvic region. Of note, GFP⁺ cells now surrounded branching ureteric epithelium unlike in the control (Fig. 4E). We conclude from this analysis that *Tbx18* is required in uncommitted precursor cells to adopt the ureteric fate. In absence of *Tbx18* these cells contribute to the renal stroma.

A spatially restricted subset of Tbx18⁺ mesenchymal cells contributes to the definite ureteric mesenchyme after E11.5

As *Tbx18* is exclusively required within the ureteric mesenchymal lineage, we wished to learn about the mechanisms that

confine *Tbx18* expression in the early metanephric field, and suppress the stromal in favor of the ureteric mesenchymal fate. To determine whether *Tbx18*⁺ cells of the early metanephric field contribute randomly or in a spatially defined manner to the ureteric mesenchyme, we isolated kidney rudiments of E11.5 *Tbx18*^{GFP/+} embryos and explanted them onto filter membranes. The red fluorescent dye Dil was injected at defined distances from the ureteric epithelium onto small cell clusters within the *Tbx18*⁺ domain (as visualized by GFP fluorescence from the *Tbx18*^{GFP} allele) and the distribution of the red fluorescence was determined after 2 days (Fig. 5A, Supplementary Fig. S6). Two outcomes were observed: Dil injected into mesenchymal cells in a distance of up to 200 μm from the ureteric epithelium contributed to the kidney stroma whereas Dil injected more distally ended up as an amorphous mass in between the Wolffian duct and the kidney. Localization of Dil⁺ cells to the GFP⁺ ureteric mesenchyme was never observed (Fig. 5B). Lysotracker staining of E11.5 metanephric rudiments explanted for 1 day detected apoptotic cells in the lateral domain of the ureteric mesenchyme that had lost *Tbx18* expression at this time but not in those adjacent to the ureteric epithelium (Fig. 5C). To exclude a culture artefact, we also analyzed apoptosis by TUNEL staining in sections of E11.5 and E12.5 embryos. At both stages we detected apoptosis in mesenchymal cells lateral to but not adjacent to the short ureter stalk. Intriguingly, apoptosis in this domain was completely lost in *Tbx18*-deficient embryos (Fig. 5D).

We conclude that only a minor fraction of the mesenchymal cells initially positive for *Tbx18* contribute to the definite ureteric mesenchyme, most likely those in direct proximity to the epithelium (that we were unable to label by this technique). Cells within a 200-μm range of the ureteric epithelium contribute to the kidney stroma whereas cells further away undergo apoptosis. In *Tbx18*-deficient embryos, lateral *Tbx18*⁺ descendants fail to undergo apoptosis but may additionally contribute to the renal stroma.

Epithelial signals impose a ureteric fate onto Tbx18⁺ cells

Given the finding that only cells in direct vicinity of the ureteric epithelium are likely to contribute to the definitive ureteric mesenchyme, we wished to test the role of epithelial signals in maintaining *Tbx18* expression and directing a ureteric fate to cells in the early metanephric field, and performed tissue recombination experiments in cultured explants of metanephric rudiments of E11.5 *Tbx18*^{GFP/+} embryos (Fig. 6A). In a control experiment, GFP expression was confined to the mesenchymal tissue layer covering the ureteric epithelium after 3 days of culture. Removal of the ureter from E11.5 kidney explants resulted in a dispersal of GFP⁺ cells and their complete loss after 3 days. We then transplanted an RFP-labeled ureteric epithelium (obtained from E12.5 *R26*^{mTmG/+} embryos) into the *Tbx18*⁺ domain in a position distant from the ureteric epithelium of the host tissue. Interestingly, GFP expression was maintained in the lateral mesenchyme and GFP⁺ cells accumulated around the ectopic RFP⁺ ureteric epithelium. In contrast, when a RFP-labeled ureteric epithelium was transplanted into the lateral GFP⁺ domain of kidney explants of E11.5 *Tbx18*^{GFP/lacZ} embryos, GFP⁺ cells did not accumulate around the ectopic ureter (Fig. 6A). Together, these results strongly suggest that epithelial signals are required and sufficient to maintain *Tbx18* expression and to impose a ureteric fate onto *Tbx18*⁺ cells. Epithelial signals do not act in a distance to induce a condensation process but merely seem to impinge onto the adjacent layer of mesenchymal cells. In absence of *Tbx18*, mesenchymal cells can no longer respond to signals from the ureteric epithelium.

We have recently shown that canonical (*Ctnnb1*-dependent) WNT signaling is required to maintain *Tbx18* expression and induce smooth muscle differentiation in the ureteric mesenchyme

(Trowe et al., 2012). The latter process also requires SHH signals from the epithelial compartment (Yu et al., 2002). In *Tbx18*-deficient ureters, *Tcf21*⁺-mesenchymal cells surrounding the ureter did not express *Axin2* and *Ptch1*, targets of the canonical WNT- and SHH-signals that are secreted from the epithelial compartment in the mutant (Fig. 6B). We conclude that *Tbx18* is required in uncommitted precursor cells to respond to epithelial signals and to adopt the ureteric fate.

To address the question whether WNT and/or SHH signals are sufficient to maintain *Tbx18* expression in the lateral domain in which it is lost after E11.5, we explanted E11.5 kidney rudiments and implanted beads soaked with SHH and/or WNT9B protein (*Wnt9b* is co-expressed with *Wnt7b* in the ureteric epithelium) into this domain (Trowe et al., 2012). Neither BSA control nor WNT9B-, SHH- or WNT9B/SHH-beads maintained GFP, i.e. *Tbx18* expression, in the lateral domain (Fig. 6C), arguing that WNTs cooperate with other as yet unknown epithelial signals to maintain *Tbx18* expression and possibly determine the ureteric fate.

Discussion

Tbx18⁺ progenitors contribute to multiple cell types in the urogenital system

We have demonstrated that descendants of *Tbx18*⁺ cells contribute to a variety of cell types within the urogenital system including cells within the gonads, the kidney, ureter, bladder and adrenal gland. Our expression analysis together with the genetic lineage tracing of *Tbx18*⁺ cells argue that cellular contribution to the adrenal gland and gonads on one hand and to the kidney, ureter and bladder on the other hand reflect two independent expression domains of *Tbx18*; one in the urogenital ridge and the other one in the metanephric field, and that the latter represents a novel subpool of progenitors from which the ureteric mesenchyme will eventually arise.

Transient expression in the epithelial lining of the urogenital ridge around E9.5 is likely to present a common precursor pool for the gonads and the adrenals. In fact, the contribution to interstitial, Sertoli and tunica albuginea cells in the gonad and steroidogenic cells of the adrenal cortex is virtually identical to that identified by a genetic approach based on expression of *Sf1*, a marker for this primordium (Bingham et al., 2006). *Tbx18* expression in the epithelial lining of the ridge is transient and seems to slightly precede that of *Sf1* in this domain. Compatible with expression in the unseparated progenitor pool for both tissues, we recently noted sex reversal and loss of adrenals in mice with conditional *Tbx18*^{cre}-mediated deletion of *Ctnnb1* (Trowe et al., 2012). In fact, identical phenotypes were observed upon an *Sf1*^{cre}-mediated deletion of this mediator of the canonical branch of WNT signaling in mice (Kim et al., 2008; Liu et al., 2009). At this point, we do not have the technical means to independently evaluate the contribution of the mesenchymal expression domain of *Tbx18* in the early urogenital ridge. However, since this domain does not overlap with *Pax2* in the mesonephros, we suggest that it does not mark progenitors for mesonephric tubules but for stromal cells that are associated with these structures.

In contrast to our initial expectations, we found that the *Tbx18*⁺ cells that are located in the metanephric field between the mesenchymal populations of the metanephros and the Wolffian duct, are not yet specified to a ureteric mesenchymal fate but are a multipotent population that contributes to interstitial cells of the kidney (cortical and medullary stromal cells, mesangial cells and vascular smooth muscle cells), to all mesenchymal cells of the ureter and to a subset of smooth muscle cells of the bladder. Most notably, our expression analysis as well as the fate mapping clearly

shows that the *Tbx18*⁺ lineage is at all time points separated from the *Six2*⁺*Uncx*⁺ progenitors from which nephrons will develop. *Tbx18* expression does not overlap with the stromal marker *Foxd1* at E11.5. However, *Foxd1* is not expressed at E10.5 in the metanephric field strongly suggesting that *Tbx18* expression at this stage encompasses progenitors of renal stromal cells as well as of the ureteric mesenchyme. Hence, within the *Osr1*⁺ metanephric field two lineages are established at E10.5: the *Six2*⁺*Uncx*⁺ nephron lineage and the *Tbx18*⁺ lineage of kidney stromal cells/ureter and bladder mesenchyme. Between E10.5 and E11.5 the *Tbx18*⁺ and *Foxd1*⁺ lineages are completely separated. *Tbx18*⁺ cells lying in direct proximity to the ureteric epithelium will maintain *Tbx18* and differentiate into all mesenchymal cell types of the ureter. Cells which lose *Tbx18* expression will either die or contribute to the renal stroma and the bladder mesenchyme. Due to lack of appropriate markers and adequate culture settings we cannot firmly state when the mesenchymal lineages of the ureter and bladder separate but assume that it occurs around the same time.

Tbx18-Cre cell lineage tracing with a BAC-based approach recently reported contribution of *Tbx18*⁺ descendants to smooth muscle cells of the bladder and the ureter in the mature urogenital system. The more restricted contribution in this genetic setting may relate to a less sensitive detection system used but more likely reflects the lack of regulatory elements in the BAC used for construction of a *Tbx18-Cre* transgene (Wang et al., 2009). Our *Tbx18*^{cre} allele was constructed by inserting a *cre* orf into the start codon of the *Tbx18* locus (Trowe et al., 2010). Analysis of *cre* expression in the urogenital system as well as at extrarenal sites showed that expression of *cre* faithfully mimics endogenous expression of *Tbx18* strongly arguing that all control elements of *Tbx18* are preserved and direct appropriate expression of *cre* from this allele (Christoffels et al., 2009; Trowe et al., 2012). Furthermore, the sensitive *Rosa26*^{mTmG} reporter line allows a cellular resolution of all recombination events. Hence, we are convinced that our genetic lineage tracing system is technically sound and provides a true image of the widespread distribution of *Tbx18*⁺ descendants in the urogenital system.

Tbx18⁺ cells do not condense to form the definitive ureteric mesenchyme

We previously suggested that the band of *Tbx18*⁺ mesenchymal cells in the E11.5 metanephric field condenses around the ureteric epithelium to form the definite ureteric mesenchyme until E12.5. Our genetic lineage tracings as well as our Dil injection in the *Tbx18*⁺ domain at E11.5 contradict this “condensation” model but suggest that only a minor fraction of the cells initially positive for *Tbx18* become the precursors for smooth muscle cells and fibroblasts of the ureter. In fact, the majority of cells in this domain switch off *Tbx18* expression, and depending on the distance from the ureter contribute to the kidney stroma (the more proximal ones) or localize to the tissue in between the kidney and the Wolffian duct (the more distal ones). The latter population undergoes apoptosis, a process that may aid in severing the connections between the two organs. Only the few cells in proximity to the ureteric epithelium maintain *Tbx18* expression. Our further experiments suggest that the ureteric mesenchyme is specified between E11.5 and E12.5 by signals from the ureteric epithelium. Data from canonical WNT pathway manipulation presented in this study as well in a recent report from our lab strongly suggest that WNT signals are required to maintain but are not sufficient to induce *Tbx18* expression (Trowe et al., 2012). We suggest that other signals from the epithelium, but not SHH, cooperate with WNT signals to maintain *Tbx18* expression and specify a ureteric fate to allow further differentiation of ureteric fibroblasts and smooth muscle cells.

Our analysis of *Tbx18*-deficient embryos has shown that *Tbx18* is not required for development of any of the components of the urogenital system except the ureter. *Tbx18* seems to act in a sub-pool of mesenchymal precursors of the metanephric field to favor a ureteric at the expense of a renal stromal fate. Since target genes for signals from the ureteric epithelium (*i.e.* SHH and WNTs) are not activated in *Tbx18*-deficient cells, we suggest that *Tbx18* acts as a pre-patterning gene to make the cells competent to receive signals emanating from the epithelial compartment. However, our analysis has also shown that transient *Tbx18* expression in mesenchymal cells of the early metanephric field is required to induce apoptosis in the lateral domain to avoid the formation of ectopic ligaments between the gonads, the kidney and the ureter as observed in *Tbx18*-deficient urogenital systems.

Acknowledgments

This work was supported by a grant from the Deutsche Forschungsgemeinschaft (German Research Foundation) to A.K. (DFG Ki728/7-1). We would like to thank Rolf Kemler, Andrew P. McMahon, Dietmar Vestweber, Tamara Rabe and Ahmed Mansouri for antibodies.

Appendix A. Supporting information

Supplementary data associated with this article can be found in the online version at <http://dx.doi.org/10.1016/j.jydbio.2013.04.036>.

References

- Airik, R., Bussen, M., Singh, M.K., Petry, M., Kispert, A., 2006. *Tbx18* regulates the development of the ureteral mesenchyme. *J. Clin. Invest.* 116, 663–674.
- Airik, R., Trowe, M.O., Foik, A., Farin, H.F., Petry, M., Schuster-Gossler, K., Schweizer, M., Scherer, G., Kist, R., Kispert, A., 2010. Hydroureteronephrosis due to loss of *Sox9*-regulated smooth muscle cell differentiation of the ureteric mesenchyme. *Hum. Mol. Genet.* 19, 4918–4929.
- Bingham, N.C., Verma-Kurvari, S., Parada, L.F., Parker, K.L., 2006. Development of a steroidogenic factor 1/Cre transgenic mouse line. *Genesis* 44, 419–424.
- Boyle, S., Misfeldt, A., Chandler, K.J., Deal, K.K., Southard-Smith, E.M., Mortlock, D.P., Baldwin, H.S., de Caestecker, M., 2008. Fate mapping using Cited1-CreERT2 mice demonstrates that the cap mesenchyme contains self-renewing progenitor cells and gives rise exclusively to nephronic epithelia. *Dev. Biol.* 313, 234–245.
- Brenner-Anantharam, A., Cebrian, C., Guillaume, R., Hurtado, R., Sun, T.T., Herzlinger, D., 2007. Tailbud-derived mesenchyme promotes urinary tract segmentation via BMP4 signaling. *Development* 134, 1967–1975.
- Bussen, M., Petry, M., Schuster-Gossler, K., Leitges, M., Gossler, A., Kispert, A., 2004. The T-box transcription factor *Tbx18* maintains the separation of anterior and posterior somite compartments. *Genes Dev.* 18, 1209–1221.
- Christoffels, V.M., Grieskamp, T., Norden, J., Mommersteeg, M.T., Rudat, C., Kispert, A., 2009. *Tbx18* and the fate of epicardial progenitors. *Nature* 458, E8–E9; discussion E9–10.
- Christoffels, V.M., Mommersteeg, M.T., Trowe, M.O., Prall, O.W., de Gier-de Vries, C., Soufan, A.T., Bussen, M., Schuster-Gossler, K., Harvey, R.P., Moorman, A.F., Kispert, A., 2006. Formation of the venous pole of the heart from an *Nkx2-5*-negative precursor population requires *Tbx18*. *Circ. Res.* 98, 1555–1563.
- Dressler, G.R., Deutsch, U., Chowdhury, K., Nornes, H.O., Gruss, P., 1990. *Pax2*, a new murine paired-box-containing gene and its expression in the developing excretory system. *Development* 109, 787–795.
- Fujiwara, Y., Komiya, T., Kawabata, H., Sato, M., Fujimoto, H., Furusawa, M., Noce, T., 1994. Isolation of a DEAD-family protein gene that encodes a murine homolog of *Drosophila vasa* and its specific expression in germ cell lineage. *Proc. Natl. Acad. Sci. USA* 91, 12258–12262.
- Gao, X., Chen, X., Taglienti, M., Rumballe, B., Little, M.H., Kreidberg, J.A., 2005. Angioblast-mesenchyme induction of early kidney development is mediated by *Wt1* and *Vegfa*. *Development* 132, 5437–5449.
- Grote, D., Souabni, A., Busslinger, M., Bouchard, M., 2006. *Pax 2/8*-regulated *Gata 3* expression is necessary for morphogenesis and guidance of the nephric duct in the developing kidney. *Development* 133, 53–61.
- Guillaume, R., Bressan, M., Herzlinger, D., 2009. Paraxial mesoderm contributes stromal cells to the developing kidney. *Dev. Biol.* 329, 169–175.
- Hatano, O., Takakusu, A., Nomura, M., Morohashi, K., 1996. Identical origin of adrenal cortex and gonad revealed by expression profiles of *Ad4BP/SF-1*. *Genes Cells* 1, 663–671.
- Hatini, V., Huh, S.O., Herzlinger, D., Soares, V.C., Lai, E., 1996. Essential role of stromal mesenchyme in kidney morphogenesis revealed by targeted disruption of Winged Helix transcription factor *BF-2*. *Genes Dev.* 10, 1467–1478.
- Heikkilä, M., Peltoketo, H., Leppaluoto, J., Ilves, M., Vuolteenaho, O., Vainio, S., 2002. *Wnt-4* deficiency alters mouse adrenal cortex function, reducing aldosterone production. *Endocrinology* 143, 4358–4365.
- Humphreys, B.D., Lin, S.L., Kobayashi, A., Hudson, T.E., Nowlin, B.T., Bonventre, J.V., Valerius, M.T., McMahon, A.P., Duffield, J.S., 2010. Fate tracing reveals the pericyte and not epithelial origin of myofibroblasts in kidney fibrosis. *Am. J. Pathol.* 176, 85–97.
- Ikeda, Y., Shen, W.H., Ingraham, H.A., Parker, K.L., 1994. Developmental expression of mouse steroidogenic factor-1, an essential regulator of the steroid hydroxylases. *Mol. Endocrinol.* 8, 654–662.
- James, R.G., Kamei, C.N., Wang, Q., Jiang, R., Schultheiss, T.M., 2006. Odd-skipped related 1 is required for development of the metanephric kidney and regulates formation and differentiation of kidney precursor cells. *Development* 133, 2995–3004.
- Karner, C.M., Das, A., Ma, Z., Self, M., Chen, C., Lum, L., Oliver, G., Carroll, T.J., 2011. Canonical *Wnt9b* signaling balances progenitor cell expansion and differentiation during kidney development. *Development* 138, 1247–1257.
- Keegan, C.E., Hammer, G.D., 2002. Recent insights into organogenesis of the adrenal cortex. *Trends Endocrinol. Metab.* 13, 200–208.
- Kim, A.C., Reuter, A.L., Zubair, M., Else, T., Serecky, K., Bingham, N.C., Lavery, G.G., Parker, K.L., Hammer, G.D., 2008. Targeted disruption of beta-catenin in *Sf1*-expressing cells impairs development and maintenance of the adrenal cortex. *Development* 135, 2593–2602.
- Kobayashi, A., Valerius, M.T., Mugford, J.W., Carroll, T.J., Self, M., Oliver, G., McMahon, A.P., 2008. *Six2* defines and regulates a multipotent self-renewing nephron progenitor population throughout mammalian kidney development. *Cell Stem Cell* 3, 169–181.
- Kraus, F., Haenig, B., Kispert, A., 2001. Cloning and expression analysis of the mouse T-box gene *Tbx18*. *Mech. Dev.* 100, 83–86.
- Lalli, E., 2010. Adrenal cortex ontogenesis. *Best Pract. Res. Clin. Endocrinol. Metab.* 24, 853–864.
- Levinson, R.S., Batourina, E., Choi, C., Vorontchikhina, M., Kitajewski, J., Mendelsohn, C.L., 2005. *Foxd1*-dependent signals control cellularity in the renal capsule, a structure required for normal renal development. *Development* 132, 529–539.
- Little, M.H., McMahon, A.P., 2012. Mammalian kidney development: principles, progress, and projections. *Cold Spring Harbor Perspect. Biol.* 4.
- Liu, C.F., Bingham, N., Parker, K., Yao, H.H., 2009. Sex-specific roles of beta-catenin in mouse gonadal development. *Hum. Mol. Genet.* 18, 405–417.
- Luo, X., Ikeda, Y., Parker, K.L., 1994. A cell-specific nuclear receptor is essential for adrenal and gonadal development and sexual differentiation. *Cell* 77, 481–490.
- Moorman, A.F., Houweling, A.C., de Boer, P.A., Christoffels, V.M., 2001. Sensitive nonradioactive detection of mRNA in tissue sections: novel application of the whole-mount *in situ* hybridization protocol. *J. Histochem. Cytochem.* 49, 1–8.
- Morais da Silva, S., Hacker, A., Harley, V., Goodfellow, P., Swain, A., Lovell-Badge, R., 1996. *Sox9* expression during gonadal development implies a conserved role for the gene in testis differentiation in mammals and birds. *Nat. Genet.* 14, 62–68.
- Morgan, S.M., Samulowitz, U., Darley, L., Simmons, D.L., Vestweber, D., 1999. Biochemical characterization and molecular cloning of a novel endothelial-specific sialomucin. *Blood* 93, 165–175.
- Mugford, J.W., Sipila, P., McMahon, A.P., McMahon, A.P., 2008. *Osr1* expression demarcates a multi-potent population of intermediate mesoderm that undergoes progressive restriction to an *Osr1*-dependent nephron progenitor compartment within the mammalian kidney. *Dev. Biol.* 324, 88–98.
- Muzumdar, M.D., Tasic, B., Miyamichi, K., Li, L., Luo, L., 2007. A global double-fluorescent Cre reporter mouse. *Genesis* 45, 593–605.
- Neidhardt, L.M., Kispert, A., Herrmann, B.G., 1997. A mouse gene of the paired-related homeobox class expressed in the caudal somite compartment, and in the developing vertebral column, kidney and nervous system. *Dev. Genes Evol.* 207, 330–339.
- Pedersen, A., Skjong, C., Shawlot, W., 2005. *Lim 1* is required for nephric duct extension and ureteric bud morphogenesis. *Dev. Biol.* 288, 571–581.
- Saxen, L., 1987. Organogenesis of the Kidney. Cambridge University Press, Cambridge, UK.
- Schneider, C.A., Rasband, W.S., Eliceiri, K.W., 2012. NIH image to image J: 25 years of image analysis. *Nat. Methods* 9, 671–675.
- Self, M., Lagutin, O.V., Bowling, B., Hendrix, J., Cai, Y., Dressler, G.R., Oliver, G., 2006. *Six2* is required for suppression of nephrogenesis and progenitor renewal in the developing kidney. *EMBO J.* 25, 5214–5228.
- So, P.L., Danielian, P.S., 1999. Cloning and expression analysis of a mouse gene related to *Drosophila odd-skipped*. *Mech. Dev.* 84, 157–160.
- Trowe, M.O., Airik, R., Weiss, A.C., Farin, H.F., Foik, A.B., Bettenhausen, E., Schuster-Gossler, K., Taketo, M.M., Kispert, A., 2012. Canonical *Wnt* signaling regulates smooth muscle precursor development in the mouse ureter. *Development* 139, 3099–3108.
- Trowe, M.O., Shah, S., Petry, M., Airik, R., Schuster-Gossler, K., Kist, R., Kispert, A., 2010. Loss of *Sox9* in the periotic mesenchyme affects mesenchymal expansion and differentiation, and epithelial morphogenesis during cochlea development in the mouse. *Dev. Biol.* 342, 51–62.

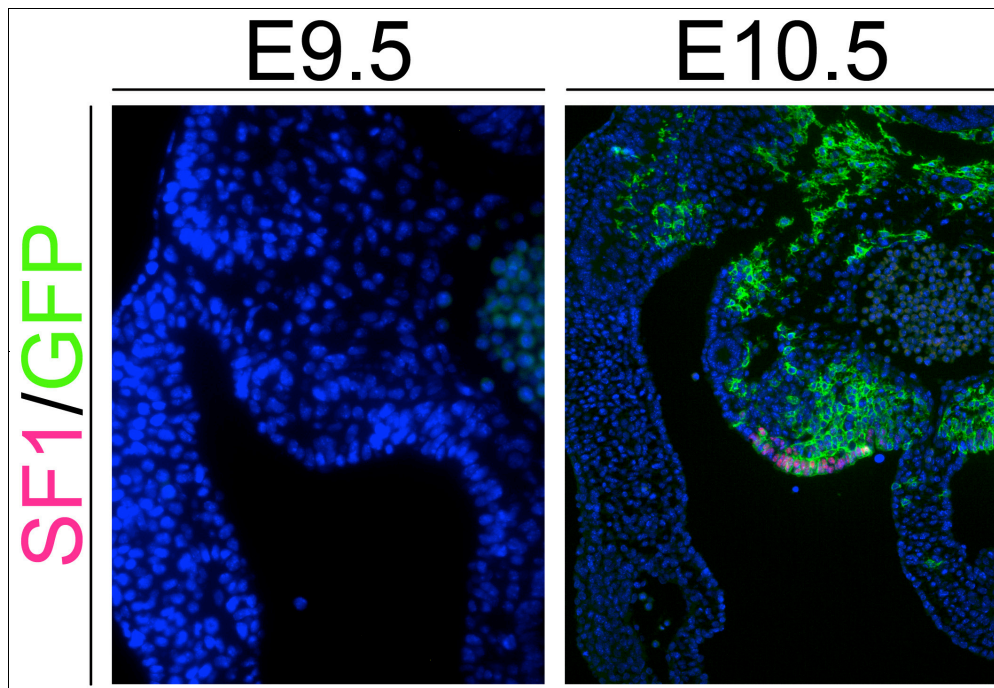
- Vestweber, D., Kemler, R., Ekblom, P., 1985. Cell-adhesion molecule uvomorulin during kidney development. *Dev. Biol.* 112, 213–221.
- Wang, C., Gargollo, P., Guo, C., Tang, T., Mingin, G., Sun, Y., Li, X., 2011. Six1 and Eya1 are critical regulators of peri-cloacal mesenchymal progenitors during genitourinary tract development. *Dev. Biol.* 360, 186–194.
- Wang, Q., Lan, Y., Cho, E.S., Maltby, K.M., Jiang, R., 2005. Odd-skipped related 1 (Odd1) is an essential regulator of heart and urogenital development. *Dev. Biol.* 288, 582–594.
- Wang, Y., Tripathi, P., Guo, Q., Coussens, M., Ma, L., Chen, F., 2009. Cre/lox recombination in the lower urinary tract. *Genesis* 47, 409–413.
- Wilkinson, D.G., Nieto, M.A., 1993. Detection of messenger RNA by *in situ* hybridization to tissue sections and whole mounts. *Methods Enzymol.* 225, 361–373.
- Yu, J., Carroll, T.J., McMahon, A.P., 2002. Sonic hedgehog regulates proliferation and differentiation of mesenchymal cells in the mouse metanephric kidney. *Development* 129, 5301–5312.

Supplementary Figures

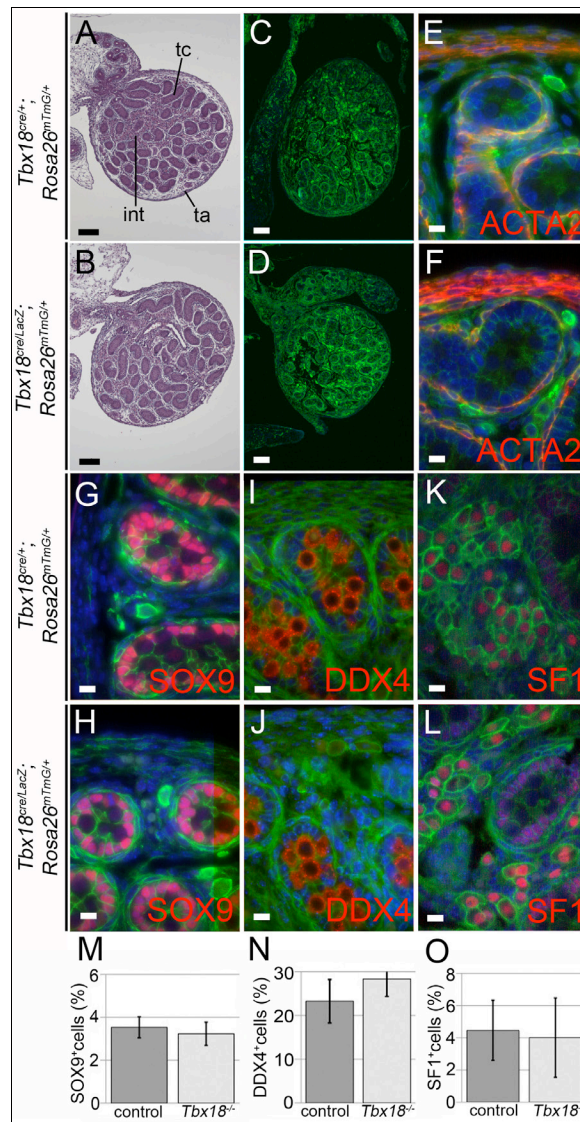
for

***Tbx18* expression demarcates multipotent precursor populations in the developing urogenital system but is exclusively required within the ureteric mesenchymal lineage to suppress a renal stromal fate**

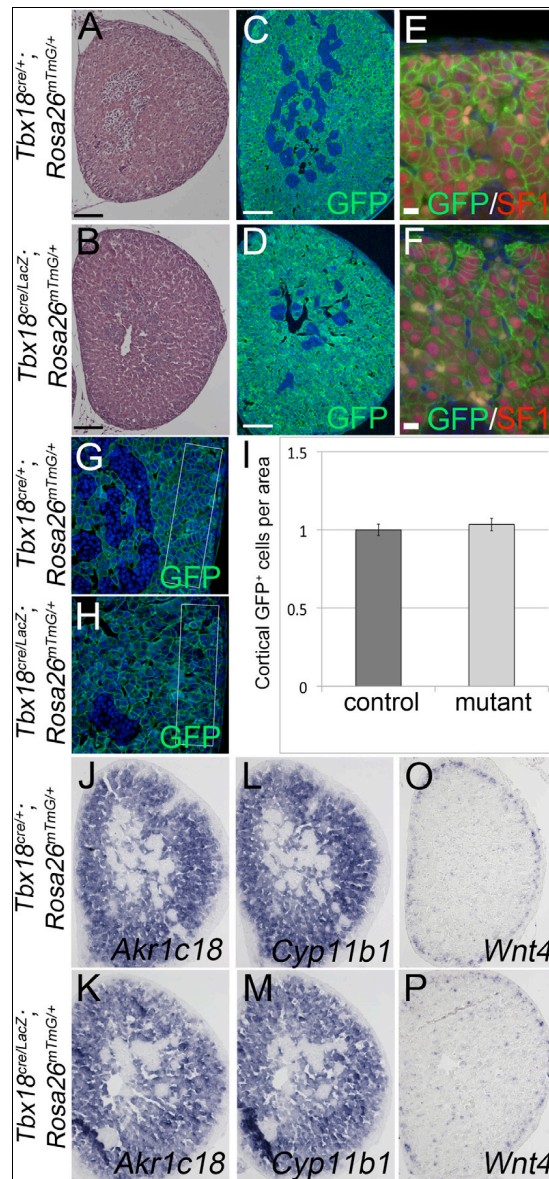
Tobias Bohnenpoll¹, Eva Bettenhausen¹, Anna-Carina Weiss, Anna B. Foik, Mark-Oliver Trowe, Patrick Blank, Rannar Airik, and Andreas Kispert*



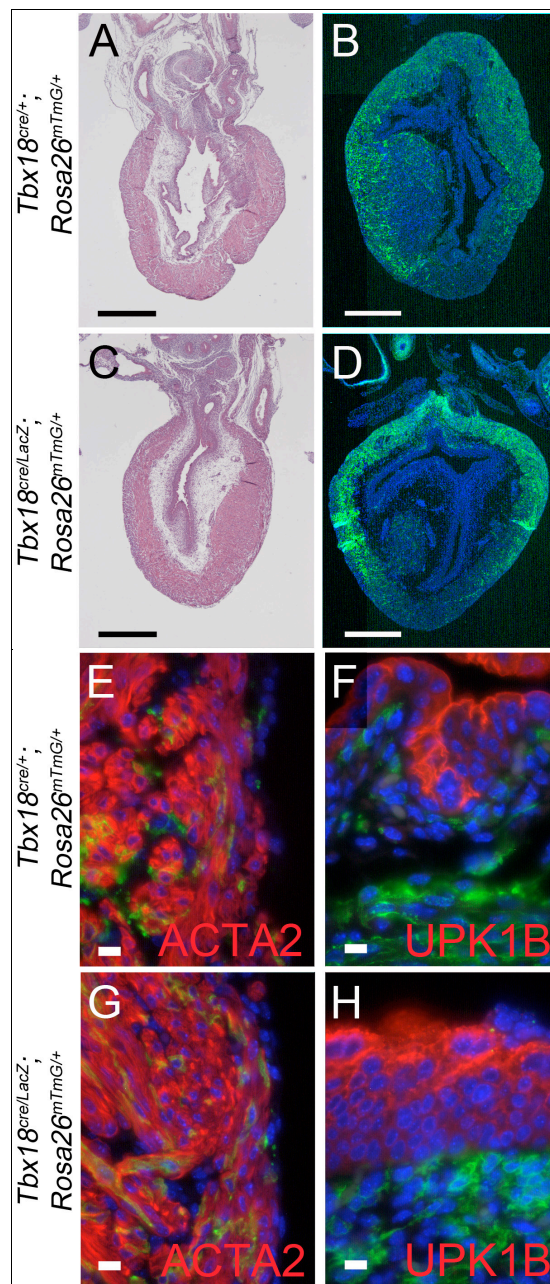
Supplementary Fig. S1. *Tbx18*⁺-descendants are positive for SF1 in the coelomic lining at E10.5. (Co-)immunofluorescence analysis of expression of the lineage marker GFP (green) and the marker for the adrenogonadal primordium, SF1 (red), on transverse sections through the posterior trunk of E9.5 and E10.5 *Tbx18*^{Cre/+}; *R26*^{mTmG/+} embryos. At E9.5, SF1 protein is not yet expressed in the coelomic lining and recombination of the lineage reporter has not yet occurred. At E10.5, cells formerly positive for *Tbx18* in the coelomic lining express SF1.



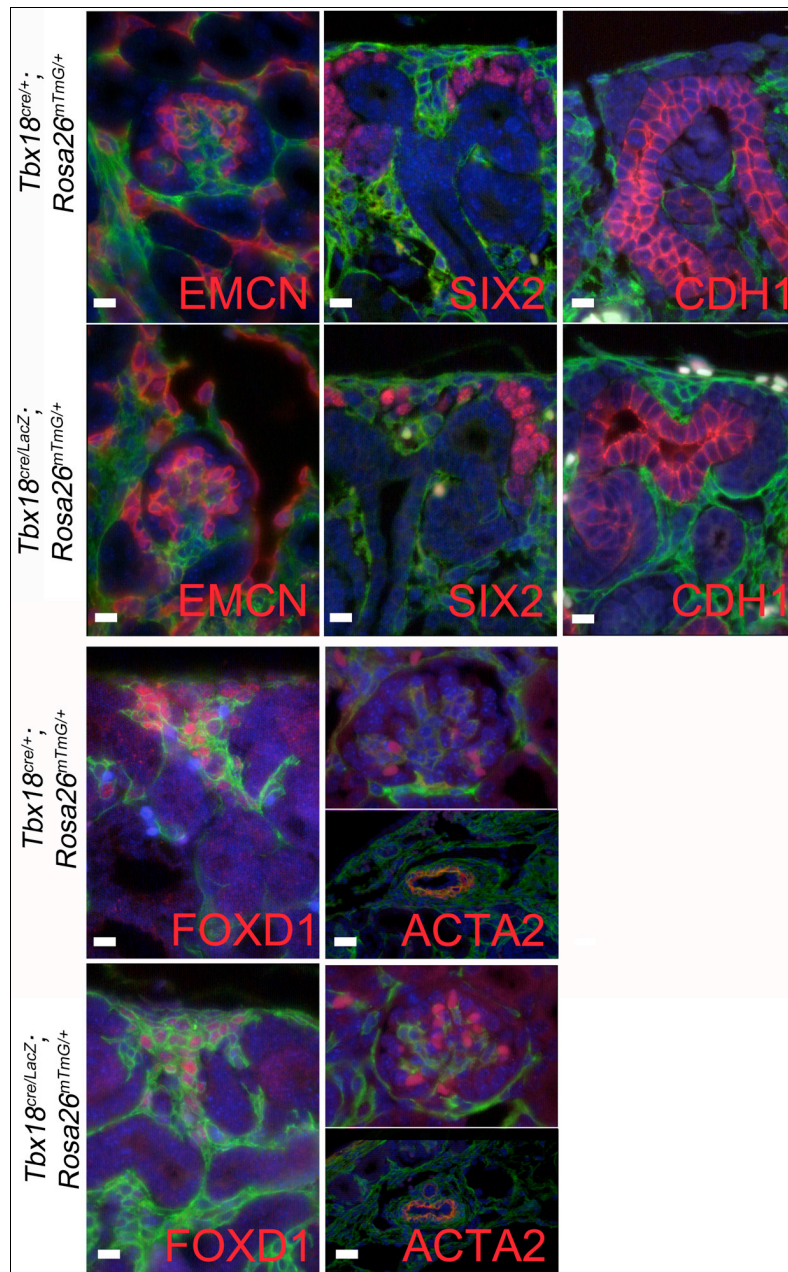
Supplementary Fig. S2. Loss of *Tbx18* does not affect testis development. (A,B) Histological analysis by haematoxylin and eosin staining of sagittal testis sections in E18.5 control ($Tbx18^{cre/+}; R26^{mTmG/+}$) and *Tbx18*-deficient embryos ($Tbx18^{cre/lacZ}; R26^{mTmG/+}$) does not detect changes of the testicular tissue organization. (C-L) (Co-)immunofluorescence analysis of expression of the lineage marker GFP and markers of differentiated cell types on sections of E18.5 testis does not detect changes in the number and distribution of smooth muscle cells of the capsule (ACTA2), of Sertoli cells (SOX9), of germ cells (DDX4) and of Leydig cells (SF1) between control and *Tbx18*-deficient embryos. Scale bars represent 100 μ m (A,B,C,D) and 10 μ m (E-L). (M-O) Quantification of SOX9⁺ Sertoli cells, DDX4⁺ germ cells and SF1⁺ Leydig cells in the testis. (M) SOX9⁺ cells/all cells in the counted area (in%), control: 3.5 \pm 0.5, mutant: 3.2 \pm 0.5 p=0.515. (N) DDX4⁺ cells/testis cord cells (somatic and germ cells) (in %). control: 23.3 \pm 5.0, mutant: 28.3 \pm 4.0 p=0.093. (O) SF1⁺ Leydig cells/all interstitial cells (in %), control: 4.5 \pm 1.9, mutant: 4.0 \pm 2.5 p=0.801.



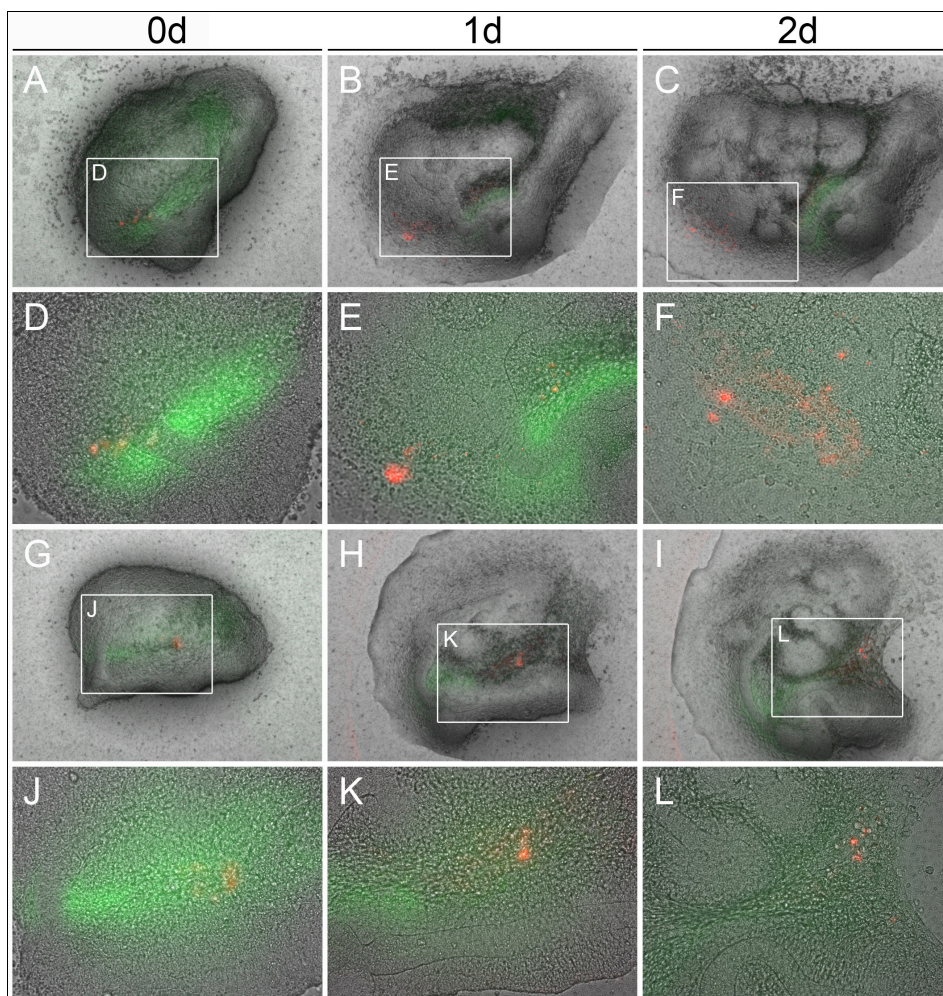
Supplementary Fig. S3. Loss of *Tbx18* does not affect adrenal development at E18.5. (A,D) Histological analysis by haematoxylin and eosin staining, (B,E) immunofluorescence analysis of expression of the lineage marker GFP, (C,F) co-immunofluorescence analysis of expression of the lineage marker GFP and of the steroidogenic marker SF1, on sections of control ($Tbx18^{cre/+}; Rosa26^{mTmG/+}$) and *Tbx18*-deficient embryos ($Tbx18^{cre/lacZ}; Rosa26^{mTmG/+}$) does not detect changes in adrenal development. Size bars represent 0.1 mm (A-D) and 10 μ m (C,F). (G-I) Immunofluorescence analysis of cells expressing the lineage marker GFP in a defined cortical area and subsequent quantification of GFP⁺ cells (control is set to 1) reveals unchanged contribution of *Tbx18*⁺ descendants to the cortical area of the *Tbx18*-deficient adrenal gland. Control: 1 ± 0.037, mutant: 1.034 ± 0.04, $p=0.26$ (J-M) *In situ* hybridization analysis of markers of the inner cortical region shows normal zonation in the mutant adrenal gland. Genotypes, probes and antigens are as shown.



Supplementary Fig. S4. Loss of *Tbx18* does not affect bladder development. (A,C) Histological analysis by haematoxylin and eosin staining, (B,D) immunofluorescence analysis of expression of the lineage marker GFP, (E,G) co-immunofluorescence analysis of expression of the lineage marker GFP and the smooth muscle marker ACTA2, (F,H) co-immunofluorescence analysis of expression of the lineage marker GFP and of the urothelial marker UPK1B on sections of control ($Tbx18^{cre/+};R26^{mTmG/+}$) and *Tbx18*-deficient embryos ($Tbx18^{cre/LacZ};R26^{mTmG/+}$) does not detect changes in contribution of *Tbx18*⁺ descendants and cellular differentiation in the bladder. Size bars represent 0.5 mm (A-D) and 10 μ m (E-H).



Supplementary Fig. S5. Loss of *Tbx18* does not affect differentiation of renal cell lineages. Co-immunofluorescence analysis of expression of the lineage marker GFP, with the endothelial marker EMCN, the cap mesenchyme marker SIX2, the epithelial marker CDH1, the cortical stroma marker FOXD1 and the smooth muscle marker ACTA2 on sections of control (*Tbx18^{cre/+}; R26^{mTmG/+}*) and *Tbx18*-deficient embryos (*Tbx18^{cre/lacZ}; R26^{mTmG/+}*) does not detect changes in contribution of *Tbx18*⁺ descendants and cellular differentiation in the kidney. Size bars represent 10 μ m.



Supplementary Figure S6. Lineage analysis of *Tbx18*⁺ mesenchymal cells in early kidney rudiments. (A) Combined brightfield and epifluorescence analysis of metanephric explants from E11.5 *Tbx18*^{GFP/+} embryos at 0, 1 and 2 days of culture. GFP (green) marks the *Tbx18* expression domain, the red fluorescence indicates Dil-injected cell clusters. Shown are two representative examples of Dil-injected cells localizing to the space between kidneys and the Wolffian duct (lower row). Boxed regions are shown in higher magnifications below.

Canonical Wnt signaling regulates smooth muscle precursor development in the mouse ureter

Mark-Oliver Trowe^{1,*}, Rannar Airik^{1,*}, Anna-Carina Weiss¹, Henner F. Farin¹, Anna B. Foik¹, Eva Bettenhausen¹, Karin Schuster-Gossler¹, Makoto Mark Taketo² and Andreas Kispert^{1,§}

¹Institut für Molekularbiologie, Medizinische Hochschule Hannover, 30625 Hannover, Germany

²Department of Pharmacology, Graduate School of Medicine, Kyoto University, Sakyo, Kyoto 606-8501, Japan

§Author for correspondence:

Email: kispert.andreas@mh-hannover.de

Tel: +49511 5324017

Fax: +49511532483

Published in Development (Development (2012) 139, 3099-3108)

Reprinted with permission

Development 139, 3099-3108 (2012) doi:10.1242/dev.077388
© 2012. Published by The Company of Biologists Ltd

Canonical Wnt signaling regulates smooth muscle precursor development in the mouse ureter

Mark-Oliver Trowe^{1,*}, Rannar Airik^{1,*}, Anna-Carina Weiss¹, Henner F. Farin¹, Anna B. Foik¹, Eva Bettenhausen¹, Karin Schuster-Gossler¹, Makoto Mark Taketo² and Andreas Kispert^{1,‡}

SUMMARY

Smooth muscle cells (SMCs) are a key component of many visceral organs, including the ureter, yet the molecular pathways that regulate their development from mesenchymal precursors are insufficiently understood. Here, we identified epithelial Wnt7b and Wnt9b as possible ligands of Fzd1-mediated β -catenin (Ctnnb1)-dependent (canonical) Wnt signaling in the adjacent undifferentiated ureteric mesenchyme. Mice with a conditional deletion of *Ctnnb1* in the ureteric mesenchyme exhibited hydronephrosis and hydronephrosis at newborn stages due to functional obstruction of the ureter. Histological analysis revealed that the layer of undifferentiated mesenchymal cells directly adjacent to the ureteric epithelium did not undergo characteristic cell shape changes, exhibited reduced proliferation and failed to differentiate into SMCs. Molecular markers for prospective SMCs were lost, whereas markers of the outer layer of the ureteric mesenchyme fated to become adventitial fibroblasts were expanded to the inner layer. Conditional misexpression of a stabilized form of Ctnnb1 in the prospective ureteric mesenchyme resulted in the formation of a large domain of cells that exhibited histological and molecular features of prospective SMCs and differentiated along this lineage. Our analysis suggests that Wnt signals from the ureteric epithelium pattern the ureteric mesenchyme in a radial fashion by suppressing adventitial fibroblast differentiation and initiating smooth muscle precursor development in the innermost layer of mesenchymal cells.

KEY WORDS: Wnt, Ctnnb1, Ureter, Tbx18, Smooth muscle cell

INTRODUCTION

The mammalian ureter is a simple tube that mediates by unidirectional peristaltic contractions the efficient removal of urine from the renal pelvis to the bladder. The structural basis of the flexibility and contractile activity of this tubular organ is a two-layered tissue architecture of an outer mesenchymal wall composed of radially organized layers of fibroelastic material, contractile smooth muscle cells (SMCs) and adventitial fibroblasts, and an inner specialized highly expandable impermeable epithelial lining. Whether acquired or inherited, compromised drainage of the urine to the bladder by physical barriers or by functional impairment of the SMC layer results in fluid pressure-mediated dilation of the ureter (hydronephrosis) and the pelvis and collecting duct system of the kidney (hydronephrosis), a disease entity that may progress to pressure-mediated destruction of the renal parenchyme (Chevalier et al., 2010; Rosen et al., 2008; Song and Yosypiv, 2011).

The three-layered mesenchymal coating of the mature ureter arises from a homogenous precursor tissue that is established in the metanephric field after formation of the ureter as an epithelial outgrowth of the Wolffian duct. In the mouse, this mesenchymal precursor pool remains undifferentiated from embryonic day (E) 11.5 to E15.5 and supports the elongation of the distal ureter stalk. From E15.5, i.e. shortly before onset of urine production in the developing kidney at E16.5, the mesenchyme in direct proximity to the ureteric epithelium differentiates in a proximal-to-distal wave

into SMCs that will form layers with longitudinal and transverse orientations. Between the SMCs and the urothelium, a thin layer of stromal cells develops that contributes to elasticity of the ureteric tube. The outer mesenchymal cells remain more loosely organized and differentiate into adventitial fibroblasts (Airik and Kispert, 2007).

Despite its simple design and the relevance of congenital defects of the ureteric wall, only a small number of genes crucial for development of the ureteric mesenchyme have been characterized in recent years (Airik and Kispert, 2007; Uetani and Bouchard, 2009). Phenotypic analyses of mutant mice suggested that the T-box transcription factor gene 18 (*Tbx18*) specifies the ureteric mesenchyme (Airik et al., 2006); that *Bmp4*, a member of the family of secreted bone morphogenetic proteins, inhibits budding and branching morphogenesis of the distal ureteric epithelium, directs a ureteric fate and/or promotes SMC differentiation (Brenner-Anantharam et al., 2007; Dunn et al., 1997; Miyazaki et al., 2003); that the transcriptional regulators GATA binding protein 2 (*Gata2*), teashirt zinc finger family member 3 (*Tshz3*) and SRY-box containing gene 9 (*Sox9*) act as downstream mediators of *Bmp4* function in the mesenchyme to activate expression of myocardin (*Myocd*), the key regulator of SMC differentiation (Airik et al., 2010; Caubit et al., 2008; Wang and Olson, 2004; Zhou et al., 1998); and that sonic hedgehog (*Shh*) signaling from the ureteric epithelium maintains *Bmp4* in the mesenchyme and dose-dependently inhibits SMC fates (Yu et al., 2002).

The Wnt gene family encodes secreted growth and differentiation factors that have been implicated in numerous processes of vertebrate development and disease. Wnt proteins signal via at least three distinct pathways, of which only the canonical pathway has been implicated in transcriptional control of cell proliferation and differentiation. This pathway uniquely and critically involves the cytoplasmic protein β -catenin (Ctnnb1),

¹Institut für Molekularbiologie, Medizinische Hochschule Hannover, 30625 Hannover, Germany. ²Department of Pharmacology, Kyoto University, Kyoto 606-8501, Japan.

*These authors contributed equally to this work

‡Author for correspondence (kispert.andreas@mh-hannover.de)

Accepted 8 June 2012

which is stabilized upon binding of a Wnt ligand to a Frizzled (Fzd) receptor complex on the cell surface, and translocates to the nucleus to activate target gene transcription (Barker, 2008; MacDonald et al., 2009; Miller and McCrea, 2010).

Here, we study the functional involvement of Wnt signaling in the development of the (distal) ureter, particularly its mesenchymal component, in the mouse. We provide evidence for a crucial function of the *Ctnnb1*-dependent sub-branch of this pathway in the specification of the SMC lineage and radial patterning of the ureteric mesenchyme.

MATERIALS AND METHODS

Mouse strains and husbandry

For the production of a conditional misexpression allele of *Tbx18*, a knock-in strategy into the X-chromosomal hypoxanthine guanine phosphoribosyl transferase (*Hprt*) gene locus was employed (Luche et al., 2007). Construction of the targeting vector, ES cell work and generation of chimeras followed exactly the procedure established for the generation of an *Hprt^{Sox9}* allele (Airik et al., 2010). *Beta-catenin^{lox}* (*Ctnnb1^{fx}*, *Ctnnb1^{tm2Kem}*) (Brault et al., 2001), *beta-catenin^{lox(ex3)}* [*Ctnnb1^{(ex3)fx}*, *Ctnnb1^{tm1Mmt}*] (Harada et al., 1999), *Hprt^{Tbx18}*, *R26^{mTmG}* [*Gi(ROSA)26Sor^{tm4(AC1B-tdTomato-EGFP)Luor}*] (Muzumdar et al., 2007) and *Tbx18^{cre}* [*Tbx18^{tm4(cre)Akis}*] mice (Trowe et al., 2010) were maintained on an NMRI outbred background. Embryos for Wnt (pathway) gene expression analysis were derived from matings of NMRI wild-type mice. *Tbx18^{cre/+}*; *Ctnnb1^{fx/fx}* mice were obtained from matings of *Tbx18^{cre/+}*; *Ctnnb1^{fx/+}* males and *Ctnnb1^{fx/fx}* females. *Tbx18^{cre/+}*; *Ctnnb1^{fx/+}* and *Tbx18^{+/+}*; *Ctnnb1^{fx/+}* littermates were interchangeably used as controls. *Tbx18^{cre/+}*; *Ctnnb1^{(ex3)fx/+}*; *R26^{mTmG/+}* and *Tbx18^{cre/+}*; *R26^{mTmG/+}* mice were obtained from matings of *Tbx18^{cre/+}*; *R26^{mTmG/mTmG}* males and *Ctnnb1^{(ex3)fx/(ex3)fx}* and NMRI females, respectively. For timed pregnancies, vaginal plugs were checked on the morning after mating and noon was taken as E0.5. Embryos and urogenital systems were dissected in PBS and fixed in 4% paraformaldehyde (PFA) in PBS and stored in methanol at -20°C. Genomic DNA prepared from yolk sacs or tail biopsies was used for genotyping by PCR.

Organ cultures

Explant cultures of embryonic kidneys or urogenital systems were performed as previously described (Airik et al., 2010). The pharmacological Wnt pathway inhibitor IWR1 (Sigma, dissolved in DMSO) was used at final concentrations of 50 μ M and 10 μ M. Culture medium was replaced every 24 hours.

Morphological, histological and histochemical analyses

Ink injection experiments to visualize the ureteropelvic lumen were performed as previously described (Airik et al., 2010). Kidneys for histological stainings were fixed in 4% PFA, paraffin embedded, and sectioned to 5 μ m. Sections were stained with Hematoxylin and Eosin. For the detection of antigens on 5- μ m paraffin sections, the following primary antibodies and dilutions were used: polyclonal rabbit antisera against Cdh1 (E-cadherin; a kind gift from Rolf Kemler, Max-Planck-Institute for Immunobiology and Epigenetics, Freiburg, Germany; 1:200), Myh11 (SMMHC, smooth muscle myosin heavy chain; a kind gift from R. Adelstein, NIH, Bethesda, MD, USA; 1:200), transgelin (Tagln, SM22a; Abcam, ab14106-100; 1:200), GFP (Santa Cruz; 1:100) and mouse monoclonal antibodies against Acta2 (alpha smooth muscle actin, aSMA; clone 1A4, NatuTec; 1:200), cytokeratin 18 (Ck18, Krt18; Acris; 1:200) and GFP (Roche; 1:200).

Fluorescent staining was performed using Alexa 488/555-conjugated secondary antibodies (Invitrogen; 1:200) or Biotin-conjugated secondary antibodies (Dianova; 1:200) and the TSA Tetramethylrhodamine Amplification Kit (PerkinElmer). Non-fluorescent staining was performed using kits from Vector Laboratories [Vectastain ABC Peroxidase Kit (rabbit IgG), Mouse-on-Mouse Kit, DAB Substrate Kit]. Labeling with primary antibodies was performed at 4°C overnight after antigen retrieval (Antigen Unmasking Solution, Vector Laboratories; 15 minutes, 100°C), blocking

of endogenous peroxidases with 3% H₂O₂/PBS for 10 minutes (required for DAB and TSA) and incubation in 2.5% normal goat serum in PBST (0.05% Tween 20 in PBS) or blocking solutions provided with the kits. For monoclonal mouse antibodies an additional IgG blocking step was performed using the Mouse-on-Mouse Kit (Vector Laboratories).

Cellular assays

Cell proliferation rates in tissues of E12.5 and E14.5 wild-type and *Ctnnb1* mutant embryos were investigated by the detection of incorporated BrdU on 5- μ m paraffin sections according to published protocols (Bussen et al., 2004). For each specimen (three embryos per genotype for E12.5, five embryos per genotype for E14.5), ten sections of the proximal ureter were assessed. The BrdU labeling index was defined as the number of BrdU-positive nuclei relative to the total number of nuclei as detected by DAPI counterstaining in histologically defined regions. Statistical analysis was performed using the two-tailed Student's *t*-test. Data are expressed as mean \pm s.d. Differences were considered significant when *P*<0.05. Apoptosis in tissues was assessed by TUNEL assay using the ApopTag Plus Fluorescein In Situ Apoptosis Detection Kit (Chemicon) on 5- μ m paraffin sections. All sections were counterstained with DAPI.

In situ hybridization analysis

Whole-mount in situ hybridization was performed following a standard procedure with digoxigenin-labeled antisense riboprobes (Wilkinson and Nieto, 1993). Stained specimens were transferred in 80% glycerol prior to documentation. In situ hybridization on 10- μ m paraffin sections was essentially as described (Moorman et al., 2001). For each marker, at least three independent specimens were analyzed.

Image documentation

Whole-mount specimens were photographed on a Leica M420 Macroscope with a Fujix HC-300Z digital camera, and sections on a Leica DM5000 B microscope with a Leica DFC300 FX digital camera. All images were processed in Adobe Photoshop CS.

RESULTS

(Canonical) Wnt signaling in ureter development

To determine the involvement of Wnt signaling in ureter development, the expression of genes encoding Wnt ligands (*Wnt1* to *Wnt16*) and Frizzled receptors (*Fzd1* to *Fzd10*) was analyzed by in situ hybridization of whole ureters at E12.5 and E16.5, i.e. before and after cell differentiation has occurred in this tissue. This screen identified *Wnt7b*, *Wnt9b* and *Fzd1* as Wnt components with specific expression in the ureter at these stages (Fig. 1). To better resolve the spatiotemporal expression profile of these genes, we performed an in situ hybridization analysis both in whole ureters and on transverse ureter sections from E11.5 to E18.5. *Wnt7b* and *Wnt9b* were co-expressed in the ureteric epithelium from E11.5 to E14.5. Expression of *Wnt9b* was downregulated after that stage, whereas *Wnt7b* was maintained at least until E18.5 (Fig. 1A-D). Expression of *Fzd1* was detected in the ureteric mesenchyme from E11.5 to E18.5, with lower levels being confined to the innermost ring after E14.5 (Fig. 1E,F).

As *Wnt7b* and *Wnt9b* have previously been associated with the canonical branch of Wnt signaling (Karner et al., 2011; Yu et al., 2009), we investigated ureteric expression of *Axin2*, a bona fide target of this pathway (Jho et al., 2002). At E11.5, expression of *Axin2* was found in the ureteric epithelium and weakly in the surrounding mesenchyme. Epithelial expression was no longer detectable at subsequent stages, whereas mesenchymal expression was maintained and confined to the innermost cell layer at E12.5 and E14.5. *Axin2* expression in this domain was markedly downregulated after the onset of SMC differentiation at E15.5 (Fig. 1G,H).

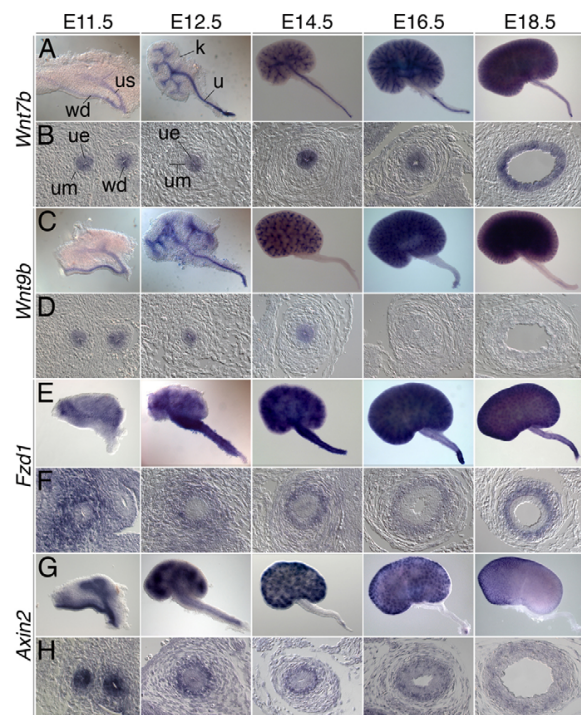


Fig. 1. Wnt expression during mouse ureter development. In situ hybridization analysis (A,C,E,G) on whole kidneys with ureters and (B,D,F,H) on transverse sections of the proximal ureter for expression of Wnt pathway components and the target of canonical Wnt signaling *Axin2* in wild-type embryos. (F,H) Note that stainings were overdeveloped to better visualize the weak expression domain. k, kidney; u, ureter; ue, ureteric epithelium; um, ureteric mesenchyme; us, ureter stalk; wd, Wolffian duct.

Together, this analysis suggests that Wnt7b and Wnt9b from the ureteric epithelium activate the canonical signal transduction pathway via Fzd1 in the adjacent undifferentiated mesenchyme.

Conditional inactivation of *Ctnnb1* in the ureteric mesenchyme results in hydroureter

To investigate the role of canonical Wnt signaling in the ureteric mesenchyme, we employed a tissue-specific gene inactivation approach using a *Tbx18^{cre}* line generated in our laboratory (Airik et al., 2010) and a floxed allele of *Ctnnb1* (*Ctnnb1^{flx}*), the unique intracellular mediator of this signaling pathway (Brault et al., 2001). We tested the efficiency of *Tbx18^{cre}*-mediated recombination in the ureteric mesenchyme with the sensitive reporter line *R26^{mTmG}*. In this line, recombination is visualized by bright membrane-bound GFP expression in a background of membrane-bound red fluorescence. Anti-GFP immunofluorescence analysis on sections provides additional cellular resolution of Cre-mediated recombination events (Muzumdar et al., 2007). In *Tbx18^{cre/+};R26^{mTmG/+}* mice, GFP activity was observed in a domain abutting the mesenchyme of the Wolffian duct and of the metanephric kidney at E11.5, as expected from the *Tbx18* expression pattern (Airik et al., 2006). Analysis of ureter sections at E12.5, E14.5 and E18.5 revealed GFP expression throughout the

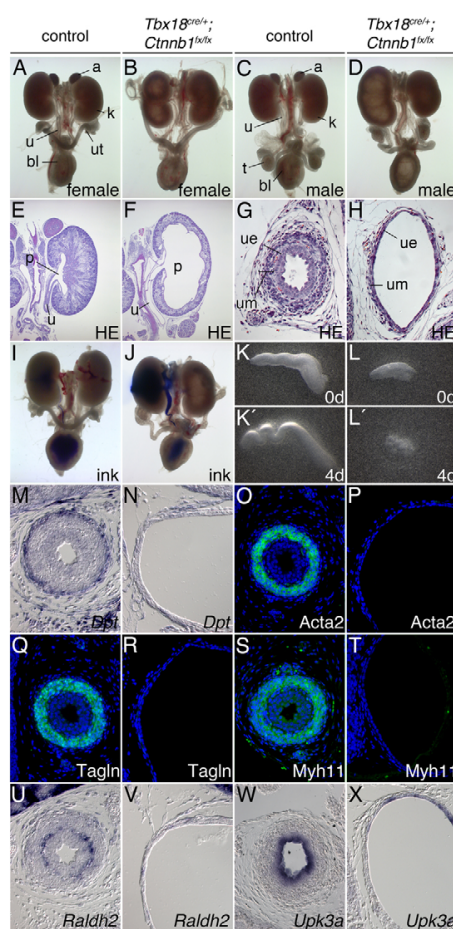


Fig. 2. Kidney and urogenital tract anomalies in *Tbx18^{cre/+};Ctnnb1^{flx/flx}* mouse embryos at E18.5. (A-D) Morphology of whole urogenital systems of female (A,B) and male (C,D) embryos. (E-H) Hematoxylin and Eosin stainings (HE) of sagittal sections of kidneys (E,F) and of transverse sections of the proximal ureter (G,H). (I,J) Absence of physical obstruction in the *Tbx18^{cre/+};Ctnnb1^{flx/flx}* ureter as revealed by ink injection experiments. (K-L') Explants of E15.5 ureters after 0 and 4 days (d) in culture. (M-X) Cytodifferentiation of the ureteric mesenchyme (M-V) and epithelium (W,X) as shown by in situ hybridization analysis (M,N,U-X) and immunohistochemistry (O-T) on transverse sections of the proximal ureter at E18.5. a, adrenal gland; bl, bladder; k, kidney; p, pelvis; t, testis; u, ureter; ue, ureteric epithelium; um, ureteric mesenchyme; ut, uterus.

entire mesenchymal compartment, confirming that *Tbx18^{cre}* mediates recombination in precursors of all differentiated cell types of the ureteric mesenchyme, i.e. fibroblasts of the inner lamina propria and outer adventitia, and SMCs (supplementary material Fig. S1). The tissue-specific inactivation of the canonical Wnt signaling pathway in *Tbx18^{cre/+};Ctnnb1^{flx/flx}* ureters was validated by the absence of *Axin2* expression in the mesenchymal but not in the epithelial compartment at E11.5 and E12.5 (supplementary material Fig. S2).

At E18.5, urogenital systems of *Tbx18^{cre/+};Ctnnb1^{flx/flx}* embryos displayed a prominent hydroureter and hydronephrosis phenotype. These abnormalities were fully penetrant and occurred bilaterally in both sexes (Fig. 2A-D). In the female mutant, the uterus appeared stretched, the translucent ovaries were attached more anteriorly to the kidneys, and the Wolffian duct had not regressed. In the male mutant, the testes and epididymides were tethered to the posterior pole of the kidneys. Adrenals were absent from the mutant urogenital systems of both sexes (Fig. 2B,D). Adrenogenital defects are compatible with a requirement of *Ctnnb1* in female differentiation and adrenal development (Chassot et al., 2008; Kim et al., 2008). They most likely derive from *Tbx18^{cre}*-mediated recombination in adrenogenital precursors in the mesonephros rather than in the ureteric mesenchyme (Kraus et al., 2001). Heterozygous loss of *Ctnnb1* in *Tbx18^{cre/+};Ctnnb1^{flx/+}* embryos was not associated with morphological defects in the urogenital system, arguing against a dose-dependent requirement for *Ctnnb1* and genetic interaction of *Tbx18* and *Ctnnb1* in ureter development (data not shown).

Histological analyses revealed dilation of the entire renal collecting system, including the collecting ducts, calyx and pelvis, and absence of the papilla in mutant kidneys (Fig. 2E,F). The ureter was strongly dilated and featured a flat and single-layered urothelium with a thin layer of surrounding mesenchyme (Fig. 2G,H).

Hydroureteronephrosis can result from structural or functional deficits of the peristaltic machinery and from physical obstruction along the ureter and its junctions. To distinguish these possibilities, we analyzed the continuity of the ureteric lumen and the patency of the junctions by injecting ink into the renal pelvis. In all genotypes the ink readily passed into the bladder (Fig. 2I,J), excluding physical barrier formation as a cause of obstruction. To further analyze the nature of functional ureter impairment, we cultured E15.5 ureter explants for 4 days, monitoring daily for peristaltic activity and contraction patterns. Wild-type ureters elongated extensively in culture and initiated unidirectional peristaltic contractions, whereas *Tbx18^{cre/+};Ctnnb1^{flx/flx}* ureters never contracted and degenerated over time (Fig. 2K-L'). To characterize the cellular changes that caused this behavior, we analyzed the expression of markers that indicate cell differentiation within the epithelial and mesenchymal tissue compartments of the ureter at E18.5. In the *Ctnnb1*-deficient ureteric mesenchyme, expression of the adventitial fibroblast marker dermatopontin (*Dpt*), the smooth muscle (SM) structural proteins *Acta2*, *Tagln* and *Myh11*, and of aldehyde dehydrogenase family 1, subfamily A2 (*Raldh2*, or *Aldh1a2*), a marker for the lamina propria, was absent (Fig. 2M-V). Urothelial differentiation was also affected in the mutant, as shown by the strong reduction of the urothelial marker *Upk3a* (Fig. 2W,X). Taken together, loss of *Ctnnb1* in the ureteric mesenchyme results in ureter dysfunction, probably caused by a complete loss of the SMC layer.

The requirement of canonical Wnt signaling for differentiation of the ureteric mesenchyme was independently confirmed by a pharmacological inhibition experiment. Exposure of explant cultures of E11.5 wild-type metanephric rudiments to 50 μ M IWR1, a Wnt pathway inhibitor that was recently shown to block expression of Wnt9b target genes in the metanephric mesenchyme at 100 μ M (Karner et al., 2011), resulted in tissue degeneration similar to that observed in explanted *Tbx18^{cre/+};Ctnnb1^{flx/flx}* ureters. Wild-type ureters cultured in 10 μ M IWR1 survived for 8 days but showed a dramatic reduction of *Acta2*-positive SMCs (supplementary material Fig. S3).

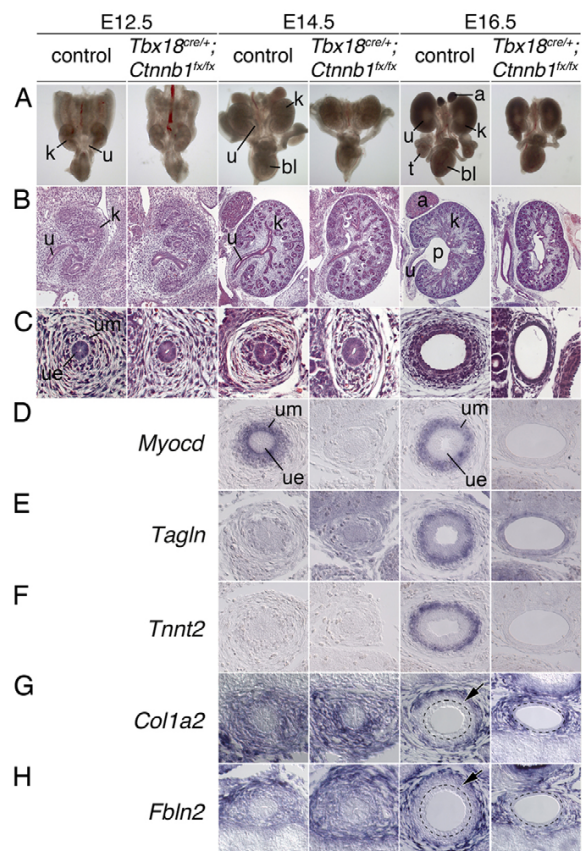


Fig. 3. Early onset of kidney and ureter anomalies in *Tbx18^{cre/+};Ctnnb1^{flx/flx}* mouse embryos. (A) Morphology of whole urogenital systems. (B, C) Hematoxylin and Eosin stainings of sagittal sections of kidneys (B) and of transverse sections of proximal ureters (C). (D-H) Cytodifferentiation of the ureteric mesenchyme into SMCs and fibroblasts as shown by in situ hybridization analysis on transverse sections of the proximal ureter. (G, H) Arrows indicate the inner ring of mesenchymal cells; the ureteric epithelium is outlined (dashed line). adrenal gland; bl, bladder; k, kidney; p, pelvis; t, testis; u, ureter; ue, ureteric epithelium; um, ureteric mesenchyme.

Early onset of ureter defects in *Tbx18^{cre/+};Ctnnb1^{flx/flx}* embryos

To define both the onset and progression of urogenital malformations in *Tbx18^{cre/+};Ctnnb1^{flx/flx}* embryos, we analyzed urogenital systems from E12.5 to E16.5. On the morphological level, *Tbx18^{cre/+};Ctnnb1^{flx/flx}* embryos were distinguished by the absence of the adrenals at E14.5. At E16.5, the failure of the testes to separate from the kidneys was apparent, and a mild dilation of the proximal ureter was observed in some mutant specimens (Fig. 3A). Histological analysis revealed the first hydronephrotic lesions (dilation of the pelvicalyceal space) in the mutant kidney at this stage, i.e. shortly after onset of urine production (Fig. 3B). In the *Ctnnb1*-deficient ureter, a mesenchymal compartment was established at E12.5 but all cells remained loosely organized with small cell bodies arranged in a tangential fashion at subsequent stages. This contrasted with the

situation in the wild-type ureteric mesenchyme, where loosely organized cells of typical fibroblast appearance with large protrusions were restricted to an outer layer, while cells adjacent to the epithelium were denser in appearance with large cell bodies from E12.5 onwards (Fig. 3C).

To examine whether these histological changes were accompanied or followed by changes in differentiation of the ureteric mesenchyme, we analyzed expression of the SM regulatory gene *Myocd*, the SM structural genes *Tagln* and troponin T2, cardiac (*Tnnt2*), and of markers of the adventitial fate collagen 1a2 (*Col1a2*) and fibulin 2 (*Fbln2*). In the wild type, *Myocd* was activated at E14.5 in the proximal region of the ureter (Fig. 3D), whereas *Tagln* and *Tnnt2* were first expressed at E16.5. *Col1a2* and *Fbln2* expression was homogenous in the ureteric mesenchyme at E14.5, but was excluded from the inner mesenchymal layers comprising lamina propria fibroblasts and SMCs at E16.5. In the mutant ureter, *Myocd* and SM structural genes were never expressed. *Col1a2* and *Fbln2* expression, by contrast, was found throughout the ureteric mesenchyme (Fig. 3D-H).

In summary, morphological and histological analyses revealed the onset of ureter anomalies in *Tbx18^{cre/+};Ctnnb1^{flx/flx}* embryos at E12.5, with a progression of phenotypic severity during subsequent embryonic stages and onset of hydronephrosis at E16.5. This, together with the absence of SMC differentiation and expanded expression of adventitial fibroblast markers argues for a function of canonical Wnt signaling in ureteric mesenchymal patterning and/or in the initiation of the SM developmental program.

Defects in mesenchymal patterning precede SM differentiation defects

In order to analyze the molecular changes that caused the defective SMC differentiation in *Tbx18^{cre/+};Ctnnb1^{flx/flx}* ureters, we screened for expression of a panel of genes that have been implicated in the early development of the ureteric mesenchyme and the initiation of the SM program by in situ hybridization analysis on ureter sections. In E12.5 wild-type ureters, *Bmp4*, *Gata2*, the target of Shh signaling patched 1 (*Ptch1*) (Ingham and McMahon, 2001), podocyte-expressed 1 (*Pod1*, also known as *Tcf21*), *Tshz3*, *Tbx18*, *Sox9* and secreted frizzled-related protein 2 (*Sfrp2*) were expressed throughout the mesenchymal compartment with increased levels in cells adjacent to the epithelium. Expression of chemokine (C-X-C motif) ligand 12 (*Cxcl12*) and BMP-binding endothelial regulator (*Bmper*) appeared uniformly high throughout the entire ureteric mesenchyme. In *Tbx18^{cre/+};Ctnnb1^{flx/flx}* ureters, only the expression of *Tbx18*, *Sox9* and *Sfrp2* was altered, as these were no longer detected at this stage (Fig. 4A-J). The normal expression of *Tbx18* in *Tbx18^{cre/+};Ctnnb1^{flx/flx}* embryos excluded a gene-dosage effect as the cause for *Tbx18* downregulation in the *Ctnnb1* mutant ureter (supplementary material Fig. S4).

In E14.5 wild-type ureters, *Bmp4*, *Gata2*, *Ptch1*, *Pod1* and *Tshz3* were expressed in the inner layer of the mesenchymal cells from which SMCs will arise. Expression of *Bmper* and *Cxcl12* was restricted to the outer layer from which adventitial fibroblasts will differentiate. In the *Ctnnb1*-deficient ureter, mesenchymal expression of *Bmp4* and *Pod1* was absent, and *Gata2* and *Tshz3* were strongly reduced. Expression of *Ptch1* was less affected, arguing that Shh signaling was still present to some degree (Fig. 4A-E). Expression of *Bmper* and *Cxcl12* was found throughout the mutant ureteric mesenchyme at this stage (Fig. 4F,G, arrows). To exclude the possibility that the *Ctnnb1*-deficient ureteric mesenchyme acquires the fate of an adjacent tissue, we additionally checked the expression of markers of the somitic mesoderm (*Tcf15*,

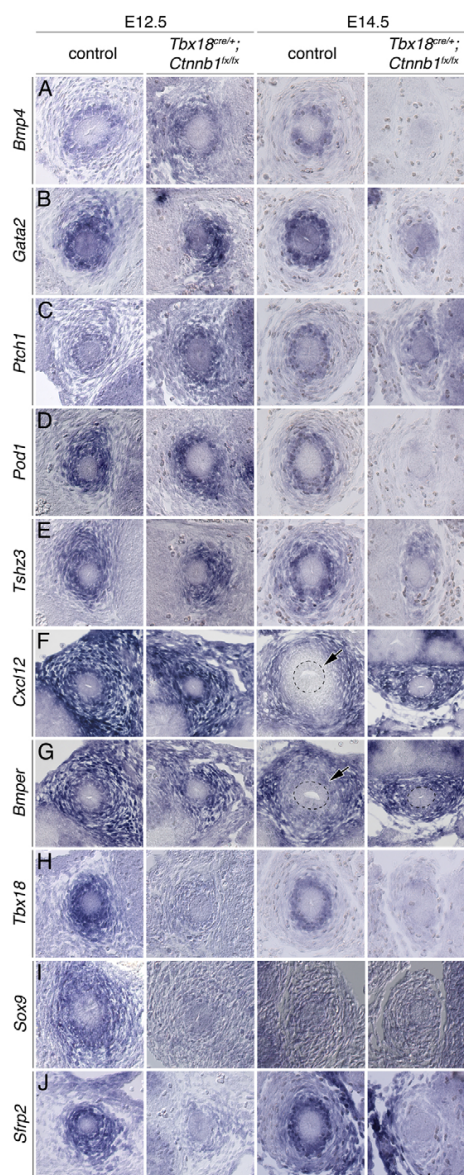


Fig. 4. Molecular characterization of *Ctnnb1*-deficient ureteric mesenchyme. (A-J) In situ hybridization analysis on transverse ureter sections at E12.5 and E14.5. (F,G) Arrows indicate the inner ring of mesenchymal cells; the ureteric epithelium is outlined (dashed line).

also known as *paraxis*), the hindlimb mesenchyme (*Tbx4*), adrenogenital tissue (*Nr5a1*, also known as *SF1*), the cap mesenchyme of nephron progenitors (*Osr1*, *Uncx4.1*, *Six2*), and chondrocytes (*Col2a1*). None of these markers was ectopically activated in the ureteric mesenchyme of *Tbx18^{cre/+};Ctnnb1^{flx/flx}* embryos (supplementary material Fig. S5). Together, this suggests that the initial specification of the ureteric mesenchyme occurs

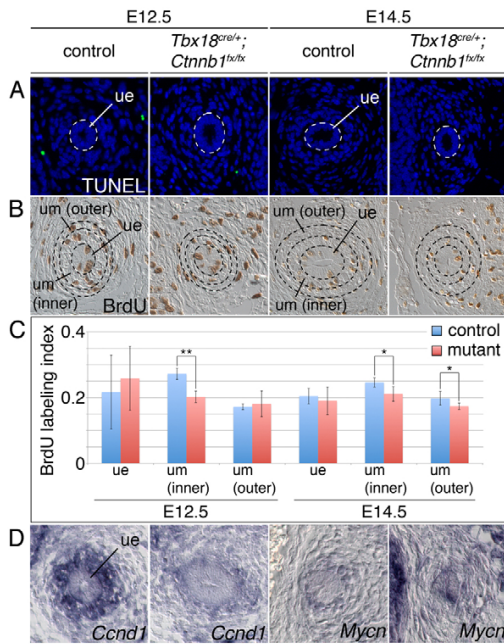


Fig. 5. Cellular defects in *Ctnnb1*-deficient ureteric mesenchyme. (A–C) Analysis of cell death by TUNEL assay (A) and of cell proliferation by BrdU incorporation assay (B, C) on transverse sections of mouse proximal ureter at E12.5 and E14.5. White dashed circles in A indicate the ureteric epithelium (ue); black dashed circles in B mark the ureteric epithelium and the inner and outer layers of ureteric mesenchymal cells (um) that were analyzed for proliferation. (C) Quantification of BrdU-positive cells. E12.5 ($n=3$), wild type versus mutant: ue, 0.217 ± 0.113 versus 0.258 ± 0.097 , $P=0.653$; um (inner layer), 0.272 ± 0.017 versus 0.202 ± 0.017 , $P=0.008$; um (outer layer), 0.172 ± 0.009 versus 0.181 ± 0.039 , $P=0.727$. E14.5 ($n=5$), wild type versus mutant: ue, 0.204 ± 0.024 versus 0.19 ± 0.042 , $P=0.527$; um (inner layer), 0.246 ± 0.014 versus 0.211 ± 0.022 , $P=0.034$; um (outer layer), 0.198 ± 0.021 versus 0.174 ± 0.01 , $P=0.047$. Error bars indicate s.d. *, $P<0.05$; **, $P<0.01$; two-tailed Student's *t*-test. (D) Expression analysis of *Ccnd1* and *Mycn* by in situ hybridization on transverse sections of the proximal ureter at E12.5.

normally in *Tbx18^{cre/+};Ctnnb1^{fx/fx}* embryos but that during the subsequent differentiation step fibroblasts expand at the expense of (prospective) SMC fates.

As *Tbx18*-deficient ureters also exhibit a severe reduction of SMCs (Airik et al., 2006), we examined whether the early loss of *Tbx18* expression contributed to the observed defects in *Ctnnb1*-deficient ureters. We tested this hypothesis by re-expressing *Tbx18* in the *Ctnnb1*-deficient ureteric mesenchyme. We generated an *Hprt^{Tbx18}* allele by integrating a bicistronic transgene cassette containing the mouse *Tbx18* ORF followed by IRES-GFP into the ubiquitously expressed X-chromosomal *Hprt* locus, similar to a previously published strategy for *Sox9* (Airik et al., 2010) (supplementary material Fig. S6). To activate transgene expression, we used the *Tbx18^{cre}* mouse line. Re-expression of *Tbx18* in *Tbx18^{cre/+};Ctnnb1^{fx/fx};Hprt^{Tbx18/Y}* embryos did not rescue hydronephrosis and loss of SMC differentiation at E18.5, nor did it reconstitute the expression of markers that were absent or reduced in *Tbx18^{cre/+};Ctnnb1^{fx/fx}* ureters at E14.5 (supplementary

material Figs S7, S8). Since we found normal expression of *Tbx18* in the ureteric mesenchyme of *Tbx18^{cre/+};Ctnnb1^{fx/fx}* embryos at E11.5 (supplementary material Fig. S9), we conclude that the loss of *Tbx18* at E12.5 or after contributes only to a minor degree, if at all, to the observed molecular and histological changes in the *Ctnnb1*-deficient ureteric mesenchyme.

Cellular changes in the ureteric mesenchyme of *Tbx18^{cre/+};Ctnnb1^{fx/fx}* mice

The loss of expression of markers of the inner, and expansion of markers of the outer, mesenchymal cell layer in *Ctnnb1*-deficient ureters might reflect a role of canonical Wnt signaling in maintaining SMC precursors. The TUNEL assay did not detect apoptotic cells at E12.5 or E14.5 in the mutant ureteric mesenchyme (Fig. 5A) making it unlikely that Wnts simply act as survival factors for these cells. However, Wnt signaling contributed to some degree to the proliferation of the inner ring of *Axin2*-positive mesenchymal cells at E12.5 and E14.5, as detected by reduced BrdU incorporation in this domain of the *Ctnnb1*-deficient ureteric mesenchyme (Fig. 5B,C). Strong reduction of the cell-cycle regulator gene cyclin D1 (*Ccnd1*) and slightly reduced expression of the pro-proliferative factor *Mycn* (Fig. 5D), which are regulated by canonical Wnt signaling in other contexts (Shtutman et al., 1999; ten Berge et al., 2008), might contribute to this finding.

Canonical Wnt signaling is sufficient to induce SMC development in the ureteric mesenchyme

Our loss-of-function analysis indicated an essential role of *Ctnnb1*-dependent Wnt signaling for SM development in the ureter, possibly by specifying an SMC precursor. To further test this hypothesis, we performed a complementary gain-of-function study with conditional (*Tbx18^{cre}*-mediated) overexpression of a stabilized form of Ctnnb1 [*Ctnnb1^{(ex3)β}*] in the ureteric mesenchyme in vivo (Fig. 6) (Harada et al., 1999). As shown above, *Tbx18^{cre}*-mediated recombination is not restricted to the SMC lineage but occurs in the precursor pool of all mesenchymal cell types of the ureter (supplementary material Fig. S1), allowing ectopic activation of canonical Wnt signaling in prospective fibroblasts as well.

We validated this experimental strategy by comparative expression analysis of the lineage marker GFP and the target of canonical Wnt signaling *Axin2* on adjacent sections. In control embryos (*Tbx18^{cre/+};R26^{mTmG/+}*), GFP expression marked a band of mesenchymal cells between the metanephric mesenchyme and the Wolffian duct at E11.5, and labeled all mesenchymal cells surrounding the distal ureter stalk at E12.5. At both stages, *Axin2* expression was barely detectable under the conditions used (we developed the color reaction for a shorter time than shown in Fig. 1) in the innermost layer of mesenchymal cells adjacent to the ureteric epithelium. In *Tbx18^{cre/+};R26^{mTmG/+};Ctnnb1^{(ex3)β/+}* embryos, *Axin2* expression was strongly activated in almost all GFP-positive cells in the E11.5 and E12.5 ureter, confirming the premature and ectopic activation of canonical Wnt signaling at high levels in precursor cells for all differentiated cell types of the ureteric mesenchyme (Fig. 6A–H'). Histological analysis revealed that the enlarged GFP⁺ *Axin2*⁺ domain in E12.5 *Tbx18^{cre/+};R26^{mTmG/+};Ctnnb1^{(ex3)β/+}* ureters almost exclusively harbored densely packed large mesenchymal cells that were rhomboid in shape. In control embryos, this cell morphology was restricted to the innermost ring of the ureteric mesenchyme at E12.5 and E14.5, whereas the rest of the GFP⁺ ureteric mesenchyme featured cells that were slender and loosely packed,

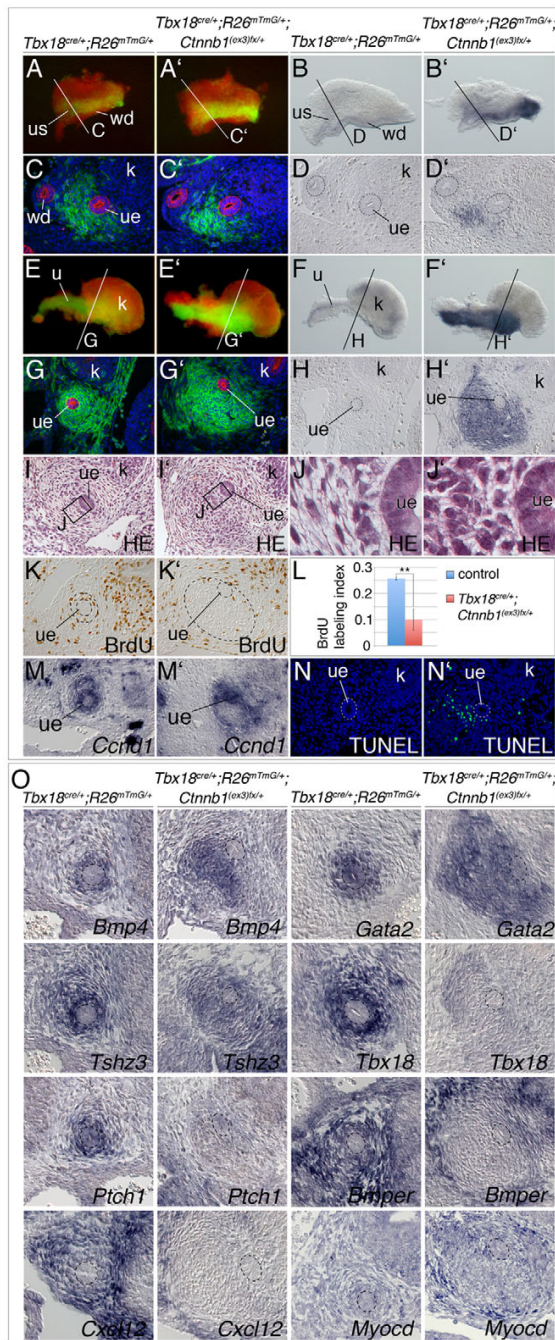


Fig. 6. Stabilization of Ctnnb1 in the ureteric mesenchyme triggers ectopic differentiation of SMC progenitors. (A,A',E,E') GFP/RFP epifluorescence in whole mouse kidneys at E11.5 (A,A') and E12.5 (E,E'). (B,B',D,D',F,F',H,H') In situ hybridization analysis of *Axin2* expression in whole kidneys at E11.5 (B,B') and E12.5 (F,F') and in sections of these kidneys (planes as indicated) (D,D',H,H'). (C,C',G,G') Immunofluorescent staining against GFP of the *R26^{mTmG}* reporter allele in sections of E11.5 (C,C') and E12.5 (G,G') kidneys. (I-J) Hematoxylin and Eosin stainings of transverse sections of the proximal ureter at E12.5. (K-L) Analysis of cell proliferation by the BrdU incorporation assay on transverse sections of the proximal ureter at E12.5. The regions counted, as marked by dashed lines in K,K', are the GFP⁺ *Axin2*⁺ region of mesenchymal cells of the ureter. (L) Quantification of BrdU-positive cells. Wild type versus mutant: 0.257±0.006 versus 0.1±0.04, *P*=0.003; *n*=3. Error bars indicate s.d. **, *P*<0.01; two-tailed Student's *t*-test. (M,M',O) In situ hybridization analysis on transverse ureter sections at E12.5. (N,N') Analysis of cell death (green) by the TUNEL assay. Sections were counterstained with DAPI. k, kidney; ue, ureteric epithelium; us, ureter stalk; wd, Wolffian duct.

expansion of putative SM progenitors by enhanced Wnt signaling but point to a reprogramming of prospective fibroblasts toward an SMC fate.

We further tested this idea by analyzing the expression of a panel of marker genes associated with differentiation of SMCs and fibroblasts in the ureter. *Bmp4*, *Gata2* and *Tshz3*, which are expressed throughout the entire ureteric mesenchyme of wild-type ureters at E12.5 and mark prospective SMCs of the inner ring in the wild type at E14.5, were expressed throughout the large GFP⁺ *Axin2*⁺ domain of the ureteric mesenchyme of *Tbx18^{cre/+};R26^{mTmG/+};Ctnnb1^(ex3)/fx</sup>+/+</sup>* embryos at E12.5. By contrast, *Tbx18*, *Pod1* and *Ptch1*, which have similar expression patterns in the wild type, were severely downregulated in the mutants. Expression of *Bmper* and *Cxcl12*, which are restricted to the non-myogenic lineage of the ureteric mesenchyme in the wild type starting from E14.5, was clearly excluded from the GFP⁺ *Axin2*⁺ mesenchymal cells in *Tbx18^{cre/+};Ctnnb1^(ex3)/fx</sup>+/+</sup>* ureters. To our surprise, we detected weak expression of *Myocd* in the mutant, whereas no expression was found in the wild-type ureteric mesenchyme at this stage (Fig. 6O). These data indicate that stabilization of Ctnnb1/enhanced Wnt signaling prevents fibroblast differentiation and promotes premature SMC differentiation in the ureteric mesenchyme.

As *Tbx18^{cre/+};Ctnnb1^(ex3)/fx</sup>+/+</sup>* mice die at ~E12.5 due to cardiovascular lesions (Norden et al., 2011), we could not observe the long-term effect of our misexpression approach on cell differentiation in vivo. Therefore, we explanted whole urogenital systems at E12.5, cultured them for 4 days and examined the histology and expression of SM structural markers on adjacent transverse sections of the proximal ureter (Fig. 7). Analyses at later time points, which might have been more representative of the full differentiation potential of the ureteric mesenchyme, were not possible owing to subsequent degeneration of the mutant ureter by apoptosis (compare with Fig. 6N'). In control specimens, the E-cadherin (Cdh1)-positive ureteric epithelium was encircled by mesenchymal cells that expressed the lineage marker GFP but were negative (at this level of signal development) for the target of canonical Wnt signaling *Axin2* (Fig. 7A,C). Cells in the outer, less dense region expressed the fibroblast marker *Colla2*, whereas an

as is typical for fibroblasts (Fig. 6I-J'). The BrdU incorporation assay demonstrated that cell proliferation was actually decreased, correlating with the absence of *Cnd1* expression, while TUNEL staining detected increased levels of apoptosis in the GFP⁺ *Axin2*⁺ domain of the ureteric mesenchyme in *Tbx18^{cre/+};R26^{mTmG/+};Ctnnb1^(ex3)/fx</sup>+/+</sup>* embryos at E12.5 (Fig. 6K-N'). Together, these findings argue against a selective proliferative

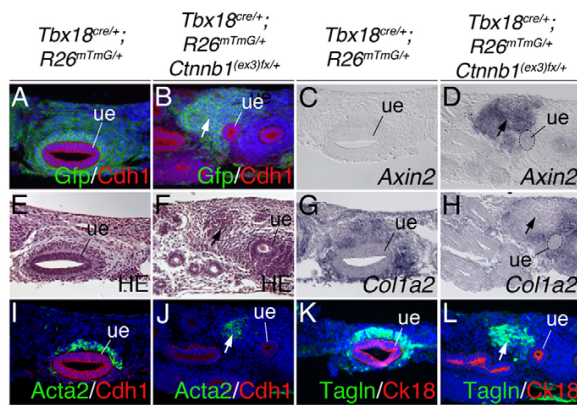


Fig. 7. Stabilization of Ctnnb1 in the ureteric mesenchyme results in ectopic SMC differentiation. Whole urogenital systems of E12.5 *Tbx18^{cre/+};R26^{mTmG/+}* (control) and *Tbx18^{cre/+};R26^{mTmG/+};Ctnnb1^{(ex3)fx/+}* mouse embryos were explanted, cultured for 4 days, sectioned through the proximal ureter region and analyzed by (A,B,I-L) co-immunofluorescence, (C,D,G,H) in situ hybridization and (E,F) Hematoxylin and Eosin staining. Arrows indicate the GFP⁺ Axin2⁺ domain in the ureteric mesenchyme of *Tbx18^{cre/+};R26^{mTmG/+};Ctnnb1^{(ex3)fx/+}* embryos. For immunofluorescent stainings, sections were counterstained with DAPI. Cdh1 and Ck18 immunofluorescence visualizes the ureteric epithelium. ue, ureteric epithelium.

inner ring of highly condensed mesenchymal cells was positive for the SMC markers Acta2 and Tagln (Fig. 7C,G,I,K). In *Tbx18^{cre/+};R26^{mTmG/+};Ctnnb1^{(ex3)fx/+}* explant cultures, the ureteric epithelium appeared mildly hypoplastic, with cells showing enlarged nuclei. An accumulation of GFP-positive mesenchymal cells in proximity to the ureteric epithelium expressed high levels of *Axin2*, demonstrating continuous activity of the canonical Wnt signaling pathway in these cells (Fig. 7B,D). These GFP⁺ *Axin2*⁺ cells were not positive for the fibroblast marker *Colla2* but expressed Acta2 and Tagln, albeit at slightly reduced levels compared with the wild type (Fig. 7H,J,L). These data strongly suggest that forced activation of the Ctnnb1-dependent Wnt signaling pathway is sufficient to induce SMC differentiation in the ureteric mesenchyme.

DISCUSSION

Specification of SMC precursors by epithelial Wnt signals in the ureteric mesenchyme

The development of the distal ureter and its surrounding mesenchymal layer lacks the complex morphogenetic processes of the proximal part. Nonetheless, it is obvious that proliferation rates and differentiation waves require spatial and temporal coordination between the epithelium and the surrounding mesenchyme to achieve continuous elongation and to acquire functional integrity at the onset of urine production in the kidney. In fact, embryological experiments have shown that the urothelium is necessary for the survival of isolated ureteric mesenchyme and induction of SMCs (Cunha, 1976), and that the mesenchymal layer controls urothelial survival, proliferation and differentiation (Airik and Kispert, 2007). However, the molecular nature of the underlying signaling systems has remained largely obscure, with the exception of epithelial Shh signals that are required for patterning and proliferation of the adjacent SMC layer (Yu et al., 2002).

Our data suggest that epithelial signals of the Wnt family play a crucial role in SMC development in the ureteric mesenchyme. Our exhaustive in situ hybridization screen identified expression of *Wnt7b* and *Wnt9b* in the ureteric epithelium but failed to detect expression of Wnt family members in the adjacent mesenchyme. By contrast, we found expression of the Wnt receptor gene *Fzd1* and of the target of canonical Wnt signaling *Axin2* in the mesenchyme but only weakly and transiently (*Axin2* at E11.5) in the epithelium, arguing that *Wnt7b* and *Wnt9b* act in a paracrine fashion on the mesenchymal tissue compartment to activate the canonical Wnt signaling pathway. Previous functional analyses of *Wnt7b* and *Wnt9b* have revealed their role as canonical Wnt ligands in the development of the renal medulla and as inducers of nephrogenesis but have not described ureter defects (Carroll et al., 2005; Yu et al., 2009), suggesting that *Wnt7b* and *Wnt9b* act redundantly in the ureteric epithelium. *Axin2* expression was confined to a single layer of mesenchymal cells directly adjacent to the epithelial compartment, indicating that, in this context, epithelial Wnt signals are largely non-diffusible and do not act as morphogens, but act from cell to cell. To our knowledge, *Axin2* is the earliest marker that molecularly distinguishes mesenchymal cells of an inner from that of an outer mesenchymal compartment. Shortly after the onset of *Axin2* expression at E12.5, cells of the inner ring undergo characteristic cell shape changes that clearly distinguish them from outer mesenchymal cells. Although lineage tracing has not yet been performed to confirm this, it is very likely that SMCs arise exclusively from the (*Axin2*⁺) inner compartment, whereas the outer compartment gives rise to adventitial fibroblasts.

Our genetic experiments and supportive pharmacological inhibition studies showed that loss of *Ctnnb1*-dependent Wnt signaling results in absence of the SMC lineage. This phenotype is compatible with a number of functions for canonical Wnt signaling, including the aggregation, specification or survival of uncommitted precursor cells, proliferation and expansion of specified precursors and/or terminal differentiation of SMCs. Our analysis of *Ctnnb1*-deficient embryos has shown that the ureteric mesenchyme aggregated normally around the distal ureter stalk and exhibited reduced proliferation but survived throughout development. In turn, stabilization of Ctnnb1 did not lead to aggregation of cells but merely to shape changes of resident cells that had reduced proliferation and increased apoptosis, strongly arguing against a primary function of canonical Wnt signaling in the aggregation and survival of the ureteric mesenchyme. We suggest that proliferation of the ureteric mesenchyme, particularly increased proliferation of SMC precursors, is mediated both by Shh (Yu et al., 2002) and by epithelial Wnt signals. We deem it unlikely that canonical Wnts act late on as terminal differentiation signals for SMCs either, as *Axin2* expression was activated early and dropped sharply after the onset of *Myocd* expression. In our opinion, our dataset is most compatible with a role of canonical Wnt signaling in initiating SMC development by specifying SMC precursors at the expense of the alternative fibroblast fate, for the following reasons. First, expression of *Axin2* preceded the characteristic cell shape changes of the inner ureteric mesenchymal cell layer. Second, these cell shape changes were largely prevented when canonical Wnt signaling was absent, whereby SMC differentiation failed completely and the fibroblast layer was expanded instead. Third, expression of all markers of SMC precursors was completely lost by E14.5. Finally, canonical Wnt signaling was sufficient to induce the characteristic cell shape

changes and marker expression in unprogrammed precursor cells, which was followed by SMC development at the expense of fibroblast fates.

Mesenchymal cells expressing stabilized Ctnnb1, i.e. possessing enhanced Wnt signaling, expressed *Myocd* and SM structural genes at much lower levels than in the wild-type ureter. It is conceivable that additional signals emitted from the ureteric epithelium are required for increased proliferation and terminal differentiation of these cells. In fact, cells with ectopic Wnt signaling lacked the Shh signaling that has previously been shown to increase the proliferation of SMCs (Yu et al., 2002). Alternatively, or additionally, prolonged activation of canonical Wnt signaling might actually prevent terminal differentiation.

A requirement for *Ctnnb1*-dependent Wnt signaling in SMC development is not without precedence but the specific function and mode of action seem to vary in different tissues. Loss of *Wnt7b* from the pulmonary epithelium resulted in decreased mesenchymal differentiation and proliferation and, later in development, decreased vascular SMC integrity in the lung (Shu et al., 2002). *Wnt4* was shown to be required in an autocrine fashion for SMC differentiation in the medullary stroma (Itäranta et al., 2006) and for SMC proliferation during intimal thickening in the vascular system (Tsaousi et al., 2011).

Canonical Wnt signaling is independent of *Tbx18* but acts upstream of other factors required for SMC differentiation

To date, only a small number of factors have been identified as crucial for ureteric SMC development (Airik and Kispert, 2007): *Tbx18* was implicated in the specification and cohesive aggregation of the ureteric mesenchyme (Airik et al., 2006), *Bmp4* and *Gata2* in control of ureter budding and SMC differentiation (Brenner-Anantharam et al., 2007; Dunn et al., 1997; Miyazaki et al., 2003; Zhou et al., 1998), Shh signaling in the proliferation and patterning of the ureteric mesenchyme (Yu et al., 2002) and *Tshz3* and *Sox9* in SMC differentiation (Airik et al., 2010; Caubit et al., 2008). *Gata2* and Shh signaling are thought to regulate *Bmp4*, which in turn regulates *Tshz3*. Although only specifically shown for *Sox9* and *Tshz3*, all of these genes are likely to act upstream of *Myocd*, the key regulator of SMC differentiation (Wang and Olson, 2004). Therefore, the loss of expression of all of these factors might collectively contribute to the loss of SMCs in the *Ctnnb1*-deficient mesenchyme. Downregulation of *Tbx18* preceded that of the other genes relevant to SMC formation, suggesting a primary requirement of this transcription factor upstream of other molecular circuits. However, re-expression of *Tbx18* in the *Ctnnb1*-deficient ureteric mesenchyme did not induce expression of any of these factors in this tissue, nor did it rescue SMC differentiation and hydroureter formation. Although this finding does not exclude the possibility that *Tbx18* is relevant for SMC differentiation, it shows that *Tbx18* is not sufficient to trigger the ureteric SMC differentiation program downstream of canonical Wnt signaling.

Early loss of expression of *Tbx18*, *Sfrp2* and *Sox9* at E12.5 and later loss of *Bmp4*, *Tshz3*, *Gata2* and *Pod1* in the *Ctnnb1*-deficient ureteric mesenchyme argue for differential regulation by Wnt signaling. In the first case, *Ctnnb1*-dependent Wnt signaling might be directly required to maintain the expression of *Tbx18* [*Sfrp2* and *Sox9* depend on *Tbx18* in turn (Airik et al., 2006)], whereas downregulation of the second set of genes might merely reflect a loss of specification of this cell type. The latter contention is

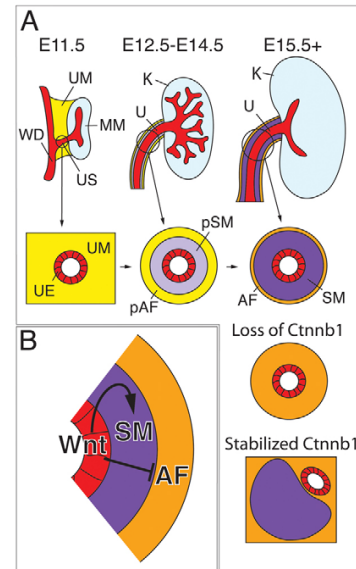


Fig. 8. Model of how canonical Wnt signaling directs the formation of SMCs in the developing mouse ureter. (A) Scheme of the developing mouse kidney and ureter. At E11.5, homogenous ureteric mesenchyme surrounds the epithelium in the distal ureter stalk region. Between E12.5 and E14.5, two mesenchymal subdomains become established whose cells differ in shape and gene expression profile. After E15.5, the inner domain differentiates into SMCs, whereas the outer domain differentiates into adventitial fibroblasts. Loss of Wnt signaling by deletion of *Ctnnb1* in the ureteric mesenchyme results in loss of the SMC lineage and expansion of fibroblast fates. Stabilization of Ctnnb1 throughout the entire ureteric mesenchyme induces ectopic SMC differentiation. (B) Scheme for radial patterning of the ureteric mesenchyme. Wnt signals from the ureter epithelium may specify SMCs and repress adventitial fibroblast fate. (p)AF, (prospective) adventitial fibroblasts; K, kidney; MM, metanephric mesenchyme; pSM, (prospective) smooth muscle cells; U, ureter; UE, ureteric epithelium; UM, ureteric mesenchyme; US, ureter stalk; WD, Wolffian duct.

supported by the concurrent expansion of markers for prospective fibroblasts. Interestingly, these markers are initially expressed uniformly as well, but become progressively restricted to the outer layer of prospective and definitive fibroblasts after E12.5. Hence, Wnt signaling may pattern the ureteric mesenchyme by inducing SMCs and/or by repressing a fibroblast fate.

Although all of these factors directly or indirectly depend on canonical Wnt signaling, they differentially respond to ectopic activation of this pathway in the prospective ureteric mesenchyme in *Tbx18^{cre/+};Ctnnb1^{(ex3)fl/+}* embryos: expression of *Tbx18* and *Pod1* is repressed, whereas *Bmp4*, *Gata2* and *Tshz3* are induced. We propose that this regulation reflects a differential cooperation of Wnt signaling with other signaling systems (e.g. Shh) in the ureteric mesenchyme.

It has recently been suggested that in the developing lung epithelial Wnt7b mediates, via the canonical pathway, the direct transcriptional activation of the extracellular matrix protein tenascin C (*Tnc*), which in turn is necessary and sufficient for expression of *Pdgfra/b* in the mesenchymal compartment (Cohen et al., 2009). We did not detect any changes in the expression of

these three genes in the *Ctnnb1*-deficient ureteric mesenchyme, arguing that the molecular pathways downstream of Wnt7b/*Ctnnb1* differ in different developmental settings (supplementary material Fig. S10).

In summary, our analysis suggests that Wnt proteins from the ureteric epithelium act as paracrine signals to initiate SM precursor development in adjacent mesenchymal cells, and thus may pattern the mesenchyme in a radial fashion (Fig. 8). Our findings emphasize the importance of epithelial-mesenchymal signaling in ureter development. They will help to further dissect the molecular pathways that are important for SMC differentiation in the excretory system and to develop strategies for the directed formation of this important cell type for therapeutic purposes.

Acknowledgements

We thank Andrew P. McMahon, Brian Parr, Cathy Mendelsohn, Charles J. Sherr, Christer Betsholtz, Gregory Shackleford, Laurent Fasano, Liz Robertson, Luc Leyns, Matthew Scott, Richard Stump, Suzanne Cory and Yingzi Yang for probes; R. Adelstein for the rabbit SMMHC antiserum; Rolf Kemler for the anti-Cdh1 antibody and *Ctnnb1^{flx}* mice; and Achim Gossler and Aravind Shekar for technical help.

Funding

This work was supported by a grant from the Deutsche Forschungsgemeinschaft [DFG KI728/7 to A.K.].

Competing interests statement

The authors declare no competing financial interests.

Supplementary material

Supplementary material available online at <http://dev.biologists.org/lookup/suppl/doi:10.1242/dev.077388/-DC1>

References

- Airik, R. and Kispert, A. (2007). Down the tube of obstructive nephropathies: the importance of tissue interactions during ureter development. *Kidney Int.* **72**, 1459-1467.
- Airik, R., Bussen, M., Singh, M. K., Petry, M. and Kispert, A. (2006). Tbx18 regulates the development of the ureteral mesenchyme. *J. Clin. Invest.* **116**, 663-674.
- Airik, R., Trowe, M. O., Foik, A., Farin, H. F., Petry, M., Schuster-Gossler, K., Schweizer, M., Scherer, G., Kist, R. and Kispert, A. (2010). Hydrourereteronephrosis due to loss of Sox9-regulated smooth muscle cell differentiation of the ureteric mesenchyme. *Hum. Mol. Genet.* **19**, 4918-4929.
- Barker, N. (2008). The canonical Wnt/beta-catenin signalling pathway. *Methods Mol. Biol.* **468**, 5-15.
- Braut, V., Moore, R., Kutsch, S., Ishibashi, M., Rowitch, D. H., McMahon, A. P., Sommer, L., Boussadia, O. and Kemler, R. (2001). Inactivation of the beta-catenin gene by Wnt1-Cre-mediated deletion results in dramatic brain malformation and failure of craniofacial development. *Development* **128**, 1253-1264.
- Brenner-Anantharam, A., Cebrian, C., Guillaume, R., Hurtado, R., Sun, T. T. and Herzlinger, D. (2007). Tailbud-derived mesenchyme promotes urinary tract segmentation via BMP4 signaling. *Development* **134**, 1967-1975.
- Bussen, M., Petry, M., Schuster-Gossler, K., Leitges, M., Gossler, A. and Kispert, A. (2004). The T-box transcription factor Tbx18 maintains the separation of anterior and posterior somite compartments. *Genes Dev.* **18**, 1209-1221.
- Carroll, T. J., Park, J. S., Hayashi, S., Majumdar, A. and McMahon, A. P. (2005). Wnt9b plays a central role in the regulation of mesenchymal to epithelial transitions underlying organogenesis of the mammalian urogenital system. *Dev. Cell* **9**, 283-292.
- Caubit, X., Lye, C. M., Martin, E., Coré, N., Long, D. A., Vola, C., Jenkins, D., Garratt, A. N., Skaer, H., Woolf, A. S. et al. (2008). Teashirt 3 is necessary for ureteral smooth muscle differentiation downstream of SHH and BMP4. *Development* **135**, 3301-3310.
- Chassot, A. A., Ranc, F., Gregoire, E. P., Roepers-Gajadien, H. L., Taketo, M. M., Camerino, G., de Rooij, D. G., Schedl, A. and Chaboissier, M. C. (2008). Activation of beta-catenin signaling by Rspo1 controls differentiation of the mammalian ovary. *Hum. Mol. Genet.* **17**, 1264-1277.
- Chevalier, R. L., Thornhill, B. A., Forbes, M. S. and Kiley, S. C. (2010). Mechanisms of renal injury and progression of renal disease in congenital obstructive nephropathy. *Pediatr. Nephrol.* **25**, 687-697.
- Cohen, E. D., Ihida-Stansbury, K., Lu, M. M., Panettieri, R. A., Jones, P. L. and Morrissey, E. E. (2009). Wnt signaling regulates smooth muscle precursor development in the mouse lung via a tenascin C/PDGFR pathway. *J. Clin. Invest.* **119**, 2538-2549.
- Cunha, G. R. (1976). Epithelial-stromal interactions in development of the urogenital tract. *Int. Rev. Cytol.* **47**, 137-194.
- Dunn, N. R., Winnier, G. E., Hargett, L. K., Schrick, J. J., Fogo, A. B. and Hogan, B. L. (1997). Haploinsufficient phenotypes in Bmp4 heterozygous null mice and modification by mutations in Gli3 and Alx4. *Dev. Biol.* **188**, 235-247.
- Harada, N., Tamai, Y., Ishikawa, T., Sauer, B., Takaku, K., Oshima, M. and Taketo, M. M. (1999). Intestinal polyposis in mice with a dominant stable mutation of the beta-catenin gene. *EMBO J.* **18**, 5931-5942.
- Ingham, P. W. and McMahon, A. P. (2001). Hedgehog signaling in animal development: paradigms and principles. *Genes Dev.* **15**, 3059-3087.
- Itäranta, P., Chi, L., Seppänen, T., Niku, M., Tuukkanen, J., Peltoketo, H. and Vainio, S. (2006). Wnt-4 signaling is involved in the control of smooth muscle cell fate via Bmp-4 in the medullary stroma of the developing kidney. *Dev. Biol.* **293**, 473-483.
- Jho, E. H., Zhang, T., Domon, C., Joo, C. K., Freund, J. N. and Costantini, F. (2002). Wnt/beta-catenin/Tcf signaling induces the transcription of Axin2, a negative regulator of the signaling pathway. *Mol. Cell. Biol.* **22**, 1172-1183.
- Karner, C. M., Das, A., Ma, Z., Self, M., Chen, C., Lum, L., Oliver, G. and Carroll, T. J. (2011). Canonical Wnt9b signaling balances progenitor cell expansion and differentiation during kidney development. *Development* **138**, 1247-1257.
- Kim, A. C., Reuter, A. L., Zubair, M., Else, T., Serecky, K., Bingham, N. C., Lavery, G. G., Parker, K. L. and Hammer, G. D. (2008). Targeted disruption of beta-catenin in Sf1-expressing cells impairs development and maintenance of the adrenal cortex. *Development* **135**, 2593-2602.
- Kraus, F., Haenig, B. and Kispert, A. (2001). Cloning and expression analysis of the mouse T-box gene Tbx18. *Mech. Dev.* **100**, 83-86.
- Luche, H., Weber, O., Nageswara Rao, T., Blum, C. and Fehling, H. J. (2007). Faithful activation of an extra-bright red fluorescent protein in "knock-in" Cre-reporter mice ideally suited for lineage tracing studies. *Eur. J. Immunol.* **37**, 43-53.
- MacDonald, B. T., Tamai, K. and He, X. (2009). Wnt/beta-catenin signaling: components, mechanisms, and diseases. *Dev. Cell* **17**, 9-26.
- Miller, R. K. and McCrear, P. D. (2010). Wnt to build a tube: contributions of Wnt signaling to epithelial tubulogenesis. *Dev. Dyn.* **239**, 77-93.
- Miyazaki, Y., Oshima, K., Fogo, A. and Ichikawa, I. (2003). Evidence that bone morphogenetic protein 4 has multiple biological functions during kidney and urinary tract development. *Kidney Int.* **63**, 835-844.
- Moorman, A. F., Houweling, A. C., de Boer, P. A. and Christoffels, V. M. (2001). Sensitive nonradioactive detection of mRNA in tissue sections: novel application of the whole-mount in situ hybridization protocol. *J. Histochem. Cytochem.* **49**, 1-8.
- Muzumdar, M. D., Tasic, B., Miyamichi, K., Li, L. and Luo, L. (2007). A global double-fluorescent Cre reporter mouse. *Genesis* **45**, 593-605.
- Norden, J., Greulich, F., Rudat, C., Taketo, M. M. and Kispert, A. (2011). Wnt/beta-catenin signaling maintains the mesenchymal precursor pool for murine sinus horn formation. *Circ. Res.* **109**, e42-e50.
- Rosen, S., Peters, C. A., Chevalier, R. L. and Huang, W. Y. (2008). The kidney in congenital ureteropelvic junction obstruction: a spectrum from normal to nephrectomy. *J. Urol.* **179**, 1257-1263.
- Shtutman, M., Zhurinsky, J., Simcha, I., Albanese, C., D'Amico, M., Pestell, R. and Ben-Ze'ev, A. (1999). The cyclin D1 gene is a target of the beta-catenin/LEF-1 pathway. *Proc. Natl. Acad. Sci. USA* **96**, 5522-5527.
- Shu, W., Jiang, Y. Q., Lu, M. M. and Morrissey, E. E. (2002). Wnt7b regulates mesenchymal proliferation and vascular development in the lung. *Development* **129**, 4831-4842.
- Song, R. and Yosypiv, I. V. (2011). Genetics of congenital anomalies of the kidney and urinary tract. *Pediatr. Nephrol.* **26**, 353-364.
- ten Berge, D., Brugmann, S. A., Helms, J. A. and Nusse, R. (2008). Wnt and FGF signals interact to coordinate growth with cell fate specification during limb development. *Development* **135**, 3247-3257.
- Trowe, M. O., Shah, S., Petry, M., Airik, R., Schuster-Gossler, K., Kist, R. and Kispert, A. (2010). Loss of Sox9 in the periotic mesenchyme affects mesenchymal expansion and differentiation, and epithelial morphogenesis during cochlea development in the mouse. *Dev. Biol.* **342**, 51-62.
- Tsaousi, A., Williams, H., Lyon, C. A., Taylor, V., Swain, A., Johnson, J. L. and George, S. J. (2011). Wnt4/beta-catenin signaling induces VSMC proliferation and is associated with intimal thickening. *Circ. Res.* **108**, 427-436.
- Uetani, N. and Bouchard, M. (2009). Plumbing in the embryo: developmental defects of the urinary tracts. *Clin. Genet.* **75**, 307-317.
- Wang, D. Z. and Olson, E. N. (2004). Control of smooth muscle development by the myocardin family of transcriptional coactivators. *Curr. Opin. Genet. Dev.* **14**, 558-566.
- Wilkinson, D. G. and Nieto, M. A. (1993). Detection of messenger RNA by in situ hybridization to tissue sections and whole mounts. *Methods Enzymol.* **225**, 361-373.
- Yu, J., Carroll, T. J. and McMahon, A. P. (2002). Sonic hedgehog regulates proliferation and differentiation of mesenchymal cells in the mouse metanephric kidney. *Development* **129**, 5301-5312.
- Yu, J., Carroll, T. J., Rajagopal, J., Kobayashi, A., Ren, Q. and McMahon, A. P. (2009). A Wnt7b-dependent pathway regulates the orientation of epithelial cell division and establishes the cortico-medullary axis of the mammalian kidney. *Development* **136**, 161-171.
- Zhou, Y., Lim, K. C., Onodera, K., Takahashi, S., Ohta, J., Minegishi, N., Tsai, F. Y., Orkin, S. H., Yamamoto, M. and Engel, J. D. (1998). Rescue of the embryonic lethal hematopoietic defect reveals a critical role for GATA-2 in urogenital development. *EMBO J.* **17**, 6689-6700.

Supplemental Figures
for

**Canonical Wnt signaling regulates smooth muscle precursor development
in the mouse ureter**

Mark-Oliver Trowe^{1,*}, Rannar Airik^{1,*}, Anna-Carina Weiss¹, Henner F. Farin¹, Anna B. Foik¹, Eva Bettenhausen¹, Karin Schuster-Gossler¹, Makoto Mark Taketo² and Andreas Kispert^{1,§}

¹Institut für Molekularbiologie, Medizinische Hochschule Hannover, 30625 Hannover, Germany

²Department of Pharmacology, Kyoto University, Kyoto 606-8501, Japan

§ Address correspondence to: Andreas Kispert, Institut für Molekularbiologie, OE5250, Medizinische Hochschule Hannover, Carl-Neuberg-Str. 1, D-30625 Hannover, Germany.
Phone: +49 511 5324017, Fax: +49 511 5324283, E-Mail: kispert.andreas@mh-hannover.de

*Authorship note: M.-O.T. and R.A. contributed equally to this work.

Short title: Wnt signaling in ureter development

Key words: Wnt, Ctnnb1, Ureter, Tbx18, smooth muscle cell

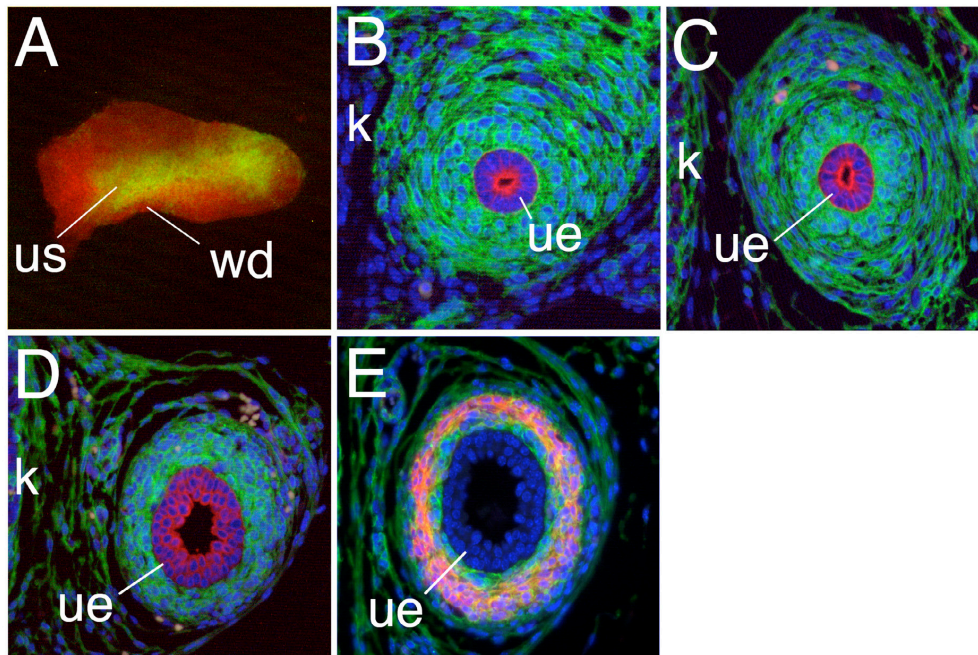


Fig. S1. *Tbx18^{cre}* mediates recombination of a reporter allele in the entire ureteric mesenchyme. (A) Analysis of GFP expression in whole E11.5 kidneys by epifluorescence, and (B-E) by anti-GFP immunofluorescence on sections through the ureter region at E12.5 (B), E14.5 (C), and E18.5 (D,E) of *Tbx18^{cre/+};R26^{mTmG/+}* embryos. GFP-positive cells are shown in green (A-E), the ureteric epithelium is marked in red by expression of Ck18 (B-D). All mesenchymal cells surrounding the ureteric epithelium are positive for the lineage marker GFP from E12.5 to E18.5. (E) Co-immunofluorescence analysis for expression of the SMC marker Acta2 (in red) shows that all differentiated cell types of the ureter mesenchyme at this stage, i.e. SMCs but also fibroblasts of the outer adventitia and the inner lamina propria derive from Tbx18-positive precursor cells. k, kidney; ue, ureteric epithelium; us, ureter stalk; wd, Wolffian duct.

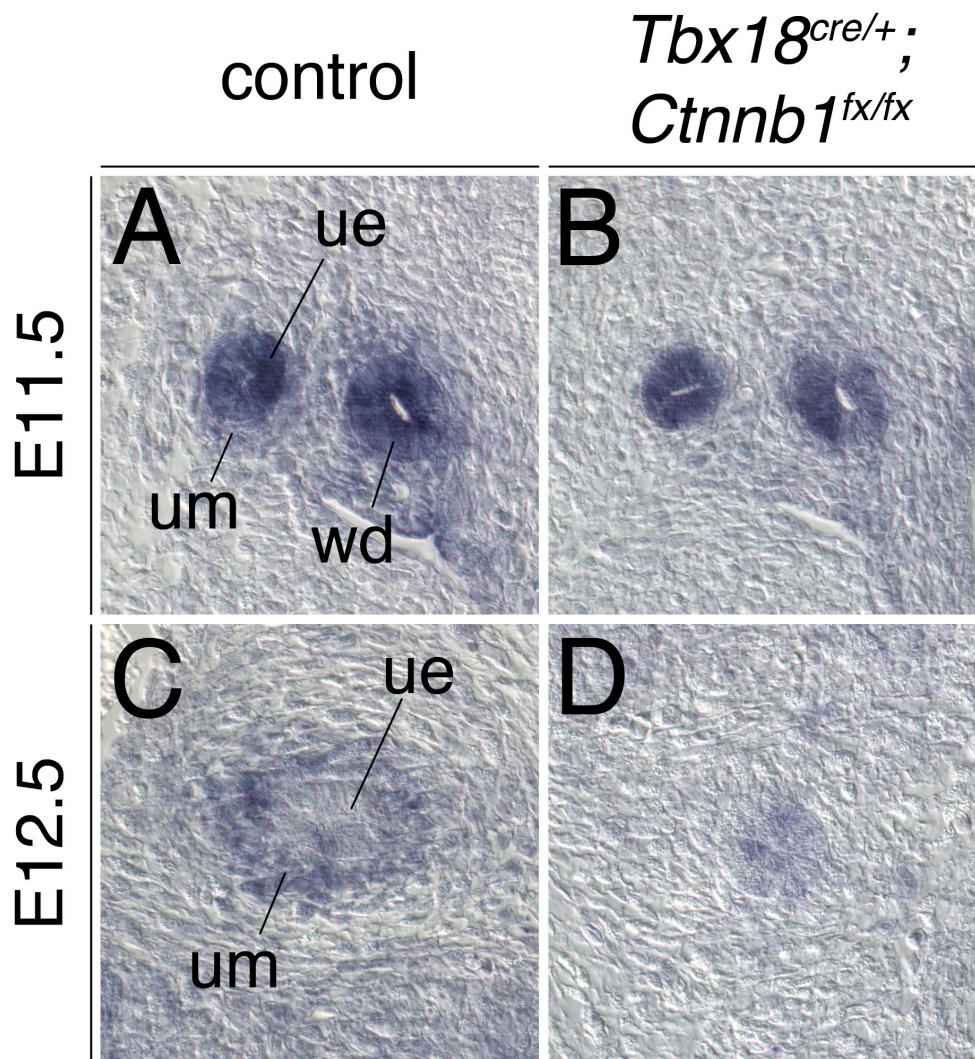


Fig. S2. Conditional inactivation of *Ctnnb1* in the ureteric mesenchyme. (A-D) Expression analysis of the *Ctnnb1* downstream target *Axin2* by *in situ* hybridization on transverse sections of the proximal ureter of *Tbx18*^{cre/+};*Ctnnb1*^{fx/fx} and control embryos at E11.5 and E12.5. Absence of *Axin2* expression indicates that *Tbx18*^{cre}-mediated deletion of *Ctnnb1* completely abrogates canonical Wnt signaling as early as E11.5. ue, ureteric epithelium; um, ureteric mesenchyme; wd, Wolffian duct.

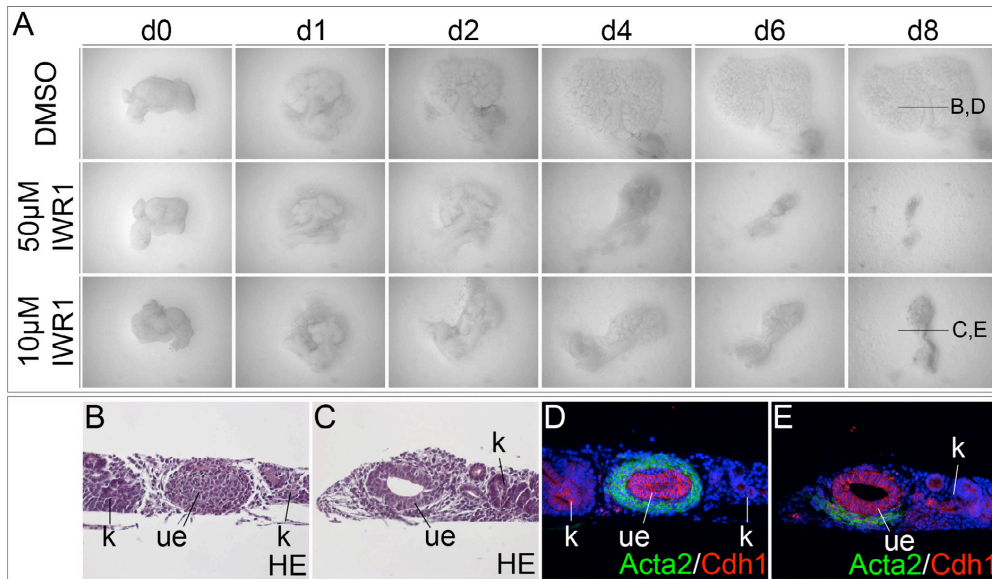


Fig. S3. Pharmacological inhibition of canonical Wnt signaling in kidney explant cultures severely affects differentiation and growth of the ureteric mesenchyme. (A) Morphological inspection of explants of E11.5 kidney rudiments at different days (d) of culture. Explants were treated with DMSO (control), and 50 μ M and 10 μ M of the inhibitor of canonical Wnt signaling IWR1, respectively. 50 μ M IWR1 results in complete degeneration of the ureter, whereas ureters survive in 10 μ M IWR1. Note that IWR1 also affects nephron induction in the metanephric mesenchyme leading to reduced branching and nephron formation at both concentrations. (B,C) Histological analysis by hematoxylin and eosin staining of sections through the ureter in 8d explant cultures treated with DMSO (B) or 10 μ M IWR1 (C) (section planes are marked in A). (D,E) Analysis of SM development by anti-Acta2 immunofluorescence (green) on adjacent sections shows severe reduction of the SMC layer surrounding the ureteric epithelium (visualized by expression of Cdh1 in red) in ureters treated with 10 μ M IWR1 (E) but not in control explants (D). k, kidney; ue, ureteric epithelium.

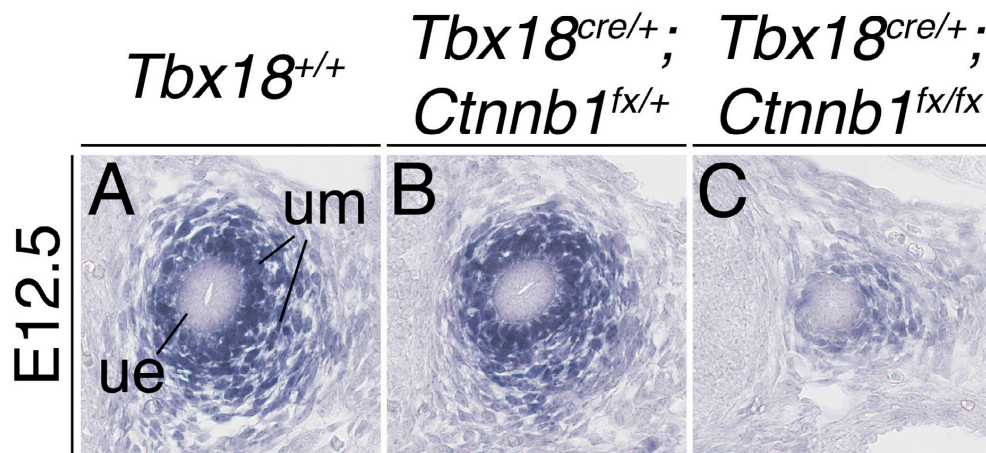


Fig. S4. Downregulation of *Tbx18* expression in the ureteric mesenchyme of *Tbx18^{cre/+};Ctnnb1^{fx/fx}* embryos at E12.5. (A-C) Expression of *Tbx18* as detected by *in situ* hybridization analysis on transverse sections of the proximal ureter at E12.5 in different genotypes. Unaltered expression of *Tbx18* in *Tbx18^{cre/+};Ctnnb1^{fx/+}* ureteric mesenchyme shows that reduction of *Tbx18* expression in *Tbx18^{cre/+};Ctnnb1^{fx/fx}* ureters is due to loss of *Ctnnb1* and not due to the presence of only one functional allele of *Tbx18*. ue, ureteric epithelium; um, ureteric mesenchyme.

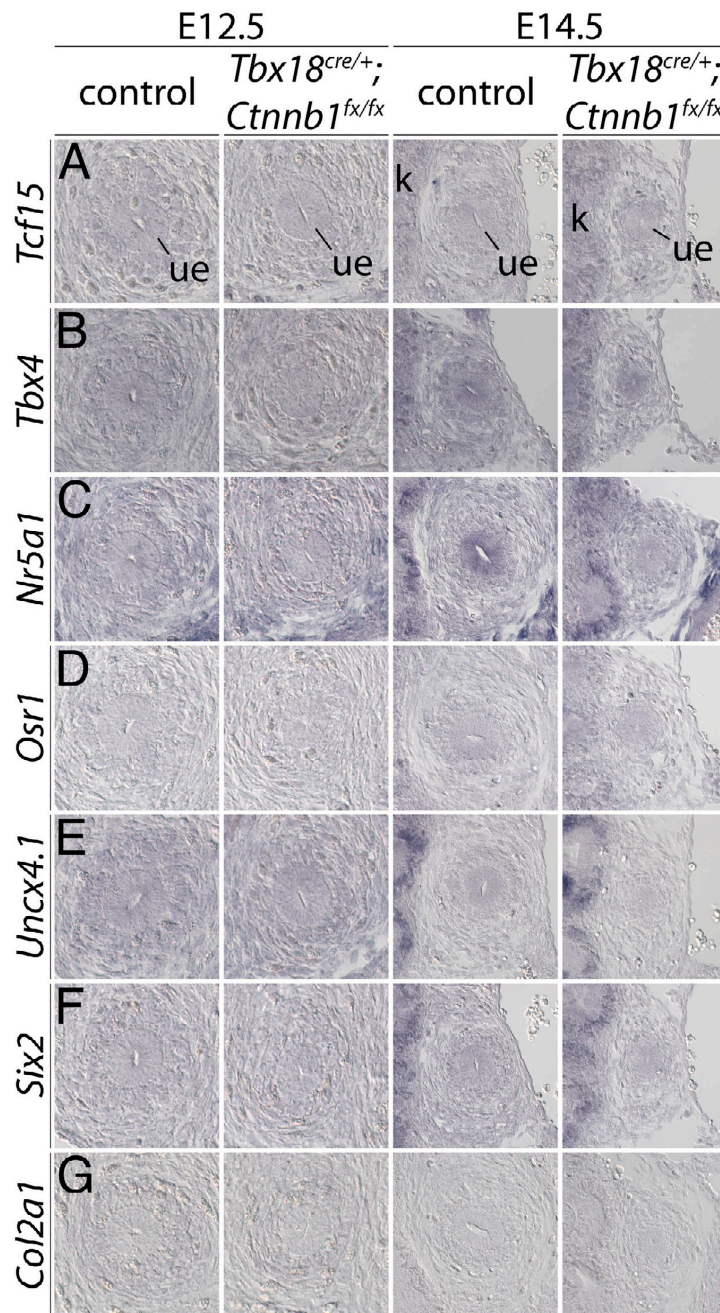


Fig. S5. Molecular characterization of the *Ctnnb1*-deficient ureteric mesenchyme. *In situ* hybridization analysis on transverse ureter sections at E12.5 and E14.5. Markers for somitic mesoderm (*Tcf15*), the hindlimb mesenchyme (*Tbx4*), adrenogenital tissue (*Nr5a1*), cap mesenchyme of nephron progenitors (*Osr1*, *Uncx4.1*, *Six2*), and chondrocytes (*Col2a1*) are not derepressed in the mesenchyme of *Tbx18^{cre/+};**Ctnnb1^{fx/fx}* ureters. Stages, probes and genotypes are as indicated. k, kidney; ue, ureteric epithelium.

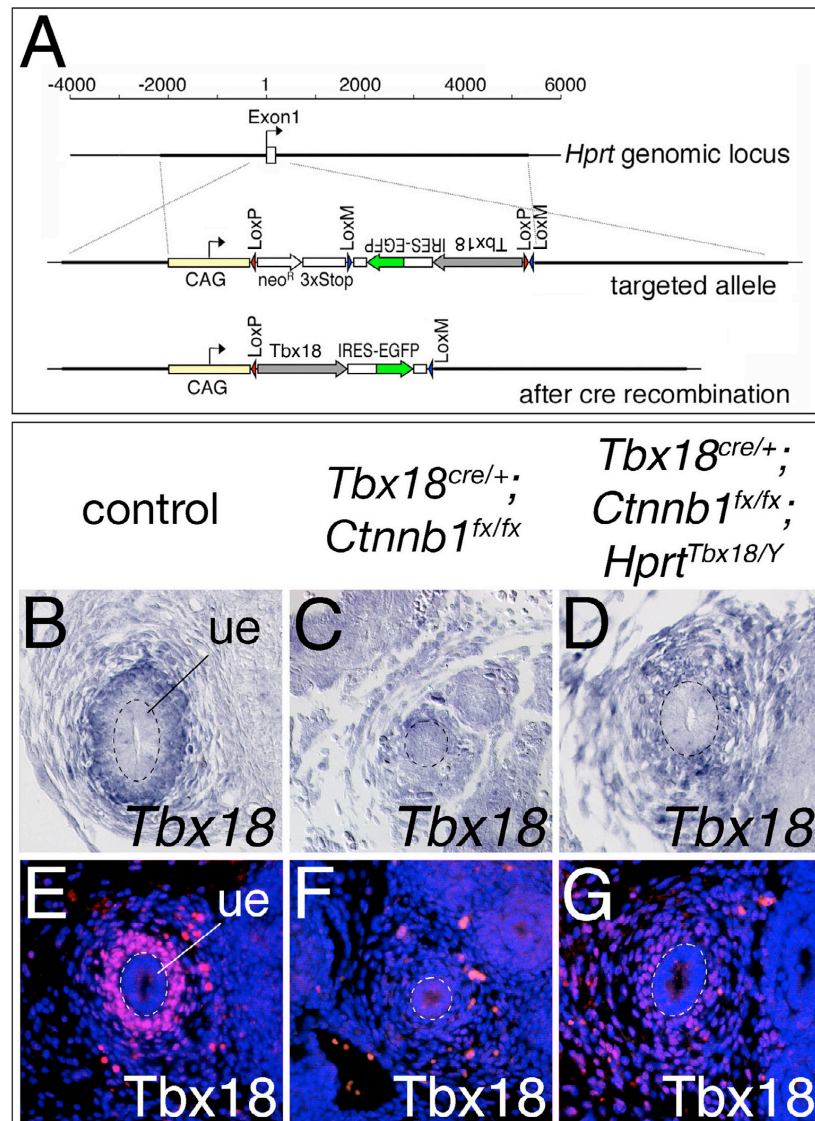


Fig. S6. Generation of an *Hprt*^{Tbx18} 'knock-in' allele. (A) Targeting strategy depicting the *Hypoxanthine guanine phosphoribosyl transferase* (*Hprt*) genomic locus in the wild-type (top), after homologous recombination in ES cells (middle) and after cre-mediated recombination (bottom), respectively. The scale bar shows distances (in base pairs) relative to the *Hprt* transcription start site; homology regions included in the targeting vectors are labeled with thick lines; asterisks mark a SV40 polyadenylation signal. Abbreviations are: 3xStop, three successive polyadenylation sequences from the bovine growth hormone gene; CAG, CMV early enhancer/chicken beta-actin promoter; IRES, internal ribosomal entry site; neo^R, neomycin resistance. (B-D) *In situ* hybridization analysis of *Tbx18* mRNA, and (E-F) immunofluorescence analysis of *Tbx18* protein expression on transverse sections of the proximal ureter at E14.5 of mice with genotypes as indicated. Expression of *Tbx18* from the *Hprt* allele reconstitutes (low level) expression of *Tbx18* mRNA and *Tbx18* protein in the ureteric mesenchyme in the *Ctnnb1*-deficient background. ue, ureteric epithelium.

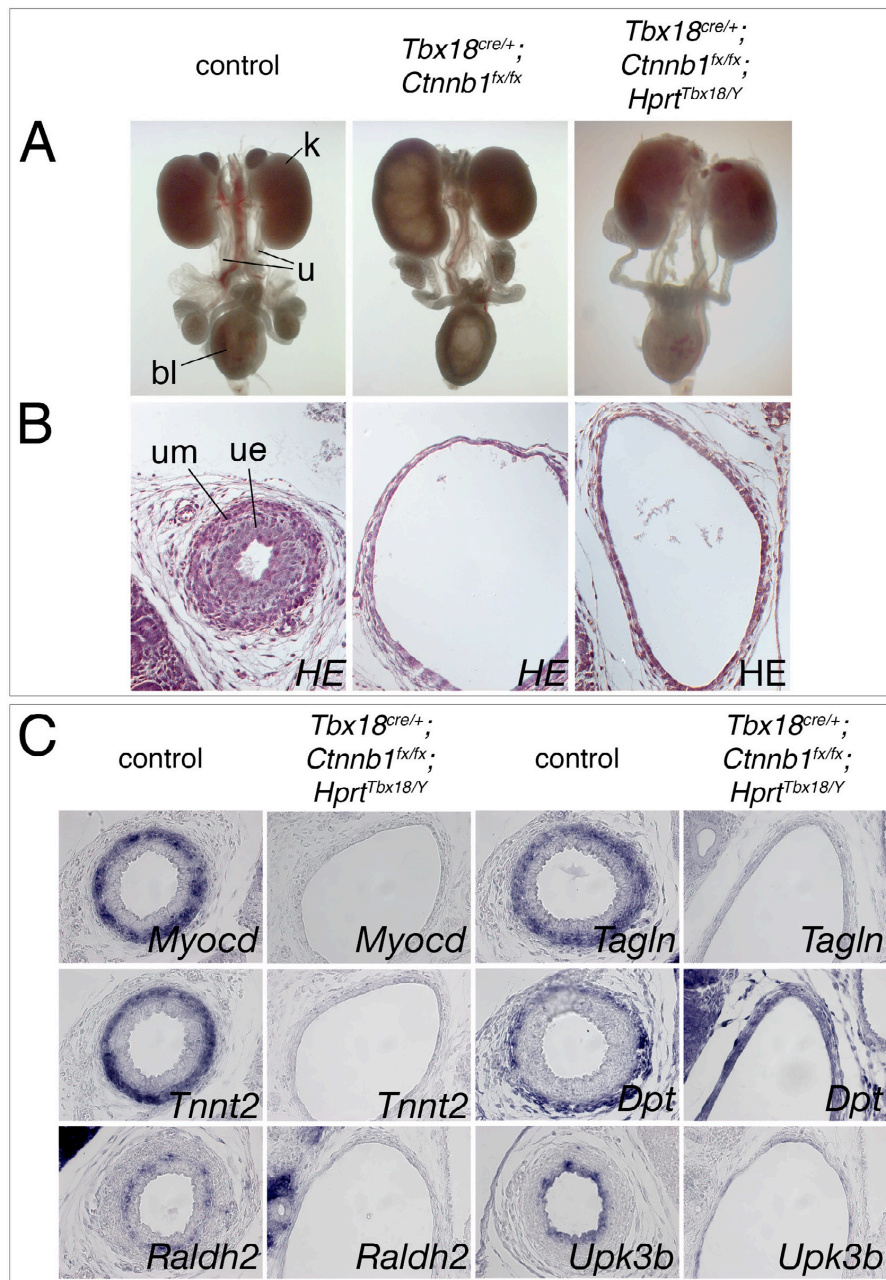


Fig. S7. Re-expression of *Tbx18* in the *Ctnnb1*-deficient ureteric mesenchyme does not rescue hydronephrosis and the lack of SMC differentiation. (A) Morphology of whole urogenital systems of male embryos, and (B) histological stainings (HE) of transverse sections of the proximal ureter at E18.5. (C) Cytodifferentiation of the ureter by *in situ* hybridization analysis on transverse sections of the proximal ureter at E18.5 for markers of SMCs (*Myocd*, *Tagln*, *Tnnt2*), adventitial fibroblasts (*Dpt*), lamina propria fibroblasts (*Raldh2*), and of the urothelium (*Upk3b*). Probes and genotypes are as indicated. bl, bladder; k, kidney; u, ureter; ue, ureteric epithelium; um, ureteric mesenchyme.

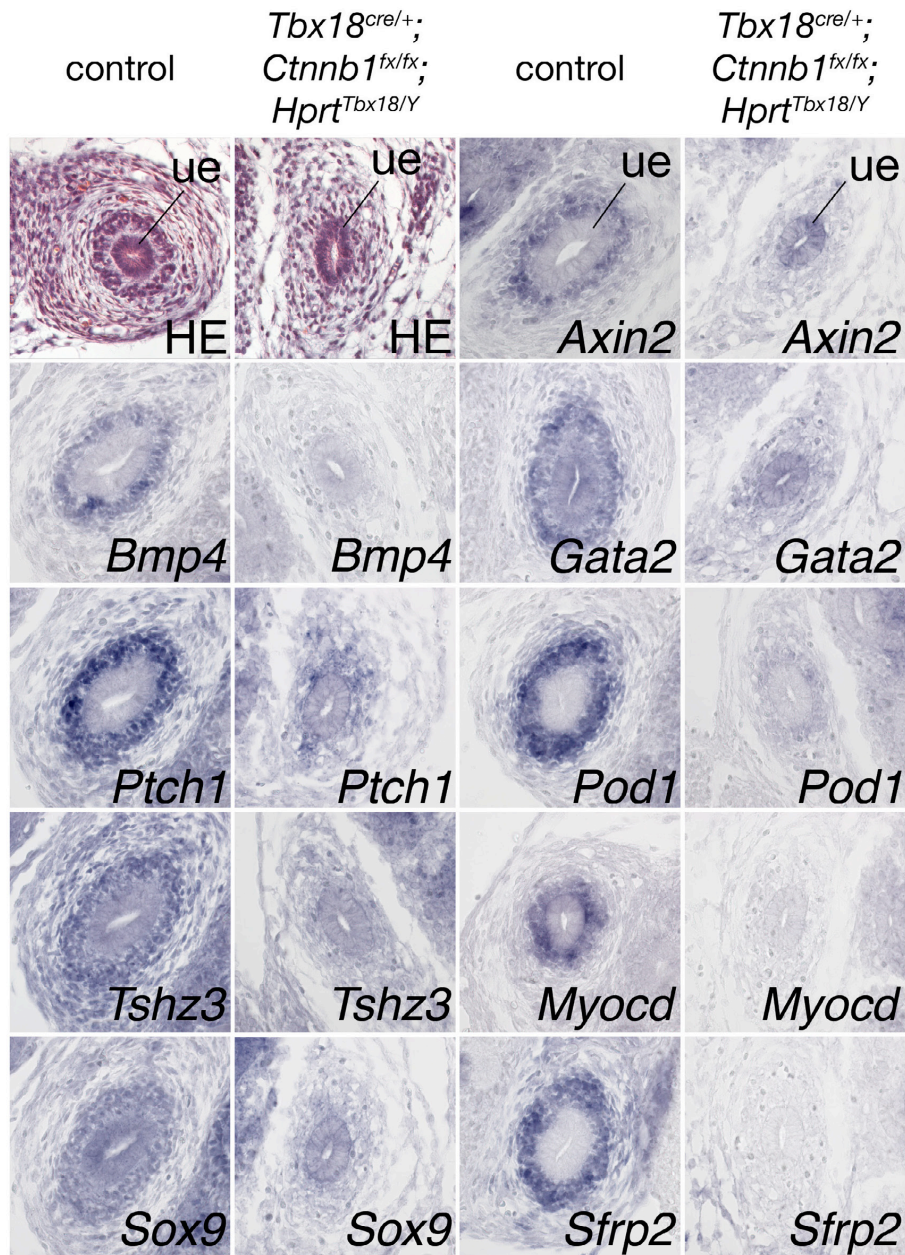


Fig. S8. Re-expression of Tbx18 in the *Ctnnb1*-deficient ureteric mesenchyme does not rescue loss of patterning and differentiation of the tissue. Histological stainings (HE) of transverse sections of the proximal ureter at E14.5, and *in situ* hybridization analysis on transverse sections of the proximal ureter at E14.5 of markers for patterning and differentiation of the ureteric mesenchyme. Probes and genotypes are as indicated. ue, ureteric epithelium.

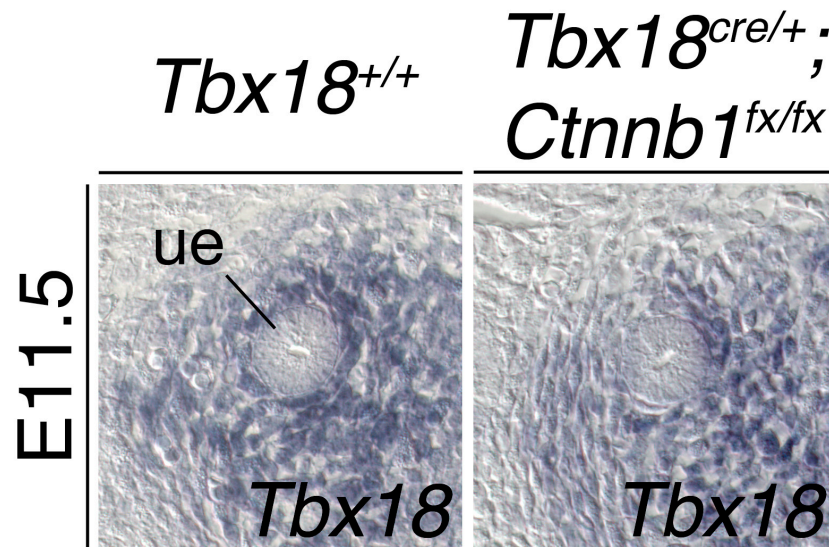


Fig. S9. Expression of *Tbx18* is not changed in the *Ctnnb1*-deficient prospective ureteric mesenchyme at E11.5. *In situ* hybridization analysis of *Tbx18* expression in transverse sections of the proximal ureter region in wildtype (*Tbx18*^{+/+}) and *Tbx18*^{cre/+};*Ctnnb1*^{fx/fx} embryos. ue, ureteric epithelium.

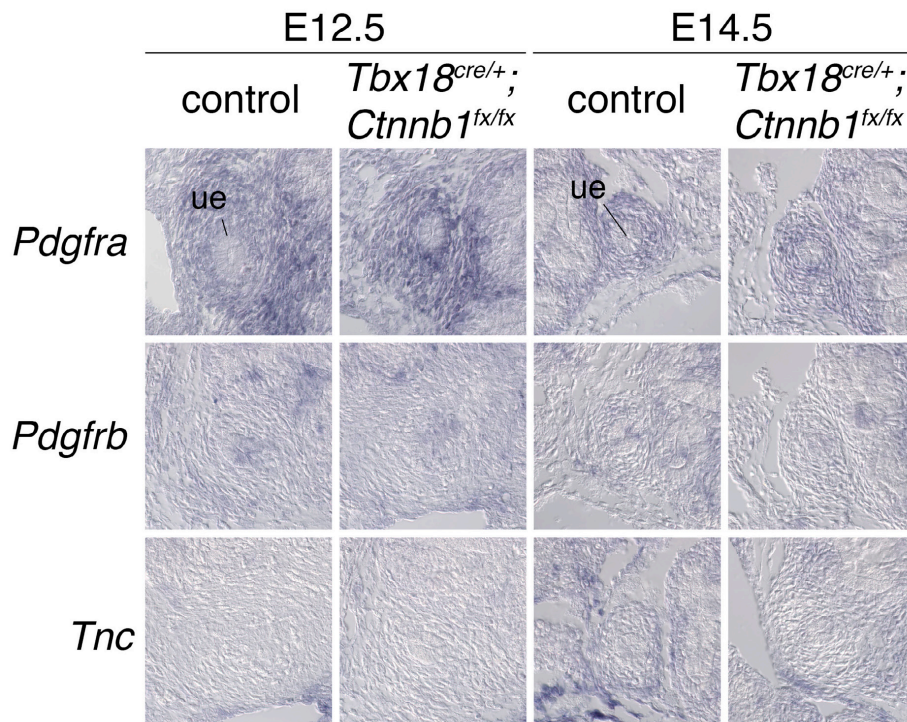


Fig. S10. *Ctnnb1* function in directing SMC development in the ureteric mesenchyme is not mediated by *Pdgfr* signaling and Tenascin C. *In situ* hybridization analysis of *Pdgfra*, *Pdgfrb* and *Tnc* expression on transverse section of the proximal ureter region in wildtype (control) and *Tbx18*^{cre/+};*Ctnnb1*^{fx/fx} embryos at E12.5 and E14.5. Probes and genotypes are as indicated. ue, ureteric epithelium.

The zinc finger transcription factor Gata2 promotes differentiation of the ureteric mesenchyme by controlling Hedgehog- and RA-signalling

Anna-Carina Weiss¹, Tobias Bohnenpoll¹, Patrick Blank¹, Rannar Airik¹, Tamrat Mamo¹, Marc-Oliver Trowe¹ and Andreas Kispert^{1,§}

¹

Institut für Molekularbiologie, Medizinische Hochschule Hannover, 30625 Hannover, Germany.

§

Author for correspondence: (kispert.andreas@mh-hannover.de)

Short title: Gata2 and differentiation of the UM

KEYWORDS: Gata2, ureter, differentiation, ureteric mesenchyme, smooth muscle

Manuscript in preparation

Introduction

Congenital anomalies of the kidney and the urinary tract (CAKUT) are amongst the most prevalent birth defects affecting up to 1% of newborns [1]. These anomalies comprise a spectrum of functional and physical obstructions of all components of the urinary tract and their junctions. Common diagnosed afflictions encompass hydro- and megaureter, ureteropelvic and vesicoureteral junction obstruction and hydronephrosis. However, the genetic causes and molecular mechanisms underlying these anomalies are poorly understood. Over the last decades, genetically modified mouse models have elucidated some factors and signaling pathways regulating normal urinary tract development and upon their deletion or perturbation cause CAKUT-like phenotypes.

The ureter, as a part of the upper urinary tract, mediates the transport of the urine from the renal pelvis towards the urinary bladder, where the urine is temporarily stored and released. The ureter is comprised of four different but tightly associated cell layers, which all fulfill different functions in its peristaltic machinery. The innermost layer is a highly specialized epithelial lining, the urothelium, which functions as a barrier against the urine. The urothelium is followed by the *lamina propria*, a fibrous tissue, which mediates the elasticity of the ureter during urine transport. The *lamina* is connected to the smooth muscle (SM) layer, which mediates the peristaltic contractions to remove the urine. The outermost lining of the ureter is the fibrous *tunica adventitia*, which is thought to anchor the ureter in the body cavity [2].

Impaired urine removal either by functional or physical obstruction of the ureter leads to pressure mediated dilatation of the ureter (hydroureter), and of the renal pelvis and collecting duct system (hydronephrosis). This in turn will cause subsequent destruction of the renal parenchyma and lead to renal failure as seen in end stage renal disease.

Ureter development starts with the emergence of the nephric duct (ND) out of the intermediate mesoderm at E8.5. The ND then migrates caudally until it joins and connects to the cloaca at E9.5. One day later, the ureteric bud (UB) emerges from the ND and invades into the metanephric mesenchyme (MM), a highly specialized mesenchymal cell mass located at hind limb level. Outgrowth of the UB is triggered by the Glial derived neurotrophic factor (*Gdnf*) from the MM. Loss of *Gdnf* leads to ureter and kidney agenesis and targeted misexpression leads to multiple ureteric buds, which will eventually terminate blindly in the bladder wall [3]. From E11.5 on, the distal part of the ureteric bud, which lies outside of the MM, simply elongates whereas the proximal part inside the MM undergoes several rounds of dichotomous branching to give rise to the renal pelvis and the collecting duct system. Concomitant with dichotomous branching, the ureteric tips induce the surrounding mesenchyme to aggregate and to form renal vesicles, the progenitor structures of the mature filtering unit of the kidney, the nephron. From E12.5 on, due to signals from the epithelium, the UM starts to condense around the ureteric stalk and eventually differentiates into the working smooth musculature of the ureter [2]. Starting at E14.5, the UM starts to differentiate into ureteric SM cells. This process is initiated by expression of the transcriptional co-activator *Myocardin*

cells. This process is initiated by expression of the transcriptional co-activator *Myocardin* (*Myocd*). Binding of *Myocd* to Srf (serum response factor) initiates transcription of typical SM structural genes, the prerequisite of proper peristaltic contractions of the ureter.

To date, only few molecular players have been identified to regulate SM development of the ureter. The T-box transcription factor (TF) *Tbx18* is a pivotal regulator of this developmental process. The analysis of a *Tbx18* null allele revealed that *Tbx18*-deficient embryos lack the ureteric SM layer, which was traced to mislocalization of the mutant UM to the surface of the kidney. This, in turn, results in functional obstruction of the ureter [4]. The SRY-box containing TF *Sox9*, a downstream target of *Tbx18*, is a further pivotal factor to control SM differentiation. Conditional deletion of *Sox9* in the UM leads to a lack of terminal SM differentiation and to an altered ECM composition [5]. The bone morphogenetic protein *Bmp4* has been suggested to inhibit ectopic ureteric budding from the ND and the ureter stalk [6]. Moreover, *Bmp4* directs a ureteric fate and promotes SM cell differentiation [7]. Furthermore, Shh-signaling from the epithelium regulates proliferation of the UM, maintains *Bmp4* expression in this tissue and by that controls SM cell differentiation [8]. In addition, recent studies identified the zinc finger transcription factor *Tshz3* together with *Sox9* to build a ternary complex with *Myocd*. This transcription factor complex then controls the timing of SM differentiation in the undifferentiated UM [9].

GATA zinc finger proteins are an evolutionary conserved family of transcription factors, which govern many processes in development and adulthood. They are known to regulate differentiation, lineage decision and differential gene expression in many tissues and cell types. The GATA transcription factor family consists of six members, which can be subdivided in two subgroups, GATA 1-3 and GATA 4-6. Name giving is their consensus nucleotide recognition sequence (A/T)GATA(A/G). GATA proteins can either directly bind to DNA or interact with other regulatory proteins to modulate transcription of target genes. The subfamily GATA 1-3 is mainly expressed in blood cell progenitors to regulate differentiation of the different hematopoietic lineages, whereas the subfamily GATA 4-6 is expressed and functionally implicated in several mesoderm- and endoderm-derived lineages like the heart, lung, liver and intestinal tract [10].

However, the functional relevance of Gata zinc finger transcription factors in urinary tract development of the mouse has remained elusive. Only two members of the Gata family have assigned functions in this developmental context to date. *Gata3* is expressed in the pronephric anlage and in the nephric duct (ND) where it is described as a downstream target of two closely related paired box genes *Pax2* and *Pax8* to facilitate nephric duct morphogenesis and guidance [11]. In *Gata3*-deficient embryos the ND fails to reach the cloacal region and to fuse with the cloacal epithelium due to increased ND cellularity and insufficient extension [12].

Gata2 expression was determined using an anti-GFP antibody in a *Gata2^{GFP}* knock in mouse line [13]. GFP staining was detected in the mesenchyme surrounding the ND and in

the mesonephric mesenchyme at E10.5. At E12.5, GFP expression was found in the ND mesenchyme and the ureteric epithelium. In the adult urogenital system, GFP protein was detectable in all derivatives of the ND and in the entire collecting duct system of the kidney, where *Gata2* maintains *Aqp2* expression and by that preserves proper water homeostasis [14].

Complete loss of *Gata2* in embryonic development has a fatal outcome. *Gata2* null embryos die around E10.5 from failure of primitive and definitive hematopoiesis [15]. In the attempt to rescue the early lethality of *Gata2* null embryos, a YAC (yeast artificial chromosome) transgene was detected (d16B YAC) that covered two hematopoietic enhancers upstream of the *Gata2* structural gene [16]. This YAC transgene was able to overcome the hematopoietic defects of the *Gata2* null allele. Phenotypical analysis of the urogenital system of YAC-rescued *Gata2*^{-/-} embryos revealed megaureter and hydronephrosis, common spectra of CAKUT. These phenotypes were traced back to a shift of the ureter budding position arising from reduced levels of the bone morphogenetic protein *Bmp4*, which lead to prenatal vesico-ureteric junction obstruction. This study suggested *Gata2* as a crucial regulator of ureter bud positioning [17]. Interestingly, urogenital tract specific (UG4-) enhancer driven reconstitution of *Bmp4* in *Gata2* hypomorphic embryos was able to extenuate the megaureter phenotype [18]. However, a detailed endogenous mRNA and protein expression analysis and the functional role of *Gata2* in the developing ureter after the initial budding process have not been addressed to date.

MATERIALS AND METHODS

Mice

Tbx18^{cre} [*Tbx18*^{tm(cre)Akis}] [5] and *Gata2*^{fx/fx} [*Gata2*^{tm1Sac}] [19] mice were maintained on an NMRI outbred background. Embryos for *Gata2* gene expression analysis were derived from matings of NMRI wild-type mice. *Tbx18*^{cre};*Gata2*^{fx/fx} mice were obtained from matings of *Tbx18*^{cre/+};*Gata2*^{fx/+} males with *Gata2*^{fx/fx} females. *Tbx18*^{cre/+};*Gata2*^{fx/+} and *Tbx18*^{+/+};*Gata2*^{fx/+} littermates were interchangeably used as controls.

For timed pregnancies, vaginal plugs were checked on the morning after mating and noon was taken as E0.5. Pregnant females were sacrificed by cervical dislocation. Embryos and urogenital systems were harvested in PBS and fixed in 4% paraformaldehyde (PFA) in PBS and stored in methanol at -20°C before further processing. Genomic DNA prepared from tissue biopsies was used for genotyping by PCR.

Morphological, histological and immunohistochemical analyses

Ink injection experiments were performed as previously described [5]. For histological and immunofluorescent stainings, organ rudiments or posterior trunks of embryos were paraffin embedded and sectioned to 5 μm . Sections were stained with haematoxylin and eosin.

For the detection of antigens, embryos or organ rudiments were sectioned to 5 μm . The following primary antibodies and dilutions were used: rabbit-anti-Gata2 (Gata2, sc-9008, Santa Cruz Biotechnologies, 1:200), mouse-anti-Acta2 (alpha smooth muscle actin, aSMA; clone 1A4, NatuTec; 1:200), rabbit-anti-Myh11 (SMMHC, smooth muscle myosin heavy chain; a kind gift from R. Adelstein, NIH, Bethesda, MD, USA; 1:200) and rabbit-anti-transgelin (Tagln, SM22a; Abcam, ab14106-100; 1:200).

Fluorescent stainings were performed using Alexa 488/555-conjugated secondary antibodies (Life Technologies; 1:200) or Biotin-conjugated secondary antibodies (Dianova; 1:200) and the TSA Tetramethylrhodamine Amplification Kit (PerkinElmer). Labeling with primary antibodies was performed at 4°C overnight after citrate antigen unmasking (#H-3300, Vector Laboratories). Secondary antibodies were incubated at RT for 2h in blocking solution.

RNA *in situ* hybridization analysis

Whole-mount RNA *in situ* hybridization was performed following a standard procedure with digoxigenin-labeled antisense riboprobes (Wilkinson and Nieto, 1993). Stained specimens were transferred to 80% glycerol prior to documentation. RNA *in situ* hybridization on 10 μm paraffin sections was essentially done as previously described (Moorman et al., 2001). For each marker at least three independent specimens were analyzed.

Image documentation

Whole-mount specimens were documented on a Leica M420 Macroscope with a Fujix HC-300Z digital camera and sections on a Leica DM5000 B microscope with a Leica DFC300 FX digital camera. Figures images were processed with Adobe PhotoshopCS3.

Results

Gata2 is expressed during ureter development in the mouse.

Since a detailed mRNA expression analysis of *Gata2* during mouse metanephric development has not been reported, we performed RNA *in situ* hybridization analyses on kidney rudiments as well as on embryonic sections from E11.5 to E16.5 (Figure 1). At E11.5 *Gata2* expression was detectable both in the ureteric mesenchyme (UM) and the ureteric epithelium (Fig. 1A,E). Expression in both compartments was maintained until E14.5 (Fig. 1B,C,F,G) but expression in the mesenchyme appeared stronger than in the epithelium. After E14.5 *Gata2* mRNA was quickly downregulated in the UM and was absent at E16.5 in the SM layer but maintained only in the superficial layer of the urothelium (Fig. 1D,H).

To determine the protein expression of *Gata2*, we performed immunofluorescence (IF) stainings on sections of the metanephros region at E11.5 and the proximal ureter from E12.5 until E16.5. *Gata2* protein was found as nuclear staining in the UM and in the ureteric epithelium at E11.5 and E12.5 (Fig. 1I,J). Expression in the UM was maintained until E14.5, whereas no *Gata2* protein was detectable in the epithelium any longer at this stage (Fig. 1K). At E16.5 *Gata2* protein was weakly detectable in the ureteric SM layer and strongly expressed in umbrella cells of the urothelium (Fig. 1L). Furthermore, weak expression of *Gata2* was visible in the metanephros after E12.5 (to be analyzed elsewhere).

With the intend to analyze the epistatic relationship of *Gata2* with other transcription factors or signaling pathways known to be involved in development of the UM, we checked *Gata2* mRNA expression on proximal ureter sections of respective mouse mutants at E12.5 and E14.5. All conditional alleles were obtained using the *Tbx18^{cre}* line that was generated in our lab [20].

E12.5, expression of *Gata2* was unchanged in the UM of conditional mutants of the Hh-coreceptor *Smoothed (Smo)*, in conditional *Bmp4*-mutants and consequentially in conditional mutants of the *Bmp4* downstream effector *Smad4*. Moreover, we did not observe an epistatic relation of *Gata2* with the signaling transducer of canonical Wnt-signaling *Ctnnb1*, as well as with the SRY-box transcription factor *Sox9* (Fig. 1 M-T). Surprisingly, we observed strong reduction of *Gata2* mRNA in *Tbx18^{GFP/GFP}* null embryos at E12.5 and E14.5 and complete loss of *Gata2* expression in *Smo*-deficient UM at E14.5, suggesting that *Gata2* might act downstream of *Tbx18* and Hh-signaling in this tissue compartment (Fig. 1 W,X and Supplementary material S2 A,B,K,L).

Loss of *Gata2* in the UM leads to strong hydronephrosis in prenatal embryos.

Earlier work has shown that YAC-rescued *Gata2^{-/-}* embryos display megaureter and hydronephrosis as a result of vesico-ureteric junction obstruction (VUJO) [5]. However, the significance of *Gata2* expression in the UM has not been addressed to date. In order to investi-

gate the role of *Gata2* in the ureteric mesenchyme, we used the tissue specific *Tbx18^{cre}* line and crossed it to a *Gata2* floxed allele (*Gata2^{fx}*).

Morphological analysis of urogenital systems of *Tbx18^{cre/+};Gata2^{fx/fx}* embryos at E18.5 revealed CAKUT-like phenotypes ranging from bilateral proximal hydronephroses to bilateral megaureters (Fig. 2 A-D, Suppl. Figure S1). The prenatal CAKUT-like phenotype of the conditional mutants was sex-independent and revealed 50% hydronephrosis and 50% megaureter occurrence. Since development of megaureter in YAC-rescued *Gata2^{-/-}* embryos has been traced back to ureter budding defects, we predominantly focused on the hydronephrosis phenotype of *Gata2* mutants in this study.

Histological analysis of mutant urogenital systems revealed a strong dilatation of the proximal ureter and partial absence of the renal pelvis and calyx in *Gata2*-deficient embryos (Fig. 2 E-H). In order to analyze the cellular changes associated with hydronephrosis formation, we performed immunofluorescence (IF) and RNA *in situ* hybridization analyses of typical smooth muscle structural genes and proteins at E18.5. *Acta2* and *Myh11*, both contractile proteins of the ureteric SM layer, were strongly reduced in *Tbx18^{cre/+};Gata2^{fx/fx}* embryos (Fig. 2 I-L). Further RNA *in situ* hybridization experiments revealed that *Myocd* (*Myocardin*) and *Tagln* (*Transgelin*, former *Sm22a*) were both strongly reduced and *Tnnt2* (*Troponin, T2, cardiac*) was completely absent in mutant embryos (Fig. 2 M-R). *Aldh1a2*, a marker for the fibrous lamina propria was not detectable in mutant ureters either. Moreover, *Dpt* (*Dermatopontin*), a marker for the fibrous adventitial layer, was slightly reduced (Fig. 2 S-V). The urothelial marker gene *Upk3b* (*Uroplakin 3B*) was unaffected in *Gata2*-deficient ureters at this stage (Fig. 2 W,X).

To rule out physical obstruction as the cause of hydronephrosis in *Tbx18^{cre/+};Gata2^{fx/fx}* embryos, we tested for the connectivity of the distal ureter and the bladder. Therefore, we performed histological stainings on sagittal bladder sections and additionally injected ink into the renal pelvis of wildtype and mutant embryos. In the wildtype, the distal ureter entered the bladder at the dorsal bladder neck and was then properly connected to the bladder lumen. In mutant embryos, we also observed connectivity of these tissues, but, consistent with earlier findings [16] the insertion point of the distal ureter was slightly shifted in cranial direction (Fig. 2 Y,Z). Furthermore, the injected ink reached the bladder in wildtype as well as in mutant embryos (Fig. 2 A',B'), indicating that the slight shift of the ureteric insertion point in the mutants did not hamper urine transport to the bladder. Taken together, we find a strong reduction of SM cell and fibroblast specific gene expression together with a functional vesico-ureteric junction in *Tbx18^{cre/+};Gata2^{fx/fx}* embryos. This analysis points to a functional obstruction of the ureter as the underlying cause of hydronephrosis in *Gata2*-deficient embryos.

Onset and progression of ureter differentiation defects in *Tbx18^{cre/+};Gata2^{fx/fx}* embryos.

To define the onset of the ureter defects in mutant embryos, we analyzed sections of urogenital systems from E12.5 until E16.5 (Figure 3 and supplementary material S3). Haematoxylin and eosin stainings of sagittal kidney sections showed no gross histological changes of mutant kidneys compared to controls at E14.5 and E15.5. Ureteric tips, cap mesenchyme and nephrogenic structures were equally detectable in control and mutant embryos. However, at E16.5 we observed a strong dilatation of the renal pelvis and calyx as well as of the proximal ureter in *Tbx18^{cre/+};Gata2^{fx/fx}* embryos (Fig. 3 A). Histology of proximal ureter sections of wildtype embryos at E12.5 showed a distinct zonation of the ureteric mesenchyme: a perpendicularly arranged mesenchyme adjacent to the ureteric epithelium and a circularly arranged outer mesenchyme. In mutant embryos, this zonation was established, but the mesenchyme of the inner domain appeared hypoplastic at this stage (Supplementary material S3). At E14.5 in the wildtype, a highly condensed ring of mesenchymal cells adjacent to the ureter stalk and an outer loosely arranged mesenchymal layer was visible. In *Gata2*-deficient embryos, the two mesenchymal compartments were evident but the inner mesenchyme appeared more loosely packed and disorganized, indicating that the initial condensation process occurred but cells of the inner UM showed an altered orientation and hypoplasia. At E15.5 in control embryos, a compact layer of SM cells was detectable around the ureter stalk, whereas in *Gata2*-mutants the UM was still perpendicularly and loosely arranged around the urothelium. At E16.5, when urine production had started, *Gata2*-mutants showed a strong dilatation of the proximal ureter and only a thin lining of urothelial cells compared to controls (Fig. 3B).

Since we observed histological defects in the *Gata2*-deficient UM on histological level, we sought to analyze whether these defects were attended or followed by alterations in SM cell differentiation.

Section RNA *in situ* hybridization analysis from E14.5 to E16.5 with the typical SM marker genes *Tnnt2*, *Tagln* and *Myocd* showed a complete absence of active SM gene transcription in the *Gata2*-deficient UM until E16.5. Contrarily, urothelial differentiation occurred in mutant embryos as shown by regular expression of the urothelial marker *Upk1b*. The fibrocyte markers *Aldh1a2* for the *lamina propria* and *Dpt* for the *tunica adventitia* were not detectable in the ureter with this method until E16.5 (Fig. 3C).

We then sought to answer the question whether programmed cell death (apoptosis) accounts for the hypoplastic UM in *Gata2*-deficient ureters at early stages. Therefore, we performed a TUNEL assay on transverse sections of the proximal ureter at E12.5 and E14.5 (supplementary material S4). At E12.5, only very few apoptotic bodies were detectable in the UM of both the wildtype and the mutant (Fig. S4 A-D). At E14.5, apoptosis neither occurred in controls nor in the mutants (Fig. S4 E-H), excluding programmed cells death as cause of hypoplasia in early *Gata2*-deficient ureters. Moreover, our analysis provides evidence of an

onset of ureter defects in *Tbx18^{cre/+};Gata2^{fx/fx}* embryos at E12.5 accompanied by complete failure of SM cell differentiation starting at E14.5.

Ureteric SM differentiation defects of *Tbx18^{cre/+}; Gata2^{fx/fx}* ureters *ex vivo*.

Hydrostatic pressure induced ureteric dilatation might eventually lead to dedifferentiation of ureteric SM cells. In order to circumvent these secondary effects in the embryo, we cultured E14.5 ureters for a period of 6 days on Corning transwell® filters and then performed IHC and RNA *in situ* hybridization analyses with SM specific marker genes on sections of these cultures, respectively (Figure 4).

In the wildtype, peristaltic movements of the ureter start after two days in culture and reach their peak after 4 days. In the *Gata2*-mutant, the explanted ureters did not show initiation of peristalsis after two days, but ureters showed contractions after 4 days and after 6 days the peristalsis of mutant ureters was indistinguishable from control explants (Fig. 4A). We then wanted to analyze the spacio-temporal expression of typical SM structural genes in mutant ureters *ex vivo*. In controls, expression of the contractile protein Acta2 (Actin, alpha 2, SM, aorta) was detectable in the ureteric SM layer after two days of culture and expression levels were equally strong after day 4 and day 6. In mutant ureters, however, Acta2 protein was barely detectable after two days, but started to be expressed after 4 days and was equally strong expressed compared to the controls after 6 days of culture (Fig. 4 B). In addition, Tagln (transgelin, former Sm22a) was found in the SM cells of the wildtype after two days and was comparably expressed to Acta2 levels until the end of the culture period. In *Tbx18^{cre/+};Gata2^{fx/fx}* ureters, Tagln expression in the SM layer was weaker than in controls after two days but was identical after 4 and 6 days of culture (Fig. 4C).

To extend these observations, we performed RNA *in situ* hybridization experiments on sections of these ureter cultures. In control ureters, the SM key regulatory gene *Myocd* was strongly expressed in the ureteric muscle after two days and (weaker) expression was maintained until day 6 of culture. In contrast, *Gata2*-deficient ureters showed weak *Myocd* expression after two days of culture and the expression level of controls was not reached until 4 days of culture (Fig. 4D). The same observations were made for gene expression of the contractile protein *Myh11* in the mutant (Fig. 4E). The SM structural genes *Tagln* and *Tnnt2* were expressed in control ureters from day 2 onwards in equal levels, whereas in *Gata2*-deficient ureters both genes were barely detectable after two days of culture. Expression of both genes became stronger after 4 days and almost reached wildtype level after 6 days of culture (Fig. 4 F,G).

This analysis revealed that ureteric SM cell differentiation in *Tbx18^{cre/+};Gata2^{fx/fx}* ureters occurred in a delay of approximately 2 days compared to controls. Moreover, the *ex vivo* culture system allows to rule out hydrostatic pressure as reason of SM differentiation defects, indicating cell autonomous changes in the ureteric mesenchyme as cause of hydroureteronephrosis of *Tbx18^{cre/+};Gata2^{fx/fx}* embryos.

Molecular changes in the ureter of *Tbx18^{cre/+};Gata2^{fx/fx}* embryos at E13.5.

With the aim to unravel the molecular changes, which lead to ureteric SM differentiation defects, we analyzed a set of genes that was recently implicated in the development of the uncommitted UM at E13.5 (Figure 5).

The Wnt-signaling modulator *Sfrp2*, the transcription factor *Tcf21* and the transcriptional target of *Sox9*, *Car3*, [17] are specifically expressed in the UM without an assigned function to date. *Tbx18*, *Sox9* and *Tshz3*, all transcription factors strongly expressed in the UM, have been shown to differentially regulate ureteric SM cell differentiation. Hedgehog-signaling, represented by its receptor and target *Ptch1*, the bone morphogenetic protein *Bmp4* and its transcriptional target *Id2* have also been shown at various steps to regulate ureter development prenatally and in the adult [5]. Moreover, Wnt- and Retinoic acid (RA)-signaling as shown by *Axin2* and *Rarb*, respectively, are further crucial factors implicated in murine ureter development [21]. In controls, *Tbx18* is expressed in the inner ring and in a few cells of the outer ring of the UM. *Tbx18* mRNA levels were unchanged in the *Gata2*-mutant compared to the wildtype (Fig. 5 A,B), whereas expression of the *Tbx18* target gene *Sox9* was significantly reduced in the ureteric epithelium in *Gata2*-deficient ureters, whereas *Sox9* expression in the UM appeared unchanged compared to controls at that stage (Fig. 5 C,D). The transcriptional target of *Sox9*, carbonic anhydrase *Car3*, was equally expressed in the *Gata2*-deficient UM compared to controls. The same observations were made for the Wnt target gene *Axin2*, the Wnt-modulator *Sfrp2* and the Shh receptor and target gene *Ptch1* (Fig. 5 K-P). According to earlier findings [22], we observed reduction of the bone morphogenetic protein *Bmp4* in the UM of *Gata2*-deficient ureters and slight downregulation of the *Bmp4* target *Id2* in the UM and the ureteric epithelium (Fig. 5 G-J). Interestingly, we saw upregulation of the transcription factors *Tcf21*, *Zfp536* and *Tshz3* in *Tbx18^{cre/+};Gata2^{fx/fx}* embryos at that stage. RA-signaling as shown by *Rarb* expression in the UM appeared unaltered in *Gata2*-mutants compared to controls (Fig. 5 W,X). Taken together, this analysis indicates decreased *Bmp4*-signalling and increased expression of several transcription factors that may potentially interfere with ureteric SM differentiation.

Molecular causes of ureter differentiation defects in *Tbx18^{cre/+};Gata2^{fx/fx}* embryos at E14.5.

To analyze the molecular changes preceding SM differentiation defects in *Gata2*-deficient ureters, we analyzed the above-mentioned set of genes in the uncommitted UM at E14.5 (Figure 6).

The mRNA expression of *Sox9*, *Bmp4*, *Id2*, *Axin2* and *Sfrp2* was unchanged in *Gata2*-deficient ureters compared to control specimens at this stage (Fig. 6 C,D,F-K), whereas slight upregulation of *Tbx18* (Fig. 6 A,B) and strong upregulation of *Tcf21*, *Ptch1*, *Zfp536* and *Rarb* was detectable in the mutant UM (Fig. 6 N-W). Contrarily, *Car3*, a transcriptional target of *Sox9* in this tissue, was slightly reduced in the UM of *Gata2*-deficient ureters (Fig. 6 D,E).

This analysis provides evidence of enhanced Hedgehog- and RA-signaling and potentially decreased Sox9 activity in the mesenchyme of the ureter, which may interfere with terminal differentiation of this tissue compartment.

Molecular changes in the UM of *Tbx18^{cre/+};Gata2^{fx/fx}* embryos proceed at E15.5.

We then intended to follow the molecular changes (increased Hh- and RA-signaling) prior to hydroureter formation and performed section RNA *in situ* hybridization analyses with the above-mentioned set of genes at E15.5 (Figure 7).

In control embryos, expression of the T-box transcription factor *Tbx18* is restricted to the innermost ring of SM cells, whereas in mutant embryos *Tbx18* was upregulated and the expression domain appeared expanded (Fig. 7 A,B). The transcription factor *Sox9* was not detectable in control embryos any longer, but weak expression was still found in the UM of mutant embryos (Fig. 7 C,D). Moreover, in control embryos, *Bmp4* mRNA was weakly detectable in the prospective *lamina propria* domain, whereas in *Gata2*-deficient embryos, *Bmp4* expression was upregulated and encompassed the inner ring of the UM (Fig. 7 E,F). Moreover, in controls, the canonical Wnt signaling component *Axin2* was expressed in a few cell clusters in the UM, whereas in *Gata2*-mutants weak *Axin2* expression was present in the entire inner mesenchymal ring (Fig. 7 I,J). Contrarily, *Id2*, a well known target of *Bmp4*, and the transcription factor *Tcf21* were unchanged at this stage (Fig. 7 GH;K,L). According to our findings at E14.5, the mRNA levels of *Sfrp2*, *Ptch1*, *Tshz3* and the RA-receptor *Rarb* were upregulated in the UM of *Tbx18^{cre/+};Gata2^{fx/fx}* embryos (Fig. 7 M-T). In summary, the mesenchyme of *Gata2*-deficient ureters may retain a progenitor state as shown by enhanced or prolonged expression of typical marker genes of the uncommitted UM.

Transcriptional profiling by RNA-microarray analysis at E14.5 and E15.5.

In order to get a deeper insight into the molecular changes in the mesenchyme of *Gata2*-deficient ureters, a RNA-microarray analysis of ureters (collected by Tobias Bohnenpoll) was performed at E14.5 and E15.5 (Supplementary material). The purpose of transcriptional profiling at E14.5 was the characterization of primary changes in the UM, and at E15.5 to explain the molecular changes of the late phenotype prior to hydroureter formation. To circumvent sex-specific differences in the transcriptional profile, male and female pools were collected for both controls and mutants. The RNA was extracted from the ureter tissue and then hybridized to whole mouse genome RNA microarray chip (Agilent, for further information: Dr. O. Dittrich-Breiholz, MHH).

At E14.5, with at least 1.3-fold deregulation (without intensity filtering), we saw 263 downregulated (Table S1) and 222 upregulated transcripts (Table S2) in ureters of *Tbx18^{cre/+};Gata2^{fx/fx}* embryos. After functional annotation analysis applying gene ontology (GO) terms [17, 23], we found 17 clusters of downregulated and 31 clusters of upregulated transcripts after filtering with a statistical ease of 0.05.

Downregulated genes of E14.5 *Gata2*-deficient ureters are functionally implicated in blood circulation and blood vessel size (Table S1_A), in cell-to-cell signaling (Table S1_B), in neuronal differentiation (Table S1_C) and in neurofilament composition (Table S1_D), in the development of muscle organs (Table S1_E) and of muscle proteins (Table S1_F) as well as in positive regulation of transcription (Table S1_G). After careful cluster selection of the upregulated transcripts, we observe functional implication in the regulation of blood circulation and blood pressure (Table S2_A), in regulation of UGS (Table S2_B) and epithelial development (Table S2_C). In addition, we detected functional relevance in cell-to-cell signaling (Table S2_D) and in cellular adhesion (Table S2_E). Interestingly, we see upregulation of Wnt signaling (Table S2_F), enhanced Bmp antagonists (Table S2_G) and upregulation of diverse homeobox genes (Table S2_H).

Since we detected strong upregulation of Hedgehog-signaling in the ureteric mesenchyme of *Tbx18^{cre/+};Gata2^{fx/fx}* embryos in our section RNA *in situ* hybridization analysis at E14.5, we looked at the intersection of downregulated genes in Cyclopamine (*bona fide* pharmacological inhibitor of Hh-signaling) treated kidney cultures (experiment performed by T. Bohnenpoll) and compared them to upregulated transcripts of *Gata2*-deficient ureters at E14.5 (Table S3).

Looking at the intersection of deregulated genes of both microarrays, 18 transcripts were commonly deregulated at least 1.3-fold (no intensity filtering applied). Amongst them, 5 genes were detectable in the ureter of E14.5 wild-type embryos (www.eurexpress.org). After GO term analysis, 17 deregulated genes were grouped into 4 clusters comprising Wnt signaling, negative regulation of signal transduction, glycoproteins and signal peptides, as well as plasma membrane integrity. Among the top hits that were expressed in the ureter, we found *Sostdc1* (4.4-fold upregulation), a member of the sclerostin family, which encodes a secreted protein, which antagonizes Bmp proteins by competitive binding to their Bmp receptors [24]. In addition, *Vwc2* (*van Willebrand factor C domain containing 2*), a secreted Bmp antagonist, was upregulated in *Gata2*-deficient ureters, indicating negative regulation of this pathway upon loss of *Gata2*. Interestingly, *Wif1* (*Wnt inhibitory factor 1*), a factor that binds to Wnt ligands and inhibits their activities, was 2-fold upregulated in *Gata2*-mutants, suggesting negative regulation of the Wnt signal transduction upon loss of *Gata2* in the UM as well. Moreover, *Avpr1a* (3-fold upregulation), which encodes the receptor of arginine vasopressin, belongs to the subfamily of the G-protein coupled receptors. *Avpr1a* orchestrates cell contraction, proliferation, vasoconstriction and, thus, regulation of blood pressure (www.genecards.org). Upregulation of this receptor in *Gata2*-mutants indicates potentially increased proliferation, decreased contractility of muscle tissues and vessels and negative regulation of neuronal excitability.

Additionally, *Enpep*, which encodes aminopeptidase A, a protein, that cleaves off acidic glutamyl and aspartyl residues of angiotensin and other active peptides to lower their activity,

was 1.8-fold upregulated (NCBI). Upregulation of this gene in *Gata2* mutants points to a deregulation of the renin/angiotensin system as well as to potentially altered proliferation. Interestingly, we found the forkhead/winged helix-box transcription factor *Foxl1* upregulated (1.6-fold) in *Gata2*-mutants, which is strongly expressed in the wildtype UM (Table S3, europepmc.org). Fox proteins are known to play pivotal roles in cell survival, proliferation and cell specification [25]. Furthermore, *Foxl1* has been shown to be expressed in myoblast precursors in the sea urchin [26]. Taken together, the majority of genes, which were deregulated both in the Cyclophamide and E14.5 *Gata2*-microarray, are mainly associated with negative regulation of the Bmp- and Wnt signaling pathways, with modulation or response to peptide hormones and with proliferation control.

Upregulation of Hh- and RA-target and effector genes in *Tbx18^{cre/+};Gata2^{fx/fx}* embryos at E15.5.

In order to check whether target and effector genes of the Hh-pathway remain upregulated in *Gata2*-mutant ureters, we performed RNA *in situ* hybridization experiments on proximal ureter sections of E15.5 embryos (Figure 8 and Table S4). *Vcan* (*Versican*) and *Sostdc1* (*Sclerostin domain containing 1*) were expressed weakly in ureteric SM cells of control embryos and were both strongly upregulated in the UM of *Gata2*-deficient ureters (Fig. 8 A-D). The aminopeptidase *Enpep*, the Hh-receptor *Ptch2*, *Ndp* (*Norries disease pseudoglioma*) a target of Shh in the retina [27], as well as the cell growth regulator *Ddit4l* were not detectable in the ureter in the wildtype as well as in the mutants with this method (Fig. 8 E-K).

Additionally, we sought to answer the question, whether RA-signaling components were changed at E15.5 as well. The retinol-carrier protein *Rbp4* was neither detectable in the wildtype nor in the mutant ureters (Fig. 8 M,N). Expression of the RA-target gene *Meis1* appeared unchanged in comparison to controls, whereas upregulation of *Meis2* was clearly detectable in the UM of *Gata2*-deficient ureters (Fig. 8 J-M). The RA synthesizing enzyme *Aldh1a2* was neither detectable in wildtype nor in mutant ureters at this stage. *Cyp26a1*, coding for a cytochrome 450 protein, which is known to metabolize RA and by that to negatively regulate its free levels, is not expressed in the UM in both genotypes (Fig. 8 P,Q). Interestingly, we find elevated mRNA levels of the RA receptor *Rarb* in the UM in *Tbx18^{cre/+};Gata2^{fx/fx}* embryos (Fig. 8 R,S).

In summary, although some genes were not detectable by the method of RNA *in situ* hybridization, we observe enhanced Hedgehog- and RA signaling in the UM of *Tbx18^{cre/+};Gata2^{fx/fx}* embryos at E15.5.

Altered Wnt-signaling in *Tbx18^{cre/+};Gata2^{fx/fx}* ureters at E14.5.

Since we observed hypoplasia of the ureteric mesenchyme in early *Gata2*-deficient embryos, we checked for signaling pathways, which are implicated in growth regulation or patterning of cell compartments. The canonical Wnt pathway is an important signaling module

regulating patterning and proliferation in several tissue contexts [28] and was upregulated and functionally clustered in the microarray (Table S2_F). Looking at components of the Wnt-signaling pathway in the E14.5 *Gata2* microarray (Table S5), we found the ligand *Wnt10a* upregulated, whereas *Wnt11* and *Wnt5b* were downregulated in *Gata2*-mutants. Furthermore, while most of the Fzd receptors were unchanged, we observed strong upregulation of *Fzd10* in *Gata2*-deficient ureters (Table S5 and S2_F). The intracellular signal transducer *Ctnnb1* was slightly reduced, while *Axin2*, the target gene of canonical Wnt signaling, was unchanged in mutant ureters. Surprisingly, *Axin1*, a scaffolding protein of the *Ctnnb1*-destruction complex, was downregulated in *Tbx18^{cre/+};Gata2^{flx/flx}* embryos, indicating a possible accumulation of Cntnb1 protein in *Gata2*-deficient ureters.

Looking at overlaps of the E14.5 *Gata2* and IWR-1 (a pharmacological inhibitor of canonical Wnt signaling) treated kidney cultures (experiment performed by Dr. M.-O. Trowe), we observed 40 common genes that were at least 1.3-fold deregulated with intensities higher than 500 (Table S6). After functional annotation analysis, the deregulated transcripts were grouped into 12 clusters encompassing extracellular matrix, development of an epithelium, cell adhesion, Wnt signaling, cell membrane, regulation of transcription incl. Hox genes, calcium and zinc ion binding, G-protein signaling and nucleotide binding. Amongst them, we found the nuclear receptor *Ahr* (*Aryl hydrocarbon receptor*) strongly upregulated in *Gata2*-deficient ureters and downregulated in IWR1-inhibited kidney cultures. *Ahr* is a CAKUT-associated gene that was shown to inhibit branching morphogenesis of the kidney [29]. Additionally, we observed upregulation of the homeobox transcription factor *Alx1* (Alx homeobox protein 1) in *Gata2*-mutants, a key transcriptional activator, which was downregulated in wildtype kidneys upon IWR-1 treatment. Moreover, we see upregulation of the transcription factor *Id4*, a HLH protein that inhibits DNA binding and harbors a Gata2-motif 3696 bp upstream of the ATG [30], indicating a potentially direct regulation of *Id4* expression by *Gata2*. Since we observe upregulation of the Wnt signaling pathway and also of Wnt target genes (IWR-1 microarray) in *Gata2*-deficient ureters, we plan to analyze these particular finding in future experiments in more detail with main focus on *Alx1*, *Ahr* and *Id4* gene expression.

A previous study in our lab showed, that conditional deletion of the SRY-box containing transcription factor *Sox9* in the UM results in loss of SM differentiation [31]. In addition to that, both transcription factors are coexpressed in the ureteric epithelium and UM until E13.5. A preliminary microarray analysis of *Sox9* deficient ureters at E13.5 (performed by Dr. M.-O. Trowe) revealed a strong overlap with 37 downregulated (Table S7) and 35 upregulated genes (Table S8) with the *Gata2* microarray at E14.5. In both microarrays, we observe strong downregulation of *Myocd* (-2.3-fold and -2.4-fold), which reflects a lack or delay of SM cell differentiation in both conditional mutants. Interestingly we see downregulation of *Sox9* in *Gata2*-deficient ureters accompanied by decrease in *Car3* mRNA expression. Surprisingly, in section RNA *in situ* hybridization analysis at E13.5 (Fig. 5), we only observe downregula-

tion of *Sox9* in the ureteric epithelium of *Gata2*-mutants. This finding explains the 1.5-fold downregulation of the microarray, since RNA was extracted from both ureteric tissue compartments. Loss of *Sox9* in the ureteric epithelium of *Gata2*-deficient ureters alludes to a paracrine signaling to the epithelium potentially by RA-signalling, as we see enhanced *Aldh1a3* mRNA levels in both conditional mutants (see Table S2_C and Table S8).

Sox9 and Gata2 do not interact genetically during ureter development.

To unravel a genetic interaction of *Gata2* and *Sox9*, we analyzed sections of proximal ureters of *Sox9*-deficient and *Gata2*-deficient embryos at E14.5 via section RNA *in situ* hybridization (Figure 9). The expression of *Sox9* appeared unaltered in *Tbx18^{cre/+};Gata2^{fx/fx}* mutants E14.5 (Fig. 9 A,B), whereas downregulation of the *Sox9* target gene *Car3* was clearly detectable in *Gata2*-deficient ureters (Fig. 9 C,D). Likewise, we tested for *Gata2* expression in *Sox9*-deficient embryos, where no changes in the mRNA expression level were apparent (Fig. 9 E,F). As an internal control, we analyzed *Car3* expression, which was, as expected, completely absent in *Sox9*-deficient embryos (Fig. 9 G,H).

Furthermore, we intended to validate the RNA *in situ* hybridization results by generation and analysis of *Gata2/Sox9* compound mutants. Therefore, we characterized the morphology of urogenital systems of prenatal single (*Tbx18^{cre/+};Gata2^{fx/+}* and *Tbx18^{cre/+};Sox9^{fx/+}*) and double heterozygous (*Tbx18^{cre/+};Gata2^{fx/+};Sox9^{fx/+}*) embryos at E18.5.

Single and double heterozygous embryos (sex-independent) were indistinguishable from controls (n=4) (Fig. 9 I-L). These findings showed that *Sox9* and *Gata2* do not interact on the genetic level. Still, we detected a downregulation of *Sox9* in the *Gata2* microarray at E14.5 (-1.3-fold) and in the ureteric epithelium at E13.5 as well as downregulation of *Car3* in *Gata2*-deficient ureters in both *in vivo* and *ex vivo*, suggesting that both factors might still act in a common pathway during ureteric SM development.

Gata2 potentially represses Hox gene transcription.

Another family of genes, which was significantly deregulated in E14.5 *Gata2* microarray, was the Homeobox (Hox) transcription factor family (Table S2_H and Table S4_H). Generally, Hox genes endow cells with a positional identity [5]. We observe upregulation of the homeobox transcription factors *Alx1* (2.5-fold), *Nkx3.1* (2.2-fold), *Pou3f1* (1.6-fold), *Hoxc11* (1.9-fold) and of members of the *Hoxd* gene family in the *Gata2*-mutant (*Hoxd10*, *Hoxd11*, *Hoxd12* and *Hoxd13*). The *Hoxd* gene family is clustered at 44.13 cM on chromosome 2 in the mouse (www.informatics.jax.org), indicating a potentially repressive function on this gene cluster by *Gata2*.

Transcriptome of E15.5 *Gata2*-deficient ureters reflects loss of structural SM genes and enhanced Wnt signaling.

In order to get a deeper insight into the molecular changes in the *Gata2*-mutant at E15.5, we analyzed the microarray results with applying a filter criterion of at least 1.3-fold deregulation. We found 360 transcripts to be downregulated (Table S9) and 361 transcripts to be upregulated (Table S10) in ureters of E15.5 *Tbx18^{cre/+};Gata2^{fx/fx}* embryos. With the help of functional annotation analysis, we found 22 clusters of downregulated and 26 clusters of upregulated genes applying a statistical ease of 0.05. After careful selection of the functional clusters, the downregulated genes recapitulated the *in vivo* phenotype of *Tbx18^{cre/+};Gata2^{fx/fx}* embryos to a large extend. We detect downregulation of muscle cell development (Table S3_C) and, hence, of muscle proteins (Table S3_B). Moreover, we observed alterations in the actin cytoskeleton (Table S3_A) and in genes regulating epithelial proliferation as well as extracellular matrix composition (Table S3_D,F). Additionally, we observe alterations in activity of MAPKs (Table S3_E) and in axon assembly (Table S3_H). Also, genes regulating blood circulation were decreased in *Gata2*-deficient ureters (Table S3_G).

Analyzing the downregulated genes by GO terms, we see functional implication in development of the UGS (Table S4_A) and in mesenchymal cell differentiation (Table S4_C). Moreover, genes were upregulated that regulate the morphogenesis of epithelia (Table S4_C) and constitute components or regulators of the ECM (Table S4_D). Interestingly, we again observe upregulated antagonism of Bmp- (Table S4_E) and Wnt signaling (Table S4_F) and in addition observe upregulation of genes that can be part of TF complexes (Table S4_G). According to earlier findings, we see genes upregulated that harbor homeobox conserved sites (Table S4_H). Taken together, this microarray analysis revealed loss of marker genes for differentiated axons (such as *Nefl*, *Prpha* and *Th*) and of the vascular system (such as *F5* and *Ednrb*). We furthermore see loss of SM differentiation and, hence, of muscle structural proteins (e.g. *Acta2*, *Myh11*, *Tagln* and *Tnnt2*). Contrarily, Wnt-signaling and Bmp antagonism are upregulated in the *Gata2*-mutant at E15.5. Finally, we detect upregulation of genes containing homeobox conserved sites, indicating a repressive function of *Gata2* on Hox genes, on Wnt-signaling as well as increased antagonism of Bmp signaling.

In a recent publication [32] direct target genes of *Gata2* in human umbilical vein cells (HUVECs) were determined via CHIP sequencing experiments. We then sought to answer the question whether these genes constitute targets of *Gata2* in the ureter as well. Therefore, we compared the targets in HUVECs with deregulated genes in the E14.5 microarray (Table S10). Surprisingly, 53 common genes were deregulated up to 1.8-fold in the *Gata2* microarray. Amongst these genes, we found 3 upregulated genes (depicted in red) particularly interesting. *Atf3* (*Activating transcription factor 3*) encodes a TF that is able to directly bind DNA to initiate transcription. *Yes1*, a non-receptor tyrosine kinase is involved in regulation of proliferation and survival, cell adhesion and differentiation [33]. Moreover, we find *Spre1*

(*Sprouty related, EVH1 domain containing 1*) upregulated, a gene, that is implicated in inhibition of MAPK signaling [34]. *Rspan3* (*R-spondin 3*) is a Wnt signaling activator [35] and is also enhanced in *Gata2*-deficient ureters at E14.5.

Looking at the downregulated *Gata2*-target genes, we detect at least three very interesting genes (depicted in blue): *Frzb* (*frizzled-related protein*) is a key modulator of Wnt signaling [36]. *Fgf18* (*fibroblast growth factor 18*) plays important roles in cell proliferation, cell differentiation and cell migration [37]. Last but not least, we detect strong downregulation of *Tgfb2* (*transforming growth factor, beta 2*), which is also a crucial factor regulating cell growth, differentiation and adhesion [38]. Canonical *Tgfb2* signaling is transduced via Smad2/3 and co-Smad4 to initiate target gene transcription. This genes together indicate upregulated mRNA expression of activating transcription factors, antagonized MAPK- and upregulated Wnt-signaling as well as reduced growth factor activity in ureters of E14.5 *Tbx18^{cre/+};Gata2^{fx/fx}* embryos, which coincides with our *in vivo* and GO term analysis.

DISCUSSION

***Gata2* is required in the uncommitted UM to allow SM cell differentiation.**

SM cell differentiation of the ureter involves a tight regulation of transcription factors and signaling pathways in space and time. *Myocd* is a transcriptional co-activator, which, together with *Srf*, initiates terminal differentiation of the mouse ureter. *Myocd* expression is driven by diverse signaling pathways and transcription factors including Shh- and Wnt-signaling and their downstream effectors *Bmp4*, *Tshz3* and *Sox9*. Here, we show that *Gata2* is expressed in mesenchymal and epithelial progenitor cells of the ureter and upon conditional loss of *Gata2* in the UM, *Myocd* expression and, hence, SM cell differentiation is delayed. Additionally, our analysis showed that the transcription factor *Sox9* is reduced in *Gata2*-deficient embryos at E13.5 and E14.5. *Sox9* downregulation in *Gata2* mutants might account for delayed *Myocd* expression since it is required in the early UM to initiate *Myocd* expression [39]. These findings coincide with the analysis of conditional *Sox9* mutants, which lack SM differentiation, display an altered ECM composition and show upregulation of *Tshz3* in the uncommitted UM [9]. Additionally, it has recently been shown that a *Gata4/Fog2* transcriptional complex directly regulates *Sox9* expression in a sex reversal mouse model [5]. Whether *Gata2* is also able to activate *Sox9* transcription in the UM directly, may be accessed by transactivation assays.

In the past only a limited number of factors has been identified to allow proper ureteric SM development. The T-box transcription factor *Tbx18* drives specification and spatial aggregation of the undifferentiated mesenchyme prior to SM differentiation [40]. In addition, Shh signaling controls proliferation and patterning of the UM and maintains *Bmp4* expression, which

is important for proper SM differentiation [4]. Moreover, canonical Wnt-signaling is essential for patterning the early UM in order to allow differentiation of the inner mesenchymal ring [8]. As already mentioned, Hedgehog signaling is a crucial long-range module known to regulate proliferation and patterning of organs during embryogenesis. In the limb, Gata6 has been shown to directly bind to *Ptch1* and *Gli3* regulatory elements and by that balances Hh-signaling activity [41]. Our study accentuates increased Hedgehog-signaling in the UM of *Gata2*-deficient ureters as shown by upregulation of *Ptch1* expression at E14.5 and E15.5 in *Gata2*-deficient embryos. Therefore, Gata2 might act as a direct repressor of Hh-signaling in the UM as it is seen in limb development. In another manuscript, we plan to culture *Gata2*-deficient ureters in the presence of Cyclopamine, the *bona fide* pharmacological inhibitor of *Smo* (*smoothened homolog*). Rescue of ureteric peristalsis with this assay would indicate that increased Hh-signaling indeed hampers SM cell differentiation in *Gata2*-deficient ureters. Whether Gata2 is able to bind to the *Ptch1* or *Gli3* promoter, could be assessed by CHIP (sequencing) experiments.

Over a decade ago, the McMahon group has shown that Shh signaling from the ureteric epithelium is necessary to maintain *Bmp4* expression in the UM [42]. Enhanced *Ptch1* expression in *Gata2*-deficient UM might consequently result in upregulation of *Bmp4* expression. However, preliminary experiments in our lab have shown that Hh-signaling is necessary but not sufficient to induce *Bmp4* expression in the UM (data not shown).

Hence, Gata2 might directly regulate Bmp-signaling independently of Shh in the uncommitted UM.

During ureteric budding, *Gata2* has been introduced by D. Engel's group as a key regulator of *Bmp4* expression [8]. YAC-rescued *Gata2* hypomorphic embryos show decreased *Bmp4* levels, which lead to UB defects and culminated in megaureter development. In our study, we showed that *Bmp4* levels were also dramatically decreased in the UM at E13.5. Gata2 might therefore directly regulate *Bmp4* signaling in the UM on the transcriptional level or it might repress an activator, which may be tested by CHIP sequencing or mass spectrometry.

Cells of the ureteric mesenchyme of *Tbx18*^{cre/+};*Gata2*^{fx/fx} embryos may retain a precursor state.

Cytodifferentiation requires the transition of precursor cells into a specialized cell type. RA-signaling is a potent signaling module, which has been implicated in many contexts to favor a precursor state of cells and to regulate their proliferation [18].

In our study, we see enhancement of this pathway, shown by upregulation of the RA receptor and internal target *Rarb*. Furthermore, we observe upregulation of *Tcf21* in the UM of *Gata2*-deficient ureters, which is a direct target of RA signaling in the epicardium, where it is known to control SM differentiation [43]. Moreover, in *Gata2*-deficient ureters we see upregulation of *Meis2*, a well-established target of RA [44], indicating enhanced RA signaling response in

this tissue. These findings strongly suggest a negative regulation of RA-signaling by Gata2 during embryogenesis.

In a separate manuscript, we intend to culture *Gata2*-deficient ureters in the presence of BMS453, a pan-RA receptor inhibitor [45]. A rescue of ureteric peristalsis would indicate that increased RA signaling interferes with SM cell differentiation in *Gata2*-mutants. In turn, wild-type ureter *ex vivo* cultures treated with RA might phenocopy *Gata2* deficiency (to some extent), which will be addressed in the future.

Hypoplasia and developmental delay of the UM upon conditional loss of Gata2.

Our study revealed hypoplasia and developmental delay of the *Gata2*-deficient UM already at E12.5. RA is able to activate or inhibit cell growth by distinct binding to two different nuclear receptors (RAR α/β and PPAR β/δ). Binding to RARs in general leads to cell growth inhibition. In contrast, binding of RA to orphan PPAR receptors facilitates proliferation and apoptosis inhibition [46]. Since we see weak RAR α and strong RAR β expression in the wild-type UM, we deem it likely that enhanced RA signaling via binding to RARs results in potential proliferation defects that we observe in the *Gata2*-mutants. Examination of cell growth still needs to be addressed in this particular mouse mutant and in which respect it accounts for the phenotype.

Potentially diminished angiogenesis in the UM of *Tbx18^{cre/+};Gata2^{fx/fx}* embryos.

Gata2 has been described as a pivotal regulator of angiogenesis [43], one process, which might be disturbed early in UM development in *Tbx18^{cre/+};Gata2^{fx/fx}* embryos (Table S6). Preliminary experiments in our lab have shown that the early metanephric field, especially the Tbx18⁺ domain, is highly vascularized (Master thesis of T. Bohnenpoll). In the *Gata2* microarray at E14.5, we find clusters of genes downregulated, which are associated with angiogenesis and blood composition. Almost all angiopoietin-like factors are downregulated in E14.5 *Gata2*-deficient ureters (except *Angptl3*). *Angptl1*, 2 and 4 participate in the formation of blood vessels (www.genecards.org). In vascular endothelial cells, *Angptl4* (*angiopoietin like 4*, -1.3-fold downregulated) is known to inhibit apoptosis (www.genecards.org). Moreover, *Aqp1* (*Aquaporin1*, *Colton blood group*), which is an important water channel for erythrocytes, is also strongly downregulated in *Gata2*-deficient ureters. Interestingly, a whole set of complement factors (*C1qa-C1qc*), which are components of the blood serum, are mutually downregulated in mutant ureters. In addition, we find a subset of hemoglobin (*Hba-x* and *Hbb-bh1*) encoding genes and *Vcam1* (*Vascular cell adhesion molecule 1*) mRNA levels decreased in *Gata2*-mutant ureters.

These findings strongly indicate abolished angiogenesis and/or vasculogenesis in *Gata2*-mutants at E14.5, which results in lower levels of hemoglobin and complement factors compared to controls. This, in turn, might hamper the nutrition and proliferation of SM precursor

cells. Consequently, insufficient nutrition might lead to retardation of UM development and to a delay in SM differentiation.

Taken together, our study introduces *Gata2* as a novel regulator of ureteric SM development. Deletion of *Gata2* in the UM results in loss of *Myocd* (the key regulator of ureteric SM differentiation) and in delayed expression of SM structural genes, which explains the delayed onset of ureteric peristalsis. Moreover, we observe enhanced and prolonged expression of three key signaling pathways of ureter development: Hh-, RA- and Wnt signaling, which might account for the potential maintenance of the mesenchymal precursor state. This leads us to the assumption, that *Gata2* is needed to repress these key signaling modules in order to allow proper development of the UM.

FIGURES and LEGENDS

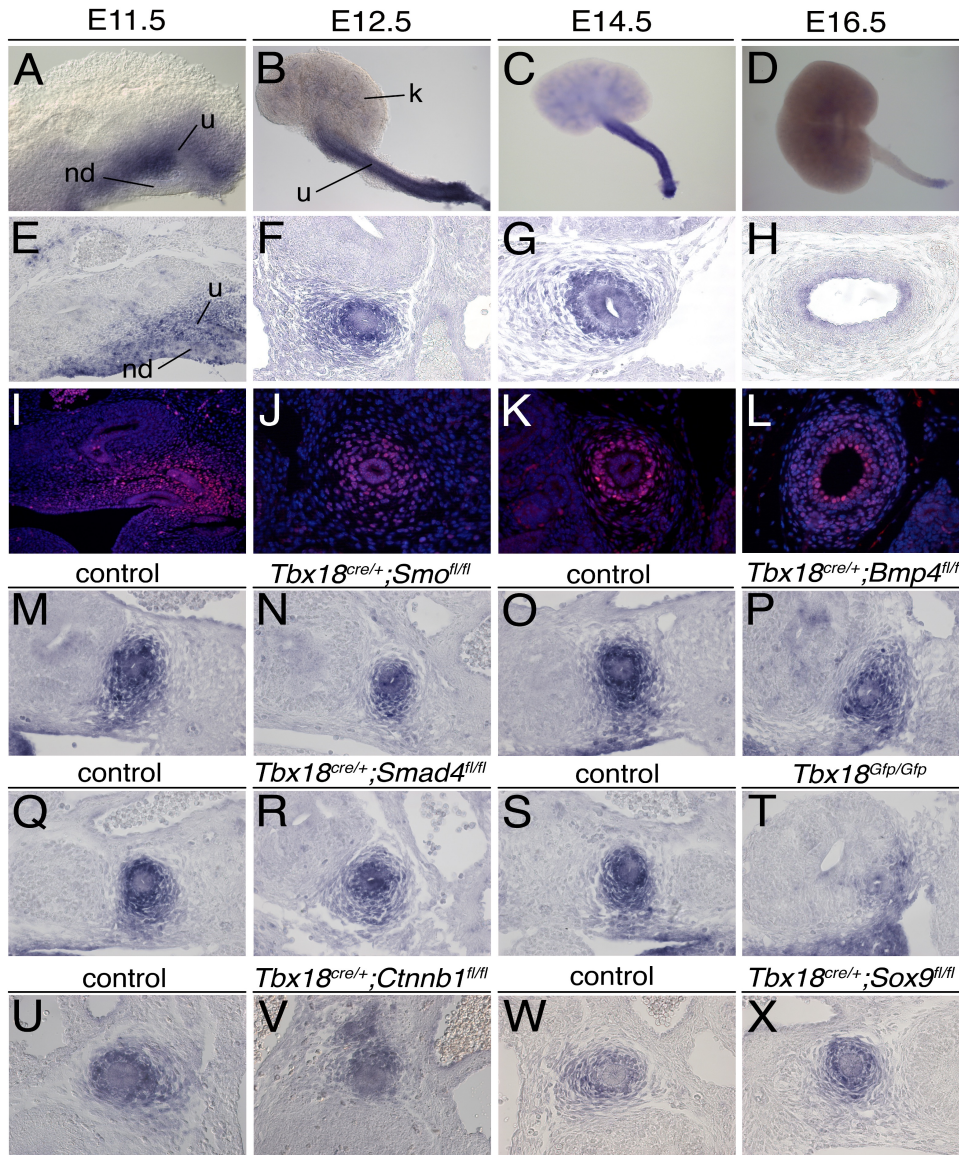


Figure 1. Expression and genetic control of *Gata2* during ureter development.

RNA *in situ* hybridization analysis of whole mount kidney rudiments (**A-D**) and on sections of the metanephros region (**E**) and on proximal ureter sections (**F-H; M-X**). Immunohistochemical analysis of the *Gata2* protein on sections of the metanephros region (**I**) and of proximal ureter sections (**J-L**). Stages and probes are indicated. k, kidney; nd, nephric duct; u, ureter.

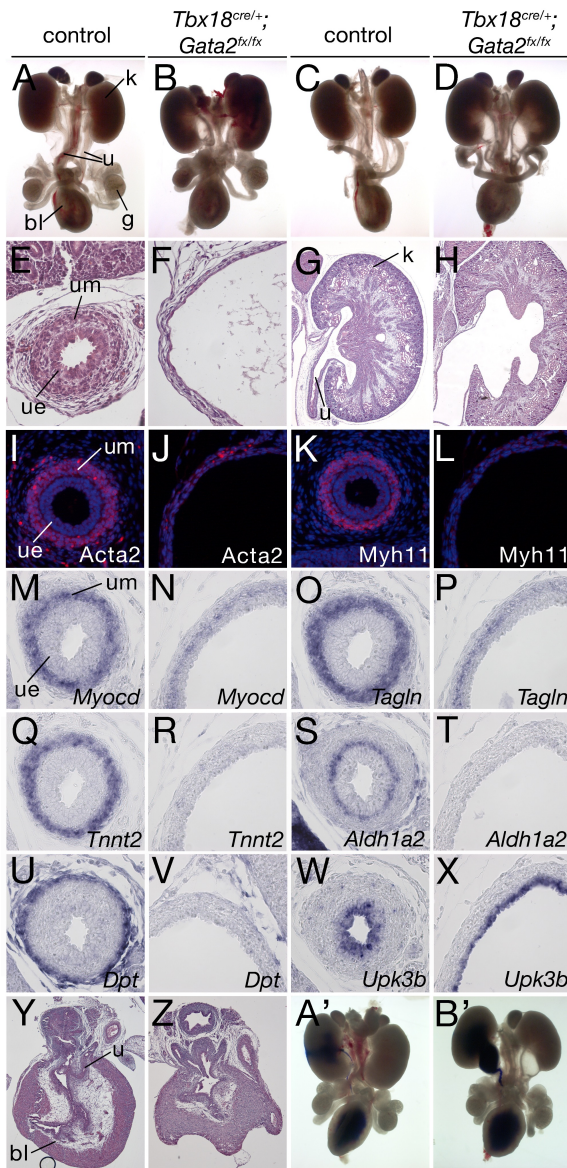


Figure 2. Ureter and kidney anomalies of *Tbx18^{cre/+};Gata2^{fx/fx}* mutants at E18.5.**

(A-D) Morphology of whole urogenital systems of male (A,B) and female embryos (C,D). (E-H) H&E stainings on transversal sections of the proximal ureter (E,F) and on sagittal kidney sections (G,H). (I-X) Cytodifferentiation of the ureteric mesenchyme (I-V) and of the urothelium (W,X) shown by immunofluorescence (I-L) and by section RNA *in situ* hybridization analysis (M-X). (Y-B') Analysis of the vesico-ureteric junction shown by H&E stainings on sagittal bladder sections (Y,Z) and by ink injection (A',B'). Probes and antibodies are indicated. bl, bladder; g, gonad; k, kidney; u, ureter; ue, ureteric epithelium; um, ureteric muscle.

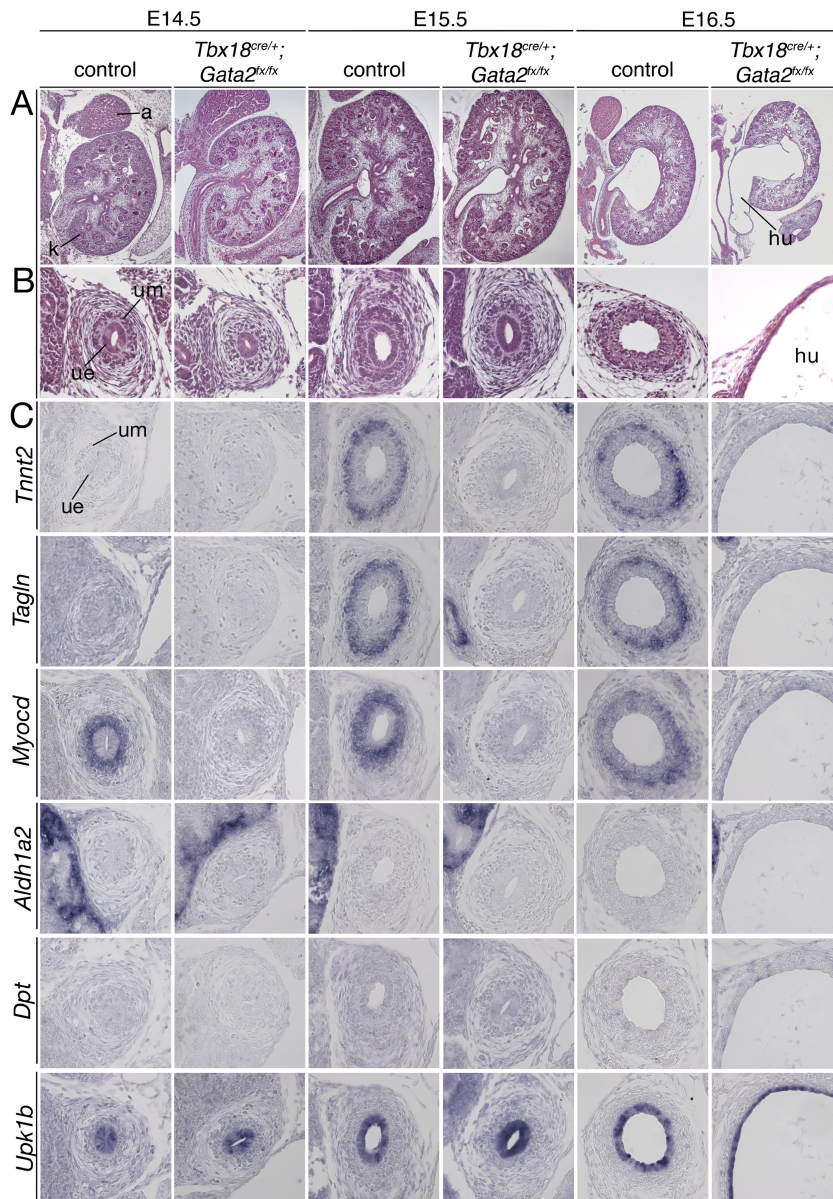


Figure 3. Onset and progression of differentiation defects of the ureteric mesenchyme in *Tbx18^{cre/+};Gata2^{flx/flx}* embryos.**

(A,B) H&E stainings on sagittal sections of the kidney (A) and on transverse sections of the proximal ureter (B). (C) Cytodifferentiation of the ureteric mesenchyme and the urothelium shown by section RNA *in situ* hybridization analysis. Stages and probes are indicated. a, adrenal gland; hu, hydronephrosis; ue, ureteric mesenchyme; um, ureteric mesenchyme, k, kidney.

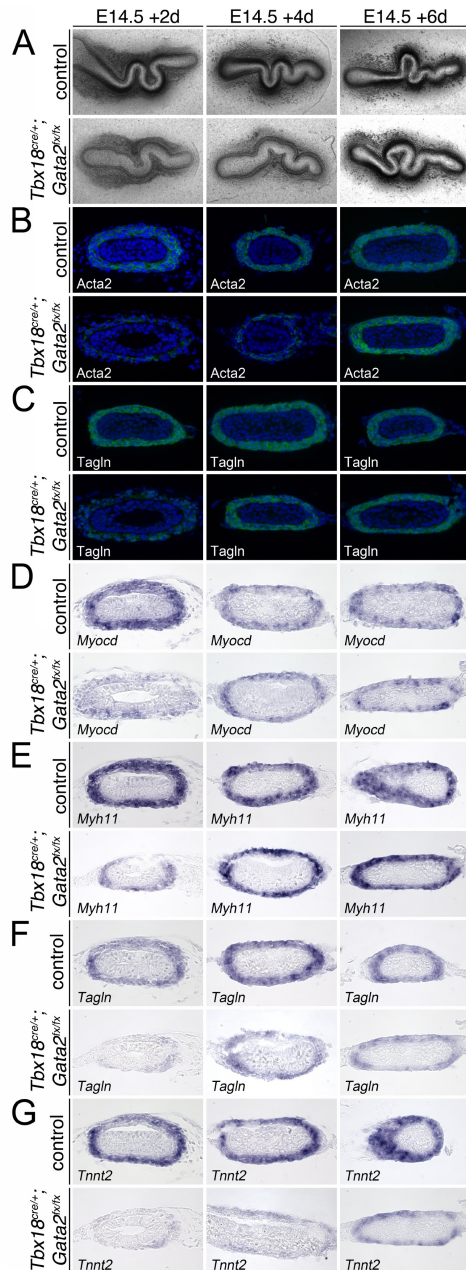


Figure 4. Ureter defects of *Tbx18^{cre/+};Gata2^{fx/fx}* embryos ex vivo.**

(A-G) Cytodifferentiation and peristalsis of *Gata2*-deficient ureters ex vivo. (A) Peristalsis assay of isolated ureters in culture. (B-G) Cytodifferentiation of cultured ureters shown by immunofluorescence (B,C) and RNA *in situ* hybridization analysis on sections of cultured ureters. Time periods, antibodies, probes and genotypes are indicated.

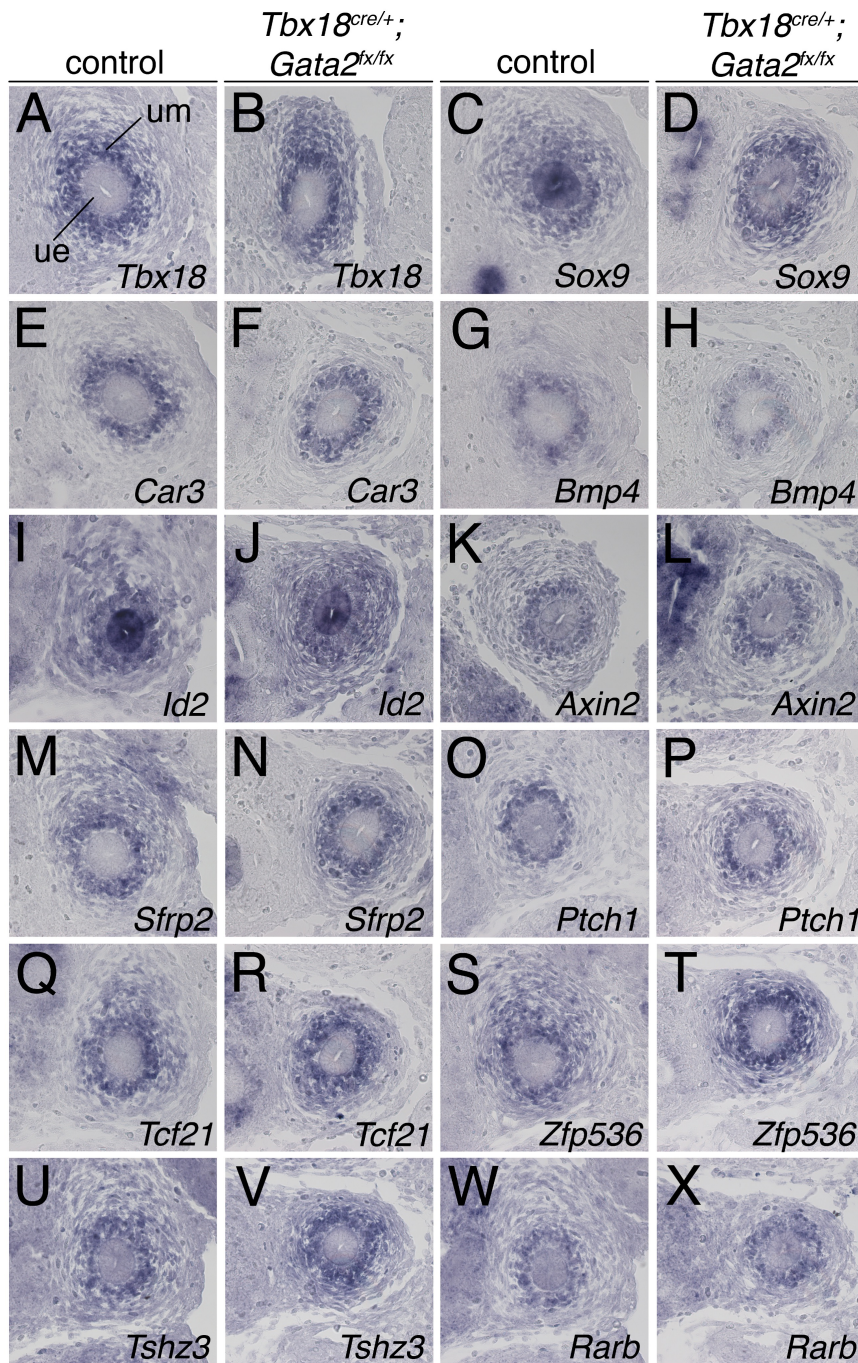


Figure 5. Molecular changes in *Tbx18^{cre/+};Gata2^{fx/fx}* embryos at E13.5.**
(A-X) RNA *in situ* hybridization analysis on sections of the proximal ureter at E13.5. Probes and genotypes are indicated. ue, ureteric epithelium; um, ureteric mesenchyme.

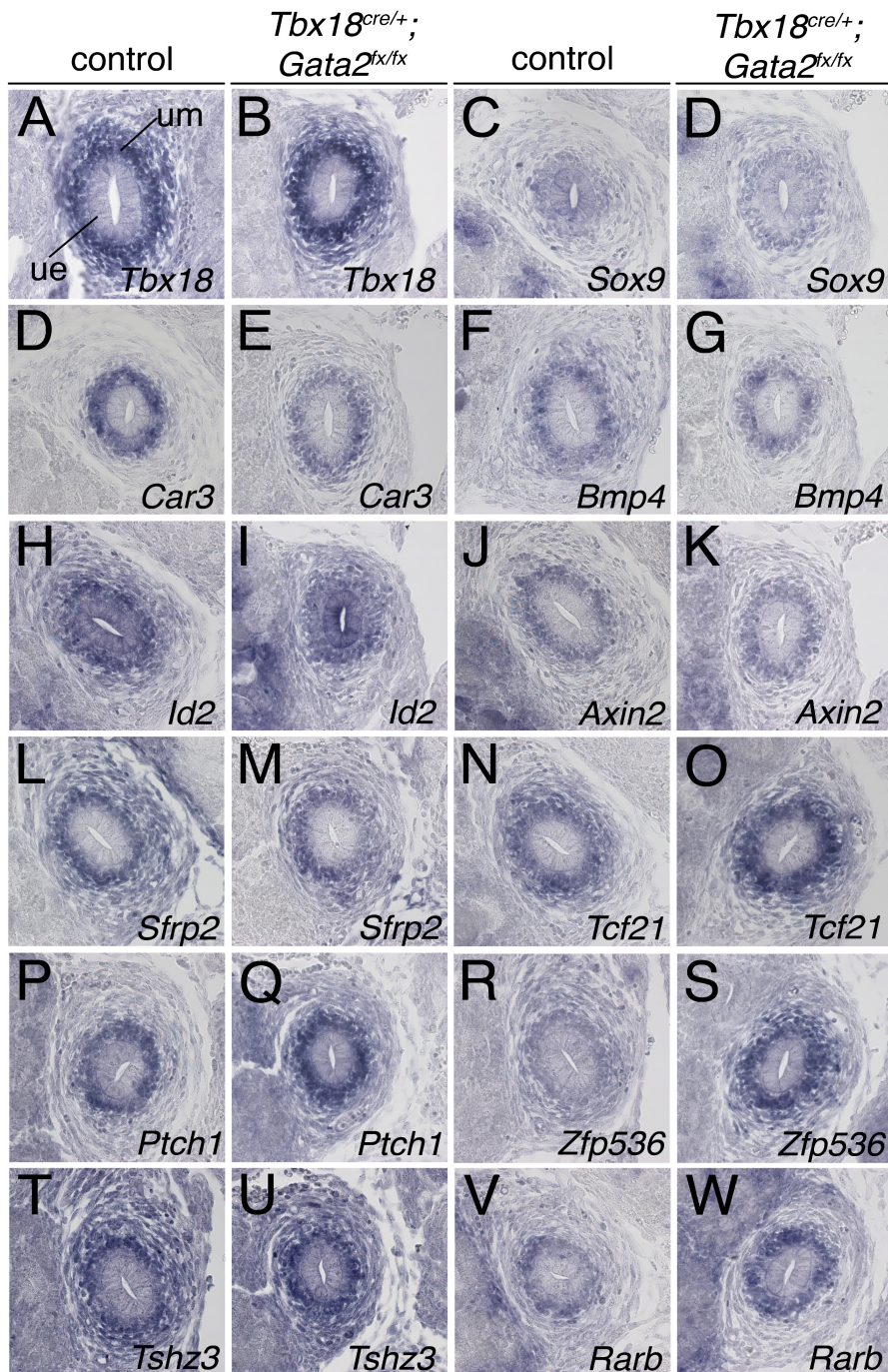


Figure 6. Molecular changes in the UM of *Tbx18^{cre/+};Gata2^{flx/flx}* embryos at E14.5.**
(A-W) RNA *in situ* hybridization analysis on sections of the proximal ureter at E14.5.
Probes and genotypes are indicated. ue, ureteric epithelium; um, ureteric mesenchyme.

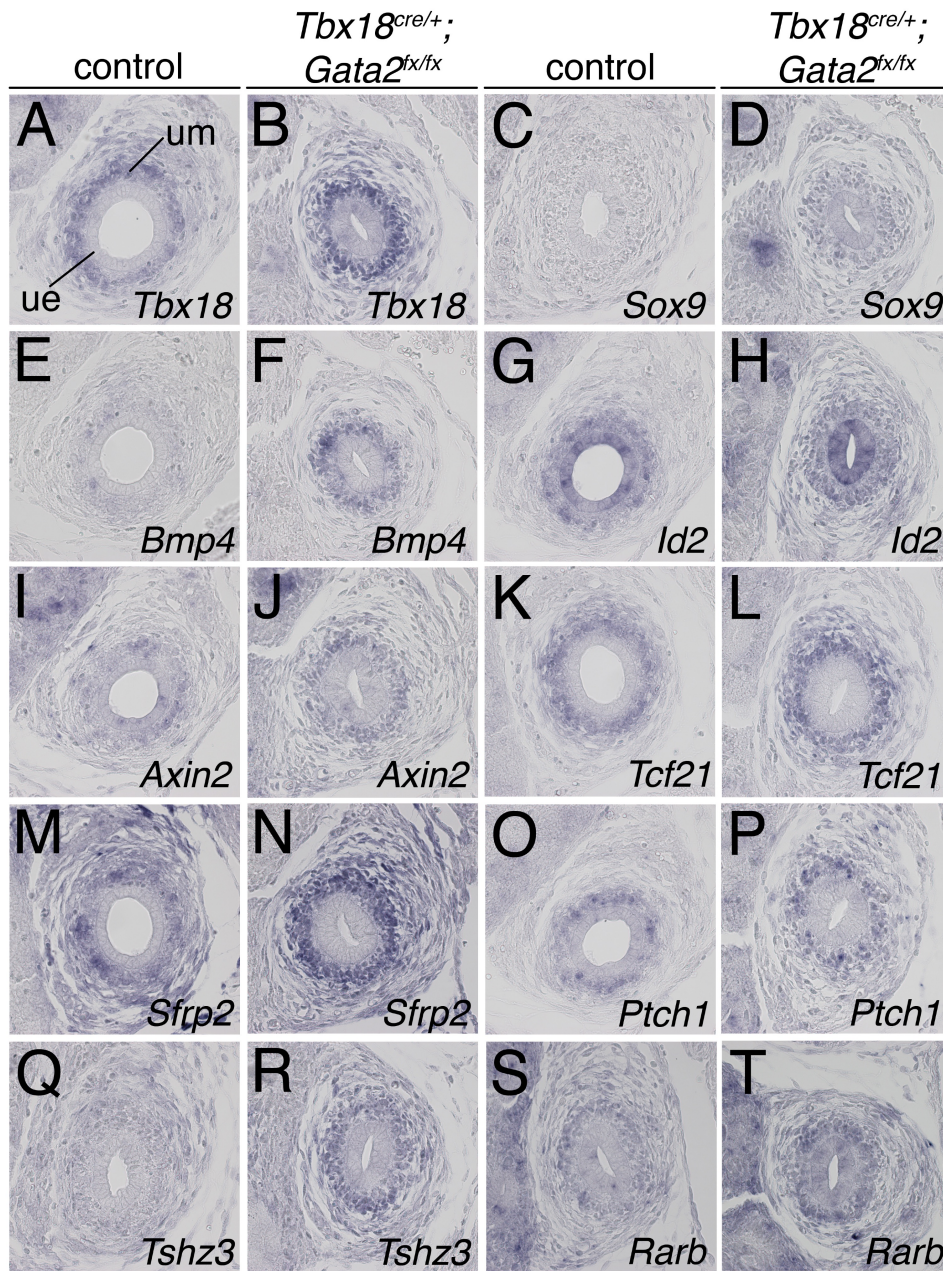


Figure 7. Molecular changes in the UM of *Tbx18^{cre/+};Gata2^{fx/fx}* embryos at E15.5.
(A-T) RNA *in situ* hybridization analysis on sections of the proximal ureter at E15.5.
Probes and genotypes are indicated. ue, ureteric epithelium; um, ureteric mesenchyme.

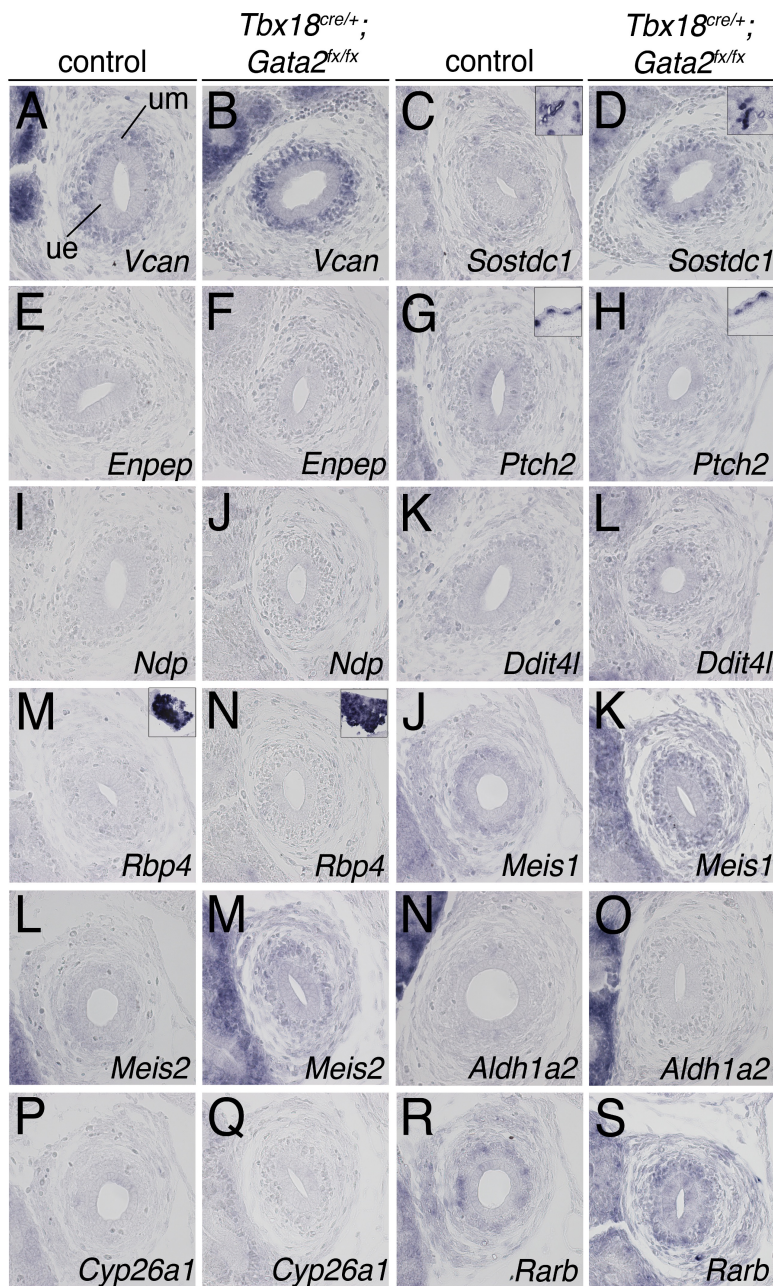


Figure 8. Molecular analysis of Hedgehog- and RA- target and effector genes in the UM of *Tbx18^{cre/+};Gata2^{fx/fx}* embryos at E15.5.**

(A-B') RNA *in situ* hybridization analysis on sections of the proximal ureter at E15.5.

Probes and genotypes are indicated. ue, ureteric epithelium; um, ureteric mesenchyme. In-sets (C,D,G,H,Q,R) show positive control regions in the embryo.

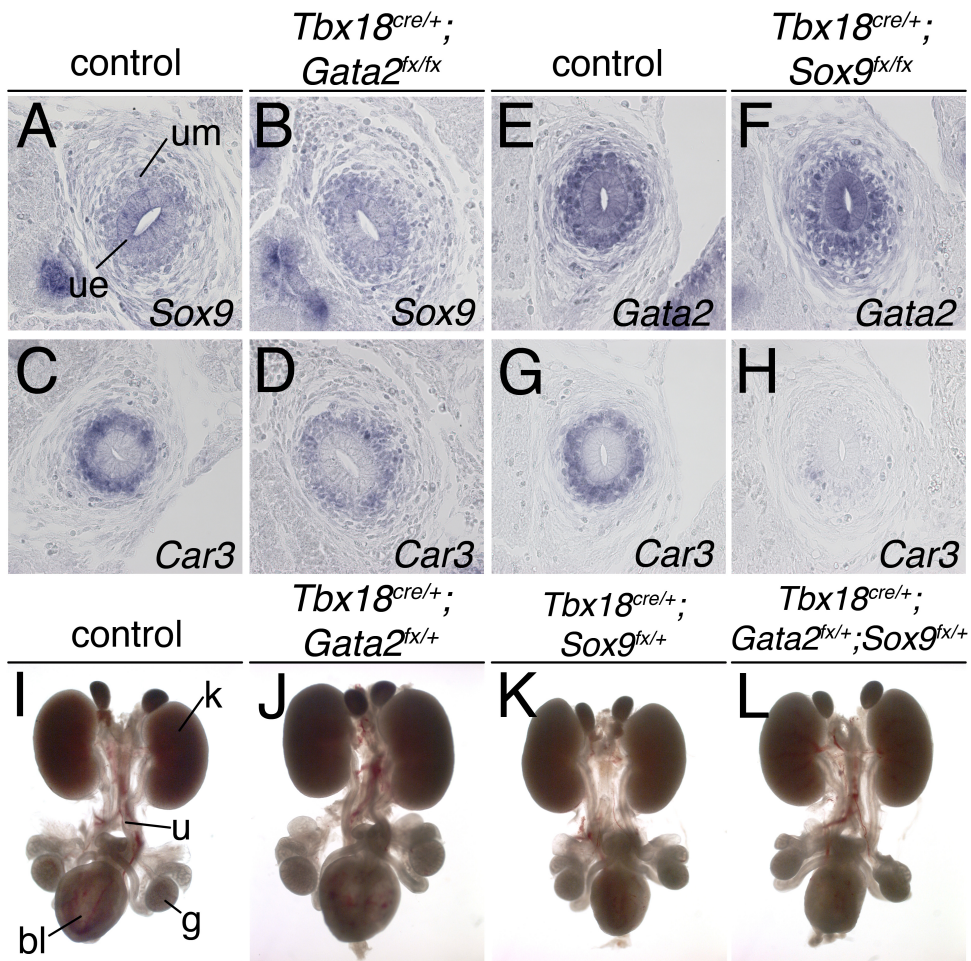


Figure 9. Analysis of the epistasis of *Gata2* and *Sox9* at E14.5 at E18.5.

(A-H) RNA *in situ* hybridization analysis on sections of the proximal ureter at E14.5. (I-L) Morphology of whole UGS of male embryos at E18.5. Probes and genotypes are indicated. bl, bladder; g, gonad; k, kidney; u, ureter; ue, ureteric epithelium, um, ureteric mesenchyme.

Bibliography

1. Renkema, K.Y., et al., Novel perspectives for investigating congenital anomalies of the kidney and urinary tract (CAKUT). *Nephrol Dial Transplant*, 2011. 26(12): p. 3843-51.
2. Bohnenpoll, T. and A. Kispert, Ureter growth and differentiation. *Semin Cell Dev Biol*, 2014. 36: p. 21-30.
3. Costantini, F. and R. Shakya, GDNF/Ret signaling and the development of the kidney. *Bioessays*, 2006. 28(2): p. 117-27.
4. Airik, R., et al., Tbx18 regulates the development of the ureteral mesenchyme. *J Clin Invest*, 2006. 116(3): p. 663-74.
5. Airik, R., et al., Hydroureteronephrosis due to loss of Sox9-regulated smooth muscle cell differentiation of the ureteric mesenchyme. *Hum Mol Genet*, 2010. 19(24): p. 4918-29.
6. Miyazaki, Y., et al., Bone morphogenetic protein 4 regulates the budding site and elongation of the mouse ureter. *J Clin Invest*, 2000. 105(7): p. 863-73.
7. Brenner-Anantharam, A., et al., Tailbud-derived mesenchyme promotes urinary tract segmentation via BMP4 signaling. *Development*, 2007. 134(10): p. 1967-75.
8. Yu, J., T.J. Carroll, and A.P. McMahon, Sonic hedgehog regulates proliferation and differentiation of mesenchymal cells in the mouse metanephric kidney. *Development*, 2002. 129(22): p. 5301-12.
9. Martin, E., et al., TSHZ3 and SOX9 regulate the timing of smooth muscle cell differentiation in the ureter by reducing myocardin activity. *PLoS One*, 2013. 8(5): p. e63721.
10. Aronson, B.E., K.A. Stapleton, and S.D. Krasinski, Role of GATA factors in development, differentiation, and homeostasis of the small intestinal epithelium. *Am J Physiol Gastrointest Liver Physiol*, 2014. 306(6): p. G474-90.
11. Grote, D., et al., Pax 2/8-regulated Gata 3 expression is necessary for morphogenesis and guidance of the nephric duct in the developing kidney. *Development*, 2006. 133(1): p. 53-61.
12. Grote, D., et al., Gata3 acts downstream of beta-catenin signaling to prevent ectopic metanephric kidney induction. *PLoS Genet*, 2008. 4(12): p. e1000316.
13. Khandekar, M., et al., Multiple, distant Gata2 enhancers specify temporally and tissue-specific patterning in the developing urogenital system. *Mol Cell Biol*, 2004. 24(23): p. 10263-76.
14. Yu, L., et al., GATA2 regulates body water homeostasis through maintaining aquaporin 2 expression in renal collecting ducts. *Mol Cell Biol*, 2014. 34(11): p. 1929-41.
15. Tsai, F.Y., et al., An early haematopoietic defect in mice lacking the transcription factor GATA-2. *Nature*, 1994. 371(6494): p. 221-6.
16. Zhou, Y., et al., Rescue of the embryonic lethal hematopoietic defect reveals a critical role for GATA-2 in urogenital development. *EMBO J*, 1998. 17(22): p. 6689-700.
17. Hoshino, T., et al., Reduced BMP4 abundance in Gata2 hypomorphic mutant mice result in uropathies resembling human CAKUT. *Genes Cells*, 2008. 13(2): p. 159-70.

18. Ainoya, K., et al., UG4 enhancer-driven GATA-2 and bone morphogenetic protein 4 complementation remedies the CAKUT phenotype in Gata2 hypomorphic mutant mice. *Mol Cell Biol*, 2012. 32(12): p. 2312-22.
19. Charles, M.A., et al., Pituitary-specific Gata2 knockout: effects on gonadotrope and thyrotrope function. *Mol Endocrinol*, 2006. 20(6): p. 1366-77.
20. Aoki, Y., et al., Id2 haploinsufficiency in mice leads to congenital hydronephrosis resembling that in humans. *Genes Cells*, 2004. 9(12): p. 1287-96.
21. Batourina, E., et al., Apoptosis induced by vitamin A signaling is crucial for connecting the ureters to the bladder. *Nat Genet*, 2005. 37(10): p. 1082-9.
22. Huang da, W., B.T. Sherman, and R.A. Lempicki, Bioinformatics enrichment tools: paths toward the comprehensive functional analysis of large gene lists. *Nucleic Acids Res*, 2009. 37(1): p. 1-13.
23. Huang da, W., B.T. Sherman, and R.A. Lempicki, Systematic and integrative analysis of large gene lists using DAVID bioinformatics resources. *Nat Protoc*, 2009. 4(1): p. 44-57.
24. Henley, K.D., et al., Inactivation of the dual Bmp/Wnt inhibitor Sostdc1 enhances pancreatic islet function. *Am J Physiol Endocrinol Metab*, 2012. 303(6): p. E752-61.
25. Myatt, S.S. and E.W. Lam, The emerging roles of forkhead box (Fox) proteins in cancer. *Nat Rev Cancer*, 2007. 7(11): p. 847-59.
26. Andrikou, C., et al., Myogenesis in the sea urchin embryo: the molecular fingerprint of the myoblast precursors. *Evodevo*, 2013. 4(1): p. 33.
27. McNeill, B., et al., Hedgehog regulates Norrie disease protein to drive neural progenitor self-renewal. *Hum Mol Genet*, 2013. 22(5): p. 1005-16.
28. Li, V.S., et al., Wnt signaling through inhibition of beta-catenin degradation in an intact Axin1 complex. *Cell*, 2012. 149(6): p. 1245-56.
29. Jeanpierre, C., et al., RET and GDNF mutations are rare in fetuses with renal agenesis or other severe kidney development defects. *J Med Genet*, 2011. 48(7): p. 497-504.
30. Daily, K., et al., MotifMap: integrative genome-wide maps of regulatory motif sites for model species. *BMC Bioinformatics*, 2011. 12: p. 495.
31. Philippidou, P. and J.S. Dasen, Hox genes: choreographers in neural development, architects of circuit organization. *Neuron*, 2013. 80(1): p. 12-34.
32. Linnemann, A.K., et al., Genetic framework for GATA factor function in vascular biology. *Proc Natl Acad Sci U S A*, 2011. 108(33): p. 13641-6.
33. Je, D.W., et al., The inhibition of SRC family kinase suppresses pancreatic cancer cell proliferation, migration, and invasion. *Pancreas*, 2014. 43(5): p. 768-76.
34. Phoenix, T.N. and S. Temple, Spred1, a negative regulator of Ras-MAPK-ERK, is enriched in CNS germinal zones, dampens NSC proliferation, and maintains ventricular zone structure. *Genes Dev*, 2010. 24(1): p. 45-56.

35. Ohkawara, B., A. Glinka, and C. Niehrs, Rspo3 binds syndecan 4 and induces Wnt/PCP signaling via clathrin-mediated endocytosis to promote morphogenesis. *Dev Cell*, 2011. 20(3): p. 303-14.
36. Bougault, C., et al., Protective role of frizzled-related protein B on matrix metalloproteinase induction in mouse chondrocytes. *Arthritis Res Ther*, 2014. 16(4): p. R137.
37. Ohbayashi, N., et al., FGF18 is required for normal cell proliferation and differentiation during osteogenesis and chondrogenesis. *Genes Dev*, 2002. 16(7): p. 870-9.
38. Schmierer, B. and C.S. Hill, TGFbeta-SMAD signal transduction: molecular specificity and functional flexibility. *Nat Rev Mol Cell Biol*, 2007. 8(12): p. 970-82.
39. Manuylov, N.L., et al., The regulation of Sox9 gene expression by the GATA4/FOG2 transcriptional complex in dominant XX sex reversal mouse models. *Dev Biol*, 2007. 307(2): p. 356-67.
40. Trowe, M.O., et al., Canonical Wnt signaling regulates smooth muscle precursor development in the mouse ureter. *Development*, 2012. 139(17): p. 3099-108.
41. Kozhemyakina, E., A. Ionescu, and A.B. Lassar, GATA6 is a crucial regulator of Shh in the limb bud. *PLoS Genet*, 2014. 10(1): p. e1004072.
42. Wolf, G., Retinoic acid as cause of cell proliferation or cell growth inhibition depending on activation of one of two different nuclear receptors. *Nutr Rev*, 2008. 66(1): p. 55-9.
43. Braitsch, C.M., et al., Pod1/Tcf21 is regulated by retinoic acid signaling and inhibits differentiation of epicardium-derived cells into smooth muscle in the developing heart. *Dev Biol*, 2012. 368(2): p. 345-57.
44. Sapin, V., et al., Differential expression of retinoic acid-inducible (Stra) genes during mouse placentation. *Mech Dev*, 2000. 92(2): p. 295-9.
45. Yang, L., et al., Retinoic acid receptor antagonist BMS453 inhibits the growth of normal and malignant breast cells without activating RAR-dependent gene expression. *Breast Cancer Res Treat*, 1999. 56(3): p. 277-91.
46. Coma, S., et al., GATA2 and Lmo2 control angiogenesis and lymphangiogenesis via direct transcriptional regulation of neuropilin-2. *Angiogenesis*, 2013. 16(4): p. 939-52.

SUPPLEMENTARY MATERIAL

for

The zinc finger transcription factor Gata2 promotes differentiation of the ureteric mesenchyme by alleviating Hedgehog- and RA-signaling activity

Anna-Carina Weiss¹, Tobias Bohnenpoll¹, Patrick Blank¹, Tamrat Mamo¹, Rannar Airik¹, Marc-Oliver Trowe¹ and Andreas Kispert^{1,§}

¹Institut für Molekularbiologie, Medizinische Hochschule Hannover, 30625 Hannover, Germany.

§ Author for correspondence: (kispert.andreas@mh-hannover.de)

SUPPLEMENTARY FIGURES

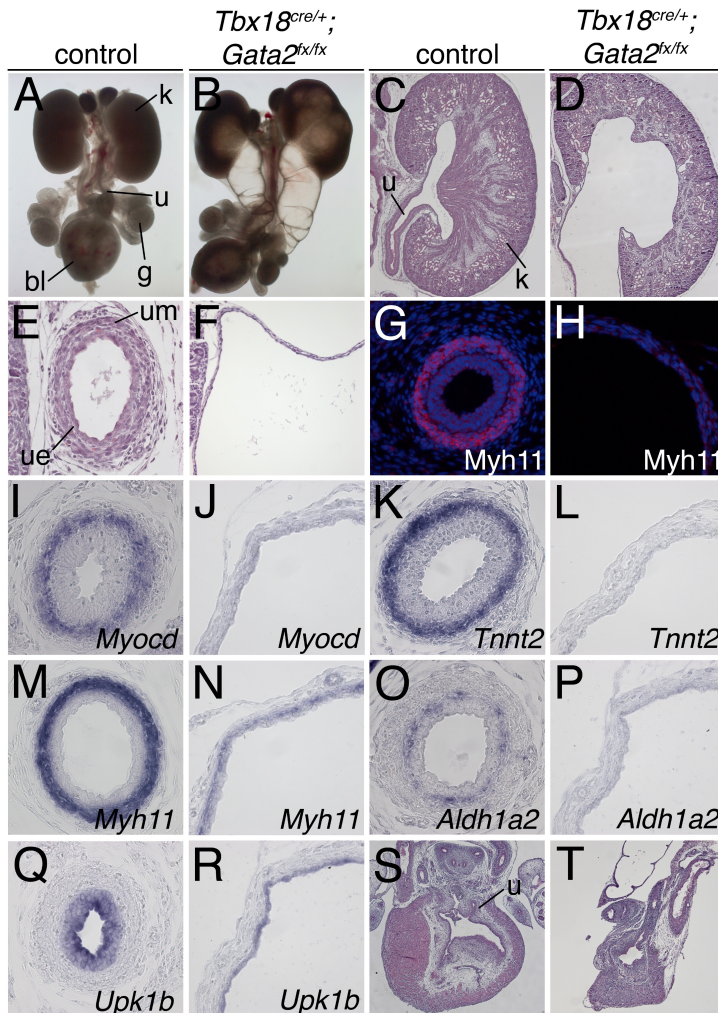


Fig. S1. Megaureter and hydronephrosis of *Tbx18^{cre/+};Gata2^{fx/fx}* embryos at E18.5.

(A,B) Morphology of urogenital systems of male embryos at E18.5. (C-F) Haematoxylin and eosin stainings on sagittal sections of kidneys and (E,F) of sections of the proximal ureter. (G-R) Cytodifferentiation of the ureteric mesenchyme (G-P) and the urothelium (Q,R) shown by immunofluorescence (G,H) and RNA *in situ* hybridizations (I-Q). Analysis of the vesico-ureteric junction by H&E stainings on sagittal sections of the bladder (S,T). Genotypes and probes are indicated. bl, bladder; g, gonad; k, kidney, u, ureter.

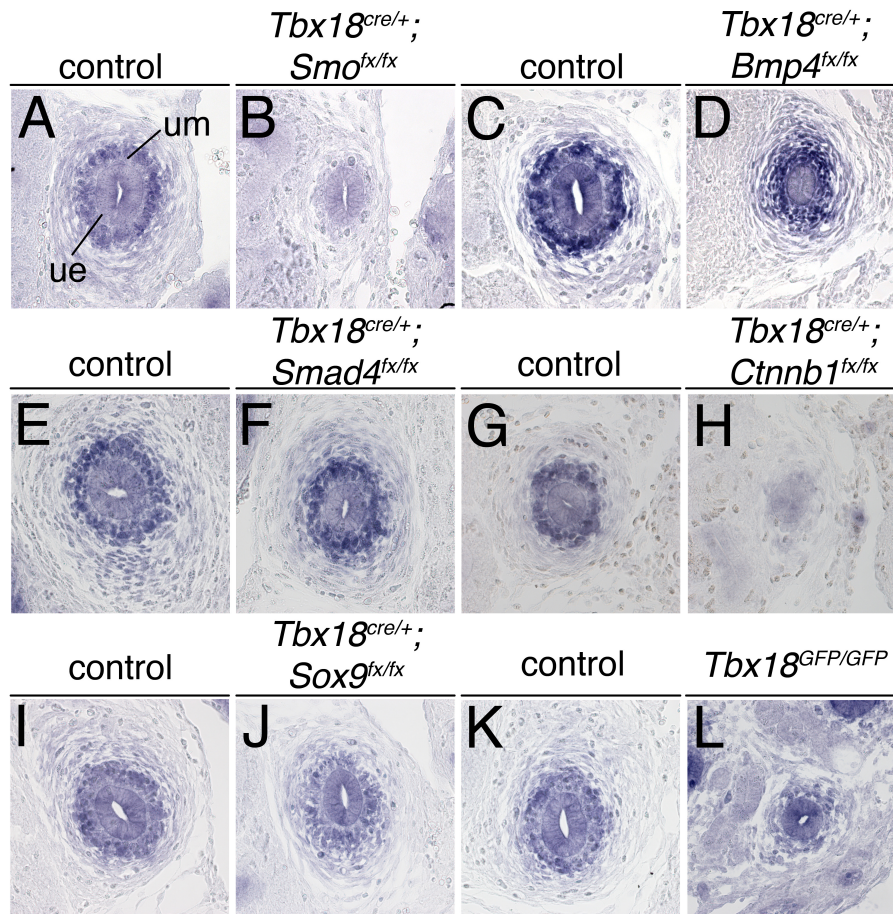


Figure S2. Genetic control of *Gata2* expression in the ureter at E14.5.

(A-N) RNA *in situ* hybridization analysis of *Gata2* expression on sections of the proximal ureter of various conditional and null mouse mutants at E14.5. Genotypes are indicated. ue, ureteric epithelium; um, ureteric mesenchyme.

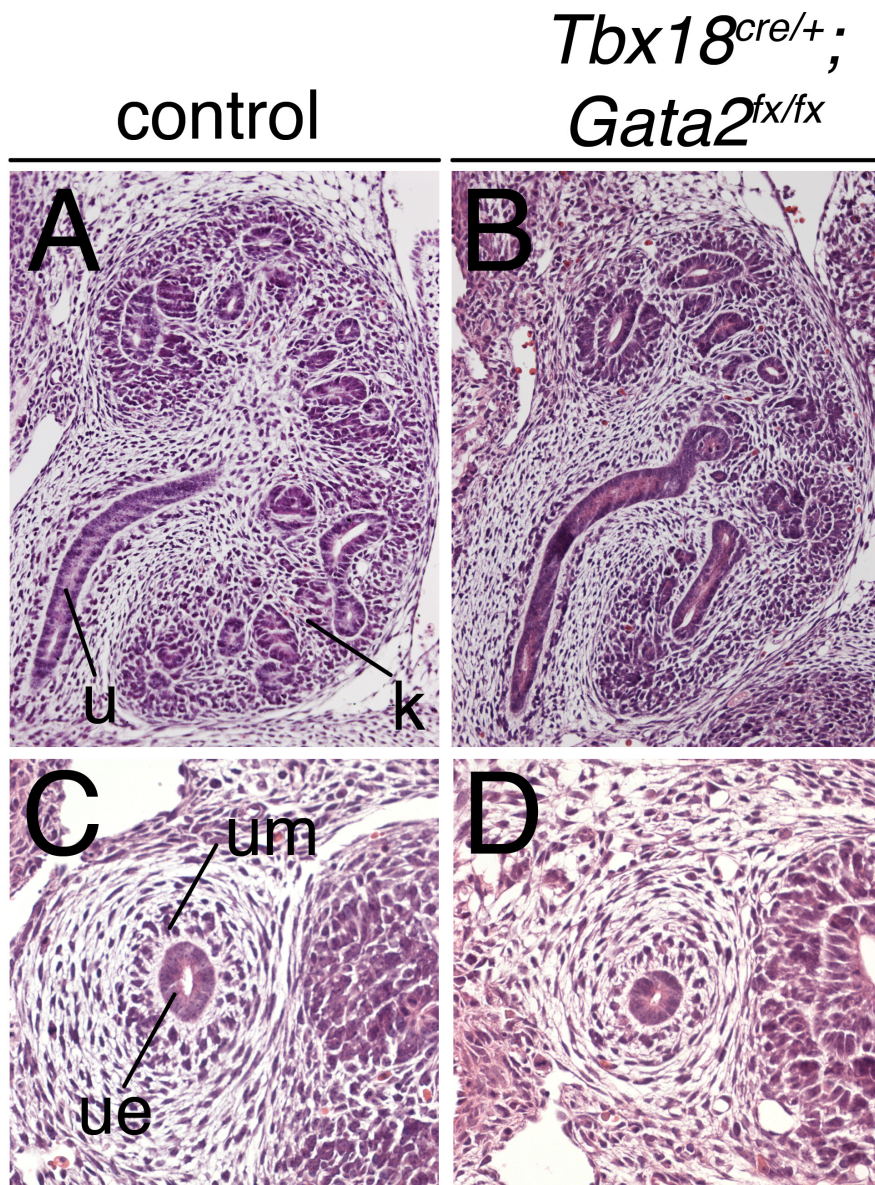


Figure S3. Hypoplasia of the proximal UM of *Tbx18*^{cre/+};*Gata2*^{fx/fx} embryos at E12.5.

(A-D) Haematoxylin and eosin stainings on (A,B) sagittal sections of kidney and on (C,D) proximal sections of the ureter. Genotypes are indicated. k, kidney; u, ureter; ue, ureteric epithelium; um, ureteric mesenchyme.

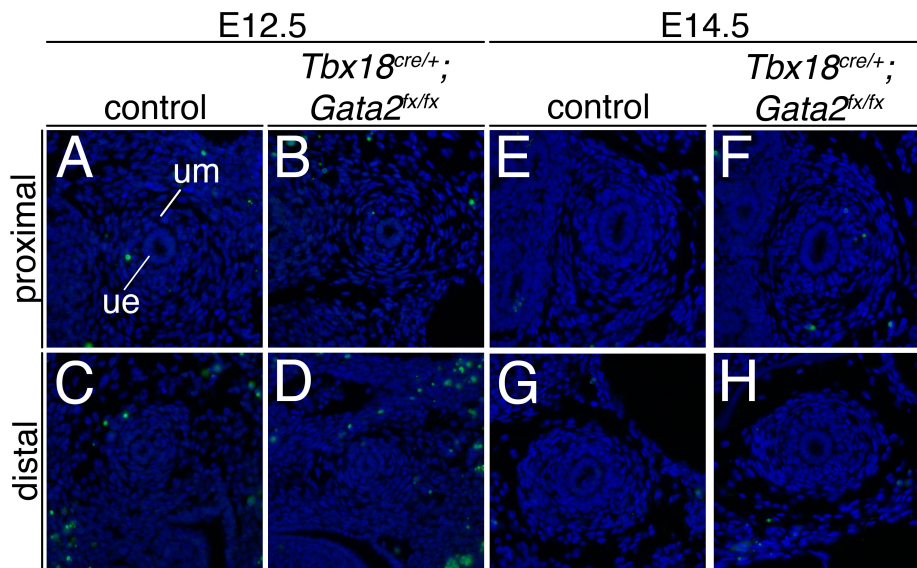


Figure S4. Programmed cell death is unchanged in *Tbx18^{cre/+};Gata2^{fx/fx}* embryos at E12.5 and E14.5. (A-H)** Analysis of programmed cell death by TUNEL assay on transverse sections of the proximal and distal ureter at E12.5 (A-D) and at E14.5 (E-H). Apoptosis is unaltered in *Gata2*-mutant embryos. Apoptotic bodies in green, nuclei in blue (DAPI). Stages and genotypes are indicated. ue, ureteric epithelium, um, ureteric mesenchyme.

SUPPLEMENTARY TABLES

OFFICIAL_GENE_SYMBOL		GENE NAME	Related Genes	Species
Cartpt	(-2.6-fold)	CART_prepropeptide	RG	Mus.musculus
Gch1	(-1.6-fold)	GTP_cyclohydrolase_1	RG	Mus.musculus
Acta2	(-1.8-fold)	actin_alpha_2_smooth_muscle_aorta	RG	Mus.musculus
ApoE	(-1.5-fold)	apolipoprotein_E	RG	Mus.musculus
Calca	(-2.2-fold)	calcitonin/calcitonin-related_polypeptide_alpha	RG	Mus.musculus
EdnrB	(-1.5-fold)	endothelin_receptor_type_B	RG	Mus.musculus
Nppc	(-2.0-fold)	natriuretic_peptide_precursor_type_C	RG	Mus.musculus
Npy	(-3.2-fold)	neuropeptide_Y	RG	Mus.musculus

Table S1_A. Downregulated genes functionally involved in “blood circulation” by gene ontology terms at E14.5. Fold change of E14.5 *Gata2*-microarray analysis in brackets.

OFFICIAL_GENE_SYMBOL		GENE NAME	Related Genes	Species
Cartpt	(-2.6-fold)	CART_prepropeptide	RG	Mus.musculus
Sox2	(-1.6-fold)	SRY-box_containing_gene_2	RG	Mus.musculus
Vgf	(-3.3-fold)	VGF_nerve_growth_factor_inducible	RG	Mus.musculus
Ache	(-1.7-fold)	acetylcholinesterase	RG	Mus.musculus
Cttna2	(-3.0-fold)	catenin_(cadherin_associated_protein)_alpha_2	RG	Mus.musculus
Chrm3	(-1.8-fold)	cholinergic_receptor_muscarinic_3_cardiac	RG	Mus.musculus
Chrm2	(-2.1-fold)	cholinergic_receptor_nicotinic_beta_polypeptide_2_(neuronal)	RG	Mus.musculus
Cplx1	(-2.5-fold)	complexin_1	RG	Mus.musculus
Fgf7	(-1.5-fold)	fibroblast_growth_factor_7	RG	Mus.musculus
Gjd2	(-3.5-fold)	gap_junction_protein_delta_2	RG	Mus.musculus
Grii2c	(-2.1-fold)	glutamate_receptor_ionotropic_NMDA2C_(epsilon_3)	RG	Mus.musculus
Lin7a	(-1.4-fold)	lin-7_homolog_A_(C_elegans)	RG	Mus.musculus
Nrxn3	(-1.4-fold)	neurexin_III	RG	Mus.musculus
Prima1	(-1.7-fold)	proline_rich_membrane_anchor_1	RG	Mus.musculus
Colq	(-2.8-fold)	similar_to_Collagen-like_tail_subunit_(single_strand_of_homotrimer)_of_asymmetric_acetylcholinesterase; collagen-like_tail_subunit_(single_strand_of_homotrimer)_of_asymmetric_acetylcholinesterase	RG	Mus.musculus
Smpd3	(-2.1-fold)	sphingomyelin_phosphodiesterase_3_neutral	RG	Mus.musculus
Th	(-2.5-fold)	tyrosine_hydroxylase	RG	Mus.musculus
Unc13c	(-1.7-fold)	unc-13_homolog_C_(C_elegans)	RG	Mus.musculus
Wnt11	(-1.7-fold)	wingless-related_MMTV_integration_site_11	RG	Mus.musculus

Table S1_B. Downregulated genes functionally involved in “cell-to-cell signaling” by gene ontology terms at E14.5. Fold change of E14.5 *Gata2*-microarray analysis in brackets.

OFFICIAL_GENE_SYMBOL	GENE_NAME	Related Genes	Species
Brsk2 (-2.3-fold)	BR_serine/threonine_kinase_2	RG	Mus_musculus
Efd1 (-1.5-fold)	EF_hand_domain_containing_1	RG	Mus_musculus
Sox2 (-1.6-fold)	SRY-box_containing_gene_2	RG	Mus_musculus
Ascl1 (-1.6-fold)	achaete-scute_complex_homolog_1 (Drosophila)	RG	Mus_musculus
Celsr3 (-2.2-fold)	cadherin_EGF_LAG_seven-pass_G-type_receptor_3 (flamingo_homolog, Drosophila)	RG	Mus_musculus
Ctnna2 (-3.0-fold)	catenin (cadherin associated protein), alpha 2	RG	Mus_musculus
Chrn2 (-2.0-fold)	cholinergic_receptor_nicotinic_beta_polypeptide_2 (neuronal)	RG	Mus_musculus
Dlx1 (-1.9-fold)	distal-less_homeobox_1	RG	Mus_musculus
Etv1 (-1.7-fold)	ets_variant_gene_1	RG	Mus_musculus
Gas1 (-1.4-fold)	growth_arrest_specific_1	RG	Mus_musculus
Isl2 (-1.4-fold)	insulin_related_protein_2 (Islet 2)	RG	Mus_musculus
Nrn1 (-1.4-fold)	neurtin_1	RG	Mus_musculus
Nefl (-2.2-fold)	neurofilament_light_polypeptide	RG	Mus_musculus
Phox2a (-2.6-fold)	paired-like_homeobox_2a	RG	Mus_musculus
Ptprr (-2.0-fold)	protein_tyrosine_phosphatase_receptor_type_B	RG	Mus_musculus
Ret (-1.8-fold)	ret_proto-oncogene	RG	Mus_musculus
Stmn3 (-2.2-fold)	stathmin-like_3	RG	Mus_musculus
Tgfb2 (-1.7-fold)	transforming_growth_factor_beta_2	RG	Mus_musculus
Tubb3 (-1.8-fold)	tubulin_beta_3; tubulin_beta_3_pseudogene_1	RG	Mus_musculus
Th (-2.5-fold)	tyrosine_hydroxylase	RG	Mus_musculus
Uchl1 (-1.5-fold)	ubiquitin_carboxy-terminal_hydrolase_L1	RG	Mus_musculus

Table S1_C. Downregulated genes functionally involved in neuron differentiation by gene ontology analysis at E14.5. Fold change of E14.5 *Gata2*-microarray analysis in brackets.

OFFICIAL_GENE_SYMBOL	GENE_NAME	Related Genes	Species
Ina (-2.5-fold)	internexin_neuronal_intermediate_filament_protein_alpha	RG	Mus_musculus
Nefl (-2.2-fold)	neurofilament_light_polypeptide	RG	Mus_musculus
Nefm (-3.0-fold)	neurofilament_medium_polypeptide	RG	Mus_musculus
Prph (-2.7-fold)	peripherin	RG	Mus_musculus
Nefh (-2.1-fold)	similar to neurofilament protein; neurofilament_heavy_polypeptide	RG	Mus_musculus

Table S1_D. Downregulated genes functionally involved in “neurofilament” by gene ontology terms at E14.5. Fold change of *Gata2*-microarray analysis in brackets.

OFFICIAL_GENE_SYMBOL	GENE_NAME	Related Genes	Species
Acta1 (-1.8-fold)	actin_alpha_1_skeletal_muscle	RG	Mus_musculus
Csrp3 (-1.6-fold)	cysteine_and_glycine-rich_protein_3	RG	Mus_musculus
Etv1 (-1.7-fold)	ets_variant_gene_1	RG	Mus_musculus
Foxp2 (-1.4-fold)	forkhead_box_P2	RG	Mus_musculus
Hand1 (-3.6-fold)	heart_and_neural_crest_derivatives_expressed_transcript_1	RG	Mus_musculus
Myog (-2.2-fold)	myogenin	RG	Mus_musculus
Myh11 (-2.5-fold)	myosin_heavy_polypeptide_11_smooth_muscle	RG	Mus_musculus
Pitx1 (-2.6-fold)	paired-like_homeodomain_transcription_factor_1	RG	Mus_musculus
Tgfb2 (-1.7-fold)	transforming_growth_factor_beta_2	RG	Mus_musculus
Tnni1 (-1.5-fold)	troponin_I_skeletal_slow_1	RG	Mus_musculus
Tnnt2 (-1.9-fold)	troponin_T2_cardiac	RG	Mus_musculus
Vgll2 (-2.2-fold)	vestigial_like_2_homolog (Drosophila)	RG	Mus_musculus

Table S1_E. Downregulated genes functionally involved in “muscle organ development” by gene ontology terms at E14.5. Fold change of E14.5 *Gata2*-microarray analysis in brackets.

OFFICIAL_GENE_SYMBOL	GENE_NAME	Related Genes	Species
Acta1 (-1.8-fold)	actin, alpha 1, skeletal muscle	RG	Mus musculus
Acta2 (-1.8-fold)	actin, alpha 2, smooth muscle, aorta	RG	Mus musculus
Actg2 (-2.3-fold)	actin, gamma 2, smooth muscle, enteric	RG	Mus musculus
Mybph (-1.9-fold)	myosin binding protein H	RG	Mus musculus
Myh11 (-2.5-fold)	myosin heavy polypeptide 11, smooth muscle	RG	Mus musculus
Myh3 (-2.0-fold)	myosin heavy polypeptide 3, skeletal muscle, embryonic	RG	Mus musculus
Myl1 (-1.8-fold)	myosin light polypeptide 1	RG	Mus musculus
Myl4 (-1.4-fold)	myosin light polypeptide 4	RG	Mus musculus
Tnnc1 (-1.7-fold)	troponin C, cardiac/slow skeletal	RG	Mus musculus
Tnni1 (-1.5-fold)	troponin I, skeletal, slow 1	RG	Mus musculus
Tnnt2 (-1.9-fold)	troponin T2, cardiac	RG	Mus musculus

Table S1_F. Downregulated genes functionally involved in “muscle protein” by gene ontology terms at E14.5. Fold change of E14.5 *Gata2*-microarray analysis in brackets.

OFFICIAL_GENE_SYMBOL	GENE_NAME	Related Genes	Species
9430076C15Rik (-1.6-fold)	RIKEN cDNA 9430076C15 gene; cAMP responsive element binding protein 5	RG	Mus musculus
Sox10 (-1.6-fold)	SRY-box containing gene 10	RG	Mus musculus
Sox2 (-1.6-fold)	SRY-box containing gene 2	RG	Mus musculus
Ascl1 (-1.6-fold)	achaete-scute complex homolog 1 (Drosophila)	RG	Mus musculus
Foxd3 (-1.7-fold)	forkhead box D3	RG	Mus musculus
Hand1 (-3.6-fold)	heart and neural crest derivatives expressed transcript 1	RG	Mus musculus
Hand2 (-2.9-fold)	heart and neural crest derivatives expressed transcript 2	RG	Mus musculus
Inhba (-1.5-fold)	inhibin beta-A	RG	Mus musculus
Myocd (-2.3-fold)	myocardin	RG	Mus musculus
Myog (-2.2-fold)	myogenin	RG	Mus musculus
Vgll2 (-2.2-fold)	vestigial like 2 homolog (Drosophila)	RG	Mus musculus

Table S1_G. Downregulated genes functionally involved in “positive regulation of transcription” by gene ontology terms at E14.5. Fold change of E14.5 *Gata2*-microarray analysis in brackets.

OFFICIAL_GENE_SYMBOL	GENE_NAME	Related Genes	Species
Wnk1 (1.6-fold)	WNK lysine deficient protein kinase 1	RG	Mus musculus
Agtr1b (1.6-fold)	angiotensin II receptor, type 1b	RG	Mus musculus
Agt (1.5-fold)	angiotensinogen (serpin peptidase inhibitor, clade A, member 8)	RG	Mus musculus
Avpr1a (3.0-fold)	arginine vasopressin receptor 1A	RG	Mus musculus
Npr3 (1.9-fold)	natriuretic peptide receptor 3	RG	Mus musculus
Nrg1 (1.5-fold)	neuregulin 1	RG	Mus musculus
Kcnma1 (2.0-fold)	potassium large conductance calcium-activated channel, subfamily M, alpha member 1	RG	Mus musculus

Table S2_A. Upregulated genes functionally involved in “blood circulation and blood pressure” by gene ontology terms at E14.5. Fold change of E14.5 *Gata2*-microarray analysis in brackets.

OFFICIAL_GENE_SYMBOL	GENE_NAME	Related Genes	Species
Nkx3-1 (2.2-fold)	NK-3 transcription factor, locus 1 (Drosophila)	RG	Mus musculus
Agtr1b (1.6-fold)	angiotensin II receptor, type 1b	RG	Mus musculus
Agt (1.5-fold)	angiotensinogen (serpin peptidase inhibitor, clade A, member 8)	RG	Mus musculus
Ahr (1.9-fold)	aryl-hydrocarbon receptor	RG	Mus musculus
Grem1 (2.3-fold)	gremlin 1	RG	Mus musculus
Hoxc11 (1.9-fold)	homeo box C11	RG	Mus musculus
Hoxd11 (1.7-fold)	homeo box D11	RG	Mus musculus
Sall1 (1.5-fold)	sall-like 1 (Drosophila)	RG	Mus musculus

Table S2_B. Upregulated genes functionally involved in “UGS development” by gene ontology terms at E14.5. Fold change of E14.5 *Gata2*-microarray analysis in brackets.

OFFICIAL_GENE_SYMBOL	GENE_NAME	Related Genes	Species
Alix1 (2.5-fold)	ALX homeobox 1	RG	Mus musculus
Elf5 (1.4-fold)	E74-like factor 5	RG	Mus musculus
Nkx3-1 (2.2-fold)	NK-3 transcription factor, locus 1 (Drosophila)	RG	Mus musculus
Pou3f1 (1.6-fold)	POU domain, class 3, transcription factor 1	RG	Mus musculus
Aldh1a3 (1.9-fold)	aldehyde dehydrogenase family 1, subfamily A3	RG	Mus musculus
Agt (1.5-fold)	angiotensinogen (serpin peptidase inhibitor, clade A, member 8)	RG	Mus musculus
Grem1 (2.3-fold)	gremlin 1	RG	Mus musculus
Hoxd11 (1.7-fold)	homeo box D11	RG	Mus musculus
Sema3c (1.6-fold)	sema domain, immunoglobulin domain (Ig), short basic domain, secreted, (semaphorin) 3C	RG	Mus musculus

Table S2_C. Upregulated genes functionally involved in “epithelial development” by gene ontology terms at E14.5. Fold change of E14.5 *Gata2*-microarray analysis in brackets.

OFFICIAL_GENE_SYMBOL	GENE_NAME	Related Genes	Species
Foxl1 (1.6-fold)	forkhead box L1	RG	Mus musculus
Grem1 (2.3-fold)	gremlin 1	RG	Mus musculus
Hoxc11 (1.9-fold)	homeo box C11	RG	Mus musculus
Hoxd11 (1.7-fold)	homeo box D11	RG	Mus musculus
Nrg1 (1.5-fold)	neuregulin 1	RG	Mus musculus
Nlgn1 (1.7-fold)	neuroligin 1	RG	Mus musculus
Ntrf3 (1.4-fold)	neurotrophin 3	RG	Mus musculus
Kcnma1 (2.0-fold)	potassium large conductance calcium-activated channel, subfamily M, alpha member 1	RG	Mus musculus
Sall1 (1.5-fold)	sall-like 1 (Drosophila)	RG	Mus musculus
Slc22a3 (1.7-fold)	solute carrier family 22 (organic cation transporter), member 3	RG	Mus musculus
Tmod2 (1.5-fold)	tropomodulin 2	RG	Mus musculus

Table S2_D. Upregulated genes functionally involved in “cell-to-cell signaling” by gene ontology terms at E14.5. Fold change of E14.5 *Gata2*-microarray analysis in brackets.

OFFICIAL_GENE_SYMBOL	GENE_NAME	Related Genes	Species
Fat3 (1.4-fold)	FAT tumor suppressor homolog 3 (Drosophila)	RG	Mus musculus
Neil1 (1.9-fold)	NEI-like 1 (chicken)	RG	Mus musculus
Agt (1.5-fold)	angiotensinogen (serpin peptidase inhibitor, clade A, member 8)	RG	Mus musculus
Cadm3 (1.6-fold)	cell adhesion molecule 3	RG	Mus musculus
Cldn1 (2.2-fold)	claudin 1	RG	Mus musculus
Cldn4 (1.6-fold)	claudin 4	RG	Mus musculus
Cntn1 (2.1-fold)	contactin 1	RG	Mus musculus
Lamc3 (1.8-fold)	laminin gamma 3	RG	Mus musculus
Mfap4 (1.6-fold)	microfibrillar-associated protein 4	RG	Mus musculus
Megf10 (2.0-fold)	multiple EGF-like-domains 10	RG	Mus musculus
Nlgn1 (1.7-fold)	neuroligin 1	RG	Mus musculus
Rhoa (1.6-fold)	ras homolog gene family, member A; similar to alysia ras-related homolog A2; predicted gene 12844	RG	Mus musculus
Ibsp (1.5-fold)	similar to Integrin binding sialoprotein; Integrin binding sialoprotein	RG	Mus musculus

Table S2_E. Upregulated genes functionally involved in “cell adhesion” by gene ontology terms at E14.5. Fold change of E14.5 *Gata2*-microarray analysis in brackets after gene symbol.

OFFICIAL_GENE_SYMBOL	GENE_NAME	Related Genes	Species
Wif1 (1.8-fold)	Wnt inhibitory factor 1	RG	Mus musculus
Fzd10 (2.3-fold)	frizzled homolog 10 (Drosophila)	RG	Mus musculus
Mapk8 (2.3-fold)	mitogen-activated protein kinase 8	RG	Mus musculus
Nkd1 (1.4-fold)	naked cuticle 1 homolog (Drosophila); similar to naked cuticle 1 homolog	RG	Mus musculus
Plicb1 (1.8-fold)	phospholipase C, beta 1	RG	Mus musculus
Rhoa (1.6-fold)	ras homolog gene family, member A; similar to alysia ras-related homolog A2; predicted gene 12844	RG	Mus musculus

Table S2_F. Upregulated genes functionally involved in “Wnt signaling pathway” by gene ontology terms at E14.5. Fold change of E14.5 *Gata2*-microarray analysis in brackets after gene symbol.

OFFICIAL_GENE_SYMBOL	GENE_NAME	Related Genes	Species
Grem1 (2.3-fold)	gremlin 1	RG	Mus musculus
Sostdc1 (4.4-fold)	sclerostin domain containing 1	RG	Mus musculus
Vwc2 (1.8-fold)	von Willebrand factor C domain containing 2	RG	Mus musculus

Table S2_G. Upregulated genes functionally involved in “Bmp antagonism” by gene ontology terms at E14.5. Fold change of E14.5 *Gata2*-microarray analysis in brackets after gene symbol.

OFFICIAL_GENE_SYMBOL	GENE_NAME	Related Genes	Species
Alix1 (2.5-fold)	ALX homeobox 1	RG	Mus musculus
Nkx3-1 (2.2-fold)	NK-3 transcription factor, locus 1 (Drosophila)	RG	Mus musculus
Pou3f1 (1.6-fold)	POU domain, class 3, transcription factor 1	RG	Mus musculus
Hoxc11 (1.9-fold)	homeo box C11	RG	Mus musculus
Hoxd11 (1.7-fold)	homeo box D11	RG	Mus musculus

Table S2_H. Upregulated genes functionally involved in “Homeobox genes” by gene ontology terms at E14.5. Fold change of E14.5 *Gata2*-microarray analysis in brackets after gene symbol.

OFFICIAL_GENE_SYMBOL	GENE_NAME	Related Genes	Species
Acta1 (-2.5-fold)	actin, alpha 1, skeletal muscle	RG	Mus.musculus
Acta2 (-3.1-fold)	actin, alpha 2, smooth muscle, aorta	RG	Mus.musculus
Alf1 (-1.6-fold)	allograft inflammatory factor 1	RG	Mus.musculus
Ctnna2 (-4.3-fold)	catenin (cadherin associated protein), alpha 2	RG	Mus.musculus
Myom1 (-1.9-fold)	myomesin 1	RG	Mus.musculus
Myh11 (-2.3-fold)	myosin, heavy polypeptide 11, smooth muscle	RG	Mus.musculus
Myl1 (-1.6-fold)	myosin, light polypeptide 1	RG	Mus.musculus
Myl4 (-1.8-fold)	myosin, light polypeptide 4	RG	Mus.musculus
Myl7 (-3.1-fold)	myosin, light polypeptide 7, regulatory	RG	Mus.musculus
Tnnt2 (-7.2-fold)	troponin T2, cardiac	RG	Mus.musculus

Table S3_A. Downregulated genes functionally involved in “actin cytoskeleton” by gene ontology terms at E15.5. Fold change of E15.5 *Gata2*-microarray analysis in brackets after gene symbol.

OFFICIAL_GENE_SYMBOL	GENE_NAME	Related Genes	Species
Acta1 (-2.5-fold)	actin, alpha 1, skeletal muscle	RG	Mus.musculus
Acta2 (-3.1-fold)	actin, alpha 2, smooth muscle, aorta	RG	Mus.musculus
Actc1 (-2.4-fold)	actin, alpha, cardiac muscle 1; similar to alpha-actin (AA 27-375)	RG	Mus.musculus
Actg2 (-3.4-fold)	actin, gamma 2, smooth muscle, enteric	RG	Mus.musculus
Myom1 (-1.9-fold)	myomesin 1	RG	Mus.musculus
Myh11 (-2.3-fold)	myosin, heavy polypeptide 11, smooth muscle	RG	Mus.musculus
Myl1 (-1.6-fold)	myosin, light polypeptide 1	RG	Mus.musculus
Myl4 (-1.8-fold)	myosin, light polypeptide 4	RG	Mus.musculus
Myl7 (-3.1-fold)	myosin, light polypeptide 7, regulatory	RG	Mus.musculus
Tagln (-2.5-fold)	transgelin	RG	Mus.musculus
Tnnt2 (-7.2-fold)	troponin T2, cardiac	RG	Mus.musculus

Table S3_B. Downregulated genes functionally involved in “muscle protein” by gene ontology terms at E15.5. Fold change of E15.5 *Gata2*-microarray analysis in brackets after gene symbol.

OFFICIAL_GENE_SYMBOL	GENE_NAME	Related Genes	Species
Acta1 (-2.5-fold)	actin, alpha 1, skeletal muscle	RG	Mus.musculus
Actc1 (-2.4-fold)	actin, alpha, cardiac muscle 1; similar to alpha-actin (AA 27-375)	RG	Mus.musculus
Myh11 (-2.3-fold)	myosin, heavy polypeptide 11, smooth muscle	RG	Mus.musculus
Pitx1 (-3.6-fold)	paired-like homeodomain transcription factor 1	RG	Mus.musculus
Tmod1 (-2.2-fold)	tropomodulin 1	RG	Mus.musculus
Tnnt2 (-7.2-fold)	troponin T2, cardiac	RG	Mus.musculus

Table S3_C. Downregulated genes functionally involved in “muscle cell development” by gene ontology terms at E15.5. Fold change of E15.5 *Gata2*-microarray analysis in brackets after gene symbol.

OFFICIAL_GENE_SYMBOL	GENE_NAME	Related Genes	Species
Egfr (-1.4-fold)	epidermal growth factor receptor	RG	Mus.musculus
Fgf7 (-1.6-fold)	fibroblast growth factor 7	RG	Mus.musculus
Fgf9 (-1.4-fold)	fibroblast growth factor 9	RG	Mus.musculus
Foxp2 (-1.4-fold)	forkhead box P2	RG	Mus.musculus

Table S3_D. Downregulated genes functionally involved in “epithelial proliferation” by gene ontology terms at E15.5. Fold change of E15.5 *Gata2*-microarray analysis in brackets after gene symbol.

OFFICIAL_GENE_SYMBOL	GENE NAME	Related Genes	Species
Cav1 (-1.5-fold)	caveolin 1, caveolae protein	RG	<i>Mus musculus</i>
Irak3 (-1.6-fold)	interleukin-1 receptor-associated kinase 3	RG	<i>Mus musculus</i>
Lpar3 (-2.7-fold)	lysophosphatidic acid receptor 3	RG	<i>Mus musculus</i>
Pde6h (-1.4-fold)	phosphodiesterase 6H, cGMP-specific, cone, gamma	RG	<i>Mus musculus</i>
Tnxb (-1.6-fold)	tenascin XB	RG	<i>Mus musculus</i>
Trib3 (-1.5-fold)	tribbles homolog 3 (Drosophila)	RG	<i>Mus musculus</i>

Table S3_E. Downregulated genes functionally involved in “regulation of MAPK activity” by gene ontology terms at E15.5. Fold change of E15.5 *Gata2*-microarray analysis in brackets after gene symbol.

OFFICIAL_GENE_SYMBOL	GENE NAME	Related Genes	Species
Clec3b (-1.5-fold)	C-type lectin domain family 3, member b	RG	<i>Mus musculus</i>
Adam28 (-1.6-fold)	a disintegrin and metallopeptidase domain 28	RG	<i>Mus musculus</i>
Col4a3 (-1.8-fold)	collagen, type IV, alpha 3	RG	<i>Mus musculus</i>
Col9a1 (-2.2-fold)	collagen, type IX, alpha 1	RG	<i>Mus musculus</i>
Dpt (-2.1-fold)	dermatopontin	RG	<i>Mus musculus</i>
Epyc (-4.8-fold)	epiphycan	RG	<i>Mus musculus</i>
Optc (-2.1-fold)	opticin	RG	<i>Mus musculus</i>
Papln (-1.6-fold)	papilin, proteoglycan-like sulfated glycoprotein	RG	<i>Mus musculus</i>
Prss12 (-1.5-fold)	protease, serine, 12 neurotrypsin (motopsin)	RG	<i>Mus musculus</i>
Prss34 (-1.8-fold)	protease, serine, 34	RG	<i>Mus musculus</i>
Tnxb (-1.6-fold)	tenascin XB	RG	<i>Mus musculus</i>
Vtn (-1.4-fold)	vitronectin	RG	<i>Mus musculus</i>
Zp3 (-1.5-fold)	zona pellucida glycoprotein 3	RG	<i>Mus musculus</i>

Table S3_F. Downregulated genes functionally involved in “ECM” by gene ontology terms at E15.5. Fold change of E15.5 *Gata2*-microarray analysis in brackets after gene symbol.

OFFICIAL_GENE_SYMBOL	GENE NAME	Related Genes	Species
Cartpt (-1.8-fold)	CART prepropeptide	RG	<i>Mus musculus</i>
Gch1 (-1.4-fold)	GTP cyclohydrolase 1	RG	<i>Mus musculus</i>
Acta2 (-3.1-fold)	actin, alpha 2, smooth muscle, aorta	RG	<i>Mus musculus</i>
Calcb (-2.4-fold)	calcitonin-related polypeptide, beta	RG	<i>Mus musculus</i>
Calca (-2.2-fold)	calcitonin/calcitonin-related polypeptide, alpha	RG	<i>Mus musculus</i>
Cav1 (-1.5-fold)	caveolin 1, caveolae protein	RG	<i>Mus musculus</i>
F5 (-2.0-fold)	coagulation factor V; similar to Murine coagulation factor V	RG	<i>Mus musculus</i>
Ednrb (-1.4-fold)	endothelin receptor type B	RG	<i>Mus musculus</i>
Nppc (-2.2-fold)	natriuretic peptide precursor type C	RG	<i>Mus musculus</i>

Table S3_G. Downregulated genes functionally involved in “blood circulation” by gene ontology terms at E15.5. Fold change of E15.5 *Gata2*-microarray analysis in brackets after gene symbol.

OFFICIAL_GENE_SYMBOL	GENE_NAME	Related Genes	Species
Calca (-2.2-fold)	calcitonin/calcitonin-related polypeptide, alpha	RG	Mus musculus
Ctnna2 (-4.3-fold)	catenin (cadherin associated protein), alpha 2	RG	Mus musculus
Nefl (-1.7-fold)	neurofilament, light polypeptide	RG	Mus musculus
Prph (-1.7-fold)	peripherin	RG	Mus musculus
Prss12 (-1.5-fold)	protease, serine, 12 neurotrypsin (motopsin)	RG	Mus musculus
Stmn2 (-1.6-fold)	stathmin-like 2	RG	Mus musculus
Tac1 (-3.8-fold)	tachykinin 1	RG	Mus musculus
Th (-1.6-fold)	tyrosine hydroxylase	RG	Mus musculus

Table S3_H. Downregulated genes functionally involved in “axon” by gene ontology terms at E15.5. Fold change of E15.5 *Gata2*-microarray analysis in brackets after gene symbol.

OFFICIAL_GENE_SYMBOL	GENE_NAME	Related Genes	Species
Nkx3-1 (1.8-fold)	NK-3 transcription factor, locus 1 (Drosophila)	RG	Mus musculus
Agtr1a (1.5-fold)	angiotensin II receptor, type 1a	RG	Mus musculus
Ahr (2.7-fold)	aryl-hydrocarbon receptor	RG	Mus musculus
Gdnf (2.2-fold)	glial cell line derived neurotrophic factor	RG	Mus musculus
Hoxa11 (1.5-fold)	homeo box A11	RG	Mus musculus
Hoxd13 (1.7-fold)	homeo box D13	RG	Mus musculus
Nog (1.7-fold)	noggin	RG	Mus musculus
Rbp4 (1.6-fold)	retinol binding protein 4, plasma	RG	Mus musculus
Sall1 (1.9-fold)	sall-like 1 (Drosophila)	RG	Mus musculus
Wnt5a (1.6-fold)	wingless-related MMTV integration site 5A	RG	Mus musculus

Table S4_A. Upregulated genes functionally involved in “UGS development” by gene ontology terms at E15.5. Fold change of E15.5 *Gata2*-microarray analysis in brackets after gene symbol.

OFFICIAL_GENE_SYMBOL	GENE_NAME	Related Genes	Species
Aix1 (3.4-fold)	ALX homeobox 1	RG	Mus musculus
Gdnf (2.2-fold)	glial cell line derived neurotrophic factor	RG	Mus musculus
Lef1 (2.0-fold)	lymphoid enhancer binding factor 1	RG	Mus musculus
Nrp2 (1.4-fold)	neuropilin 2	RG	Mus musculus
Nog (1.7-fold)	noggin	RG	Mus musculus

Table S4_B. Upregulated genes functionally involved in “mesenchymal cell differentiation” by gene ontology terms at E15.5. Fold change of E15.5 *Gata2*-microarray analysis in brackets after gene symbol.

OFFICIAL_GENE_SYMBOL	GENE_NAME	Related Genes	Species
Aix1 (3.4-fold)	ALX homeobox 1	RG	Mus musculus
Nkx3-1 (1.8-fold)	NK-3 transcription factor, locus 1 (Drosophila)	RG	Mus musculus
Gdnf (2.2-fold)	glial cell line derived neurotrophic factor	RG	Mus musculus
Hoxa11 (1.5-fold)	homeo box A11	RG	Mus musculus
Hoxd13 (1.7-fold)	homeo box D13	RG	Mus musculus
Lama1 (1.4-fold)	laminin, alpha 1	RG	Mus musculus
Nog (1.7-fold)	noggin	RG	Mus musculus
Ptch1 (2.0-fold)	patched homolog 1	RG	Mus musculus
Pml (1.4-fold)	promyelocytic leukemia	RG	Mus musculus
Wnt5a (1.6-fold)	wingless-related MMTV integration site 5A	RG	Mus musculus

Table S4_C. Upregulated genes functionally involved in “morphogenesis of an epithelium” by gene ontology terms at E15.5. Fold change of E15.5 *Gata2*-microarray analysis in brackets after gene symbol.

OFFICIAL_GENE_SYMBOL	GENE NAME	Related Genes	Species
Crtac1 (1.7-fold)	cartilage_acidic_protein_1	RG	Mus.musculus
Col4a1 (1.5-fold)	collagen_type_IV_alpha_1	RG	Mus.musculus
Col4a2 (1.6-fold)	collagen_type_IV_alpha_2	RG	Mus.musculus
Dmp1 (1.7-fold)	dentin_matrix_protein_1	RG	Mus.musculus
Ecm1 (2.4-fold)	extracellular_matrix_protein_1	RG	Mus.musculus
Lamc3 (2.6-fold)	laminin_gamma_3	RG	Mus.musculus
Lama1 (1.4-fold)	laminin_alpha_1	RG	Mus.musculus
Ntn3 (1.6-fold)	netrin_3	RG	Mus.musculus
Thsd4 (1.4-fold)	thrombospondin_type_I_domain_containing_4	RG	Mus.musculus
Vcan (1.9-fold)	versican	RG	Mus.musculus
Vwc2 (1.9-fold)	von_Willebrand_factor_C_domain_containing_2	RG	Mus.musculus
Wnt5a (1.6-fold)	wingless-related_MMTV_integration_site_5A	RG	Mus.musculus

Table S4_D. Upregulated genes functionally involved in “ECM” by gene ontology terms at E15.5. Fold change of E15.5 *Gata2*-microarray analysis in brackets after gene symbol.

OFFICIAL_GENE_SYMBOL	GENE NAME	Related Genes	Species
Nog (1.7-fold)	noggin	RG	Mus.musculus
Sostdc1 (8.3-fold)	sclerostin_domain_containing_1	RG	Mus.musculus
Vwc2 (1.9-fold)	von_Willebrand_factor_C_domain_containing_2	RG	Mus.musculus

Table S4_E. Upregulated genes functionally involved in “negative regulation of Bmp signalling” by gene ontology terms at E15.5. Fold change of E15.5 *Gata2*-microarray analysis in brackets after gene symbol.

OFFICIAL_GENE_SYMBOL	GENE NAME	Related Genes	Species
Ndp (1.5-fold)	Norrie_disease_(pseudoglioma)_human	RG	Mus.musculus
Rspo1 (3.3-fold)	R-spondin_homolog_(Xenopus_jevis)	RG	Mus.musculus
Wif1 (2.4-fold)	Wnt_inhibitory_factor_1	RG	Mus.musculus
Fzd1 (1.6-fold)	frizzled_homolog_1_(Drosophila)	RG	Mus.musculus
Fzd10 (3.6-fold)	frizzled_homolog_10_(Drosophila)	RG	Mus.musculus
Lef1 (2.0-fold)	lymphoid_enhancer_binding_factor_1	RG	Mus.musculus
Nkd1 (1.6-fold)	naked_cuticle_1_homolog_(Drosophila);_similar_to_naked_cuticle_1_homolog	RG	Mus.musculus
Sostdc1 (8.3-fold)	sclerostin_domain_containing_1	RG	Mus.musculus
Sfrp2 (1.5-fold)	secreted_frizzled-related_protein_2	RG	Mus.musculus
Sfrp5 (2.1-fold)	secreted_frizzled-related_sequence_protein_5	RG	Mus.musculus
Wnt5a (1.6-fold)	wingless-related_MMTV_integration_site_5A	RG	Mus.musculus

Table S4_F. Upregulated genes functionally involved in “Wnt signalling” by gene ontology terms at E15.5. Fold change of E15.5 *Gata2*-microarray analysis in brackets after gene symbol.

OFFICIAL_GENE_SYMBOL	GENE NAME	Related Genes	Species
Alx1 (3.4-fold)	ALX homeobox 1	RG	Mus musculus
Irx4 (1.5-fold)	Iroquois related homeobox 4 (Drosophila)	RG	Mus musculus
Smad9 (1.4-fold)	MAD homolog 9 (Drosophila)	RG	Mus musculus
Pou3f1 (2.7-fold)	POU domain class 3 transcription factor 1	RG	Mus musculus
Ahr (2.7-fold)	aryl-hydrocarbon receptor	RG	Mus musculus
Dach1 (1.9-fold)	dachshund 1 (Drosophila)	RG	Mus musculus
Hoxa10 (1.4-fold)	homeo box A10	RG	Mus musculus
Hoxa11 (1.5-fold)	homeo box A11	RG	Mus musculus
Hoxd12 (1.7-fold)	homeo box D12	RG	Mus musculus
Lef1 (2.0-fold)	lymphoid enhancer binding factor 1	RG	Mus musculus

Table S4_G. Upregulated genes functionally involved in “transcription factor complex” by gene ontology terms at E15.5. Fold change of E15.5 *Gata2*-microarray analysis in brackets after gene symbol.

OFFICIAL_GENE_SYMBOL	GENE NAME	Related Genes	Species
Alx1 (3.4-fold)	ALX homeobox 1	RG	Mus musculus
Irx4 (1.5-fold)	Iroquois related homeobox 4 (Drosophila)	RG	Mus musculus
Nkx3-1 (1.8-fold)	NK-3 transcription factor, locus 1 (Drosophila)	RG	Mus musculus
Pou3f1 (2.7-fold)	POU domain class 3 transcription factor 1	RG	Mus musculus
Hoxa10 (1.4-fold)	homeo box A10	RG	Mus musculus
Hoxa11 (1.5-fold)	homeo box A11	RG	Mus musculus
Hoxd12 (1.7-fold)	homeo box D12	RG	Mus musculus
Hoxd13 (1.7-fold)	homeo box D13	RG	Mus musculus
Msx1 (1.7-fold)	homeobox, msh-like 1	RG	Mus musculus
Tshz3 (1.6-fold)	teashirt zinc finger family member 3	RG	Mus musculus

Table S4_H. Upregulated genes functionally involved in “homeobox conserved sites” by gene ontology terms at E15.5. Fold change of E15.5 *Gata2*-microarray analysis in brackets after gene symbol.

OFFICIAL_GENE_SYMBOL	GENE NAME	Related Genes	Species
Agtr1a (1.5-fold)	angiotensin II receptor type 1a	RG	Mus musculus
Avpr1a (4.9-fold)	arginine vasopressin receptor 1A	RG	Mus musculus
Hsd11b2 (1.6-fold)	hydroxysteroid 11-beta dehydrogenase 2	RG	Mus musculus
Npr3 (2.9-fold)	natriuretic peptide receptor 3	RG	Mus musculus
Nrg1 (2.0-fold)	neuregulin 1	RG	Mus musculus
Kcnma1 (2.8-fold)	potassium large conductance calcium-activated channel, subfamily M, alpha member 1	RG	Mus musculus

Table S4_I. Upregulated genes functionally involved in “blood circulation” by gene ontology terms at E15.5. Fold change of E15.5 *Gata2*-microarray analysis in brackets after gene symbol.

Gene Symbol	Gene Name	*	Expressed in ureter (eurexpress.org)	e145gata2::max_int	>1,3	e145gata2::relevant_ratio1	>1,3	e145gata2::relevant_ratio2	>1,3	e145gata2::av_ratio	<-1,3	E125cyclopamine::max_int	<-1,3	E125cyclopamine::relevant_ratio1	<-1,3	E125cyclopamine::relevant_ratio2	<-1,3	E125cyclopamine::av_ratio
2700046A07Rik	RIKEN cDNA 2700046A07 gene	other		40	1,4	1,4	1,4	1,4	1,4	1,4	-2,3	53	-2,3	-1,9	-1,9	-2,1	-2,1	
4833424O15Rik	lipid phosphate phosphatase-related protein type 5	other		196	1,5	2	1,7	2	1,7	67	-2,6	67	-2,6	-4,5	-4,5	-3,5	-3,5	
Avpr1a	arginine vasopressin receptor 1A	G-protein coupled receptor	yes	852	2,7	3,3	3	3,3	3	1224	-2,7	1224	-2,7	-2,3	-2,3	-2,5	-2,5	
Cd83	CD83 molecule	transmembrane receptor	no	2685	1,9	2,3	2,1	2,3	2,1	576	-2,2	576	-2,2	-1,7	-1,7	-1,9	-1,9	
Cyb52	cytochrome b5 reductase 2	enzyme	not available	24	1,4	1,6	1,5	1,6	1,5	63	-1,6	63	-1,6	-1,6	-1,6	-1,6	-1,6	
D630033O11Rik	RIKEN cDNA D630033O11 gene	other		831	1,5	1,5	1,5	1,5	1,5	114	-1,6	114	-1,6	-1,4	-1,4	-1,5	-1,5	
Efcab6	EF-hand calcium binding domain 6	other	not available	37	1,4	1,4	1,4	1,4	1,4	67	-2,9	67	-2,9	-1,9	-1,9	-2,4	-2,4	
Enpep	glutamyl aminopeptidase (aminopeptidase A)	peptidase	yes	4312	1,8	1,8	1,8	1,8	1,8	2583	-2,1	2583	-2,1	-2	-2	-2	-2	
Fam179a	family with sequence similarity 179, member A	other	not available	47	1,7	1,6	1,7	1,6	1,7	33	-1,6	33	-1,6	-2,2	-2,2	-1,9	-1,9	
Foxl1	forkhead box L1	transcription regulator	yes	3859	1,5	1,7	1,6	1,7	1,6	3306	-3,9	3306	-3,9	-4	-4	-3,9	-3,9	
Ibsp	integrin-binding sialoprotein	other	no	25	1,5	1,5	1,5	1,5	1,5	50	-3,3	50	-3,3	-3	-3	-3,1	-3,1	
Kcnd3	potassium voltage-gated channel, Shal-related subfamily, member 3	ion channel	no	2866	1,9	2,2	2	2,2	2	621	-2,2	621	-2,2	-2,2	-2,2	-2,2	-2,2	
Ndp	Norris disease (pseudoglioma)	growth factor	no	2029	1,4	1,6	1,5	1,6	1,5	1218	-2,6	1218	-2,6	-2,3	-2,3	-2,4	-2,4	
Nell1	NEL-like 1 (chicken)	growth factor	not available	2038	1,9	1,9	1,9	1,9	1,9	895	-1,8	895	-1,8	-1,5	-1,5	-1,7	-1,7	
Sostdc1	sclerostin domain containing 1	other	weak	1618	4,5	4,2	4,4	4,2	4,4	156	-2,9	156	-2,9	-2,2	-2,2	-2,6	-2,6	
Vstm4	V-set and transmembrane domain containing 4	other	not available	155	1,4	1,4	1,4	1,4	1,4	50	-1,5	50	-1,5	-1,6	-1,6	-1,5	-1,5	
Vwv2	von Willebrand factor C domain containing 2	other	not available	208	1,7	1,8	1,8	1,8	1,8	30	-1,9	30	-1,9	-1,9	-1,9	-1,9	-1,9	
Wf1	WNT inhibitory factor 1	other	yes (weak)	430	2,2	1,5	1,8	1,5	1,8	1026	-2,2	1026	-2,2	-2	-2	-2,1	-2,1	

Table S5. Commonly deregulated genes of E14.5 Gata2 and Cyclopamine microarray

Gene Symbol	Gene Name	Type	e155gata2:: max_int	>1,3 e155gata2::r elevant ratio1	>1,3 e155gata2::r elevant ratio2	>1,3 e155gata2:: av_ratio	E125cyclop amine::max _int	<-1,3 E125cyclop amine::relev ant ratio1	<-1,3 E125cyclop amine::relev ant ratio2	<-1,3 E125cyclop amine::av_f ratio
2700046A07Rik	RIKEN cDNA 2700046A07 gene	other	31	2	1,8	1,9	53	-2,3	-1,9	-2,1
4833424O15Rik	lipid phosphate phosphatase-related protein type 5	other	168	1,8	1,8	1,8	67	-2,6	-4,5	-3,5
Atad2	ATPase family, AAA domain containing 2	other	114	1,6	1,4	1,5	101	-1,9	-1,6	-1,7
Avpr1a	arginine vasopressin receptor 1A	G-protein coupled receptor	1139	4,2	5,6	4,9	1224	-2,7	-2,3	-2,5
Bdkrb2	bradykinin receptor B2	G-protein coupled receptor	39	2,2	2,2	2,2	63	-2,4	-2,3	-2,4
Cd83	CD83 molecule	transmembrane receptor	2363	2,6	2,8	2,7	576	-2,2	-1,7	-1,9
Cdh22	cadherin 22, type 2	other	132	1,5	1,6	1,5	97	-1,4	-1,4	-1,4
Cyb5r2	cytochrome b5 reductase 2	enzyme	27	1,5	1,8	1,7	63	-1,6	-1,6	-1,6
Ddit4l	DNA-damage-inducible transcript 4-like	other	630	1,5	1,7	1,6	402	-3,7	-2,6	-3,2
Enpep	glutamyl aminopeptidase (aminopeptidase A)	peptidase	3115	2,9	2,3	2,6	2583	-2,1	-2	-2
ENSMUST0000048109	RIKEN cDNA 2700046A07 gene	other	342	1,5	1,5	1,5	132	-2	-2,1	-2
ENSMUST0000051253	netrin G1	other	959	1,4	2,7	2,1	1748	-2,8	-3	-2,9
Fam150b	family with sequence similarity 150, member B	other	164	2	2,3	2,1	241	-1,5	-1,4	-1,5
Fgl1	fibrinogen-like 1	other	121	1,9	1,9	1,9	46	-1,8	-1,7	-1,7
Foxl1	forkhead box L1	transcription regulator	2931	2	2,5	2,2	3306	-3,9	-4	-3,9
Ibsp	integrin-binding sialoprotein	other	77	1,5	2,1	1,8	50	-3,3	-3	-3,1
Il23a	interleukin 23, alpha subunit p19	cytokine	24	1,5	1,6	1,5	29	-1,8	-1,6	-1,7
Itga4	integrin, alpha 4 (antigen CD49D, alpha 4 subunit of VLA-4 receptor)	transmembrane receptor	2375	2,1	2	2	1658	-1,6	-1,5	-1,5
Kcnd3	potassium voltage-gated channel, Shal-related subfamily, member 3	ion channel	1666	2,3	2,8	2,6	621	-2,2	-2,2	-2,2
Kirrel3	kin of IRRE like 3 (Drosophila)	other	144	1,9	2,1	2	294	-2,1	-1,9	-2
Ndp	Norrie disease (pseudoglioma)	growth factor	1211	1,4	1,6	1,5	1218	-2,6	-2,3	-2,4
Nell1	NEL-like 1 (chicken)	growth factor	1232	1,8	1,9	1,9	895	-1,8	-1,5	-1,7
Ntn3	netrin 3	other	2496	1,5	1,8	1,6	2710	-1,4	-1,5	-1,5
Pappa	pregnancy-associated plasma protein A, pappalysin 1	peptidase	1559	2,9	1,8	2,3	1274	-1,7	-1,5	-1,6
Ptch1	patched 1	transmembrane receptor	100	1,5	2,4	2	1238	-3,6	-2,8	-3,2
Ptch2	patched 2	transmembrane receptor	2830	1,4	2	1,7	12132	-3,6	-3,7	-3,6
Rbp4	retinol binding protein 4, plasma	transporter	3059	1,5	1,7	1,6	197	-1,7	-1,4	-1,6
Sostdc1	sclerostin domain containing 1	other	3931	6,8	9,7	8,3	156	-2,9	-2,2	-2,6
Sybu	syntabulin (syntaxin-interacting)	other	161	1,9	2,3	2,1	33	-1,4	-1,4	-1,4
Thsd4	thrombospondin, type I, domain containing 4	other	2964	1,4	1,5	1,4	2477	-1,5	-1,6	-1,5
Tmem90b	synapse differentiation inducing 1	other	843	1,6	1,9	1,7	657	-1,4	-1,7	-1,6
Trim63	tripartite motif containing 63, E3 ubiquitin protein ligase	enzyme	76	2,8	2,2	2,5	55	-2,8	-1,8	-2,3
Vwc2	von Willebrand factor C domain containing 2	other	212	1,9	2	1,9	30	-1,9	-1,9	-1,9
Wif1	WNT inhibitory factor 1	other	237	2	2,8	2,4	1026	-2,2	-2	-2,1

Table S6. Commonly deregulated genes of E15.5 Gata2 and Cyclopamine microarray

Gene Symbol	Gene Name	Type	e145gata2:: max_int	e145gata2::r elevant ratio1	e145gata2::r elevant ratio2	e145gata2:: av_ratio
Wnt1	wingless-type MMTV integration site family, member 1	cytokine	259	-1,2	-1	-1,1
Wnt10a	wingless-type MMTV integration site family, member 10A	other	113	1,4	1,2	1,3
Wnt10b	wingless-type MMTV integration site family, member 10B	other	15	1	1	1
Wnt11	wingless-type MMTV integration site family, member 11	other	1720	-1,5	-1,6	-1,5
Wnt16	wingless-type MMTV integration site family, member 16	other	26	1	-1,2	-0,1
Wnt2	wingless-type MMTV integration site family member 2	cytokine	15	1	1	1
Wnt2b	wingless-type MMTV integration site family, member 2B	other	15	1	1	1
Wnt3	wingless-type MMTV integration site family, member 3	other	15	1	1	1
Wnt3a	wingless-type MMTV integration site family, member 3A	cytokine	15	1	1	1
Wnt4	wingless-type MMTV integration site family, member 4	cytokine	4194	1,3	1,2	1,2
Wnt5a	wingless-type MMTV integration site family, member 5A	cytokine	418	-1,2	1,2	0
Wnt5b	wingless-type MMTV integration site family, member 5B	other	4650	-1,4	-1,2	-1,3
Wnt6	wingless-type MMTV integration site family, member 6	other	206	1,2	1,1	1,1
Wnt7a	wingless-type MMTV integration site family, member 7A	cytokine	15	1	1	1
Wnt7b	wingless-type MMTV integration site family, member 7B	other	759	1,2	-1	0,1
Wnt8a	wingless-type MMTV integration site family, member 8A	other	15	1	1	1
Wnt8b	wingless-type MMTV integration site family, member 8B	other	18	-1,2	1	-0,1
Wnt9a	wingless-type MMTV integration site family, member 9A	other	201	-1	-1,1	-1
Wnt9b	wingless-type MMTV integration site family, member 9B	other	266	1,3	1	1,2
Fzd1	frizzled family receptor 1	G-protein coupled receptor	15111	1	1,2	1,1
Fzd10	frizzled family receptor 10	G-protein coupled receptor	636	2,5	2	2,3
Fzd2	frizzled family receptor 2	G-protein coupled receptor	11249	-1	-1,1	-1,1
Fzd3	frizzled family receptor 3	G-protein coupled receptor	649	-1	1	0
Fzd4	frizzled family receptor 4	G-protein coupled receptor	747	-1,2	-1	-1,1
Fzd5	frizzled family receptor 5	G-protein coupled receptor	45	1	-1,2	-0,1
Fzd6	frizzled family receptor 6	G-protein coupled receptor	1554	1,1	-1	0
Fzd7	frizzled family receptor 7	G-protein coupled receptor	5756	1,2	-1	0,1
Fzd8	frizzled family receptor 8	G-protein coupled receptor	381	-1,2	-1,6	-1,4
Fzd9	frizzled family receptor 9	G-protein coupled receptor	192	-1,1	-1,1	-1,1
Axin1	axin 1	other	588	-1,3	-1	-1,2
Axin2	axin 2	other	44	-1,2	1,1	0
Ctnnb1	catenin (cadherin-associated protein), beta 1, 88kDa	transcription regulator	15657	-1	-1	-1

Table S7. Regulation of Wnt signalling components of E14.5 *Gata2* microarray

Gene Symbol	Gene Name	Type	* >500 e145gata2:: max_int	>500 e145gata2::r elevant ratio1	>1,3 e145gata2::r elevant ratio2	>1,3 e145gata2:: av_ratio	>500 E125IWR1:: max_int	>500 E125IWR1:: relevant ratio1	>500 E125IWR1:: relevant ratio2	<-1,3 E125IWR1:: av_ratio
Ahr	aryl hydrocarbon receptor	ligand-dependent nuclear receptor	9809	1,8	2,1	1,9	3922	-3,3	-3,5	-3,4
Alx1	ALX homeobox 1	transcription regulator	1682	2,6	2,4	2,5	814	-1,6	-1,6	-1,6
Avpr1a	arginine vasopressin receptor 1A	G-protein coupled receptor	952	2,7	3,3	3	1221	-4,6	-5,3	-4,9
AW549542	expressed sequence AW549542	other	4710	1,4	1,6	1,5	5156	-1,6	-1,5	-1,6
Cadm3	cell adhesion molecule 3	other	651	1,4	1,7	1,6	595	-2,4	-1,9	-2,2
Cfh	complement factor H	other	12676	1,6	1,9	1,7	935	-1,4	-1,8	-1,6
Cfhr2	complement factor H-related 2	other	548	1,8	1,7	1,8	511	-1,5	-1,9	-1,7
Dach1	dachshund homolog 1 (Drosophila)	transcription regulator	6996	1,3	1,4	1,4	5024	-1,4	-1,6	-1,5
Darc	Duffy blood group, chemokine receptor	G-protein coupled receptor	795	2,1	1,4	1,8	614	-2,9	-2,3	-2,6
Dlc1	deleted in liver cancer 1	other	1918	1,2	1,6	1,4	1930	-1,9	-1,5	-1,7
Enpep	glutamyl aminopeptidase (aminopeptidase A)	peptidase	4312	1,8	1,8	1,8	3427	-1,2	-1,7	-1,5
ENSMUST0000167348	chromosome 9 open reading frame 78	other	10953	1	1,9	1,5	4158	-1,3	-1,9	-1,6
ENSMUST0000178312	SAM domain, SH3 domain and nuclear localization signals 1	other	15098	1,4	1,7	1,6	15296	-1,3	-1,8	-1,5
Epha8	EPH receptor A8	kinase	544	2,7	2	2,4	703	-5	-4	-4,5
Foxl1	forkhead box L1	transcription regulator	3859	1,5	1,7	1,6	3438	-3	-2,4	-2,7
Fzd10	frizzled family receptor 10	G-protein coupled receptor	636	2,5	2	2,3	1380	-4,6	-3,8	-4,2
Gcm1	glial cells missing homolog 1 (Drosophila)	transcription regulator	9638	1,3	1,5	1,4	4778	-1,6	-2,4	-2
Gm17821	DDB1 and CUL4 associated factor 5 pseudogene	other	8079	1,2	1,8	1,5	11939	-1,4	-1,4	-1,4
Gm4951	predicted gene 4951	other	1400	1,5	1,7	1,6	3053	-1,4	-1,7	-1,6
Id4	inhibitor of DNA binding 4, dominant negative helix-loop-helix protein	transcription regulator	10864	1,4	1,3	1,4	9458	-1,8	-1,8	-1,8
ligp1	interferon inducible GTPase 1	enzyme	2279	1,5	1,9	1,7	3417	-1,3	-1,8	-1,5
Kcnd3	potassium voltage-gated channel, Shal-related subfamily, member 3	ion channel	2866	1,9	2,2	2	608	-2	-1,9	-2
Lamc3	laminin, gamma 3	other	984	2	1,7	1,8	633	-2	-1,6	-1,8
Lix1	Lix1 homolog (chicken)	other	604	1,9	2	1,9	884	-1,4	-1,5	-1,4
Mal	mal, T-cell differentiation protein	transporter	6129	1,5	1,5	1,5	7620	-1,5	-1,5	-1,5
Megf10	multiple EGF-like-domains 10	other	1094	1,8	2,2	2	687	-1,3	-2,1	-1,7
N6amt1	N-6 adenine-specific DNA methyltransferase 1 (putative)	enzyme	1339	1,2	1,7	1,5	520	-1,4	-1,4	-1,4
Ndp	Norrie disease (pseudoglioma)	growth factor	2029	1,4	1,6	1,5	1032	-1,8	-2,3	-2
Nell1	NEL-like 1 (chicken)	growth factor	2038	1,9	1,9	1,9	889	-2,1	-2,3	-2,2
Nkd1	naked cuticle homolog 1 (Drosophila)	other	5743	1,4	1,4	1,4	6986	-2,5	-2,2	-2,3
Pappa	pregnancy-associated plasma protein A, pappalysin 1	peptidase	1525	1,2	1,6	1,4	1491	-1,5	-1,8	-1,6
Pla2g7	phospholipase A2, group VII (platelet-activating factor acetylhydrolase, plasma)	enzyme	2345	1,4	1,5	1,5	3508	-2,5	-2,6	-2,6
Pou3f1	POU class 3 homeobox 1	transcription regulator	2576	1,9	1,4	1,6	2911	-1,8	-1,5	-1,7
Rhox8	reproductive homeobox 8	other	10139	1,1	1,8	1,4	3968	-1,6	-2,3	-1,9
Sema3c	sema domain, immunoglobulin domain (lg), short basic domain, secreted, (semaphorin) 3C	other	10060	1,5	1,7	1,6	6517	-1,5	-2,1	-1,8
Sprr1a	small proline-rich protein 1A	other	3597	2,3	1	1,6	2580	-1,9	-2,1	-2
Sprr2a2	small proline-rich protein 2G	other	45181	1,9	1,4	1,7	56469	-2,2	-1,5	-1,8
Tbc1d4	TBC1 domain family, member 4	other	2979	1,5	1,7	1,6	2290	-2	-1,9	-2
Tmem132c	transmembrane protein 132C	other	802	1,5	2	1,7	920	-1,6	-1,5	-1,6
Ulk3a	uropod protein 3A	other	5377	1,8	1,1	1,5	1620	-1,5	-1,3	-1,4

Table S8. Commonly deregulated genes of the E14.5 Gata2 and IWR-1 microarray

	*			<-1,3	<-1,3	<-1,3		<-1,3	<-1,3	<-1,3
Gene Symbol	Gene Name	Type	e145gata2:: max_int	e145gata2::r elevant ratio1	e145gata2::r elevant ratio2	e145gata2:: av_ratio	E135Sox9fl:: max_int	E135Sox9fl:: relevant ratio1	E135Sox9fl:: relevant ratio2	E135Sox9fl:: av_ratio
8430436N08Rik	RIKEN cDNA 8430436N08 gene	other	25	-1,7	-1,5	-1,6	30	-1,4	-2	-1,7
Angptl7	angiopoietin-like 7	other	791	-1,6	-1,5	-1,6	329	-1,9	-2,4	-2,1
Aspa	aspartoacylase	enzyme	182	-1,5	-1,4	-1,5	130	-2	-2	-2
Aspn	asporin	other	672	-1,5	-1,9	-1,7	233	-3,4	-6,5	-5
Balf	basic leucine zipper transcription factor, ATF-like	transcription regulator	414	-1,8	-1,6	-1,7	449	-1,4	-1,4	-1,4
C1ql3	complement component 1, q subcomponent-like 3	other	274	-3,3	-4,2	-3,7	113	-2,1	-4,1	-3,1
Car3	carbonic anhydrase III, muscle specific	enzyme	36190	-2,1	-1,4	-1,7	31659	-11	-12,9	-12
Chrm3	cholinergic receptor, muscarinic 3	G-protein coupled receptor	30	-1,8	-1,8	-1,8	44	-2,1	-2,3	-2,2
Col2a1	collagen, type II, alpha 1	other	1248	-1,5	-1,4	-1,4	8132	-2,7	-1,9	-2,3
Col9a1	collagen, type IX, alpha 1	other	9637	-1,9	-1,9	-1,9	9066	-2,2	-2,2	-2,2
Crym	crystallin, mu	enzyme	6939	-1,5	-1,4	-1,5	4650	-1,9	-2	-2
Ctnna2	catenin (cadherin-associated protein), alpha 2	other	745	-3,2	-2,8	-3	745	-1,8	-1,6	-1,7
Cyp26a1	cytochrome P450, family 26, subfamily A, polypeptide 1	enzyme	268	-8,2	-4,4	-6,3	450	-16,9	-14,6	-15,8
D930019F10Rik	RIKEN cDNA D930019F10 gene	other	192	-2,1	-2,4	-2,3	162	-3,4	-2,5	-2,9
Dpt	dermatopontin	other	132	-1,8	-1,4	-1,6	100	-1,4	-2	-1,7
Ednrb	endothelin receptor type B	G-protein coupled receptor	3748	-1,5	-1,5	-1,5	4863	-1,9	-1,7	-1,8
Epyc	epiphycan	other	196	-2,4	-3	-2,7	83	-3	-3,6	-3,3
Etv1	ets variant 1	transcription regulator	3198	-2	-1,5	-1,7	4658	-1,8	-1,7	-1,7
Fam189a1	family with sequence similarity 189, member A1	other	107	-1,5	-1,6	-1,5	52	-1,4	-1,6	-1,5
Fam46a	family with sequence similarity 46, member A	other	639	-1,8	-1,6	-1,7	1109	-2,2	-1,7	-1,9
Fgf7	fibroblast growth factor 7	growth factor	1467	-1,7	-1,4	-1,5	1530	-3,1	-2,1	-2,6
Fmo1	flavin containing monooxygenase 1	enzyme	1653	-1,6	-1,7	-1,6	376	-2,6	-3,4	-3
Foxp2	forkhead box P2	transcription regulator	386	-1,4	-1,5	-1,4	502	-1,8	-2	-1,9
Grem2	gremlin 2, DAN family BMP antagonist	other	168	-1,5	-2,6	-2,1	112	-1,5	-1,4	-1,4
Mgat4c	mannosyl (alpha-1,3-)-glycoprotein beta-1,4-N-acetylglucosaminyltransferase, isozyme C (putative)	enzyme	48	-1,9	-1,8	-1,9	30	-1,5	-2	-1,7
Morf4l2	mortality factor 4 like 2	other	45665	-1,6	-1,6	-1,6	39418	-1,7	-1,5	-1,6
Myocd	myocardin	transcription regulator	56	-2,4	-2,1	-2,3	99	-2,8	-2,1	-2,4
Nppc	natriuretic peptide C	other	64	-2,1	-1,9	-2	43	-1,4	-2	-1,7
Plod2	procollagen-lysine, 2-oxoglutarate 5-dioxygenase 2	enzyme	4240	-1,5	-1,4	-1,4	2089	-2,6	-1,5	-2
Slc24a4	solute carrier family 24 (sodium/potassium/calcium exchanger), member 4	transporter	80	-1,6	-1,5	-1,5	129	-2,8	-2	-2,4
Smoc1	SPARC related modular calcium binding 1	other	619	-1,4	-1,5	-1,5	1492	-2,4	-1,4	-1,9
Sntg1	syntrophin, gamma 1	other	162	-1,5	-1,4	-1,4	248	-1,9	-1,5	-1,7
Stxbp5l	syntaxin binding protein 5-like	other	94	-2	-2,1	-2	268	-2,5	-1,7	-2,1
Wfdc18	WAP four-disulfide core domain 18	other	67	-1,6	-3,2	-2,4	51	-3	-3,3	-3,2
Wnk2	WNK lysine deficient protein kinase 2	kinase	1405	-1,5	-1,4	-1,4	1994	-2,1	-1,4	-1,8

Table S9. Commonly downregulated genes of the E14.5 Gata2 and E13.5 Sox9 MA

	*			>1,3	>1,3	>1,3		>1,3	>1,3	>1,3
Gene Symbol	Gene Name	Type	e145gata2::max_int	e145gata2::relevant_ratio1	e145gata2::relevant_ratio2	e145gata2::av_ratio	E135Sox9fl::max_int	E135Sox9fl::relevant_ratio1	E135Sox9fl::relevant_ratio2	E135Sox9fl::av_ratio
2310065F04Rik	RIKEN cDNA 2310065F04 gene	other	308	5,7	1,7	3,7	487	2,4	4,9	3,6
A730054J21Rik	RIKEN cDNA A730054J21 gene	other	165	1,8	1,5	1,6	492	1,7	2,3	2
Aldh1a3	aldehyde dehydrogenase 1 family, member A3	enzyme	775	2,2	1,5	1,9	2822	2,7	1,9	2,3
Ano2	anoctamin 2	ion channel	40	1,8	1,5	1,7	48	1,6	2,3	2
C530044C16Rik	RIKEN cDNA C530044C16 gene	other	31	1,5	1,4	1,4	74	4	3,1	3,6
C920006O11Rik	RIKEN cDNA C920006O11 gene	other	196	4,3	3	3,6	190	2,2	2	2,1
Cfh	complement factor H	other	12676	1,6	1,9	1,7	6496	1,9	1,5	1,7
Cfhr2	complement factor H-related 2	other	548	1,8	1,7	1,8	589	1,7	1,5	1,6
Cntn1	contactin 1	enzyme	971	2,5	1,7	2,1	970	1,9	1,7	1,8
D230018H15Rik	RIKEN cDNA D230018H15 gene	other	187	1,7	1,7	1,7	354	1,8	2,9	2,3
Dach2	dachshund homolog 2 (Drosophila)	other	1262	2,3	2,2	2,3	1643	1,7	1,7	1,7
Eddm3b	epididymal protein 3B	other	208	1,7	1,5	1,6	409	1,7	1,8	1,8
Efcab6	EF-hand calcium binding domain 6	other	37	1,4	1,4	1,4	37	1,7	1,4	1,6
Fam155a	family with sequence similarity 155, member A	other	3791	1,8	1,7	1,7	3361	1,6	1,9	1,7
Fam19a5	family with sequence similarity 19 (chemokine (C-C motif)-like), member A5	other	662	1,7	1,7	1,7	718	1,8	2	1,9
Fat3	FAT tumor suppressor homolog 3 (Drosophila)	other	140	1,4	1,4	1,4	339	2,1	2,4	2,2
Fbxw15	F-box and WD repeat domain containing 12	other	36	1,5	1,6	1,5	33	1,8	1,6	1,7
Fzd10	frizzled family receptor 10	G-protein coupled receptor	636	2,5	2	2,3	1178	2,4	2,4	2,4
Gabra2	gamma-aminobutyric acid (GABA) A receptor, alpha 2	ion channel	60	2,5	2,4	2,5	99	3,7	2,9	3,3
Gm5144	predicted gene 5144	other	66	2,1	2,4	2,2	43	1,5	1,6	1,5
Htr2b	5-hydroxytryptamine (serotonin) receptor 2B, G protein-coupled	G-protein coupled receptor	445	3,1	3,8	3,4	322	1,6	1,4	1,5
Kcnv2	potassium channel, subfamily V, member 2	ion channel	131	1,5	1,9	1,7	149	2,4	1,9	2,2
Lix1	Lix1 homolog (chicken)	other	604	1,9	2	1,9	1134	1,7	1,8	1,7
Lrriq1	leucine-rich repeats and IQ motif containing 1	other	303	3,3	3,4	3,4	314	1,9	2	1,9
Nell1	NEL-like 1 (chicken)	growth factor	2038	1,9	1,9	1,9	1454	2,1	1,6	1,9
Neto2	neuropilin (NRP) and tolloid (TLL)-like 2	other	2063	1,6	1,6	1,6	1626	1,5	1,5	1,5
Nhlrc2	NHL repeat containing 2	enzyme	452	1,7	1,4	1,6	678	1,5	1,4	1,4
Npr3	natriuretic peptide receptor C/ guanylate cyclase C (atrionatriuretic peptide receptor C)	G-protein coupled receptor	976	1,8	2,1	1,9	431	1,4	1,6	1,5
Pla2g7	phospholipase A2, group VII (platelet-activating factor acetylhydrolase, plasma)	enzyme	2345	1,4	1,5	1,5	4533	2	2,2	2,1
Pnp2	purine nucleoside phosphorylase	enzyme	76	1,4	1,6	1,5	41	2,1	1,8	2
Slc22a3	solute carrier family 22 (extraneuronal monoamine transporter), member 3	transporter	223	1,9	1,6	1,7	439	2,8	2	2,4
Sorcs3	sortilin-related VPS10 domain containing receptor 3	transporter	38	1,5	1,5	1,5	82	1,8	2,3	2,1
Sostdc1	sclerostin domain containing 1	other	1618	4,5	4,2	4,4	324	1,4	1,4	1,4
Tmod2	tropomodulin 2 (neuronal)	other	295	1,5	1,5	1,5	191	1,4	1,4	1,4

Table S10. Commonly upregulated genes of the E14.5 *Gata2* and E13.5 *Sox9* microarray

Table 1

Gene symbol	Gene name	Notes	max intensity	average fold change E14.5 Gata2
Centpe	centromere protein E, 312kDa		11176	+1,3
Pde3a	phosphodiesterase 3A, cGMP-inhibited		239	+1,3
Atf3	activating transcription factor 3	binds DNA directly to initiate transcription	1511	+1,3
Yes1	v-yes-1 Yamaguchi sarcoma viral oncogene homolog 1		645	+1,2
Spred1	sprouty-related, EVH1 domain containing 1	inhibitor of MAPK signalling	4232	+1,2
Zfp361	ZFP36 ring finger protein-like 1		17322	+1,2
Rfx3	regulatory factor X, 3 (influences HLA class II expression)	Ciliogenesis factor	59	+1,2
Depdc1a	DEP domain containing 1		1734	+1,2
Prkce	protein kinase C, epsilon		42	+1,2
Kif18a	kinesin family member 18A		596	+1,2
Sema3a	sema domain, immunoglobulin domain (Ig), short basic domain, secreted, (semaphorin) 3A		262	+1,2
Gem	GTP binding protein overexpressed in skeletal muscle	Receptor mediated signal transduction	1379	+1,2
Rspo3	R-spondin 3	activates Wnt-signaling	2215	+1,2
Ifit2	interferon-induced protein with tetratricopeptide repeats 2		277	+1,2
Sipa1l3	signal-induced proliferation-associated 1 like 3		1843	+1,1
Fyco1	FYVE and coiled-coil domain containing 1		1492	+1,1
S100a6	S100 calcium binding protein A6		15928	+1,1
Cd47	Cd47 molecule		5206	+1,1
Rnf141	ring finger protein 141		1940	+1,1
Cdca7	cell division cycle associated 7		7323	+1,1
Nucks1	nuclear casein kinase and cyclin-dependent kinase substrate 1		4127	+1,1
Dpysl2	dihydropyrimidinase-like 2		7899	+1,1
Runx1t1	runt-related transcription factor 1		2878	+1,1
Pcdh17	protocadherin 17		522	+1,1
Fam108c	abhydrolase domain containing 17C		6736	+1,1
Tslp	thymic stromal lymphopoietin		108	+1,1
Arid5b	AT rich interactive domain 5B (MRF1-like)		4891	+1,1
Syde2	synapse defective 1, Rho GTPase, homolog 2		233	+1,1
Cd200	CD200 molecule		365	+1,1
Gsto2	glutathione S-transferase omega 2		377	+1,1
Dkk1	dickkopf 1 homolog (Xenopus laevis)	Wnt antagonist	689	+1,1
Rein	reelin		54	+1,1
Stt3a	STT3A, subunit of the oligosaccharyltransferase complex (catalytic)		3611	-1,1
Srpx	sushi-repeat containing protein, X-linked		3093	-1,1
Tmem87b	transmembrane protein 87B		918	-1,1
Cyb5r3	cytochrome b5 reductase 3		3277	-1,1
Atg16l2	autophagy related 16-like 2 (S. cerevisiae)		395	-1,1
Nfkbib	nuclear factor of kappa light polypeptide gene enhancer in B-cells inhibitor, beta		1444	-1,1
Map1lc3b	microtubule-associated protein 1 light chain 3 beta		12797	-1,1
Lrrfp1	leucine rich repeat (in FLII) interacting protein 1		2670	-1,1
Dcbld2	discoidin, CUB and LCCL domain containing 2		349	-1,1
Plau	plasminogen activator, urokinase		114	-1,1
Frzb	frizzled-related protein	Wnt modulator	424	-1,2
Rgs2	regulator of G-protein signaling 2, 24kDa		12315	-1,2
Cd55	CD55 antigen		1263	-1,2
Ddah1	dimethylarginine dimethylaminohydrolase 1		1213	-1,2
Plekha1	pleckstrin homology domain containing, family B (evectins) member 1		317	-1,3
Kitl	KIT ligand		503	-1,4
Fgf18	fibroblast growth factor 18		2722	-1,4
Dlx2	distal-less homeobox 2		59	-1,5
Inhba	inhibin, beta A		711	-1,5
Tgfb2	transforming growth factor, beta 2		8963	-1,7
Mfi2	antigen p97 (melanoma associated)		74	-1,8

Table S11. Overlay of Gata2 CHIP targets in HUVECs and E14.5 Gata2 microarray

7. Concluding remarks

Over the last decades the analyses of various genetically modified mouse models have shed light on the molecular mechanisms controlling fundamental processes in development of the UGS such as nephric lineage induction, ureteric budding, SM differentiation, ureteric branching or nephrogenesis. However, the riddle of the aetiology of CAKUT has not been solved so far. We know, that during development cells and tissues have to interact, adhere or disperse from each other to allow proper organogenesis. These processes are mediated by a variety of signalling pathways and modules, which have to be molecularly integrated in time and space. How this is achieved has remained largely elusive. The importance of tissue interactions has become clear e.g. from tissue separation and recombination experiments. If one removes the metanephric mesenchyme from the ureteric tip, nephrogenesis is paused [64]. On the other hand, if the tissue surrounding a migrating neuron is removed, the neuron loses its orientation [49].

The Eph-ephrin signalling pathway is known to guide neurons to their targets [56], to establish tissue boundaries [65], to separate tissues [66], to mediate adhesion or repulsion events [67] and to regulate programmed cell death [62] in various cellular contexts. In the first part of this thesis, I identified the Eph receptors *EphA4* and *EphA7* as pivotal regulators of selective adhesion in the caudal nephric duct and in the fusion process between the distal ND and the cloacal epithelium. Moreover, I showed that disintegration of the caudal ND resulted in delayed or absent fusion with the urogenital sinus. This often neglected process is essential for proper function of the entire UGS, since ND fusion defects lead to severe phenotypic outcomes such as ureterocele, blind or ectopic ending ureters and secondary hydroureteronephrosis, respectively. However, it is still unclear how cooperative EphA4/EphA7 signalling influences the transcriptional control of the receptor tyrosine kinase *Ret* or the transcription factors *Gata3* and *Lhx1* or whether down-regulation of these genes is secondary to caudal ND dispersal. Moreover, since the CND in DKO embryos massively increases in size, one needs to determine how and if proliferation accounts for this fact. This might be addressed in future experiments.

In the second part of this thesis, I gave experimental support in the study that showed that *Tbx18* positive cells contribute to various cell lineages of the mature UGS including the testis, the adrenals, the kidney stroma, the UM and the bladder. However, *Tbx18* is dispensable for the differentiation of the majority of these organs except the ureter. Studies in *Tbx18*-deficient embryos revealed that *Tbx18* expression is essential in the UM to prevent a metanephric fate and for the perception of epithelial survival signals [63]. I assume, in this context *Tbx18* facilitates a selective adhesion process within the UM that prohibits cells to leave the UM cell community and on the other hand prevents cells from the MM to acquire a ureteric fate. Briefly, *Tbx18* might serve as a specification factor for the UM. How this is achieved needs to be in focus of future studies by e.g. the identifica-

tion of target genes by RNA-microarray analysis or by identification of Tbx18 interaction partners via mass spectrometry.

In part 3 and 4, I mainly focused on the molecular processes controlling terminal differentiation of the UM into SM cells. Cytodifferentiation of the UM requires clear subdivision into an inner and an outer mesenchymal domain as well as proliferation of these sub-compartments. In part 3, we showed that canonical Wnt signalling governs these processes in the UM by exerting paracrine signals from the epithelium to the mesenchyme. Upon conditional deletion of *Ctnnb1*, the intracellular signal transducer of the canonical Wnt pathway, prenatal embryos displayed hydroureter and hydronephrosis as a consequence of reduced proliferation and differentiation of the inner mesenchymal domain. Contrarily, the outer mesenchymal domain terminally differentiated into fibrocytes at the expense of ureteric SM cells. This study greatly contributed to the molecular understanding of early patterning processes in the UM and adjoined one signalling module to global knowledge of SM differentiation regulators. However, it has remained elusive how Wnt-signalling differentially regulates the subset of UM markers, which were lost in the conditional *Ctnnb1*-mutants. It also remains questionable, whether those genes that were downregulated at E14.5 in *Tbx18^{cre/+};Ctnnb1^{fx/fx}* embryos are genuine transcriptional targets or whether the loss of the inner UM cell population accounts for the absence of this markers, respectively. This issue might be solved utilizing microarray screens combined with CHIP sequencing experiments at different stages of development to unravel the primary molecular targets of this signalling module. Terminal differentiation of the UM requires proliferation of precursor cells and downregulation of certain molecular factors in space and time [68, 69]. In the search for transcriptional regulators that are present in the undifferentiated mesenchyme and downregulated in the course of development, we found the zinc finger transcription factor *Gata2* to be present in the early UM and epithelium. *Gata2* is functionally implicated in cell lineage decision and in balancing proliferation versus differentiation in various developmental processes [70]. During the analysis of a conditional *Gata2*-mutant, a delay in SM differentiation and upregulation of Hh- and RA signalling became apparent.

Microarray analysis of the conditional *Gata2*-mutant at E14.5 recapitulated the loss of SM specific marker genes and revealed astonishing alterations in the neuronal and vascular marker genes, indicating that loss of *Gata2* in the UM may hamper neuronal differentiation and angiogenesis/vasculogenesis in the UM. Consistent with the finding that *Gata2* constitutes a key regulator of angiogenesis [68], loss of a majority of blood components suggests a similar function of *Gata2* in the UM as in endothelial cells.

Therefore, I compared direct target genes of *Gata2* in HUVECs (human umbilical vein endothelial cells), which were obtained by CHIP sequencing experiments, with our microarray data at E14.5. I observed upregulation of *Atf3* (activating transcription factor 3)

and *Rfx3* (regulatory factor x, 3) upon conditional loss of *Gata2*. Furthermore *Rspo3* was upregulated, a factor implicated in modulation of the Wnt signalling pathway. This suggests a repressive function of *Gata2* in the UM, which can be validated by identification of interaction partners by mass spectrometry or reporter assays. In addition to that, I observed upregulation of some members of the *Hox* gene family. Strikingly, we saw enhanced mRNA levels of *Hoxd* genes, which are all clustered at 44.13 cM on murine chromosome 2. Whether *Gata2* is able to directly repress transcription of *Hoxd* factors or whether it does so with other protein interaction partners, needs to be investigated by CHIP sequencing or transactivation assays. Interestingly, the loss of markers of differentiated neurons suggests a function of *Gata2* in neuronal differentiation in the UM. It remains to be seen whether neurons in the UM either remain undifferentiated or whether this cell type is completely absent in *Gata2*-deficient embryos, which should be in focus of future studies.

All four independent studies of this dissertation emphasized the importance of tissue interactions and gene regulatory networks in early development of the UGS.

ND fusion was introduced as the prerequisite for proper distal ureter function and the tightly regulated control of the expression and activity of UM-specific transcription factors and signalling modules were shown to be mandatory for proper ureteric SM development. However, future studies in genetically modified mouse models, advanced *in vitro* culture systems and viral approaches will clarify the epistatic relationships orchestrating the process of ureter development.

8. Acknowledgements

First, I would like to kindly thank my supervisor Prof. Dr. Andreas Kispert for giving me the opportunity to work on many fascinating and challenging projects, for his support and helpful discussions, for his offer to participate in the IWDN workshop and for his patience in bad times.

I would like to thank the head of the IfM, Prof. Dr. Achim Gossler, for this great research environment and his wife Dr. Karin Schuster-Gossler for some mice I worked with in my studies.

I want to thank PD Dr. Sandra Ciesek and Prof. Monika Hassel for their kind offer to co-examine my thesis and to Prof. Dr. Bernhard Huchzermeyer for accepting the duty as chair of my disputation.

Thanks to all the past and present lab members (in particular Dr. Anna Foik, Dr. Julia Norden, Dr. Franziska Greulich, Dr. Marc Kleppa, Eva Bettenhausen, Dr. Timo Lüdtkke and Dr. Carsten Rudat) for their support, the nice lunchtimes, coffee breaks and “off-topics” discussions and Dr. Rannar Airik for supervising me in the very beginning.

Especially, I would like to thank Dr. Carsten Rudat and Dr. Timo Lüdtkke for their kind support during my thesis writing and their constructive and humorous criticism.

Last but not least, I would like to deeply thank my family, especially my mother and my husband, without whom this work would never have been possible and who always backed me up.

Finally, I would like to thank my son Elias Manuel for being the light of my life.

9. Curriculum vitae

Personal information

Name: Anna-Carina Weiss
 Date of birth: 31/08/1983
 Place of birth: Hannover
 Citizenship: German
 Email: weiss.carina@mh-hannover.de

School education

1990 – 1994 Grundschole Kurt-Schumacher-Schole, Hannover
 1994 – 1996 Orientierungsstufe Anderten, Hannover
 1996 – 2003 Gymnasium St.-Ursula Schule, Hannover
 Degree: Abitur

University studies

2003 – 2009 Undergraduate (“Vordiplom”) and Graduate studies (“Diplom”) in Biology at the Leibniz Universitat Hannover
 2006 – 2007 DAAD-funded graduate studies in Biology at Northeastern University and seminar classes in Biochemistry at Massachusetts Institute of Technology, Boston and Cambridge, USA
 2008 - 2009 Diploma thesis at the Institute for Molecular Biology at the Hannover Medical School (MHH) under supervision of Prof. Dr. Andreas Kispert
 Degree: Diplom-Biologin
 2009 - Research assistant in the laboratory of Prof. Dr. Andreas Kispert at the Institute for Molecular Biology at Hannover Medical School (MHH)

Practical experiences

2004 – 2005 Research assistant at the Institute for Quantum optics at the Leibniz Universitat Hannover
 2004 – 2006 Tutor in Organic Chemistry at the Institute of Food Chemistry at the Leibniz Universitat Hannover
 2007 – 2008 Research assistant at the Institute for Botany at the Leibniz Universitat Hannover
 2008 Supervision of a B.Sc. student during long-term internship at the Northeastern University, Boston, USA
 2013 Supervision of a B.Sc. student (internship and thesis) at the Institute of Molecular Biology, MHH, Hannover

Prizes and stipends Stipend of the Deutsche Akademischer Austauschdienst (DAAD) for one year “studies abroad” in Boston, USA

Language skills Fluent in English both written and spoken, IELTS Certificate, basic knowledge in Spanish and Latin (Groes Latinum)

10. List of publications

Weiss AC, Airik R, Greulich F, Foik AB, Trowe MO, Rudat C, Costantini F, Adams RH and Kispert A. "Nephric duct insertion requires EphA4/EphA7 signaling from the pericloacal mesenchyme".

Development 2014, September 141(17) 3420-30.

Airik R, Slaats GG, Weiss AC, Khan N, Ghosh A, Hurd TW, Bekker-Jensen S, Schroder JM, Elledge SJ, Andersen JS, Kispert A, Castelli M, Boletta A, Giles RH and Hildebrandt F.

"Renal-Retinal Ciliopathy Gene Sdccag8 Regulates DNA Damage Response Signaling".

Journal Of The American Society Of Nephrology 2014, April 10.

Bohnenpoll T and Bettenhausen E, Weiss AC, Foik AB, Trowe MO, Blank P, Airik R and Kispert A. "Tbx18 expression demarcates multipotent precursor populations in the developing urogenital system but is exclusively required within the ureteric mesenchymal lineage to suppress a renal stromal fate".

Developmental Biology 2013, August 380(1), 25-36.

Trowe MO, Zhao L, Weiss AC, Christoffels V, Epstein DJ and Kispert A.

"Inhibition of Sox2-dependent activation of Shh in the ventral diencephalon by Tbx3 is required for formation of the neurohypophysis".

Development 2013, June 140(11), 2299-309.

Trowe MO and Airik R, Weiss AC, Farin HF, Foik AB, Bettenhausen E, Schuster-Gossler K, Taketo MM and Kispert A. "Canonical Wnt signaling regulates smooth muscle precursor development in the mouse ureter."

Development 2012, September 139(17), 3099-108.

11. Declaration

“I hereby declare and confirm that this dissertation is entirely the result of my own work except otherwise indicated. This thesis has not been part of any other examination.”

Erklärung zur Dissertation

Gemäß §6(1) der Promotionsordnung der Naturwissenschaftlichen Fakultät der Gottfried Wilhelm Leibniz Universität Hannover

für die Promotion zum Dr. rer. nat.

Hiermit erkläre ich, dass ich meine Dissertation mit dem Titel

“Molecular control of ureter development in the mouse”

selbstständig verfasst sowie die Hilfsmittel und Quellen und gegebenenfalls die zu Hilfeleistungen herangezogenen Institutionen vollständig angegeben habe.

Die Inhalte dieser Dissertation wurden nicht zuvor als Masterarbeit, Diplomarbeit oder andere Prüfungsarbeit verwendet.

12. Bibliography

1. Costantini, F. and R. Kopan, Patterning a complex organ: branching morphogenesis and nephron segmentation in kidney development. *Dev Cell*, 2010. 18(5): p. 698-712.
2. Lang, R.J., et al., Pyeloureteric peristalsis: role of atypical smooth muscle cells and interstitial cells of Cajal-like cells as pacemakers. *J Physiol*, 2006. 576(Pt 3): p. 695-705.
3. Batinic, D., et al., Vesicoureteral reflux and urodynamic dysfunction. *Urol Int*, 2013. 90(4): p. 480-3.
4. Rosen, S., et al., The kidney in congenital ureteropelvic junction obstruction: a spectrum from normal to nephrectomy. *J Urol*, 2008. 179(4): p. 1257-63.
5. Mendelsohn, C., Using mouse models to understand normal and abnormal urogenital tract development. *Organogenesis*, 2009. 5(1): p. 306-14.
6. Renkema, K.Y., et al., Novel perspectives for investigating congenital anomalies of the kidney and urinary tract (CAKUT). *Nephrol Dial Transplant*, 2011. 26(12): p. 3843-51.
7. Miyazaki, Y. and I. Ichikawa, Ontogeny of congenital anomalies of the kidney and urinary tract, CAKUT. *Pediatr Int*, 2003. 45(5): p. 598-604.
8. Nakanishi, K. and N. Yoshikawa, Genetic disorders of human congenital anomalies of the kidney and urinary tract (CAKUT). *Pediatr Int*, 2003. 45(5): p. 610-6.
9. Hofmann, A.D., J.W. Duess, and P. Puri, Congenital anomalies of the kidney and urinary tract (CAKUT) associated with Hirschsprung's disease: a systematic review. *Pediatr Surg Int*, 2014. 30(8): p. 757-61.
10. Caruana, G. and J.F. Bertram, CAKUT genetics in mice and men. *Nephrology (Carlton)*, 2015.
11. Sultan, S., et al., Evaluation of ureteropelvic junction obstruction (UPJO) by diuretic renography. *J Pak Med Assoc*, 1996. 46(7): p. 143-7.
12. Tripathi, M., et al., Reflux in native kidneys mimicking urine leak postrenal transplant. *Clin Nucl Med*, 2005. 30(5): p. 344-6.
13. Shapiro, E., Clinical implications of genitourinary embryology. *Curr Opin Urol*, 2009. 19(4): p. 427-33.
14. Airik, R., et al., Tbx18 regulates the development of the ureteral mesenchyme. *J Clin Invest*, 2006. 116(3): p. 663-74.
15. Uetani, N., et al., Maturation of ureter-bladder connection in mice is controlled by LAR family receptor protein tyrosine phosphatases. *J Clin Invest*, 2009. 119(4): p. 924-35.
16. Weiss, A.C., et al., Nephric duct insertion requires EphA4/EphA7 signaling from the pericloacal mesenchyme. *Development*, 2014. 141(17): p. 3420-30.
17. Lechner, M.S. and G.R. Dressler, The molecular basis of embryonic kidney development. *Mech Dev*, 1997. 62(2): p. 105-20.

18. Bouchard, M., et al., Nephric lineage specification by Pax2 and Pax8. *Genes Dev*, 2002. 16(22): p. 2958-70.
19. Gerlach, G.F. and R.A. Wingert, Kidney organogenesis in the zebrafish: insights into vertebrate nephrogenesis and regeneration. *Wiley Interdiscip Rev Dev Biol*, 2013. 2(5): p. 559-85.
20. Saxen, L. and H. Sariola, Early organogenesis of the kidney. *Pediatr Nephrol*, 1987. 1(3): p. 385-92.
21. Kobayashi, A. and R.R. Behringer, Developmental genetics of the female reproductive tract in mammals. *Nat Rev Genet*, 2003. 4(12): p. 969-80.
22. Costantini, F. and R. Shakya, GDNF/Ret signaling and the development of the kidney. *Bioessays*, 2006. 28(2): p. 117-27.
23. Batourina, E., et al., Apoptosis induced by vitamin A signaling is crucial for connecting the ureters to the bladder. *Nat Genet*, 2005. 37(10): p. 1082-9.
24. Chia, I., et al., Nephric duct insertion is a crucial step in urinary tract maturation that is regulated by a Gata3-Raldh2-Ret molecular network in mice. *Development*, 2011. 138(10): p. 2089-97.
25. Gandhi, D., et al., Retinoid signaling in progenitors controls specification and regeneration of the urothelium. *Dev Cell*, 2013. 26(5): p. 469-82.
26. Bohnenpoll, T. and A. Kispert, Ureter growth and differentiation. *Semin Cell Dev Biol*, 2014. 36: p. 21-30.
27. Grote, D., et al., Pax 2/8-regulated Gata 3 expression is necessary for morphogenesis and guidance of the nephric duct in the developing kidney. *Development*, 2006. 133(1): p. 53-61.
28. Grote, D., et al., Gata3 acts downstream of beta-catenin signaling to prevent ectopic metanephric kidney induction. *PLoS Genet*, 2008. 4(12): p. e1000316.
29. Pedersen, A., C. Skjong, and W. Shawlot, Lim 1 is required for nephric duct extension and ureteric bud morphogenesis. *Dev Biol*, 2005. 288(2): p. 571-81.
30. Moore, M.W., et al., Renal and neuronal abnormalities in mice lacking GDNF. *Nature*, 1996. 382(6586): p. 76-9.
31. Brodbeck, S., B. Besenbeck, and C. Englert, The transcription factor Six2 activates expression of the Gdnf gene as well as its own promoter. *Mech Dev*, 2004. 121(10): p. 1211-22.
32. Xu, P.X., et al., Eya1-deficient mice lack ears and kidneys and show abnormal apoptosis of organ primordia. *Nat Genet*, 1999. 23(1): p. 113-7.
33. Miyazaki, Y., et al., Bone morphogenetic protein 4 regulates the budding site and elongation of the mouse ureter. *J Clin Invest*, 2000. 105(7): p. 863-73.
34. Wellik, D.M., P.J. Hawkes, and M.R. Capecchi, Hox11 paralogous genes are essential for metanephric kidney induction. *Genes Dev*, 2002. 16(11): p. 1423-32.
35. Donovan, M.J., et al., Initial differentiation of the metanephric mesenchyme is independent of WT1 and the ureteric bud. *Dev Genet*, 1999. 24(3-4): p. 252-62.

36. Yu, C.T., et al., COUP-TFII is essential for metanephric mesenchyme formation and kidney precursor cell survival. *Development*, 2012. 139(13): p. 2330-9.
37. Drummond, I.A., D. Mukhopadhyay, and V.P. Sukhatme, Expression of fetal kidney growth factors in a kidney tumor line: role of FGF2 in kidney development. *Exp Nephrol*, 1998. 6(6): p. 522-33.
38. Nie, X., et al., SIX1 acts synergistically with TBX18 in mediating ureteral smooth muscle formation. *Development*, 2010. 137(5): p. 755-65.
39. Airik, R., et al., Hydroureteronephrosis due to loss of Sox9-regulated smooth muscle cell differentiation of the ureteric mesenchyme. *Hum Mol Genet*, 2010. 19(24): p. 4918-29.
40. Yu, J., T.J. Carroll, and A.P. McMahon, Sonic hedgehog regulates proliferation and differentiation of mesenchymal cells in the mouse metanephric kidney. *Development*, 2002. 129(22): p. 5301-12.
41. Brenner-Anantharam, A., et al., Tailbud-derived mesenchyme promotes urinary tract segmentation via BMP4 signaling. *Development*, 2007. 134(10): p. 1967-75.
42. Retting, K.N., et al., BMP canonical Smad signaling through Smad1 and Smad5 is required for endochondral bone formation. *Development*, 2009. 136(7): p. 1093-104.
43. Tripathi, P., et al., Absence of canonical Smad signaling in ureteral and bladder mesenchyme causes ureteropelvic junction obstruction. *J Am Soc Nephrol*, 2012. 23(4): p. 618-28.
44. Yan, J., et al., Smad4 regulates ureteral smooth muscle cell differentiation during mouse embryogenesis. *PLoS One*, 2014. 9(8): p. e104503.
45. Nakahiro, T., et al., Identification of BMP-responsive elements in the mouse *Id2* gene. *Biochem Biophys Res Commun*, 2010. 399(3): p. 416-21.
46. Aoki, Y., et al., *Id2* haploinsufficiency in mice leads to congenital hydronephrosis resembling that in humans. *Genes Cells*, 2004. 9(12): p. 1287-96.
47. Hirai, H., et al., A novel putative tyrosine kinase receptor encoded by the *eph* gene. *Science*, 1987. 238(4834): p. 1717-20.
48. Drescher, U., Eph family functions from an evolutionary perspective. *Curr Opin Genet Dev*, 2002. 12(4): p. 397-402.
49. Kullander, K. and R. Klein, Mechanisms and functions of Eph and ephrin signalling. *Nat Rev Mol Cell Biol*, 2002. 3(7): p. 475-86.
50. Himanen, J.P., et al., Crystal structure of an Eph receptor-ephrin complex. *Nature*, 2001. 414(6866): p. 933-8.
51. Chrencik, J.E., et al., Structural and biophysical characterization of the EphB4*ephrin-B2 protein-protein interaction and receptor specificity. *J Biol Chem*, 2006. 281(38): p. 28185-92.
52. Lisabeth, E.M., G. Falivelli, and E.B. Pasquale, Eph receptor signaling and ephrins. *Cold Spring Harb Perspect Biol*, 2013. 5(9).

53. Binns, K.L., et al., Phosphorylation of tyrosine residues in the kinase domain and juxtamembrane region regulates the biological and catalytic activities of Eph receptors. *Mol Cell Biol*, 2000. 20(13): p. 4791-805.
54. Klein, R., Eph/ephrin signalling during development. *Development*, 2012. 139(22): p. 4105-9.
55. Palmer, A., et al., EphrinB phosphorylation and reverse signaling: regulation by Src kinases and PTP-BL phosphatase. *Mol Cell*, 2002. 9(4): p. 725-37.
56. Cowan, C.A., et al., Ephrin-B2 reverse signaling is required for axon pathfinding and cardiac valve formation but not early vascular development. *Dev Biol*, 2004. 271(2): p. 263-71.
57. Bong, Y.S., et al., ephrinB1 signals from the cell surface to the nucleus by recruitment of STAT3. *Proc Natl Acad Sci U S A*, 2007. 104(44): p. 17305-10.
58. Segura, I., et al., Grb4 and GIT1 transduce ephrinB reverse signals modulating spine morphogenesis and synapse formation. *Nat Neurosci*, 2007. 10(3): p. 301-10.
59. Salvucci, O. and G. Tosato, Essential roles of EphB receptors and EphrinB ligands in endothelial cell function and angiogenesis. *Adv Cancer Res*, 2012. 114: p. 21-57.
60. Redeker, C., et al., Normal development in mice over-expressing the intracellular domain of DLL1 argues against reverse signaling by DLL1 in vivo. *PLoS One*, 2013. 8(10): p. e79050.
61. Kerecuk, L., M.F. Schreuder, and A.S. Woolf, Renal tract malformations: perspectives for nephrologists. *Nat Clin Pract Nephrol*, 2008. 4(6): p. 312-25.
62. Depaepe, V., et al., Ephrin signalling controls brain size by regulating apoptosis of neural progenitors. *Nature*, 2005. 435(7046): p. 1244-50.
63. Bohnenpoll, T., et al., Tbx18 expression demarcates multipotent precursor populations in the developing urogenital system but is exclusively required within the ureteric mesenchymal lineage to suppress a renal stromal fate. *Dev Biol*, 2013. 380(1): p. 25-36.
64. Kispert, A., S. Vainio, and A.P. McMahon, Wnt-4 is a mesenchymal signal for epithelial transformation of metanephric mesenchyme in the developing kidney. *Development*, 1998. 125(21): p. 4225-34.
65. Watanabe, T., et al., EphrinB2 coordinates the formation of a morphological boundary and cell epithelialization during somite segmentation. *Proc Natl Acad Sci U S A*, 2009. 106(18): p. 7467-72.
66. Dravis, C. and M. Henkemeyer, Ephrin-B reverse signaling controls septation events at the embryonic midline through separate tyrosine phosphorylation-independent signaling avenues. *Dev Biol*, 2011. 355(1): p. 138-51.
67. Sakamoto, H., et al., Cell adhesion to ephrinb2 is induced by EphB4 independently of its kinase activity. *Biochem Biophys Res Commun*, 2004. 321(3): p. 681-7.
68. Coma, S., et al., GATA2 and Lmo2 control angiogenesis and lymphangiogenesis via direct transcriptional regulation of neuropilin-2. *Angiogenesis*, 2013. 16(4): p. 939-52.

69. Martin, E., et al., TSHZ3 and SOX9 regulate the timing of smooth muscle cell differentiation in the ureter by reducing myocardin activity. *PLoS One*, 2013. 8(5): p. e63721.
70. Aronson, B.E., K.A. Stapleton, and S.D. Krasinski, Role of GATA factors in development, differentiation, and homeostasis of the small intestinal epithelium. *Am J Physiol Gastrointest Liver Physiol*, 2014. 306(6): p. G474-90.